LONG CHAIN FATTY ACID UPTAKE BY AND TRAFFICKING WITHIN 3T3-L1 ADIPOCYTES

By

BERNARDO L. TRIGATTI, B.Sc.

A Thesis

Submitted to the School of Graduate Studies

in Partial Fulfilment of the Requirements

for the Degree

Doctor of Philosophy

McMaster University

LONG CHAIN FATTY ACID UPTAKE BY 3T3-L1 ADIPOCYTES

DOCTOR OF PHILOSOPHY (1995)
(Biochemistry)

McMASTER UNIVERSITY
Hamilton, Ontario

TITLE: Long chain fatty acid uptake by and trafficking within 3T3-L1 adipocytes

AUTHOR: Bernardo L. Trigatti, B.Sc. (McMaster University)

SUPERVISOR: Professor G.E. Gerber

NUMBER OF PAGES: xxiv, 231

ABSTRACT

Long chain fatty acids (LCFA's) are important metabolic substrates for mammalian cells. They are utilized as energy sources, through β-oxidation, and as substrates for the synthesis of lipids, including phospholipids and triglycerides, as well as lipids involved in cellular signalling. LCFAs, themselves can also participate in a variety of crucial cell signalling cascades. Adipocytes, through the storage of LCFAs as triglycerides and the mobilization of stored LCFAs are important regulators of energy balance in mammals. A variety of pathogenic conditions involve impaired storage or utilization of LCFAs.

The involvement of LCFAs in these events involves their initial interaction with, uptake by and trafficking within cells. These processes were studied in murine 3T3-L1 cells, which differentiate from preadipocytes to adipocytes. Upon differentiation, they acquired increased levels of LCFA uptake, which was saturable, exhibiting high affinities both for oleate, a natural LCFA, and for 11-*m*-diazirinophenoxy-[11-^{3}H]undecanoate, a photoreactive LCFA. This established them as a convenient cellular model in which to study LCFA uptake and trafficking. Furthermore, it established the photoreactive LCFA as an analogue of LCFAs which could prove useful for the identification and characterization of cellular LCFA binding proteins which might be involved in LCFA uptake and trafficking.

It has been proposed that cellular uptake and trafficking of LCFAs is a multi-step

process involving the delivery of LCFAs to the cell surface, their movement across the plasma membrane and their delivery to intracellular sites. The involvement of each step in LCFA uptake and trafficking in 3T3-L1 adipocytes were studied. Serum albumin, the major carrier of LCFA's in plasma had a saturable, stimulatory effect on oleate uptake by 3T3-L1 adipocytes. Serum albumin which had been photo-labeled with the photoreactive LCFA, bound to 3T3-L1 adipocytes saturably. This implicated the involvement of cellular receptors for serum albumin in the delivery of LCFAs to the cell surface.

The photoreactive LCFA was also used to identify a novel 22 kDa protein as the only high affinity LCFA receptor in the plasma membrane of 3T3-L1 cells. It was localized to the caveolae fraction of the plasma membrane and was identified immunologically as caveolin, a resident component of caveolae. Caveolin was resolved by 2-dimensional polyacrylamide gel electrophoresis into at least two forms, differing in their reaction towards an antibody recognizing a stretch of amino acids found in the predicted amino-terminal sequence of caveolin. Both forms, however had similar affinities toward the photoreactive LCFA (K_d's of 373 and 388 nM). Caveolae in the plasma membrane are believed to act as sites of transport of a variety of compounds; the localization of the only high affinity, plasma membrane LCFA receptor within caveolae suggested that they may also be sites of LCFA transport or signalling events.

A 15 kDa, cytoplasmic protein was also labeled by the photoreactive LCFA. It was identified immunologically as the adipocyte lipid binding protein (ALBP), a member of the family of low molecular weight cytoplasmic fatty acid binding proteins. Its

affinities for the photoreactive probe and natural LCFAs were determined by photoaffinity labeling and by ligand displacement, respectively. The labeling of ALBP by the photoreactive LCFA in intact 3T3-L1 adipocytes was dynamic. The time-dependence of its labeling revealed that the newly internalized photoreactive probe initially bound to and then became released by ALBP, consistent with a role for ALBP in the delivery of newly internalized LCFAs to sites of utilization within cells.

The labeling of ALBP by the photoreactive LCFA in intact cells was sensitive to inhibitors of different steps in LCFA uptake was also demonstrated. This confirmed that LCFA binding to ALBP occurred as an intermediate step in LCFA uptake. It also provided a means of discriminating between effects of various manipulations on early steps (upstream of LCFA binding to ALBP) and late steps (downstream of LCFA binding to ALBP) in LCFA uptake. Using this approach, the dependence of the movement of the photoreactive LCFA across the plasma membrane on ΔpH was demonstrated. This indicated that it traversed the membrane as the protonated species by diffusion across the lipid bilayer. Using this approach, α-iodopalmitate, an inhibitor of LCFA uptake originally thought to affect the movement of LCFAs across the plasma membrane, was shown to inhibit uptake by acting at a step downstream of LCFA binding to ALBP. This led to the identification of the specific target for delivery of LCFAs as the lipid droplet. This was the first *in vivo* demonstration of the delivery of LCFAs and of a specific target organelle for the delivery of newly internalized LCFAs by the ALBP in intact cells. It also led to the demonstration of the importance of long chain fatty acyl-CoA synthetase

in LCFA uptake. This enzyme catalyzes the first step in LCFA metabolism, namely, the activation of LCFAs by conversion to their CoA thioester derivative. Its inhibition by α-iodopalmitate was shown to result in the inhibition of LCFA uptake, suggesting that the uptake process was driven by the conversion of LCFAs to their CoA thioester derivatives.

LIST OF PUBLICATIONS

1. Trigatti, B.L., Mangroo, D. and Gerber, G.E. (1991) Photoaffinity labeling and fatty acid permeation in 3T3-L1 adipocytes. *J. Biol. Chem.* **266**, 22621-22625.

2. Trigatti, B.L., Baker, A.D., Rajaratnam, K., Rachubinski, R.A. and Gerber, G.E. (1992) Fatty acid uptake in *Candida tropicalis*: Induction of a saturable process. *Biochem. Cell Biol.* **70**, 76-80.

3. Gerber, G.E., Mangroo, D. and Trigatti, B.L. (1993) Identification of high affinity membrane-bound fatty acid-binding proteins using a photoreactive fatty acid. *Mol. Cell. Biochem.* **123**, 39-44.

4. Trigatti, B.L. and Gerber, G.E. (1995) A direct role for serum albumin in the cellular uptake of long chain fatty acids. *Biochem. J.* **308**, 155-159.

5. Mangroo, D., Trigatti, B.L., and Gerber, G.E. (1995) Membrane permeation and intracellular trafficking of long chain fatty acids: Insights from *Escherichia coli* and 3T3-L1 adipocytes. *Biochem. Cell Biol.* in press.

ACKNOWLEDGMENTS

I would like to thank Professor G.E. Gerber for his guidance, encouragement and support. I would like to thank the members of my supervisory committee, Professors J.P. Capone, R.M. Epand and E. Regoeczi for their guidance and helpful discussions. I also thank Professor R.A. Rachubinski for his encouragement. I would also like to thank Professor J.P. Capone for the use of his cell culture facilities, Professor R.M. Epand for the use of his luminescence spectrophotometer, and Professors R.G.W. Anderson and D.A. Bernlohr for supplying antibodies for caveolin and the adipocyte lipid binding protein, respectively.

I thank Dr. Dev Mangroo for his guidance and helpful discussions as well as for the synthesis of α-iodopalmitate. I am also grateful to Drs. K. Rothberg and L. Craig for providing protocols for immunoprecipitation and immunoblotting, respectively.

I would like to acknowledge the excellent technical assistance of the many undergraduate students that I have had the pleasure of working with over the years, in particular, Andrew Baker, Nick Cheng, Natasha Fernandes, Pauline Henry, Zubin Punthakee, Krishan Rajaratnam and Derek Zuccolo. I would also like to acknowledge the expert assistance of Bonnie Murphy, Barbara Sweet and Dale Tomlinson in the preparation of this and other manuscripts.

Finally, I would like to thank my family for their patience, love and support. In

particular, I thank my wife, Gabriella, who has been a constant source of encouragement, inspiration and support.

I acknowledge the financial support of the Medical Research Council of Canada.

CONTENTS

LIST OF FIGURES

LIST OF TABLES

LIST OF ABBREVIATIONS

AAT	aspartate aminotransferase
ACS	acyl-CoA synthetase
ADD	adipocyte determination and differentiation
ADIFAB	acrylodated-intestinal-FABP
ADRP	adipose differentiation related protein
ALBP	adipocyte lipid binding protein
AMP	adenosine 5'-monophosphate
APMSF	(4-amidinophenyl)methanesulfonyl fluoride
ATP	adenosine 5'-triphosphate
BCECF	2',7'-bis-(2-carboxyethyl)-5-(and 6)-carboxyfluorescein
BCECF-AM	acetoxymethyl ester of BCECF
BSA	bovine serum albumin
c-	centi-
c	concentration
°C	degrees, Celsius
cAMP	adenosine *cyclic*-3',5'-monophosphate
C/EBP	CCAAT/enhancer binding protein
cDNA	complementary deoxyribonucleic acid
CDP	cytidine diphosphate
CHAPS	3-[(3-chloramidopropyl)dimethylammonio]-1-propane-sulfonate
Ci	Curie
CoASH	coenzyme A
conc.	concentrated

CRBP	cellular retinol binding protein
CUP	C/EBPα undifferentiated protein
2-D	two-dimensional
DAP	11-*m*-diazirinophenoxy
DIDS	4,4'-diisothiocyanatostilbene-2,2'-disulfonic acid
DMEM	Dulbecco's Modified Eagles Medium
DMF	N,N-dimethylformamide
DMSO	dimethylsulfoxide
DNase	deoxyribonuclease
DTT	dithiothreitol
EDTA	ethylenediaminetetraacetic acid
EGTA	ethylenebis(oxyethylenenitrilo)tetraacetic acid
ER	endoplasmic reticulum
FAA	fatty acid activation
FAAR	fatty acid-activated receptor
FABP	fatty acid binding protein
fad, Fad	fatty acid degradation
FAT	fatty acid transporter
FATP	fatty acid transport protein
g	gram
g	gas
×*g*	acceleration of gravity
GluT	glucose transporter
H-bond	hydrogen-bond
HEPES	N-2-hydroxyethylpoperazine-N'-2-ethanesulfonic acid
HMPT	hexamethylphosphoric triamide
HNF	hepatocyte nuclear factor
HPLC	high performance liquid chromatography

h	hour
IbMX	3-isobutyl-1-methylxanthine
Ig	immunoglobulin
IGF	insulin-like growth factor
K_d	dissociation constant
kDa	kiloDalton
l	liter
l	liquid
LCFA	long chain fatty acid
LCFA-CoA	long chain fatty acyl-CoA
LDL	low density lipoprotein
LPS	lipopolysaccharide
μ-	micro-
M	molar
m	meter
m-	milli-
mAb	monoclonal antibody
MES	2-(N-morpholino)ethanesulfonic acid
mGOT	mitochondrial isoform of glutamate-oxaloacetate transaminase
min	minutes
MNNG	N-Methyl-N'-nitro-N-nitrosoguanidine
mol	moles
MOPS	3-(N-morpholino)propanesulfonic acid
mP2	myelin P2 protein
N	normality
n-	nano-
NE-IEF	Non-equilibrium Isoelectric Focusing
NP-40	ethylphenyl-polyethylene glycol

p-	pico-
PAGE	Polyacrylamide Gel Electrophoresis
PBS	Phosphate Buffered Saline
pI	isoelectric point
pK_a	negative $\log_{10}$ of the acid dissociation constant
PM	plasma membrane
PMSF	phenylmethane sulfonyl fluoride
PPAR	peroxisome proliforator-activated receptor
PPO	2,5-diphenoxazole
PRE	preadipocyte response element
PSM	post stimulation medium
PVDF	polyvinyldifluoride
RA	retinoic acid
R_f	mobility relative to the front
RNase	ribonuclease
RXR	retinoid X receptor
SA	serum albumin
SDS	sodium dodecylsulfate
sec	seconds
S.E.M.	standard error of the mean
TBS	tris-buffered saline
TLC	Thin Layer Chromatography
tris	tris-(hydroxymethyl)aminomethane
v	rate
V_{max}	maximal rate

A. INTRODUCTION

A.1. Importance of Long Chain Fatty Acids and Long Chain Fatty Acid Uptake

Long chain fatty acids (LCFA; containing 12-20 carbons; Table 1) are perhaps the most important energy source in mammals (Noy et al., 1986). They are the major fuel source for the heart (Sorrentino et al., 1988; Stremmel, 1988) and serve as an important fuel source for the brain during starvation (Stryer, 1988). The liver and adipose tissue are the major regulators of LCFA metabolism and energy balance in mammals. The liver is involved in LCFA synthesis and export (Gibbons, 1990), as well as degradation to generate fuel sources such as ketone bodies. Adipose tissue is involved in LCFA storage as triglycerides and mobilization (Greenberg et al., 1991). Consequently, these organs have been the focus of much of the work on LCFA uptake and metabolism. LCFAs are also substrates for phospholipid synthesis in virtually all cell types (Stryer 1988) and polyunsaturated fatty acids, such as arachidonic acid (Table 1) are precursors in the synthesis of a variety of signalling molecules including thromboxanes, leukotrienes, and prostaglandins (Campbell et al., 1994).

Recently, LCFAs have also been found to participate in a variety of crucial signalling cascades. For example, they induce the expression of genes involved in β-oxidation in *E. coli* (Black and DiRusso, 1994) and in yeast peroxisomes (Einerhand et al., 1993). LCFAs also induce the expression of a variety of genes in mammalian

preadipocytes, including those encoding transcription factors and enzymes involved in triglyceride synthesis and storage, leading to their differentiation to adipocytes (Amri et al., 1991a and b, 1994; Distel et al., 1992; Grimaldi et al., 1992; Safonova et al., 1994).

LCFAs also exert effects on a variety of processes other than gene expression. For example, LCFAs stimulate translocation of muscle/adipose type glucose transporters (GluT 4) to the plasma membrane in adipocytes, leading to increased glucose uptake (Hardy et al., 1991). They stimulate insulin release in pancreatic β-cells (Opara et al, 1994; Warnotte et al., 1994). LCFAs also regulate a number of ion channels in mammalian cells (Ordway et al., 1989, 1991).

In addition to their importance to normal cellular physiology, LCFAs are also important in a variety of pathogenic conditions in mammals. These include diabetes and obesity, which involve impaired storage and mobilization of LCFAs (Flier, 1995). Obesity involves an increase in adipose tissue mass resulting both from an increase in adipose cell size and numbers; the former may result from increased LCFA accumulation and storage as triglyceride, while the latter may be related to defects in the control of preadipocyte differentiation (Flier, 1995) which (as mentioned above and discussed in Section A.9) is stimulated by LCFAs.

Other conditions, such as atherosclerosis and neutral lipid storage disease, also involve the conversion of cells to an adipocyte-like morphology, in which they become packed with cytoplasmic lipid droplets. This affects macrophages and smooth muscle cells of artery walls in atherosclerosis (Brown and Goldstein, 1983; Minor et al., 1989)

and most cells of the body in neutral lipid storage disease (Chanarin et al., 1975). Whether this involves similar signals to those controlling adipose conversion (Section A.9) is unclear at present, however. Finally, the failure of placental transport of LCFA contributes to intrauterine growth retardation (Campbell et al., 1994). Because initial events in the response of cells to LCFA's (either utilization in metabolic reactions or responses to signalling events) involve their cellular uptake and intracellular trafficking, an understanding of the mechanisms of these processes will have broad implications for an understanding of the control of LCFA metabolism and signalling in both normal and diseased states.

Table 1. **Some common, natural LCFAs** (adapted from Stryer, 1988 p. 470).

Trivial Name	Systematic Name	Formula
Lauric Acid	*n*-Dodecanoic acid	$CH_3(CH_2)_{10}COOH$
Myristic Acid	*n*-Tetradecanoic acid	$CH_3(CH_2)_{12}COOH$
Palmitic Acid	*n*-Hexadecanoic acid	$CH_3(CH_2)_{14}COOH$
Stearic Acid	*n*-Octadecanoic acid	$CH_3(CH_2)_{16}COOH$
Oleic Acid	*cis*-Δ^9-Octadecenoic acid	$CH_3(CH_2)_7CH{=}CH(CH_2)_7COOH$
Arachidonic Acid	all *cis*-Δ^5,Δ^8,Δ^{11},Δ^{14}-Eicosatetraenoic acid	$CH_3(CH_2)_4(CH{=}CHCH_2)_4(CH_2)_2COOH$

A.2. Biological Membranes and Transport

The cellular uptake of small molecules such as LCFAs involves their movement across biological membranes. Membranes from different sources vary greatly in their protein and lipid composition, however the main structural unit of all biological membranes is the lipid bilayer (Figure 1). This consists of membrane lipids arranged in two leaflets, such that their hydrophilic portions are exposed to the aqueous environment while their hydrophobic portions are juxtaposed and shielded from the aqueous environment. Proteins can be associated with the membrane through interactions with either the polar or hydrophobic regions of the bilayer; proteins associated with the hydrophobic region might span the membrane or be attached via covalently linked lipid groups (Fig 1; Clarke, 1992; Ferguson and Williams, 1988; Houslay and Stanley, 1982; Johnson et al., 1994a; Resh, 1994; Stryer, 1988).

The constituents of biological membranes are relatively free to diffuse laterally, in the plane of the membrane; however the polar regions of most membrane constituents will not dissolve in the hydrophobic region of the membrane, impeding their transbilayer movement ("flip-flop"; Houslay and Stanley, 1982). This impermeability to polar compounds is the basis of the ability of biological membranes to act as barriers, maintaining the integrity of cells and subcellular compartments.

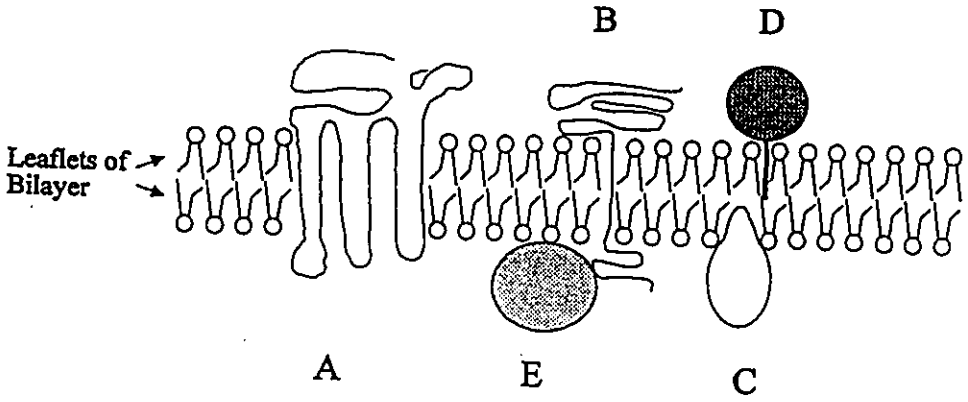

Figure 1. **Schematic representation of a cross-section of a biological membrane** (Houslay and Stanley, 1982 p.23). The two leaflets of the lipid bilayer with a number of proteins associated in a variety of ways are shown. **A.** is an integral membrane protein spanning the lipid bilayer six times. **B.** is an integral membrane protein with only one membrane spanning segment. **C.** is a protein with a hydrophobic domain inserted into but not spanning the hydrophobic interrior of the bilayer. **D.** is a protein anchored to the membrane by a covalently attached lipid. **E.** is a peripheral membrane protein associated with hydrophillic lipid headgroups and the hydrophillic portion of an integral membrane protein.

Cells and subcellular compartments, however, must exchange solutes with their environments in order to acquire nutrients, eliminate waste products and communicate with other cells or subcellular compartments. Transport of solutes across membranes can be accomplished in a variety of ways. Most simply, if the biological molecule is sufficiently hydrophobic, it can partition into the lipid portion of one leaflet of the membrane and by dissolving into the apolar phase, diffuse across the lipid bilayer (Stein, 1989). The transport of polar solutes across membranes is mediated by specific integral membrane proteins (Sachs and Fleischer, 1989). The membrane spanning segments of one or more integral proteins can be arranged to form aqueous solute-selective channels or pores, which can be gated (Nikaido, 1994; Sachs and Fleischer, 1989).

In contrast to channels and pores, carriers facilitate the transport of solutes by a mechanism which involves the binding of the solute to be transported, eliciting a conformational change in the carrier which exposes the bound solute to the other side of the membrane where it can dissociate (Andersen, 1989; Stein, 1989). Mammalian facilitative glucose transporters (GluT's), of which there are five related proteins expressed in a variety of mammalian cells, facilitate the diffusion of glucose or fructose across cell membranes in this way (Bell et al., 1993).

In both passive and facilitated diffusion, solutes move across biological membranes down their electrochemical gradients. Certain carriers can participate in the active transport of solutes across biological membranes against their electrical or chemical gradients; this process requires the input of energy (Jencks, 1989). ATP-driven ion

pumps, such as the Ca^{2+}-ATPase of muscle cells, couple the hydrolysis of ATP to the transport of ions against their electrochemical gradient (Jencks, 1989). The Ca^{2+}-ATPase transports two Ca^{2+} ions across the sarcoplasmic reticulum membrane (from the cytoplasm to the lumen) for each ATP molecule hydrolysed to ADP and inorganic phosphate (Jencks, 1989). This is an example of primary active transport, in which the hydrolysis of ATP drives the generation of ion gradients. These ion gradients, in turn, can drive the transport of other solutes against their electrochemical gradients (Jencks, 1989). For example, glucose is concentrated in mammalian intestinal cells; its transport into the cell, against its concentration gradient is coupled to the flow of Na^+ down its electrochemical gradient by a Na^+-glucose co-transporter (Bell et al., 1993).

A.3. LCFA Uptake in *E. coli*.

LCFA uptake has been studied extensively in *E. coli*. This organism possesses the only membrane protein (the FadL protein) known unequivocally to be required for LCFA movement across a cell membrane (Black et al., 1987; Nunn et al., 1979). Gram negative bacteria, such as *E. coli*, differ from mammalian cells in that they possess an outer membrane surrounding their inner, or plasma membrane. The outer and inner membranes are separated by an aqueous compartment called the periplasm. Therefore, LCFA internalization in *E. coli* involves numerous steps including the movement of LCFA across the outer membrane, through the periplasm, across the inner membrane and conversion to long chain fatty acyl-coenzyme A (LCFA-CoA) within the cell (figure 2).

A.3.1. Movement of LCFAs Across the Outer Membrane of *E. coli*.

The outer membrane of *E. coli* has a unique lipid composition; its outer leaflet contains a large proportion of lipopolysaccharide (LPS), which, due to its highly negatively charged nature, is an effective barrier to hydrophobic, anionic compounds, including LCFAs (Hancock, 1991; Nikaido, 1976; Nikaido and Vaara, 1985). The FadL protein allows the growth *of E. coli* on LCFA by allowing LCFA to cross the outer membrane (figure 2, step 1; Black and DiRusso, 1994; Black et al., 1987). The mechanism by which this occurs is not clear.

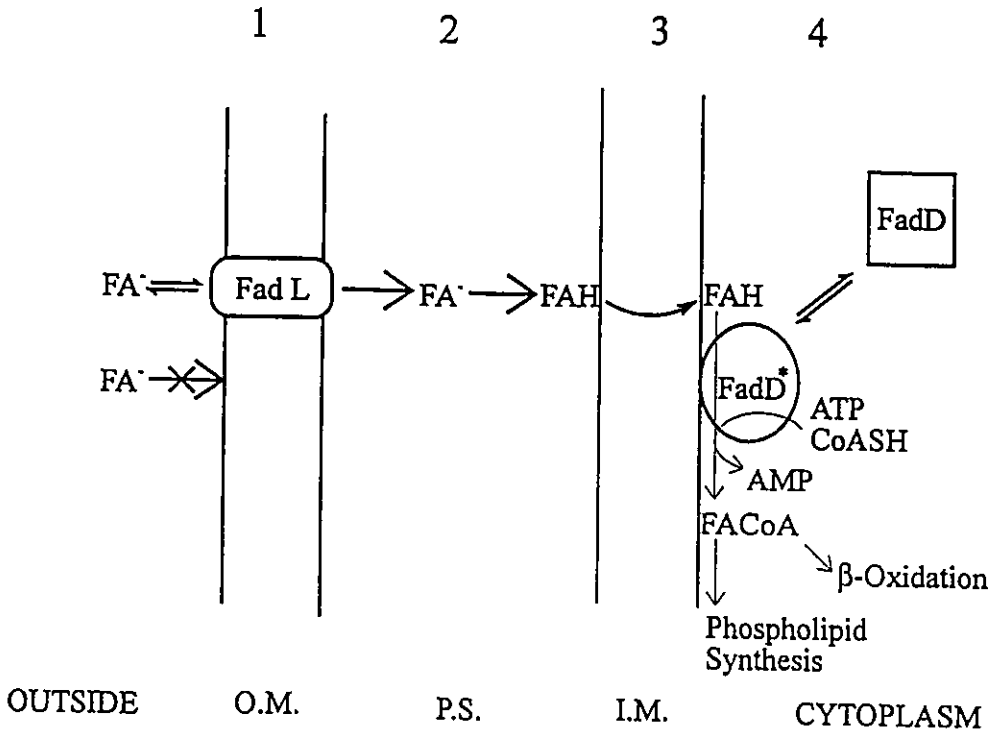

Figure 2. **Model of LCFA uptake by *E. coli*.** The process of LCFA uptake in *E. coli* involves four distinct steps. FadL binds to and transfers LCFA across the outer membrane (**O.M.**) barrier. LCFAs cross the periplasmic space (**P.S.**), most likely by diffusion, and partition into the inner membrane (**I.M.**). The protonated species (FAH) diffuses across to the cytoplasmic face of the bilayer. FadD, upon exposure to an unidentified agent, is recruited to the membrane and becomes activated (FadD*). FadD* may facilitate the removal of LCFAs from the membrane and converts them to their CoA-thioester derivative which can then be utilized for phospholipid synthesis and energy production by β-oxidation.

Studies making use of a photoreactive LCFA analogue, 11-*m*-diazirinophenoxy[11-^{3}H]undecanoate (11-DAP-[11-^{3}H]undecanoate) have shown that FadL binds LCFAs specifically and with high affinity (K_d of 63 nM; Mangroo and Gerber, 1992). Mutational analysis has demonstrated that amino acid substitutions in the carboxyl terminal region of the protein led to different effects on LCFA uptake and binding, suggesting that the two functions of the protein were separable (Kumar and Black, 1991, 1993). This suggested that the FadL protein might act as a channel, the LCFA binding activity possibly being related to a gating mechanism, as found for other ligand-binding outer membrane proteins (Nikaido, 1994).

A.3.2. Movement of LCFAs Across the Periplasm and Inner Membrane of *E. coli*.

LCFA's are thought to diffuse from the outer to the inner membrane through the periplasm (figure 2, step 2), without the aid of fatty acid binding proteins (FABP's) (Azizan and Black, 1994; Mangroo, 1992). Genetic (Azizan and Black, 1994; Black and DiRusso, 1994) and biochemical evidence (Mangroo and Gerber, 1992) suggests the absence of high affinity FABP's from the inner membrane. Consequently, LCFA's are believed to cross the inner membrane by diffusive flip-flop as the relatively non-polar protonated species (figure 2, step 3; Mangroo and Gerber, 1992).

A.3.3. The Involvement of Long Chain Acyl-Coenzyme A Synthetase.

The *fadD* gene, which encodes the bacterial long chain acyl-coenzyme A synthetase (ACS; also called LCFA:CoA ligase) is also required for growth on LCFAs and for LCFA uptake (Black and DiRusso, 1994; Klein et al., 1971). In fact, the

conversion of LCFA to LCFA-CoA (figure 2, step 4) has been shown to be the rate limiting step in LCFA uptake by *E. coli* (Mangroo, 1992).

The FadD protein appears to be cytoplasmic (Kameda and Nunn, 1981; Mangroo and Gerber, 1993). However, conditions which lead to a stimulation of LCFA uptake in *E. coli* have also been shown to result in an increase in the long chain ACS activity associated with the inner membrane and a corresponding decrease in the long chain ACS activity in the cytoplasm, suggesting that the FadD protein translocates from the cytoplasm to the cytoplasmic face of the inner membrane (figure 2; Mangroo and Gerber, 1993). Thus in addition to driving LCFA uptake in *E. coli*, the conversion of LCFA to LCFA-CoA appears to be a key regulatory point in the uptake process (Mangroo and Gerber, 1993).

A.4 Steps Involved in LCFA Uptake in Mammalian Cells

LCFA uptake in mammalian cells differs in certain respects from that in *E. coli*. The majority of unesterified LCFA to which mammalian cells are exposed is complexed to carrier proteins, the major one being serum albumin (SA; Lichenstein et al., 1994). In addition, mammalian cells do not have a membrane analogous to the outer membrane of *E. coli*, which is impermeable to LCFAs; there is, therefore, no *a priori* requirement for a transport protein to facilitate the movement of LCFAs across the cell membrane. This has been the subject of much controversy, as will be discussed in subsequent sections (A.3.2 and C.6).

"Uptake" as routinely used in the case of LCFAs, is an operational term based on the methodology used to measure their internalization. This involves the measurement of the total accumulation of either radioactively labeled or fluorescent analogues of LCFAs (Abumrad et al., 1981; Luxon and Weisiger, 1993; Storch et al., 1991; Stremmel and Berk, 1986) but does not distinguish between different forms of LCFAs, such as those tightly associated with the exterior of the cell, internalized but not metabolized, or metabolized (Knoll and Gordon, 1993).

Therefore, as for *E. coli*, LCFA uptake by mammalian cells involves a number of potential steps. These include the delivery of LCFAs to the cell surface, their movement across the plasma membrane, delivery to sites of metabolism and conversion to LCFA-

CoA (Noy and Zakim, 1993). The mechanism of LCFA movement across the plasma membrane is highly controversial, although it is known that some degree of permeation of the plasma membrane by protonated LCFA occurs by passive diffusion (Hamilton et al., 1994). As a result, the final step of LCFA uptake, the conversion of LCFA to LCFA-CoA (whose structure is shown in figure 3), is potentially significant because it results in the intracellular trapping of LCFA as a highly charged species that does not permeate the plasma membrane (Noy and Zakim, 1993). To fully understand the mechanism by which cells take up LCFAs, the contribution of each of these steps to the overall process must be studied.

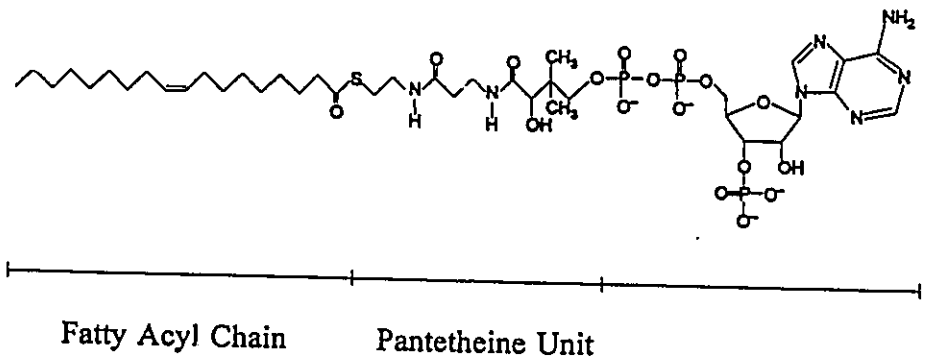

Figure 3. **Structure of oleoyl-CoA** (adapted from Stryer, 1983 p. 322). The long chain fatty acid, pantethein and ADP units are identified by the horizontal bars beneath the figure.

A.5. Uptake of Molecules Bound to SA

A.5.1. Delivery of LCFAs to Cells

Serum albumin-complexed LCFA and triglycerides (in the form of very low density lipoprotein particles) are the major forms of non-esterified and esterified LCFAs, respectively, circulating in the plasma of mammals (Peterson et al., 1990; Spector, 1975; Spector et al., 1969). SA and LCFA-SA complexes are transferred from the lumen of capillaries by transcytosis, or receptor-mediated vesicular transport across vascular endothelial cells, and into the space surrounding underlying cells such as adipocytes and cardiomyocytes (figure 4; Schnitzer and Oh, 1994; Schnitzer et al., 1994). Triglycerides are hydrolyzed to LCFAs by lipoprotein lipase at the luminal surfaces of endothelial cells lining capillaries (figure 4; Scow and Blanchette-Mackie, 1992). This enzyme, synthesized by underlying adipocytes and cardiomyocytes, is transported by transcytosis across vascular endothelium (in the opposite direction of transcytosis of SA), and becomes bound to the luminal surface of the cells (Schnitzer and Oh, 1994). LCFAs released by triglyceride hydrolysis either become bound to SA at the luminal surface of vascular endothelium and are delivered to underlying cells by transcytosis, or partition in endothelial cell membranes and migrate across endothelial cells by lateral diffusion through membranes surrounding transendothelial channels (figure 4; Scow and Blanchette-Mackie, 1992).

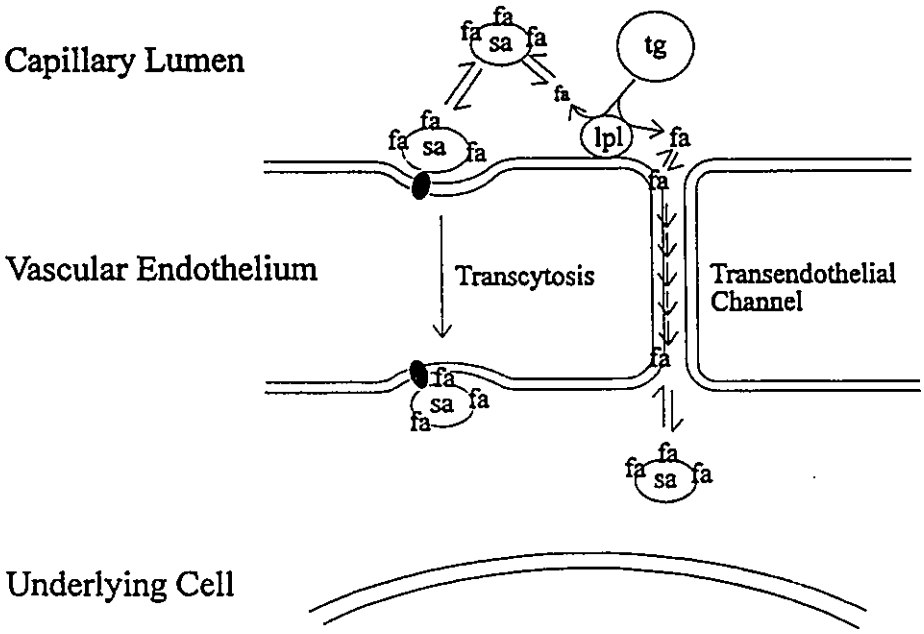

Figure 4. **Routes by which unesterified LCFAs are delivered across vascular endothelium to underlying cells for utilization** (Schnitzer and Oh, 1994; Schnitzer et al., 1994; Scow and Blanchette-Mackie, 1992). Triglycerides (**tg**; in the form of very low density lipoproteins) are hydrolyzed by lipoprotein lipase (**lpl**) at the surface of vascular endothelial cells. The resulting unesterified long chain fatty acids (**fa**) can be transported across the vascular endothelium either through putative transendothelial channels or as complexes with serum albumin (**sa**), by transcytosis mediated by caveolae.

As a result of these processes the concentration of uncomplexed LCFA in equilibrium with LCFA-SA complexes in extracellular fluids is extremely small, under normal physiological conditions (Spector., 1975; Spector et al., 1969). Thus, SA is expected to have a profound effect on the cellular uptake of LCFA.

A.5.2. Albumin Receptor Effect

The effects of SA on the uptake of LCFAs and other hydrophobic, anionic ligands have largely been studied in the perfused liver (reviewed in Noy and Zakim, 1993; Sorrentino and Berk, 1993; and Weisiger, 1993) where it was noted early on (Weisiger et al., 1981) that while SA was not internalized during LCFA uptake, LCFA uptake varied saturably with the SA concentration when the LCFA:SA ratio was held constant (conditions in which the concentration of uncomplexed LCFA remained constant). This was called the albumin receptor effect since it led to the proposal for an albumin receptor on the cell surface (Weisiger et al., 1981). It has subsequently been shown to occur in a variety of cells including hepatocytes, adipocytes and heart myocytes (Sorrentino and Berk, 1993; Sorrentino et al., 1989), for other SA ligands, such as bilirubin and sulfobromophthalein (Weisiger, 1993; Wolkoff, 1987), and for related carrier proteins, such as α-fetoprotein (Torres et al., 1992a and b; Uriel et al., 1994). Three main hypotheses have been proposed to explain this effect. These are the dissociation-limited uptake, codiffusion, and facilitation models.

A.5.3. Dissociation-Limited Uptake

Berk and co-workers have proposed that the albumin receptor effect was due to a shift in the rate limiting step in LCFA uptake from LCFA dissociation from SA at low SA concentrations to LCFA movement across the plasma membrane at higher SA concentrations (Sorrentino and Berk, 1993; Sorrentino et al., 1989). They argued that the involvement of SA in LCFA uptake was restricted to the solubilization of LCFA in the aqueous environment to provide a pool of bound LCFA to replenish uncomplexed LCFA depleted by cellular uptake. It has been shown, however, that the dissociation of LCFAs from BSA is very fast, arguing against dissociation-limited uptake (Daniels et al., 1985; Noy and Zakim, 1993).

A.5.4. Codiffusion Versus Facilitation

The codiffusion model proposes that the enhancement of the rate of LCFA uptake by SA is the result of an increased diffusional flux of LCFAs through the thin layer of unstirred fluid surrounding each cell (Weisiger, 1993; Weisiger et al., 1989). The contribution of this effect to total uptake has been found to be minor, however (Burczynski et al., 1989, 1993). Instead, the major contributor to the albumin receptor effect has been proposed to be facilitation of LCFA uptake at the cell surface (Burczynski et al., 1989, 1993). The mechanism by which facilitation might occur is not known, although it may involve the interaction of SA with the cell surface via specific receptors (Ghinea et al., 1989; Schnitzer, 1992; Torres et al., 1992b; Weisiger, 1993).

A.6. Involvement of Plasma Membrane Proteins in LCFA Uptake by Mammalian Cells.

A.6.1. Evidence in Favour of Involvement

The mechanism by which LCFAs traverse the plasma membrane is controversial. One possibility is that it is mediated by one or more proteins. Consistent with this, a large body of evidence has implicated the involvement of plasma membrane proteins in LCFA uptake. This includes the finding that LCFA uptake is saturable and demonstrates a high affinity for uncomplexed LCFA in the presence of BSA. This is the case for a variety of cells including mammalian hepatocytes (Stremmel and Theilmann, 1986), adipocytes (Abumrad et al., 1981; Schwieterman et al., 1988; Zhou et al., 1992), cardiomyocytes (Sorrentino et al., 1988; Stremmel, 1988), alveolar pneumocytes (Maniscalco et al., 1990), and keratinocytes (Schürer et al., 1994), and in *Xenopus laevis* oocytes (Zhou et al., 1994). This has been interpreted as evidence that the cellular uptake of LCFAs was mediated by a transporter with high affinity for LCFAs (Abumrad et al., 1981, 1984; Stremmel and Berk, 1986; Stremmel and Theilmann, 1986), although others have argued that this saturation may reflect intracellular events, such as LCFA binding or conversion to LCFA-CoA (Degrella and Light, 1980; Noy and Zakim, 1993).

LCFA uptake by hepatocytes and adipocytes is, however, sensitive to protease treatment, suggesting the importance of proteins in the process (Abumrad et al., 1984;

Mahadevan and Sauer, 1974). To date, studies have implicated the involvement of three plasma membrane proteins in LCFA uptake in mammalian cells. These include a 43 kDa protein first isolated from hepatocyte plasma membranes (called $FABP_{PM}$ for Plasma Membrane FABP; Stremmel et al., 1985 a; Stremmel and Theilmann, 1986), an 88 kDa adipocyte plasma membranes protein (called FAT for Fatty Acid Transporter; Abumrad et al., 1984, 1993) and a 63 kDa 3T3-L1 adipocyte protein identified by expression cloning (called FATP for Fatty Acid Transport Protein; Schaffer and Lodish, 1994).

A.6.2. $FABP_{PM}$

Berk and coworkers have isolated a 43 kDa protein ($FABP_{PM}$) by passage of either triton X-100 or NaCl extracts of hepatocyte plasma membranes over a column consisting of oleate coupled to agarose via its carboxylate group (Potter et al., 1987; Stremmel et al., 1985a). This protein has been shown to bind oleate by co-chromatography with radioactively labeled oleate (Stremmel et al., 1985a and b), with a reported K_d of 83 nM, suggesting that it has a high affinity for LCFAs (Berk et al., 1990). The $FABP_{PM}$ is expressed in a variety of tissues besides liver, including adipose, heart, gut, lung and placenta (Campbell et al., 1994; Maniscalco et al., 1990; Potter et al, 1987; Stremmel et al., 1985a and b). Furthermore, antibodies raised against the purified liver protein partially inhibit oleate uptake in rat hepatocytes, rat and 3T3-L1 adipocytes, rat heart myocytes, and *X. laevis* oocytes, suggesting that the $FABP_{PM}$ is involved in LCFA uptake in these cell types (Schwieterman et al., 1988; Sorrentino et al., 1988; Stremmel, 1988; Stremmel and Theilmann, 1986; Zhou et al., 1992, 1994).

The amino acid sequence of the amino-terminus of the protein was identical to that of the mitochondrial isoform of glutamate-oxaloacetate transaminase (mGOT, also called aspartate aminotransferase, or AAT; Berk et al., 1990). Purified $FABP_{PM}$ and mGOT behaved identically upon SDS-PAGE, isoelectric focussing, separation by HPLC on four different columns, and binding to radioactively labeled oleate as measured by co-chromatography (Berk et al., 1990; Potter and Berk, 1993; Stump et al., 1993). Plasma membranes containing $FABP_{PM}$ contained GOT enzymatic activity, and antibodies to mGOT partially inhibited LCFA uptake in rat hepatocytes (Berk et al., 1990). Purified $FABP_{PM}$ and mGOT cross-reacted with a number of polyclonal and monoclonal antibodies, although certain monoclonal antibodies react strongly with the $FABP_{PM}$ but only weakly or not at all with mGOT (Berk et al., 1990; Diede et al., 1992; Potter and Berk, 1993).

Together, these results indicated that $FABP_{PM}$ and mGOT were very similar, though not identical (Berk et al., 1990; Diede et al., 1992; Potter and Berk, 1993; Stump et al., 1993). It has been suggested that $FABP_{PM}$ may represent a third form of GOT which is targeted to the plasma membrane, in addition to the two known forms targeted to the mitochondria and cytoplasm (Potter and Berk, 1993). The nature of its involvement in LCFA uptake is presently unclear, although, contrary to what has been proposed (Potter and Berk, 1993), it is unlikely to act as a LCFA transporter due to its peripheral association with the membrane (Potter et al., 1987, Stump et al., 1993).

A.6.3. FAT

Abumrad and co-workers have found that LCFA uptake by rat adipocytes could be irreversibly inhibited by treatment of the cells with 4,4'-diisothiocyanatostilbene-2,2'-disulfonic acid (DIDS) or sulfo-*N*-succinimidyl esters of LCFAs (Abumrad et al., 1984; Harmon et al., 1991). These compounds also labeled an 85-88 kDa plasma membrane protein in these cells (Abumrad et al., 1984; Harmon and Abumrad, 1991). This protein (Harmon et al., 1993) and the corresponding cDNA (Abumrad et al., 1993) have been isolated. The deduced amino acid sequence of this so called FAT protein was 79 % identical to that of human CD36 (Abumrad et al., 1993, Harmon et al., 1993), an integral membrane protein, containing two transmembrane helices (Greenwalt et al., 1992). It was suggested that the FAT cDNA represented the rat version of CD36 (Abumrad et al., 1993). This protein is expressed in platelets, lactating mammary epithelium, different types of endothelium, and heart and skeletal muscle in addition to adipocytes (Abumrad et al., 1993; Bull, et al., 1994; Greenwalt et al., 1992; Lisanti et al., 1994b).

CD36 binds collagen (Greenwalt et al., 1992), thrombospondin (Greenwalt et al., 1992; Li et al., 1993), oxidized- (Endemann et al., 1993) and acetylated-, but not native low density lipoprotein (LDL; Acton et al., 1994) and maleylated BSA (Acton et al., 1994). By virtue of its broad binding specificity, CD36 is believed to act as a scavenger receptor (Acton et al., 1994). It is not clear, however, whether its scavenger receptor activity is related to its role in LCFA uptake; the effects of DIDS or sulfo-*N*-succinimidyl LCFAs on the binding of CD36 to any of its ligands has not been investigated.

CD36/FAT (the adipocyte CD36) may have a regulatory rather than a direct role in LCFA uptake (Abumrad et al., 1993). In platelets and endothelial cells, CD36 is closely associated with Fyn, Lyn, and Yes, tyrosine kinases related to the cellular proto-oncogene, Src (Huang et al., 1991; Bull et al., 1994). Thus, it is optimally placed to participate in signalling via these associated tyrosine kinases.

A.6.4. FATP

Recently, Schaffer and Lodish (1994) have used expression cloning to isolate a 3T3-L1 adipocyte cDNA (FATP) which conferred increased uptake of a fluorescent LCFA by COS cells. This cDNA coded for a 646 amino acid protein with a predicted molecular weight of 71 kDa, although the protein migrated with an apparent molecular weight of 63 kDa upon SDS-PAGE (Schaffer and Lodish, 1994). Sequence analysis also predicted that the protein possessed 6 transmembrane helices and a stretch of 11 amino acids common to a number of enzymes which bind pantetheine groups or derivatives (Schaffer and Lodish, 1994). These enzymes included rat liver long chain ACS and coumarate-CoA ligase 1 (Schaffer and Lodish, 1994). Whether the FATP possessed a similar enzymatic activity, or indeed contained a bound pantetheine group or derivative was not investigated (Schaffer and Lodish, 1994). The role of this protein in LCFA uptake is presently unclear. Although it has been assumed to be a LCFA transporter, its ability to bind LCFAs was not investigated. Furthermore, its expression in cell lines stably transfected with its cDNA resulted in only modest increases (two- to three-fold) in LCFA uptake (Schaffer and Lodish, 1994).

A.6.5. Physico-Chemical Hypothesis for the Transbilayer Movement of LCFAs.

Although the studies described above have demonstrated the involvement of plasma membrane proteins in LCFA uptake, they have not demonstrated that they specifically mediate the translocation of LCFAs across the plasma membrane. As indicated previously (Section A.4), LCFAs are relatively hydrophobic. This has led some to propose that there should be no need for a protein to facilitate their transbilayer movement (DeGrella and Light, 1980; Noy et al., 1986; Noy and Zakim, 1993).

Evidence from studies with model membrane systems indicates that LCFAs can permeate across lipid bilayers passively. For example, LCFAs distribute across lipid bilayers in response to imposed pH gradients due to lipid bilayer permeability to the protonated but not the ionized species (Hope and Cullis, 1987). However, for the permeation of protonated LCFAs to support LCFA uptake by mammalian cells, the proportion of protonated versus ionized species must be significant (i.e., the pK_a of LCFAs must be sufficiently high) and the rate of permeation of the protonated species must be high.

LCFAs are sparingly soluble in water but partition readily into the lipid bilayer (Cistola et al., 1988a; Noy et al., 1986; Noy and Zakim, 1993). Furthermore, their pK_a's have been reported to shift from 3-4 in aqueous solution to 7-8 upon partitioning into membranes; thus, greater than 50 % of LCFAs partitioned into lipid bilayers should be protonated at physiological pH (Hamilton and Cistola, 1986). Therefore, under normal

physiological conditions, the proportion of LCFAs partitioned into cell membranes and protonated, and therefore able to undergo flip-flop, should be large.

Rates of LCFA permeation in model lipid bilayers are fast (Doody et al., 1980; Kamp and Hamilton, 1992, 1993; Noy and Zakim, 1993). Recently, Hamilton and co-workers have developed methodology allowing the measurement of LCFA-dependent changes in pH across a membrane, as an indication of the transmembrane movement of protonated LCFA (Kamp and Hamilton, 1992, 1993; Hamilton et al., 1994). The methodology was characterized with lipid vesicles containing a trapped pH sensitive fluorescent probe (Kamp and Hamilton, 1992, 1993). It has also been applied to the measurement of LCFA movement across plasma membranes of mammalian cells by the use of a fluorescent, cytoplasmic pH indicator (Hamilton et al., 1994). Results obtained were consistent with LCFA permeation of the plasma membrane occurring by diffusion of the protonated species (Hamilton et al., 1994). However, the high concentrations (35 μM) of LCFAs used bring into question the physiological relevance of their results; under normal physiological conditions, concentrations of uncomplexed LCFAs are in the nanomolar range (Spector, 1975; Spector et al., 1969).

A.7. Cytoplasmic FABP's

A.7.1. Structure and LCFA Binding

Mammalian cells with large capacities for LCFA metabolism posses one or more cytoplasmic FABPs, members of a family of low molecular weight (approximately 15 kDa), cytoplasmic lipid binding proteins (Table 2; Bass, 1993; Kaikaus et al., 1990; Veerkamp et al., 1991). The structural, functional and physiological features of a number of these proteins have been the subject of several recent reviews (Bass, 1993; Kaikaus et al., 1990; Sacchettini and Gordon, 1993; Veerkamp et al., 1991, 1993). Amino acid sequence similarities between cytoplasmic FABPs identified to date range from as low as 22 %, between the adipocyte lipid binding protein (ALBP) and the liver-FABP, to 65 % between the ALBP and either the heart-FABP or the myelin P2 protein (mP2) (Veerkamp et al., 1991). The ALBP, mP2, and heart- and intestinal-FABPs primarily bind LCFAs, while others bind retinoids, bile salts or a combination of lipids (Table 2).

The high resolution, three dimensional structures of many of these proteins (including mouse ALBP, bovine mP2, human and bovine heart FABP, rat intestinal FABP, chicken liver basic FABP, MFB2 and rat liver CRBP I and II), both without and with bound ligands have been solved by X-ray crystallography. All have the same general structure. This consists of two α-helices and 10 antiparallel β-strands; the latter form two β-sheets whose arrangement resembles a clam shell (Benning et al., 1992;

Table 2. Members of the lipid binding protein family.[a]

Name	Occurrence	Ligand
Mammalian:		
Adipocyte lipid binding protein (ALBP, aP2)	Adipocytes	LCFA, RA
Brain-FABP[b]	Brain	Unknown
Cellular retinoic acid binding protein (CRABP)	Testis, seminal vesicles, eye, brain and skin	RA
Cellular Retinol-binding protein, type I (CRBP I)	Liver, kidney, testis, epididymis	all-*trans*-retinol
CRBP II	Intestinal villus epithelium	all-*trans*-retinol all-*trans*-retinal
Heart-FABP (Mammary derived growth inhibitor, MGDI)[c]	Heart and skeletal myocytes, kidney and mammary gland	LCFA
Ileal lipid binding protein	Ileal enterocytes	Bile salts
Intestinal-FABP	Intestine, stomach	LCFA
Liver-FABP	Liver, intestine, stomach, kidney	LCFA, bile salts, heme,chol-esterol, lysophospholipids
Myelin P2 protein (mP2)[d]	Schwann cells	LCFA, retinoic acid
Others:		
Liver-Basic FABP[e]	Chicken liver	Unknown
Locust M-FABP[f]	Locust (*Locusta migratoria*) flight muscle	LCFA
MFB 1[g]	Anterior mid-gut of tobacco hornworm, *Manduca sexta*, larva	LCFA
MFB 2[g]	Posterior mid-gut of *M. sexta* larva	LCFA
Sj-FABP[h]	From human blood fluke, *Schistosoma japonicum*	LCFA

a. Unless otherwise indicated, taken from Bass, 1993.
b. Bennett et al., 1994; Kurtz et al., 1994.
c. Bass, 1993; Yang et al., 1994.
d. Bass, 1993; Bennett et al., 1994; Kurtz et al., 1994.
e. Scapin et al., 1988.
f. Maatman et al., 1994.
g. Smith et al., 1992.
h. Becker et al., 1994.

Cowan et al., 1993; Jones et al., 1988; Lalonde et al., 1994a and b; Sacchettini et al., 1988, 1989a and b; Sacchettini and Gordon, 1993; Scapin et al., 1990, 1992; Winter et al., 1993; Xu et al., 1992, 1993; Young et al., 1994; Zanotti et al., 1992). The ligand binding site is in the interior of the clam shell; a channel leading from the exterior of the protein provides access to it (Lalond et al., 1994a and b; Sacchettini and Gordon, 1993; Xu et al., 1993; Young et al., 1994). Ligands are oriented within the binding site with their polar head group towards the interior and their apolar tails toward the exterior of the protein (Lalond et al., 1994a and b; Sacchettini and Gordon, 1993; Xu et al., 1993; Young et al., 1994).

Ligands with carboxylate groups (LCFAs and retinoic acid, RA) appear to bind as the ionized species, undergoing electrostatic and H-bonding interactions with internal arginines and tyrosines (Sacchettini and Gordon, 1993; Xu et al., 1993). Arg-126 and Tyr-128 of the ALBP appear to be involved in such interactions; upon their substitution with Gln and Trp, respectively, LCFA binding to the ALBP was abolished (Sha et al., 1993). Hydrophobic residues lining the interior of the channel interact with the hydrophobic portion of the ligand (Lalond et al., 1994; Sacchettini and Gordon, 1993; Xu et al., 1993).

A.7.2. Phosphorylation and LCFA Binding

Both the ALBP and the heart-FABP are phosphorylated at Tyr-19 upon insulin stimulation of adipocytes and heart myocytes, respectively (Bernier et al., 1987; Hresko et al., 1990; Nielsen and Spener, 1993). LCFA binding to and phosphorylation of Tyr-19

of the ALBP have reciprocal regulatory effects on each other *in vitro*; oleate binding to the unphosphorylated ALBP activates its phosphorylation, while the phosphorylation of apo-ALBP results in a dramatic reduction in its affinity for LCFAs (Buelt et al., 1991, 1992; Hresko et al., 1990).

In the absence of bound LCFA, Tyr-19 is believed to be relatively inaccessible to kinases (Buelt et al., 1992; Hresko et al., 1990). It has been proposed that upon LCFA binding, the portion of the protein comprising the two α-helices and intervening loop undergoes a conformational change (about a hinge region) making Tyr-19 accessible (Buelt et al., 1992; Hresko et al., 1990). Because this residue resides toward the exterior end of the channel leading to the LCFA binding site, its phosphorylation is believed to sterically restrict the entry and exit of LCFAs to and from the binding site (Buelt et al., 1992; Xu et al., 1993). This has led to the suggestion that the phosphorylation of the ALBP might be a means of locking LCFAs in a bound state. It has been proposed that this might represent a mechanism by which LCFA binding to and release from the protein is regulated *in vivo* (Buelt et al., 1992; Xu et al., 1993). This is therefore thought to be important for the proposed role of the protein in LCFA trafficking *in vivo* (Buelt et al., 1992; Xu et al., 1993).

A.7.3. Involvement of Cytoplasmic FABPs in LCFA Uptake.

Despite the large amount of work on the structures and *in vitro* binding properties of cytoplasmic FABP's, their intracellular functions remain unclear (Veerkamp et al., 1991, 1993). It has been proposed that they provide a large binding capacity for LCFAs

in or increase their diffusional flux through the cytoplasm, thereby driving cellular uptake of LCFAs (Luxon and Weisiger, 1993; Stewart, 1991; Veerkamp et al., 1991; Vork et al., 1991, 1993). The cloning of cDNAs corresponding to cytoplasmic FABPs, and their expression in cells normally lacking such proteins, have enabled these proposals to be tested. However, conflicting results have been obtained from such experiments. Schaffer and Lodish (1994) have reported that the expression of ALBP did not affect LCFA uptake by COS-7 cells. In contrast, Bernlohr and co-workers did find moderate increases (2- to 2.5-fold) in LCFA uptake upon expression of ALBP in Chinese hamster ovary cells (Sha et al., 1993). In agreement with the results of Schaffer and Lodish (1994), the expression of the rat liver-FABP in murine L-cells resulted in only minor increases in LCFA uptake (Schroeder et al., 1993).

Studies in model systems have, however, suggested a role for cytoplasmic FABPs in LCFA trafficking. It has been demonstrated that LCFAs could be transferred from lipid vesicles to the rat liver FABP (Brecher et al., 1984), and from various cytoplasmic FABP's to lipid vesicles (Kim and Storch, 1992a; Kim and Storch, 1992b; Storch and Bass, 1990; Wootan et al., 1993; Wootan and Storch, 1994). LCFA transfer to lipid vesicles from different cytoplasmic FABP's occurs by distinct mechanisms: LCFAs are transferred from the liver-FABP to membranes via aqueous diffusion (Kim and Storch, 1992a) while their transfer from the ALBP and heart-FABP to model membranes involves a direct interaction with the membrane and is regulated by the membrane lipid composition (Kim and Storch, 1992b; Wootan and Storch, 1994; Wootan et al., 1993).

These results suggest that different cytoplasmic FABPs may have distinct functions in different intracellular contexts (Storch, 1993).

A.8. LCFA Metabolism

A.8.1. LCFA Activation

The first step in LCFA metabolism (both β-oxidation and lipid synthesis) is the activation of LCFAs by their conversion to LCFA-CoA (Coleman, et al., 1978; Lazo et al., 1990). This reaction is rate limiting for LCFA metabolism (Noy and Zakim, 1993). It is catalyzed by ACS in the presence of fatty acids, ATP, CoASH and Mg^{2+} (Groot et al., 1976). The generally accepted mechanism involves the formation of an acyl adenylate intermediate as shown in equations 1 and 2 below (Groot et al., 1976), although others have proposed the formation of an AMP-enzyme intermediate (Parsons and Scribner, 1988).

$$H^+ + RCOO^- + ATP^{4-} + CoASH \overset{Mg^{2+}}{\rightleftarrows} E{\bullet}RCO\ AMP^- + PP_i^{3-} \qquad (1)$$

$$E{\bullet}RCO\ AMP^- + CoASH \rightleftarrows E + RCOSCoA + AMP^{2-} + H^+ \qquad (2)$$

A.8.2. Long Chain ACS

Distinct enzymes are responsible for the activation of short (2 to 4 carbons), medium (4 to 12 carbons) and long (12 to 22 carbons) chain fatty acids (Groot et al., 1976). There also appear to be distinct enzymes for the activation of arachidonic acid (Laposata, 1990; Neufeld et al., 1984) and very long chain (> 22 carbons) fatty acids

(Lazo et al., 1988, 1990). Long chain ACS activities have been found in bacteria (Kameda and Nunn, 1981), yeast (Knoll et al., 1994, Mishina et al., 1978a) and in mammals in a variety of different tissues including the liver (Bar-Tana et al., 1971; Pande and Mead, 1968), adipose tissue (Hall and Saggerson, 1985), brain (Fujino and Yamamoto, 1992) and heart and gut (De Jong and Hülsmann, 1970). Of these, the liver enzyme has been most fully characterized.

In mammalian cells, long chain ACS activities in different organelles (mitochondria, endoplasmic reticulum and peroxisomes) are believed to be mediated by identical enzymes (Suzuki et al., 1990). In contrast, yeasts are known to express distinct forms of long chain ACS involved in the activation of LCFAs destined for different metabolic fates; *Candida lipolytica* expresses two such enzymes (Mishina et al., 1978a and b), while *Saccharomyces cerevisiae* expresses as many as five, apparently encoded by distinct genes (Johnson et al., 1994b).

A.8.3. Structure and Function of Long Chain ACS

To date the sequences corresponding to the cDNA's of 9 long chain ACSs have been determined. These include those expressed by *E. coli* (Black et al., 1992) and *Pseudomonas oleovarans* (van Beilen et al., 1992), four of the five (fatty acid activation genes, *FAA 1-4*) from *S. cerevisiae* (Johnson et al., 1994b), long chain ACS from rat liver (Suzuki et al., 1990) and brain (Fujino and Yamamoto, 1992) and human liver (Abe et al., 1992). The predicted sequence identities between these enzymes range from 23% between *FAA 2* and *4* (Johnson et al., 1994b) to 64.7 % between rat liver and brain long

chain ACS (Fujino and Yamamoto, 1992) and 84.9 % between rat and human liver long chain ACS (Abe et al., 1992). They also share a region (amino acids 458-591 of rat liver long chain ACS) of significant sequence similarity (35.8 % identity) with firefly luciferase (Black et al., 1992; Fujino and Yamamoto, 1992; Suzuki et al., 1990). This enzyme catalyzes the conversion of luciferin to oxyluciferin with the formation of light; because this reaction proceeds with the formation of a luciferyl-adenylate intermediate analogous to the acyl-adenylate formed by ACS, it has been suggested that this region might be involved in the binding of ATP or carboxyl groups or in the formation of a carboxyl-adenylate (Black et al., 1992; Suzuki et al., 1990).

Long chain ACS from *E.coli* and rat liver and *FAA1* from *S. cerevisiae* share another region of high sequence identity (32-35 % for all three sequences) corresponding to amino acids 262-334 of the rat liver enzyme (Black et al., 1992). The lack of similarity with firefly luciferase in this region has led to the proposal that it might be involved in a long chain ACS specific function, such as either LCFA or CoASH binding (Black et al., 1992).

A.8.4. Membrane Association and Subcellular Localization of Long Chain ACS

Despite the high degree of sequence similarities displayed among the long chain ACS cDNAs sequenced to date, they display quite different characteristics with regards to their interaction with membranes. The rat liver ACS appears to traverse the membrane as indicated by its accessibility to proteolytic digestion from either side of the membrane (Hesler et al., 1990). In contrast, FadD, the *E. coli* long chain ACS, is cytoplasmic

(Kameda and Nunn, 1981), but translocates to the inner membrane under conditions in which LCFA uptake is stimulated (Mangroo and Gerber, 1993). However, the nature of its association with the membrane is not known. The *S. cerevisiae* ACSs, Faa1p, Faa2p and Faa3p, also appear to be soluble when expressed in *E. coli* (Knoll et al., 1994), however, it is not known whether they also undergo reversible association with membranes.

The subcellular localization of mammalian long chain ACS is also unusual. As mentioned above, mammalian long chain ACS associated with mitochondria, endoplasmic reticulum (ER) and peroxisomes are believed to be identical (Suzuki et al., 1990). Similarly, in *C. lipolytica*, long chain ACS-1 is found in mitochondria and ER, whereas long chain ACS-2 is peroxisomal (Mishina et al., 1978a). The subcellular distribution of the five *S. cerevisiae* long chain ACSs has not been reported. Interestingly, none of the eukaryotic long chain ACSs sequenced to date contain known targeting signals for specific organelles (Johnson et al., 1994b). Thus, the mechanism by which they are targeted to different organelles in mammalian cells and *C. lipolytica* is currently unknown.

A.8.5. Triglyceride Synthesis and Storage in Adipocytes

Adipocytes are specialized for the storage of LCFAs as triacylglycerol (Flier, 1994; Greenberg et al., 1991). The reactions involved in the triacylglycerol biosynthesis from LCFAs are shown in figure 5. The first of these is, as indicated above, the activation of LCFAs to LCFA-CoA by long chain ACS (Lazo et al., 1990). Glycerol-phosphate acyl transferase utilizes LCFA-CoA for the acylation of glycerol-3-phosphate, forming

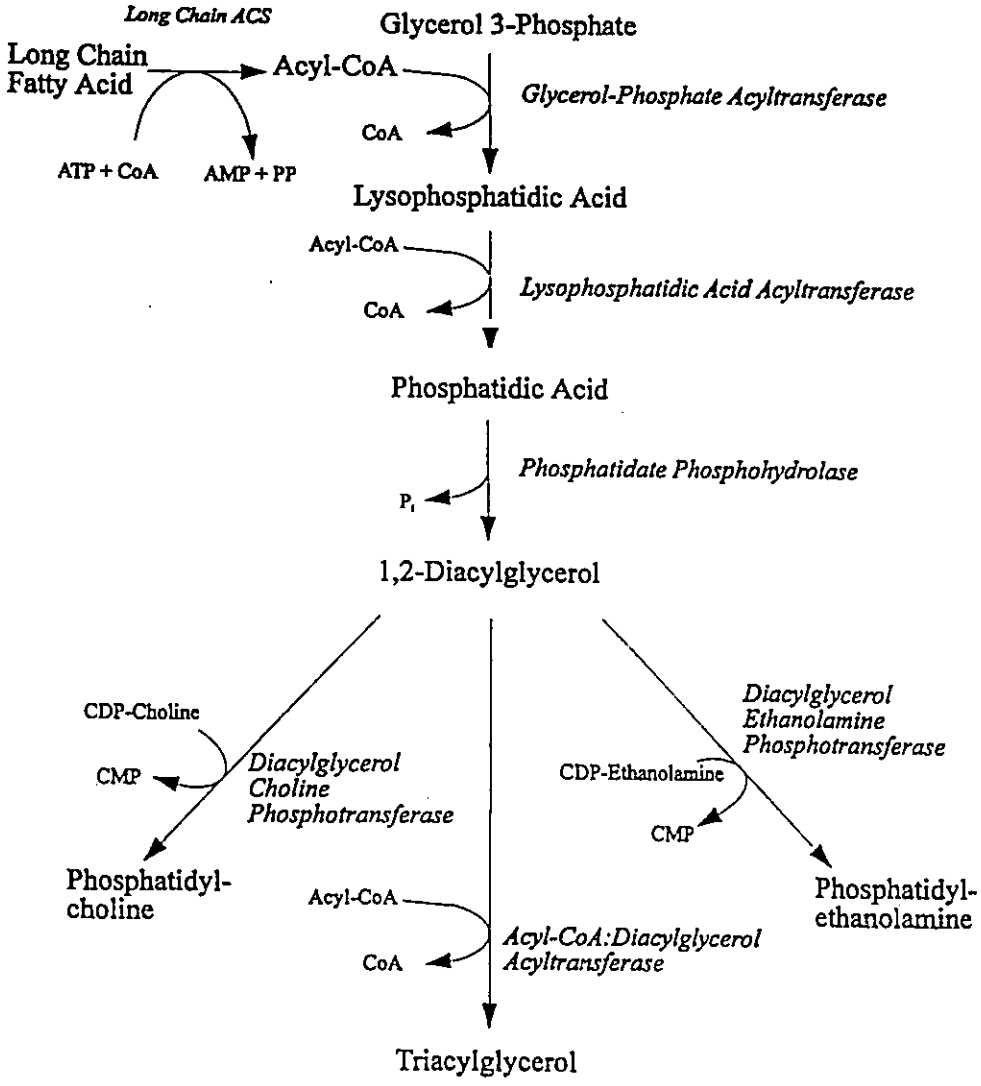

Figure 5. **Biosynthetic pathway for the incorporation of LCFAs into triglycerides and phospholipids** (adapted from Coleman et al., 1978).

lysophosphatidate which is acylated again to form phosphatidate (Coleman et al., 1978; Jamdar and Fallon, 1973). This is converted to diacylglycerol by a Mg^{2+}-dependent phosphatidate phosphohydrolase (Coleman et al., 1978; Jamdar and Fallon, 1973). Diacylglycerol can be converted to phosphatidyl choline or phosphatidyl ethanolamine through reaction with CDP-choline or CDP-ethanolamine, respectively. Otherwise, acyl-CoA:diacylglycerol acyl transferase catalyzes the acylation of diacylglycerol with LCFA-CoA to form triacylglycerol (Coleman et al., 1978; Hare et al., 1994). These enzymes have been reported to be localized to the ER membrane, although they have not yet been isolated (Hare et al., 1994; Moller et al., 1981).

While their *de novo* synthesis occurs at the ER, triglycerides are stored in large cytoplasmic lipid droplets (also called lipid storage vacuoles) (Greenberg et al., 1991; Hare et al., 1994). These are bound by a lipid bilayer that appears to be derived from the ER (Greenberg et al., 1991; Hare et al., 1994; Scow and Blanchette-Mackie, 1992). It is not known, however, whether lipid droplets acquire their membrane during or after their formation (Hare et al., 1994). Furthermore, the membrane of the mature lipid droplet differs in protein composition from the ER membrane, suggesting that it acquires specific proteins during maturation (Greenberg et al., 1991; Hare et al., 1994).

A.8.6. Lipolysis of Triglycerides in Adipocytes

The lipid droplet surface is not smooth, but contains channels leading into its interior, maximizing the total surface area available for lipolysis (Greenberg et al., 1991). Stimulation of adipocytes with lipolytic hormones such as epinephrine, norepinephrine or

glucagon, leads to the increased phosphorylation of hormone sensitive lipase and its translocation from the cytoplasm to the lipid droplet surface (Egan et al., 1992). This results in the stimulation of lipolysis and the mobilization of LCFA from the lipid droplet.

While a portion of LCFA released from adipocytes by lipolysis becomes bound to SA and enters the circulation for delivery to other tissues, a significant fraction becomes re-activated and re-used for triglyceride synthesis (Edens et al., 1990). This deacylation-reacylation cycle might serve to control the amounts of LCFA mobilized during lipolysis (Edens et al., 1990). LCFAs destined for re-esterification in the cycle appear first to be exported from the adipocyte and then taken up again rather than being re-esterified within the cell directly upon deacylation (Edens et al., 1990). The understanding of LCFA uptake by adipocytes is therefore central to the understanding of their role in LCFA storage and mobilization.

A.9. Adipose Differentiation

A.9.1. Agents Which Stimulate Differentiation

Several adipogenic cell lines have been described as convenient cell culture models for the study of the processes involved in the differentiation of adipocyte precursors (preadipocytes) to adipocytes, and of the metabolism and physiology of adipocytes (Cornelius et al., 1994). Of these, 3T3-L1 and 3T3-F442A cells have been most extensively characterized (Cornelius et al., 1994). Adipogenesis in these cells (reviewed in Cornelius et al., 1994) involves their conversion, at confluence, from a fibroblastic to an adipocyte morphology. This is characterized by a rounded shape and numerous, large cytoplasmic lipid droplets. Adipogenesis is accompanied by the induction in the transcription of a number of genes encoding adipocyte specific proteins (Table 3; for a more extensive list, see Cornelius et al., 1994).

Several agents promote the differentiation of confluent preadipocytes to adipocytes. These include fetal bovine serum, insulin, 3-isobutyl-1-methylxanthine (IbMX) and dexamethasone (Cornelius et al., 1994; Kuri-Harcuch and Green, 1978; Rubin et al., 1978). Growth hormone has been identified as the component of fetal bovine serum essential for differentiation (Cornelius et al., 1994; Doglio et al., 1986; Kuri-Harcuch and Green, 1978; Zezulak and Green,1986); it stimulates preadipocytes to synthesize insulin-like growth factor-1 (IGF-1; Doglio et al., 1987; Gaskins et al., 1990) which promotes

Table 3. **Some proteins induced upon adipose differentiation.**

Involvement	Protein	Reference	Protein	Reference
LCFA Uptake	CD36/FAT	Abumrad et al., 1993	FATP	Schaffer and Lodish, 1994
	$FABP_{PM}$	Zhou et al., 1992		
Lipid Binding	Acyl-CoA Binding Protein	Hansen et al., 1992	CRBP	Zovich et al., 1992
	ALBP	Spiegelman et al., 1983		
Lipid Synthesis	Diacylglycerol Acyltransferase	Coleman et al., 1978	Long Chain ACS	Amri et al., 1994 Coleman et al., 1978
	Fatty Acid Synthetase	Moustaid and Sul, 1991	Lysophosphatidate Acyltransferase	Coleman et al., 1978
	Glycerol-3-P Acyltransferase	Coleman et al., 1978		
Lipolysis	Hormone Sensitive Lipase	Kawamura et al., 1981	Lipoprotein Lipase	Semenkovich et al., 1989
Signalling	β_1, β_2 and β_3 Adrenergic Receptors	Fève et al., 1991 Guest et al., 1990	IGF-1 Binding Protein	Gaskins et al., 1990
	cGMP-Inhibited Cyclic Nucleotide Phosphodiesterase	Tiara et al., 1993	Insulin Receptor (IR)	Reed and Lane, 1980
			IR substrate/pp160	Rice et al., 1992
	$G_{\alpha s}$, $G_{i\alpha}$ and $G_{o\alpha}$	Watkins et al., 1987	Phospholipase A2	Gao and Serrero, 1990
	IGF-1	Gaskins et al., 1990	Rab 3D	Baldini et al., 1992
Transcription Factors	Adipocyte Determination and Differentiation Factor (ADD1)	Tontonoz et al., 1993	FAAR	Amri et al., 1995
			Glucocorticoid Receptor	Cornelius et al., 1994
	C/EBPα	Birkenmeier et al., 1989	PPARγ2	Tontonoz et al., 1994a
Other plasma membrane proteins	α2 Subunit of Na^+/K^+ ATPase	Russo et al., 1990	GluT 4	Kaestner et al., 1989
	Caveolin	Scherer et al., 1994	Scavenger Receptor (SR)-BI	Acton et al., 1994
Proteins of Unknown Function	Adipose Differentiation Related Protein	Jiang and Serrero, 1992	Perilipin	Greenberg et al., 1991, 1993

their differentiation (Cornelius et al., 1994; Smith et al., 1988). The differentiation promoting effect of insulin is thought to be mediated by the IGF-1 receptor, to which insulin binds when present at high concentrations (Cornelius et al., 1994; Smith et al., 1988).

IbMX, an inhibitor of the cyclic nucleotide phosphodiesterase (Beavo et al., 1970), results in increased intracellular levels of cAMP. Insight into a possible mechanism by which this promotes differentiation of confluent preadipocytes to adipocytes has been obtained from the study of the regulation of the aP2 gene, encoding ALBP (Yang et al., 1989). cAMP has been shown to increase the transcription of that gene by overcoming inhibition by an unknown negative regulatory factor (Yang et al., 1989). The mechanism by which this occurs is not understood. Whether similar events are involved in the increased transcription of genes encoding other adipocyte specific proteins or transcription factors, concomitant with differentiation, is also unknown. An unrelated negative regulatory element has been identified in the control region of the stearoyl-CoA desaturase 2 gene (Swick and Lane, 1992). This element, called the preadipocyte repressor element (PRE), binds a 58 kDa protein which is expressed in preadipocytes but is lost upon differentiation to adipocytes (Swick and Lane, 1992)

Dexamethasone, a synthetic glucocorticoid, also results in the stimulation of differentiation (Ringold et al., 1986). It is not clear, however, whether this represents direct effects of the glucocorticoid receptor on the expression of adipocyte specific genes

or is mediated by one or more transcription factors whose transcription is controlled by the glucocorticoid receptor (Ringold et al., 1986).

A.9.2. CCAAT/Enhancer Binding Protein α

Several genes whose transcription is elevated during differentiation contain regulatory elements recognized by the CCAAT/enhancer binding protein (C/EBP) α (Cornelius et al., 1994; Vasseur-Cognet and Lane, 1993a). This protein is expressed mainly in liver and adipose tissue (Cornelius et al., 1994; Vasseur-Cognet and Lane, 1993a). Its induction during differentiation of preadipocytes to adipocytes precedes the induction of most other adipocyte specific genes (Vasseur-Cognet and Lane, 1993a). These results suggest a role for C/EBPα in controlling the differentiation process. In support of this, the expression of C/EBPα cDNA in non-differentiating fibroblast cell lines is sufficient to induce their differentiation to adipocytes (Lin and Lane 1994). This is inhibited by coexpression of c-Myc (Freytag and Geddes, 1992). c-Myc is thought to inhibit differentiation by binding to a specific element in the promoter of the C/EBPα gene repressing its expression (Freytag and Geddes, 1992).

Transcription of the C/EBPα gene also appears to be negatively regulated by a preadipocyte factor called the C/EBPα-undifferentiated protein (CUP); C/EBPα induction during differentiation occurs concomitantly with the disappearance of CUP activity (Vasseur-Cognet and Lane, 1993b). CUP does not appear to be related to the cAMP-sensitive negative regulatory factor or the PRE binding factor (mentioned above), which

are involved in repression of the aP2 and stearoyl-CoA desaturase 1 genes, respectively (Swick and Lane, 1992; Vasseur-Cognet and Lane, 1993b; Yang et al., 1989).

A.9.3. Stimulation of Differentiation by LCFAs: Role of Peroxisome Proliferator Activated Receptors.

Recent evidence from a number of groups suggests that both saturated and unsaturated LCFAs are able to stimulate preadipocytes to differentiate to adipocytes (Amri et al., 1991a and b, 1994; Distel et al., 1992; Grimaldi et al., 1992; Safonova et al., 1994). This is believed to result from the activation, upon LCFA binding, of transcription factors belonging to the peroxisome proliferator activated receptor (PPAR) family, leading to the increased transcription of adipocyte specific genes (Amri et al., 1995; Chawla and Lazar, 1994; Chawla et al., 1994; Safonova et al., 1994; Tontonoz, et al., 1994a and b). These factors, PPARγ2 and the fatty acid-activated receptor (FAAR), appear to heterodimerize with the retinoid X receptor (RXR)α, to form a complex which trans-activates the expression of a variety of adipocyte-specific genes (Amri et al., 1995; Tontonoz et al., 1994a and b). PPARγ2 exhibits a strikingly adipose specific expression pattern, while FAAR appears to be expressed in a variety of tissues (Amri et al., 1995; Tontonoz et al., 1994a). These factors also differ in the ligands which activate them; PPARγ2-mediated transcription is activated by polyunsaturated LCFAs and fibric acid derivatives, while FAAR is activated strongly by both saturated and mono-unsaturated LCFAs but only weakly by fibric acid derivatives (Amri et al., 1995; Tontonoz et al., 1994a).

As observed with C/EBP, the enforced expression of PPARγ2 in non-differentiating fibroblast cell lines is also sufficient for their differentiation to adipocytes; this is enhanced by coexpression of RXRα (Tontonoz et al., 1994b). This suggests that either C/EBPα or PPARγ2 might constitute differentiation signals. However, neither of these proteins is expressed in preadipocytes; instead, they first become expressed after the initiation of differentiation, the expression of PPARγ2 slightly preceeding that of C/EBPα (Tontonoz et al., 1994b).

A transcription factor signalling differentiation should be expressed in preadipocytes. The expression of FAAR begins to increase in preadipocytes at confluence, prior to the initiation of differentiation (Amri et al., 1995). Furthermore, the enforced expression of FAAR in non-differentiating fibroblasts results in the induction of transcription of two adipocyte specific genes in a fatty acid-dependent manner. This suggests that it might represent a key factor in the control of the initiation of differentiation. It has not been demonstrated, however, whether the expression of FAAR in preadipocytes is sufficient for their differentiation based on morphological criteria, as well as the increased expression of a variety of other adipocyte specific genes (Amri et al., 1995).

A.9.4. Other Transcription Factors Implicated in Adipose Differentiation

Other transcription factors which are expressed at early stages in adipogenesis include HNF (hepatocyte nuclear factor)-3-like proteins, expressed in preadipocytes at confluence (Enerbäck et al., 1992) and ADD1 (adipocyte determination and differentiation

factor), which may be expressed in proliferating preadipocytes (Cornelius et al., 1994; Tontonoz et al., 1993). It is not clear, however, whether either HNF-3, ADD1 are sufficient to induce differentiation (Cornelius et al., 1994).

A.10. Rationale and Objectives

LCFAs are substrates for lipid synthesis and for energy producing reactions such as β-oxidation. In addition, they are involved in signalling processes in a variety of cell types. Adipocytes are the major sites of regulation of whole body metabolism, due to their essential role in energy storage and mobilization in the form of triglycerides and LCFAs, respectively. A variety of diseases involve alterations in LCFA metabolism. Some, such as diabetes and obesity affect the ability of adipocytes to regulate LCFA storage and mobilization.

The initial events in the response of cells to LCFAs involves the cellular uptake of LCFAs and their trafficking within the cell. Therefore, the understanding of the mechanisms of these processes will have broad implications for the understanding of the control of LCFA metabolism and signalling in both normal and diseased states.

The adipogenic cell line, 3T3-L1 was chosen as a system in which to study the mechanism of LCFA uptake for various reasons. First, an adipogenic cell line would represent a convenient tool for the identification of cellular components involved in LCFA uptake which might be induced during the course of differentiation. Of the various adipogenic cell lines available, 3T3-L1 was chosen as it was the most extensively characterized when these studies were initiated. Finally, the central involvement of adipocytes in LCFA metabolism and energy storage made them an attractive system in

which to study LCFA uptake; results obtained with adipocytes should also provide insight into the mechanisms of uptake of LCFAs by other cell types.

LCFA uptake by 3T3-L1 adipocytes was studied using radiolabeled, natural and photoactivatable LCFAs. Radiolabeled, natural LCFAs were used as probes to follow LCFA uptake and metabolism. 11-*m*-Diazirinophenoxy-[11-^{3}H]undecanoate (11-DAP-[11-^{3}H]undecanoate), a radiolabeled, photoreactive LCFA, was used for the identification of cellular LCFA binding proteins which might be involved in the uptake process and for the development of novel methods allowing the direct measurement of LCFA movement across the plasma membrane and trafficking within the intact cell.

Photoactivatable reagents are ideally suited for the identification of cellular binding proteins and the analysis of intracellular trafficking for a variety of reasons. For example, the reactive species generated by exposure of photoreactive compounds to light are generally much more reactive than chemical affinity reagents (Bayley, 1983). This is important for the identification of LCFA binding sites on proteins, since such sites should be devoid of functional groups (Bayley, 1983; Brunner, 1993). While chemical affinity reagents would not be expected to react with such sites, many photoactivatable groups give rise, upon exposure to light, to species sufficiently reactive to insert across C–C and C–H bonds. Photoactivatable LCFAs should therefore be well suited to react with such groups in a hydrophobic LCFA binding site. The covalent attachment of the radioactive probe upon photolysis has the advantage of allowing labeled samples to be fractionated and proteins to be separated without the loss or redistribution of the probe. This enables

the identification of binding proteins in complex samples, which cannot be accomplished with non-reactive, radiolabeled probes. Furthermore, because photoaffinity reagents, such as the photoreactive LCFA, are chemically inert in the dark, the labeling reaction can be initiated at a predetermined point in time by exposure to light, allowing sufficient time for the reagent to reach target sites, for example within cells (Bayley, 1983). Photoaffinity reagents are thus better suited for kinetic experiments, such as those designed to measure intracellular trafficking, than are chemical affinity reagents which begin to react immediately upon addition to biological samples or non-reactive probes which cannot be used to gain information concerning binding to individual proteins in complex samples.

The objectives of this work were therefore the following: 1. The characterization of LCFA uptake in 3T3-L1 adipocytes, and the demonstration of their suitability as a model system in which to study LCFA uptake; 2. the dissection of the uptake process into its component steps (outlined in section A.4.); 3. the characterization of the steps involved in the LCFA uptake process; 4. the investigation of the mechanisms by which each step occurs; and 5. the identification of cellular components involved in each step.

B. MATERIALS AND METHODS

B.1. Materials

N-Methyl-*N*'-nitro-*N*-nitrosoguanidine (MNNG), osmium tetroxide (9.0 % solution in t-butanol), NaH, and Rydon's reagent (methyltriphenoxyphosphonium iodide) were purchased from Aldrich. 3T3-L1 preadipocytes were bought from the American Type Culture Collection. Amplify fluorography reagent, Aqueous Counting (AC) scintillant, ECL chemiluminescence detection reagents and horseradish peroxidase conjugated to goat-anti-mouse immunoglobulin (Ig) G were purchased from Amersham. Biolyte carrier ampholytes, tween-20 and all electrophoresis equipment were purchased from Biorad. Tris-(hydroxymethyl)aminomethane (tris) was from Boehringer Mannheim. Chloroform and *n*-heptane were purchased from Caledon Laboratories. Disposable (polystyrene) cuvettes were purchased from Canlab. Cat serum was obtained from the Colorado Serum Company. Plasticware for cell culture was purchased from Corning, except for trays containing 4×1.5 cm diameter wells, which were from Nunc. Optical filters (Corning 7-51) were purchased from Corning Glass works. Hexamethylphosphoric triamide (HMPT) and XAR-5 x-ray film were purchased from Eastman Kodak. Polypropylene tubes (14 ml; #2059) were purchased from Falcon. Butanol, *N*,*N*-dimethylformamide (DMF), 2,5-diphenoxazole (PPO), hydrochloric acid, methanol (HPLC grade), oleic acid, potassium hydrogen phthalate, sodium potassium tartarate, sulphuric acid and scintillation vials were

purchased from Fisher Scientific. Calf and fetal bovine sera, Dulbecco's modified Eagles medium (DMEM), L-glutamine, penicillin-streptomycin solution, trypsin-EDTA solution and all reagents for sodium dodecylsulfate polyacrylamide gel electrophoresis (SDS-PAGE) were purchased from GIBCO-BRL Life Technologies. Urea (ultra-pure) was from ICN. Absolute and 95 % ethanol were from McMaster University. Analytical thin layer chromatography (TLC) silica plates (0.20 mm thickness) were purchased from Merck. Immobilon-P (polyvinyl difluoride; PVDF) membranes were obtained from Millipore. The acetoxymethyl ester of 2',7'-bis-(2-carboxyethyl)-5-(and 6)-carboxyfluorescein (BCECF-AM) was purchased from Molecular Probes Inc. Atomlight scintillation cocktail, Solvable Tissue and Gel Solubilizer, [9,10-^{3}H]oleic acid (10 Ci/mmol) and NaB[$^{3}H_4$] (13-15 Ci/mmol) were purchased from NEN Research Products. *cis*-Vaccenic acid was from Serdary Research Laboratories. Adenosine 5'-monophosphate (AMP), adenosine 5'-triphosphate (ATP), 4-amidinophenyl methanesulfonyl fluoride (APMSF), bestatin, bromophenol blue, BSA (prepared from fraction V, essentially fatty acid free), 3-[(3-cholamidopropyl)dimethylammonio]-1-propane-sulfonate (CHAPS), coenzyme A (CoASH; lithium salt), deoxyribonuclease (DNase) 1, dexamethasone, dithiothreitol (DTT), Folin-Ciocalteau's 2 N phenol reagent, horseradish peroxidase conjugated to donkey-anti-rabbit IgG, hydroxyalkoxypropyl-dextran (lipidex 1000), N-2-hydroxyethylpiperazine-N'-2-ethanesulfonic acid (HEPES), insulin (cell culture grade), IbMX, leupeptin, 2-(N-morpholino)-ethanesulfonic acid (MES), mouse IgG, pepstatin, phloretin, protein A-sepharose, ribonuclease (RNase) A, Triton X-100 and trypan blue dye were purchased

from the Sigma Chemical Company. μ-Bondapack C18 hydrophobic resin was from Waters. Preparative silica TLC plates (1.0 mm thickness, with preadsorbent area) and GF/C glass fibre filters (24 mm diameter) were purchased from Whatman. Ethylphenyl-polyethylene glycol (NP-40) was purchased from United States Biochemical. Affinity purified, rabbit anti-murine ALBP antibody was kindly provided by Professor D.A. Bernlohr (University of Minnesota). Anti-caveolin monoclonal antibodies (mAbs), 2234 and 2297, and polyclonal antibodies (from rabbit) specific for the N-terminal portion, C-terminal portion, or entire protein (expressed as a glutathione S-transferase-fusion) were generously supplied by Professor R.G.W. Anderson (University of Texas, Southwestern Medical Center, Dallas). α-Iodopalmitic acid was synthesized by Dr. Dev Mangroo. *m*-Diazirinophenol was synthesized by Lynne Wrona. All other reagents were purchased from BDH.

B.2. Synthesis of 11-*m*-Diazirinophenoxy-[11-^{3}H]undecanoic Acid

The synthesis of 11-*m*-diazirinophenoxy-[11-^{3}H]undecanoic acid (11-DAP-[11-^{3}H]undecanoic acid; shown schematically in figure 6) was carried out essentially as described previously (Leblanc, 1991; Leblanc et al., 1982; Mangroo, 1992) with some modifications.

B.2.1. Oxidation of *cis*-Vaccenic Acid

cis-Vaccenic acid (compound 1 in figure 6; 90 mM, in 80.0 % aqueous dioxane in the presence of 1.1 equivalent of NaOH) was oxidized to heptanal and 10-formyldecanoic acid (compound 2 in figure 6) by reaction at room temperature, overnight and in the dark, with OsO_4 (4.6 %) and $NaIO_4$ (1.0 g per mmol of *cis*-vaccenic acid, added at the beginning of the reaction, and again after 5, 15 and 60 min). The reaction was monitored by TLC on silica plates developed in diethyl ether:petroleum ether (4:1, v/v; solvent 1). Spots were visualized with iodine vapour. The R_f values for *cis*-vaccenic acid, heptanal and 10-formyldecanoic acid were 0.5, 0.3 and 0.1, respectively.

After removal of the solvent from the reaction mixture (under vacuum), the desired products were recovered by extraction into diethyl ether:petroleum ether (1:1,v/v;solvent 2). The ether was removed under vacuum, and the oily residue was suspended in 6.0 ml of 0.25 M Na_2CO_3. Heptanal was removed by extraction with petroleum ether. The aqueous phase was acidified and the 10-formyldecanoic acid was extracted into solvent

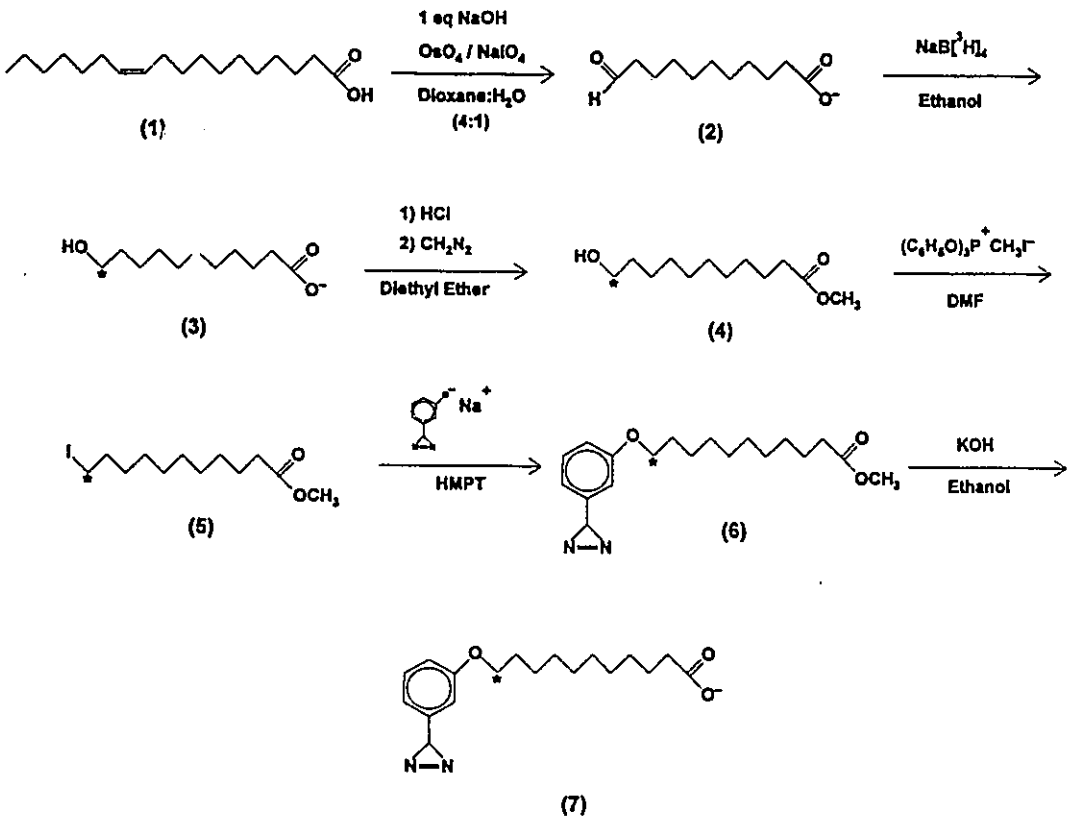

Figure 6. **Scheme for the chemical synthesis of 11-DAP-[11-^{3}H]undecanoate** (adapted from Leblanc et al., 1982). **1.** *cis*-Vaccenic acid. **2.** 10-Formyldecanoate. **3.** 11-Hydroxy-[11-^{3}H]undecanoate (the position of the tritium label is indicated with an asterisk. **4.** Methyl-ester of compound 3. **5.** Methyl-11-iodo-[11-^{3}H]undecanoate. **6.** Methyl-11-*m*-diazirinophenoxy-[11-^{3}H]undecanoate. **7.** 11-DAP-[11-^{3}H]undecanoate.

2. The solvent was removed and the residue was dried completely for 5 minutes under vacuum in a speed-vac concentrator.

B.2.2. Reduction of 10-Formyldecanoic Acid with Sodium [^{3}H]Borohydride

Four equivalents of 10-formyldecanoic acid (0.50 M in absolute ethanol, in the presence of 1.1 equivalent of NaOH) were added to solid NaB[^{3}H]$_4$ (500 mCi of 13-15 Ci/mmol). This was allowed to react for 10 min at room temperature before another four equivalents were added. Additions were again made after 15 min (one addition) and 30 min (five additions). After the final addition, the reaction was allowed to proceed for 2.5 h, or until complete. This was determined either by the evolution of H_2 (*g*) when 1.0 µl of the reaction mixture was added to 10.0 ml of diethyl ether containing 20 µl of HCl (*conc.*) or by the recovery of radioactivity in the ether phase.

Upon completion of the reaction, the mixture was acidified with 1.1 equivalent of HCl and diluted with 10 volumes of H_2O. The resulting precipitate was extracted into diethyl ether. The recovery of 11-hydroxy-[11-^{3}H]undecanoic acid in the ether extracts was monitored by liquid scintillation counting. 11-Hydroxy-[11-^{3}H]undecanoic acid was purified by preparative TLC using diethyl ether:petroleum ether (15:1, v:v; solvent 3) as the mobile phase. The position of the desired product (R_f of 0.065) was identified by autoradiography. It was recovered from the TLC plate by extraction of the silica scrapings with diethyl ether.

B.2.3. Formation of Methyl Ester of 11-Hydroxy-[11-^{3}H]undecanoic Acid

Diazomethane (0.50 M in diethyl ether) was prepared by reaction of solid MNNG (1.25 mmoles) with 1 equivalent of KOH in 0.50 ml H_2O. The diazomethane which was evolved dissolved into 1.25 ml of diethyl ether overlaying the reaction mixture. This was distilled into a second test tube containing an equal volume of diethyl ether on ice.

11-Hydroxy-[11-^{3}H]undecanoic acid (0.050 M) was allowed to react on ice for 10 minutes with a ten-fold molar excess of diazomethane in diethyl ether. The reaction mixture was applied to a preparative TLC plate and developed in solvent 3. Methyl-11-hydroxy-[11-^{3}H]undecanoate (compound 4 in figure 6; R_f 0.26) was located by autoradiography and recovered by extraction with diethyl ether. The molar yield of methyl-11-hydroxy-[11-^{3}H]undecanoate was routinely 75 %. Any unreacted starting compound (R_f 0.065) was recovered from the preparative TLC plate as described above and was stored at -20°C.

B.2.4. Preparation of Methyl-11-Iodo-[11-^{3}H]undecanoate

From this point onward, all reactions and products were protected from exposure to light. Methyl-11-hydroxy-[11-^{3}H]undecanoate (0.10 M in DMF) was allowed to react with a 10-fold molar excess of methyltriphenoxyphosphonium iodide under N_2 (*g*) for 3 h at room temperature. The reaction mixture was diluted with 10 volumes of H_2O and chromatographed on μ-bondapack C18. The desired product (methyl-11-iodo-[11-^{3}H]undecanoate; compound 5 in figure 6) was eluted with diethyl ether and applied to a

preparative TLC plate which was developed with solvent 1. The desired product (R_f 0.9) was located by autoradiography and recovered by extraction with diethyl ether.

B.2.5. Preparation of Methyl-11-*m*-diazirinophenoxy-[11-^{3}H]undecanoate

Methyl-11-iodo-[11-^{3}H]undecanoate was allowed to react with 1.1 molar equivalent of sodium *m*-diazirinophenoxide (0.10 M in HMPT) for 1.0 h at room temperature, under N_2 (*g*) and shielded from light. The reaction mixture was applied to preparative TLC plates (no more than 0.4 ml of HMPT per preparative plate) which were developed in solvent 1 (again, shielded from exposure to light). The desired product, methyl-11-DAP-[11-^{3}H]undecanoate (R_f of 0.7; compound 6 in figure 6), was located by autoradiography and was recovered by extraction with diethyl ether.

B.2.6. Saponification of Ester

Methyl-11-DAP-[11-^{3}H]undecanoate was allowed to react with ten molar equivalents of KOH (0.10 M in 93 % ethanol) for 15 hours under N_2 (*g*), in the dark to yield the potassium salt of 11-DAP-[11-^{3}H]undecanoate (compound 7 in figure 6). After removal of the solvent, the residue was dissolved in 1.0 ml of H_2O and acidified with 16 equivalents of HCl. The free acid was extracted into diethyl ether and applied onto a preparative TLC plate which was developed with solvent 1. 11-DAP-[11-^{3}H]-undecanoic acid (R_f of 0.39) was located by autoradiography and was recovered by extraction with diethyl ether.

B.3. Cell Culture

B.3.1. Long Term Storage of Cells

3T3-L1 preadipocytes were stored in N_2 (*l*) upon receipt. When needed, frozen cells were quickly thawed at 37°C and plated in growth medium: DMEM supplemented with 10% bovine calf serum (heat inactivated) and 2.0 mM L-glutamine and containing penicillin (50 units/ml) and streptomycin (50 µg/ml) (Rubin et al., 1978). Cells were grown at 37°C in a humidified atmosphere containing 5.0% CO_2. The medium was changed on the following day.

Frozen stocks were prepared from cells just prior to confluence. After removal of the growth medium, cells from each 10 cm diameter plate were washed twice with 5.0 ml of 37°C phosphate buffered saline (PBS, containing 0.14 M NaCl, 2.7 mM KCl, 15 mM Na_2HPO_4, and 1.5 mM KH_2FO_4, at pH 7.4). The cells were incubated for 30 sec with 1.0 ml of 37°C trypsin-EDTA solution (0.050 % trypsin in PBS containing 0.53 mM EDTA). After removal of this solution, cells were dislodged from the plate by gentle agitation and were suspended in 10.0 ml of freezing medium (growth medium containing 5.0 % DMSO). A portion (1.0 ml) was transferred to each of ten cryogenic vials. These were cooled for 15 min on ice, frozen at -80°C (overnight) and then placed in a N_2 (*l*) storage tank for long term storage.

B.3.2. Growth and Maintenance of Cells.

Frozen stocks of 3T3-L1 cells were thawed and grown as described above (section B.3.1). Just prior to confluence cells were released from plates with trypsin-EDTA solution as described above, and suspended in 5.0 ml of 37°C growth medium. 0.50 ml were added to 10 ml of growth medium in a 10 cm diameter tissue culture dish. The cells were grown as described above (section B.3.1) and were again split at a one in ten dilution into 10 cm dishes approximately three days later. Cells were routinely passed 5-6 times before a new stock was thawed and used. Cells to be propagated were never allowed to become fully confluent (as instructed by supplier).

B.3.3. Differentiation of Preadipocytes to Adipocytes.

One day following confluence, 3T3-L1 cells were stimulated to differentiate to adipocytes by replacing the growth medium with stimulation medium: DMEM supplemented with 10% fetal bovine serum (heat inactivated), 2.0 mM L-glutamine, insulin (0.010 mg/ml), 250 nM dexamethasone and 0.50 mM IbMX, penicillin (50 units/ml) and streptomycin (50μg/ml) (Rubin et al., 1978). After two days, this was replaced by post-stimulation medium (PSM; stimulation medium lacking dexamethasone and IbMX; Rubin et al., 1978). PSM was changed each day afterward.

To maintain cells in an undifferentiated state, growth medium was replaced just prior to confluence with one containing 9.0 % cat serum and 1.0 % calf serum (rather than 10 % calf serum), and cells were maintained beyond confluence for 4-6 days, with

medium changes every two days (Kuri-Harcuch and Green, 1978; Spiegelman and Green, 1980).

B.3.4. Harvesting of Cells

Unless otherwise indicated, stimulated cells were harvested on the fifth or sixth day after initiation of the stimulation procedure. Monolayers were washed twice with 5.0 ml of PBS and cells were released from the plates by gentle agitation following a one minute incubation at 37°C with 5.0 ml of 1.0 mM EDTA in PBS (Spiegelman and Green, 1980). The cells, recovered in 5.0 ml of ice-cold PBS, were routinely counted with a haemocytometer and were considered viable if greater than 90 % excluded trypan blue dye (Stremmel and Berk, 1986). The cells, collected by centrifugation for 10 min at 4°C and 2000 rpm in a Sorvall RC-5B centrifuge with an SS34 rotor, were resuspended in ice-cold PBS to the desired working concentration and used immediately.

B.4. LCFA Uptake and Incorporation into Cellular Lipids

B.4.1. Preparation of LCFA Solutions

[9,10-^{3}H]oleic acid was diluted to the desired specific radioactivity (normally 50-250 mCi/mmol) with non-radioactive oleic acid. LCFAs were neutralized with 1.1 equivalent of KOH in 47.5% ethanol. The solvent was removed under vacuum in a speed-vac concentrator. The dry residue was dissolved in PBS in the presence or absence of BSA where indicated, to provide a two-fold stock. This solution was equilibrated at 37°C for one hour prior to use. In all cases 11-DAP-[11-^{3}H]undecanoate was protected from exposure to light until photolysis.

The specific radioactivities of [^{3}H]-LCFA solutions were determined by liquid scintillation counting in 10 ml of AC scintillant in 15 ml opaque scintillation vials. Radioactivity due to tritium was determined with a Beckman LS-800 scintillation counter, using a 1.0 min preset counting time and preprogrammed quench correction. The quench correction curve was generated using [^{3}H]toluene of known specific radioactivity and varying amounts of methanol as the quenching agent.

B.4.2. Measurement of LCFA Binding to BSA

LCFA binding to BSA was measured by the method of Spector et al. (1969, 1971). This involved the measurement of the equilibrium partitioning of a series of concentrations of [^{3}H]-LCFA between PBS and an equal volume (0.50 ml) of *n*-heptane,

according to Goodman (1958); incubations were typically carried out for 16 h at 37°C. The concentrations of [^{3}H]-LCFA in the aqueous phase were plotted versus the corresponding concentrations in the *n*-heptane phase. The partitioning was repeated with BSA in the aqueous phase, so that uncomplexed [^{3}H]-LCFA in the aqueous phase was in equilibrium with [^{3}H]-LCFA complexed with BSA in the aqueous phase and with uncomplexed [^{3}H]-LCFA in the *n*-heptane phase (Spector et al., 1969). The concentration of [^{3}H]-LCFA in the *n*-heptane phase was measured directly, and used, along with the calibration curve established from the partitioning of the [^{3}H]-LCFA in the absence of BSA to determine the concentration of uncomplexed [^{3}H]-LCFA in the aqueous phase. This was subtracted from the total concentration of [^{3}H]-LCFA measured in the aqueous phase to give the concentration of BSA-complexed [^{3}H]-LCFA in the aqueous phase (Spector et al., 1969). The ratio of complexed [^{3}H]-LCFA to BSA was plotted versus the log of the inverse of the concentration of uncomplexed [^{3}H]-LCFA in the aqueous phase allowing the concentration of uncomplexed LCFA at different LCFA:BSA ratios to be determined (Spector et al., 1969, 1971).

B.4.3. Assay for LCFA Uptake

Cellular uptake of [^{3}H]-LCFAs was measured with a filtration assay using conditions described by Abumrad et al. (1981) and Stremmel and Berk (1986). Whatman GF/C filters were pre-saturated with BSA by filtering 15.0 ml of 0.10% BSA in PBS (room temperature). Pre-saturated filters were chilled for at least 60 min at 4°C prior to use. Four washes with 5.0 ml of ice-cold PBS containing 0.10% BSA and 200 μM

phloretin (wash solution) were sufficient to minimize the amount of [^{3}H]-LCFA sticking to filters in the absence of cells (data not shown). Cells (harvested as described in Section B.3.4) were suspended in ice-cold PBS at 1.0 mg of cellular protein/ml. Aliquots of 0.50 ml were added to 14 ml polypropylene tubes and incubated for 5.0 min at 37°C with agitation (180 min^{-1}). Assays were initiated upon the addition of 0.50 ml of two-fold stock [^{3}H]-LCFA:BSA solution. At various times 200 µl of the sample were diluted into 5.0 ml of ice-cold wash solution and vacuum-filtered. Cells retained by the filter were rapidly washed three more times with 5.0 ml of cold wash solution and filters were soaked overnight in 10.0 ml of AC scintillant prior to scintillation counting. The level of radioactivity remaining associated with the filters after washing was routinely measured in the absence of cells and subtracted from the amount of radioactivity retained by filters in the presence of cells. It normally did not exceed 10 % of the signal due to [^{3}H]-LCFA taken up by cells.

The rates of [^{3}H]-LCFA uptake at different substrate concentrations were modeled by equation 3, where v is the rate, c is the substrate concentration, V_{max} is the maximum rate and $K_{0.5}$ is the Michaelis constant for the saturable process, and k is the coefficient for non-saturable uptake.

$$v = \frac{V_{max} c}{K_{0.5} + c} + k c \qquad (3)$$

B.4.4. Incorporation of [9,10-^{3}H]Oleate into Cellular Lipids

3T3-L1 Adipocyte monolayers in 6-well trays (3.5 cm diameter wells) were incubated with 2.0 ml of [9,10-^{3}H]oleate in PBS containing BSA as described above (Section B.4.3). Immediately after washing, the monolayers were extracted twice with 2.0 ml of $CHCl_3$:CH_3OH:H_2O (1:2:0.8; *v/v/v*) according to Bligh and Dyer (1958) as modified by Abumrad et al. (1991). The extracts were combined and phase separation was brought about by the addition of 0.50 ml each of $CHCl_3$ and H_2O. Each phase was concentrated under vacuum using a speed-vac concentrator and analyzed by TLC using the following developing solvent mixtures: 1) *n*-butanol:acetic acid:H_2O (5:2:3; *v/v/v*) for the aqueous phase, containing LCFA-CoA; 2) $CHCl_3$:CH_3OH:H_2O (65:25:4; *v/v/v*) for polar lipids in the organic phase; and 3) *n*-heptane:isopropyl ether:acetic acid (60:40:4; *v/v/v*) for neutral lipids in the organic phase (Kates, 1986). TLC plates were treated with PPO (7.0 % in diethyl ether) and exposed to X-ray film at -80°C (Raderath, 1970). Radioactive spots were scraped from the plates into 10 ml of AC scintillant and the amount of radioactivity was determined by scintillation counting.

B.5. Measurement and Manipulation of Intracellular pH (pH_c).

B.5.1. pH_c Manipulation by Acid Loading with NH_4Cl

Cells were loaded with 45 mM NH_4Cl for 60 minutes in PBS containing 10 mM glucose (Frelin et al., 1988; Moolenaar et al., 1983, 1984). NH_4Cl was removed by centrifugation (5 min at 600×g) for cells in suspension or by aspiration for monolayers. Immediately thereafter, PBS containing 10 mM glucose was added and cells were used.

B.5.2. Measurement of pH_c

3T3-L1 adipocytes grown on 7×25 mm microscope slides (Moolenaar et al., 1983, 1984) were loaded with the BCECF-AM (10 μM in 2.0 ml of serum-free DMEM) in 35 mm (diameter) culture dishes at 37°C for one hour in a humidified atmosphere containing 5.0 % CO_2 (Moolenaar et al., 1983, 1984; Thomas et al., 1979; van Adelsberg et al., 1989). The loaded cells were washed and the cytoplasm was acid loaded as described above. Slides were placed in 2.0 ml of PBS in disposable, 3.0 ml fluorescence cuvettes to which test solutions were added. Fluorescence emission at 530 nm, with excitation at 500 nm (Moolenaar et al., 1984), was monitored in a Aminco Bowman series 2 luminescence spectrometer. Fluorescence was calibrated to internal pH by setting the internal and external pH's equal with nigericin in medium in which NaCl was replaced with KCl (Frelin et al., 1988; Moolenaar et al., 1984) as well as by lysis of the cells with 0.10 % triton X-100 and titration with MES (Rotin et al., 1987).

B.6. Subcellular Fractionation

B.6.1. Preparation of Total Homogenates and Isolation of Total Cellular Membranes

Cells suspensions (3-6 mg of cell protein/ml in 0.50-1.0 ml of ice cold PBS) were drawn rapidly through a 1 ml syringe fitted with a 23-gauge needle (fifteen times). Homogenates were centrifuged for one hour at $10^5 \times g$ and 4°C in a TLA-100.2 rotor in a Beckman TL-100 ultracentrifuge. The supernatant was removed and the pellet was resuspended to a protein concentration of 4.0 mg/ml in PBS, containing 0.10 mM PMSF. Each fraction was stored at -20°C until used.

B.6.2. Isolation and Delipidation of Cytoplasm

3T3-L1 adipocytes (3-6 mg of cell protein/ml in ice-cold 20 mM sodium phosphate, pH 7.4) were homogenized with five strokes, at moderate speed, of a Teflon pestle in a glass-Teflon homogenizer. Homogenates were centrifuged as described above (Section B.6.1). The cytoplasmic fraction was recovered as the supernatant below the fat cake with a syringe fitted with a 23-gauge needle. PMSF (0.10 M in isopropanol, freshly prepared) was added to a final concentration of 0.10 mM, and the sample was warmed to 37°C. This was delipidated at 37°C by passage through 1.0 ml of packed lipidex 1000 in the barrel of a 3 ml syringe in a 14 ml polypropylene tube by centrifugation at $500 \times g$ (Glatz and Veerkamp, 1983).

B.6.3. Isolation of Lipid Droplets

All manipulations were carried out at 4°C. Cells from three tissue culture dishes (10 cm diameter) were harvested as described in Section B.3.4, except that they were suspended in 1.5 ml of homogenization buffer A (10.0 mM HEPES, pH 7.4, containing 1.0 mM EDTA and 0.14 M NaCl). The cells were homogenized with 25 strokes of a motor-driven Teflon pestle (moderate speed) in a 2.0 ml glass homogenization vessel. The homogenate was diluted with 2.5 ml of homogenization buffer A and was layered onto a discontinuous sucrose gradient (1.0 ml of each of 0.125 M, 0.25 M, 0.45 M, 0.65 M, 0.85 M, 1.05 M, 1.25 M, and 1.5 M sucrose in homogenization buffer A). Gradients were centrifuged for 90 min at 21,000×*g* in a Beckman SW 41 rotor.

The lipid droplet was recovered as the fat cake at the top of the gradient (Egan et al., 1992). Because of the difficulty of pipetting the fat cake, this was accomplished by selectively freezing the fat cake by dripping N_2 (*l*) on to the surface of the gradient, and lifting the frozen fat cake out of the tube with a bent 23 gauge needle. The remainder of the gradient was fractionated by carefully pipetting 1.0 ml aliquots from the top of the gradient.

B.6.4. Isolation of Plasma Membranes, Low Density Microsomes and Mitochondrial Fractions

Except where indicated, all manipulations were carried out at 4°C. Subcellular fractions were prepared as described originally by Cushman and Wardzala (1980) and modified by Lange and Brandt (1990) with some further modifications. Cells from one

tissue culture dish of 10.0 cm diameter (10 mg total protein) were harvested as described in Section B.3.4, except that they were collected in 1.0 ml of homogenization buffer B (1.0 mM HEPES, 1.0 mM EDTA, pH 7.4, containing 0.25 M sucrose) and then stored on ice. Cell suspensions were homogenized with 10 strokes of a motor-driven Teflon pestle (moderate speed) in a glass homogenization vessel. Homogenates were diluted with an equal volume of ice-cold homogenization buffer B and centrifuged at 16,000×g for 20 minutes using a sorvall SS-34 rotor in an RC-5B centrifuge. The supernatant (S_{16}) was saved. Pellets were washed with homogenization buffer B (2.0 ml per 10.0 mg of original cell protein) and centrifuged as above. The washes were pooled with the S_{16} fraction. Washed pellets were resuspended in homogenization buffer B (1.0 ml per 10 mg of original cell protein) with 5 strokes of a motor-driven Teflon pestle (moderate speed) in a glass homogenization vessel and were layered onto a discontinuous sucrose gradient (per 1.0 ml of resuspended pellet: 1.0 ml each of 0.87 M, 1.12 M, and 1.50 M sucrose in 10 mM HEPES and 1.0 mM EDTA, pH 7.4). This was centrifuged at 23,000×g for 90 min using a Beckman SW 50.1 rotor.

For large scale preparations, cells from twenty tissue culture dishes (10.0 cm diameter; 200 mg total cellular protein) were used and all concentrations of total cellular protein were doubled. Furthermore, sucrose gradients (10.0 ml of each sucrose concentration) were centrifuged as above using a Beckman SW 28 rotor.

Plasma membranes were recovered from the 0.25 M-0.87 M sucrose interface and mitochondria were recovered from the 1.12 M-1.5 M sucrose interface. The recovered

bands were diluted 5-fold with ice-cold 20 mM sodium phosphate (unless otherwise indicated) and centrifuged at $10^5 \times g$ for 60 min using a Beckman Ti80 rotor. Low density microsomal membranes were recovered from the S_{16} fraction by centrifugation at $10^5 \times g$ as described for the plasma membrane fraction. Pellets were resuspended to 5.0-10 mg of protein/ml in PBS (unless otherwise indicated) containing 0.10 mM PMSF (freshly prepared as a 0.10 M stock in isopropyl alcohol) and were either used immediately or frozen in N_2 (*l*) and stored at -80°C.

B.6.5. Isolation of Caveolae.

Caveolae were isolated from plasma membranes as described by Chang et al. (1994) with some modifications. All procedures were carried out at 4°C. Briefly, plasma membranes (500 µl) in isolation buffer (50 mM MOPS pH 7.1 containing 300 mM NaCl, 5.0 mM EDTA, 5.0 mM EGTA, 1.0 mM dithiothreitol, 0.1 mM PMSF and 1.0% Triton X-100) were homogenized 15× with a motor-driven Teflon pestle (moderate speed) in a 2.0 ml glass homogenization vessel, and then allowed to incubate with rocking for 30 min. They were then layered onto a discontinuous sucrose gradient consisting of 800 µl each of 2.0%, 7.5%, 15%, 25% and 45% sucrose in isolation buffer. Centrifugation was for 90 min at 23,000×*g* in an SW 50.1 rotor. The supernatant, containing Triton X-100 soluble components, was recovered from the top of the gradient. Caveolae (recovered from the 2.0-7.5% interface) and the pellet of the gradient were diluted 5-fold with isolation buffer (lacking Triton X-100) and were pelleted by centrifugation for 18 min at 4°C and 10^5 rpm using a TLA 100.2 rotor in a Beckman TL-100 ultracentrifuge. Pellets

were resuspended to 5.0 mg protein/ml in PBS containing 0.10 mM PMSF and were stored at -80°C prior to use.

B.7. Enzyme, Inorganic Phosphate and Protein Assays

B.7.1. Long Chain ACS

3T3-L1 cell homogenates and subcellular fractions were prepared as described in Sections B.6.1 and B.6.3, respectively. ACS assays were carried out according to Leblanc and Gerber (1984) using the conditions of Hall and Saggerson (1985). Cellular fractions (0.10 mg protein/ml) were incubated for 2.0 min at 37°C in 0.35 M tris-HCl pH 7.5 (unless otherwise indicated) containing 0.10 % Triton X-100, 5.0 mM DTT, 10 mM ATP and 0.50 mM CoASH. Assays were initiated with the addition of [9,10-^{3}H]oleate to a final concentration of 50 μM. Aliquots of 100 μl were withdrawn at various times and were diluted into 0.50 ml of heptane:isopropanol:1.0 N sulphuric acid (40:10:1, by volume). Heptane and water (0.30 ml of each) were added to bring about phase separation and the aqueous phase, containing [9,10-^{3}H]oleoyl-CoA, was extracted four times with 1.0 ml of diethyl ether. The radioactivity remaining in the aqueous phase was determined by liquid scintillation counting as described in Section B.4.3.

B.7.2. 5'-Nucleotidase

5'-Nucleotidase activity (plasma membrane marker enzyme) was assayed as described by Touster et al. (1971). All plasticware and glassware were precleaned and phosphate-free. Membrane fractions were diluted into 10 mM HEPES, 1.0 mM EDTA, pH 7.4 (ice-cold) and pelleted by centrifugation at 4°C and 10^5 rpm using a TLA 100.2

rotor in a Beckman TL-100 ultracentrifuge. Pellets were resuspended in ice-cold, 10 mM HEPES, 1.0 mM EDTA, pH 7.4. Fractions (0.050 mg protein) were incubated for 5.0 min at 37°C in 0.90 ml of 55.6 mM imidazole, pH 7.4, containing 11.1 mM $MgCl_2$ and 0.011 % Triton X-100. Reactions were initiated with the addition of 0.10 ml of 50 mM AMP, pH 7.4. Blanks lacking enzyme or AMP were routinely included. The reaction was found to be linear for at least 60 min at 37°C (data not shown), but was typically stopped after 30 min by the addition of 1.0 ml of ice-cold 10 % trichloroacetic acid. Samples were centrifuged in an Beckman Microfuge E for 15 min at 4°C and 1.0 ml aliquots were removed for the determination of inorganic phosphate as described below (Section B.7.4).

B.7.3. Glucose-6-Phosphatase

Glucose-6-Phosphatase (ER marker) was assayed according to Canfield and Arion (1988). All plasticware and glassware were precleaned and phosphate-free. Briefly, fractions (50-100 μg of protein, prepared as described for 5'-nucleotidase assays) were incubated at 30°C in 0.30 ml of 50 mM HEPES, pH 7.0, containing 0.10 % Triton X-100 and 30 mM glucose-6-phosphate for varying times up to 60 min. Blanks lacking enzyme or substrate (glucose-6-phosphate) were routinely included. Reactions were terminated by pipetting 0.050 ml into 0.25 ml of 10 % SDS. Inorganic phosphate was assayed as described in the following section.

B.7.4. Inorganic Phosphate

Inorganic phosphate was measured according to Ames (1966). Again, all tubes were free of phosphate. Samples and standards containing varying concentrations of sodium phosphate (0.30 ml) were added to 0.70 ml of a freshly prepared solution containing 0.36 % ammonium molybdate•$4H_2O$ and 1.42 % ascorbic acid in 0.86 N H_2SO_4, and were incubated at 45°C for 20 min. Samples were then cooled to room temperature and their absorbance was determined at 820 nm.

B.7.5. NADH-dehydrogenase

NADH-dehydrogenase activity (ER marker) was measured spectrophotometrically as described by Record et al. (1982). Samples (10-50 µg protein) were incubated at room temperature in 1.2 ml of 0.10 M tris-HCl, pH 7.4, containing 0.70 mM $K_3Fe(CN)_6$, 0.70 mM β-NADH (reduced) and 0.10 % Triton X-100. Reactions were carried out in polystyrene, semi-micro cuvettes, and the decrease in absorbance at 410 nm was monitored continuously. Blanks lacking enzyme or β-NADH were routinely included.

B.7.6. Cytochrome C-Oxidase

Cytochrome C-oxidase activity (mitochondrial marker) was assayed according to the method of Appelmans et al. (1955). Briefly, cytochrome C (1.2 ml of 0.38 mg/ml in 30 mM ammonium acetate, pH 7.4, containing 0.010 % Triton X-100) in a disposable, semi-micro cuvette, was reduced with a few crystals of sodium dithionite. The absorbance of this was determined at 550 nm. Fractions to be tested (up to 50 µl) were added and rapidly mixed. The decrease in absorbance at a wavelength of 550 nm was

measured, and the initial rate was taken as a measure of the cytochrome C-oxidase activity.

B.7.7. Catalase

Catalase activity (peroxisomal marker) was determined as the rate of the decrease in the absorbance at 240 nm of a solution containing 0.070 % H_2O_2 and 0.010 % Triton X-100 in 50 mM sodium phosphate, pH 7.4, upon the addition of membrane fractions (Beers and Sizer, 1952).

B.7.8. Protein

Protein concentrations in delipidated cytoplasmic fractions were determined using the Biorad protein assay kit, with BSA as the standard. The concentrations of protein in cell homogenates and membrane fractions were determined by the method of Lowry et al. (1951). Briefly, samples were solubilized with 1.0 % SDS in a final volume of 0.20 ml. A solution of 2.0 % Na_2CO_3 and 0.020 % sodium potassium tartarate in 0.10 N NaOH was mixed with 0.50 % $CuSO_4 \cdot 5H_2O$ at a ratio of 50:1 and 1.0 ml of this was added to the samples. The reaction was allowed to proceed for 30 min at room temperature prior to the addition of 0.10 ml of 1.0 N Folin-Ciocalteau's Phenol Reagent. The reaction was then allowed to proceed at room temperature for 60 min. The absorbance at 660 nm was then determined spectrophotometrically using a Cary-210 spectrophotometer. BSA was used as the protein standard.

B.8. Photoaffinity Labeling with 11-DAP-[11-^{3}H]undecanoate

B.8.1. Labeling of Samples in Suspension

Samples to be labeled (cells, isolated membranes, or BSA, in PBS, or cytoplasm in 10 mM sodium phosphate, pH 7.4) were prepared as 2-fold stocks and were incubated at 37°C for 5.0 min in disposable semi-micro cuvettes. Equal volumes of stock solutions of 11-DAP-[11-^{3}H]undecanoate (prepared in the same buffers) were added and samples were incubated in the dark for the indicated times. Photolysis was carried out with a 1000 W, Xe-Hg arc lamp (Spectral Irradiation Corp.) in an LH151N/2 lamp housing with a LPS255HR power supply (Schoeffel Instruments Corp.). Cuvettes containing samples to be irradiated were placed in a cuvette holder at the focal point. The beam of light was filtered by passage through 0.020 % potassium hydrogen phthalate (5.0 cm pathlength in a quartz cell), which absorbs light of wavelengths below 300 nm (data not shown). Otherwise, the beam was filtered through two Corning 7-51 optical filters, the first of which was in a water-filled quartz cell of 5.0 cm pathlength (Leblanc et al., 1982). These have a peak transmittance at 360 nm (manufacturer's specifications). Photolysis was routinely for 5.0 sec (potassium hydrogen phthalate filter) or 30 sec (Corning 7-51 filters) by removal of a metal shield blocking the path of the light beam.

Cells, labeled in suspension, were pelleted in 1.5 ml Eppendorf tubes at 450×*g* for 10 minutes at 4°C, and the supernatant was discarded. Labeled membranes were pelleted

at 356,000×*g* for 40 minutes at 4°C using a Beckman TLA 100.2 rotor and the supernatant was discarded. If BSA was included in the labeling reaction, membrane pellets were washed twice in PBS containing 0.50 % BSA and once in PBS (both at room temperature) and were pelleted as above. All pellets were stored at -20°C until used. Labeled cytoplasm was stored at -20°C and then dried under vacuum using a speed-vac concentrator.

B.8.2. Photoaffinity Labeling of Cell Monolayers

Cell monolayers in 1.5 cm diameter wells in 4-well tissue culture trays were washed twice with 500 µl of PBS (37°C) and were placed in a tray of water (37°C) on a platform so that a single well was at the correct position for irradiation (see below). The monolayer was overlaid with 200 µl of PBS containing BSA and 11-DAP-[11-^{3}H]undecanoate at the specified concentrations and incubated for various times at 37°C prior to photolysis. For photolysis, a mirror was placed at a 45° angle at the focal point of the lamp to redirect the beam vertically onto the cell monolayer. The area irradiated was slightly larger than the 1.5 cm diameter well of a 4-well tissue culture tray. Photolysis was done routinely for 2 sec.

After photolysis, the irradiated photoreactive fatty acid:BSA solution was removed from cell monolayers, which were then washed four times with 300 µl of 1.0 % BSA in PBS and twice with 300 µl of PBS. All washes were at 37°C. Monolayers were suspended in 300 µl of distilled water and stored at -20°C after the addition of PMSF to 0.10 mM.

B.9. Cellular Binding of BSA

BSA was labeled with 11-DAP-[11-^{3}H]undecanoate as described in Section B.8.1. The binding of labeled BSA by intact 3T3-L1 adipocytes was measured as described by Reed and Burrington (1989) under conditions which paralleled oleate uptake assays. Briefly, 3T3-L1 adipocytes (2.0 mg of cellular protein/ml in 50 µl of PBS) were incubated at 37°C for 5.0 minutes. An equal volume of 11-DAP-[11-^{3}H]undecanoate-labeled BSA was added and the incubation was allowed to continue with gentle agitation for 60 sec. Cells were pelleted by centrifugation for 10 sec in a Beckman Microfuge E, and supernatants were recovered. The pellet surfaces were gently washed with 100 µl of PBS and then centrifuged as described above. Portions of each pellet and supernatant fraction were analyzed by SDS-PAGE (Section B.10.2) and the amount of labeled BSA was determined by quantitation of radioactivity in gel slices (Section B.10.6). Data plotted as the amount of BSA bound to cells versus the BSA concentration were fit by equation (3) (Section B.4.3) where v is the amount of BSA bound, c is the concentration of BSA, V_{max} is the maximal binding for the saturable process, $K_{0.5}$ is the apparent dissociation constant for the saturable process, and k is the coefficient for non-saturable binding.

B.10. Immunoprecipitation, Electrophoresis and Immunoblotting

B.10.1. Immunoprecipitation

This was done according to a protocol supplied by Dr. Karen Rothberg (R.G.W. Anderson Laboratory, Univ. Texas, S.W. Medical Inst., Dallas). All procedures were carried out at 4°C. Plasma membrane proteins to be immunoprecipitated (0.52 mg protein/ml) were solubilized at 4°C with 1.0% Triton X-100 and 60 mM octylglucoside (Lisanti, et al., 1993) in 25 mM tris-HCl, pH 7.5, 5.0 mM EDTA, 250 mM NaCl, 20 μM APMSF, bestatin (40 μg/ml), 1.0 μM leupeptin and 1.0 μM pepstatin with constant mixing for 4.0 h. Solubilized proteins were precleared after a 2.0 h incubation with 1.0 μg of mouse IgG by a 30 min treatment with protein A-Sepharose beads. Complexes were removed by centrifugation for 5.0 min in a Beckman microfuge E. Precleared, solubilized membrane proteins (0.091 mg membrane protein/ml) were incubated with antibodies in 25 mM tris-HCl, pH 7.5, containing 5.0 mM EDTA, 250 mM NaCl 1.0% Triton X-100 and BSA (30 mg/ml). Immunocomplexes were precipitated after incubation with protein A-Sepharose by centrifugation as described above. Pelleted protein A-Sepharose beads were washed twice with 1.0 ml of 25 mM tris-HCl pH 7.4 containing 5.0 mM EDTA, 500 mM NaCl and 1.0% Triton X-100, twice with the same solution containing 250 mM NaCl and twice with 10 mM tris-HCl pH 7.5 containing 5.0 mM EDTA. Immunoprecipitated proteins were released from the protein A-Sepharose beads

by boiling for 1.5 min after the addition of 40 µl of 0.25 M tris-HCl pH 6.8, containing 10% SDS, 100 mM DTT, 24% glycerol and 0.014 % bromophenol blue.

B.10.2. SDS-PAGE

Whole cell extracts were prepared for SDS-PAGE by incubation (at 1.0 mg of cell protein/ml) in 2.0 mM $MgSO_4$ containing 1.0 mM PMSF and DNase 1 and RNase A (each at 10 µg/ml) for 15 minutes at 37°C. Each sample was then dried under vacuum in a speed-vac concentrator. Samples for SDS-PAGE were solubilized by boiling for 5.0 min in SDS-PAGE sample buffer (125 mM tris-HCl, pH 6.8, containing 5.0 % SDS, 10.0 % β-mercaptoethanol, 12.0 % glycerol and 0.0070 % bromophenol blue; where indicated, 10.0 % β-mercaptoethanol was replaced with 5.0 mM DTT).

SDS-PAGE was performed according to Laemmli (1970), using a Mini-Protean II apparatus (Biorad). Separating gels were composed of either 10, 12.5 or 15 % polyacrylamide (acrylamide:*N*,*N*'-methylenebisacrylamide ratio of 37.5), in 0.375 M tris-HCl, pH 8.8, containing 0.10 % SDS and 1.0 % (v/v) glycerol. All separating gels were overlaid with stacking gels composed of 4.0 % polyacrylamide in 0.125 M tris-HCl, pH 6.8 containing 0.10 % SDS. Electrophoresis was done at 200 V in 0.0249 M tris, 0.192 M glycine, pH 8.3, containing 0.10 % SDS.

B.10.3. Two Dimensional-PAGE

2D-PAGE was performed by non-equilibrium-isoelectric focussing (NE-IEF) in the first dimension and SDS-PAGE in the second dimension. Membrane samples were solubilized for NE-IEF according to Ames and Nikaido (1976). Samples (14.9 µl of 2.5

μg of membrane protein/μl) were mixed with 3.7 μl of SDS-solubilization solution (0.25 M tris-HCl, pH 6.8 containing 2.6 % SDS and 2.46 mM $MgCl_2$) and were boiled for 5.0 min. After the addition of 7.5 μl of NP-40 sample dilution solution (10.4 % NP-40, containing 7.0 % ampholytes and either 20 % β-mercaptoethanol or 10.0 mM DTT), 15.5 mg of urea was added. For NE-IEF of cytoplasmic samples, 4.0 mg cytoplasmic protein were added to a solution containing 1.8 % CHAPS, 8.0 M urea and 1.0 % ampholytes (Bernier et al., 1987).

Samples were loaded onto 1.0 mm diameter tube gels in a Biorad Mini-IEF chamber, and were overlaid with 25 μl of a solution containing 1.0 % urea and 1.0 % ampholytes. NE-IEF gels consisted of 4.0 % polyacrylamide (acrylamide:*N*,*N*'-methylenebisacrylamide ratio of 17.5), 9.0 M urea, 2.0 % ampholytes and either 2.0 % NP-40 (for membrane samples) or CHAPS (for cytoplasmic samples). For the separation of membrane proteins, a 2:2:1 mixture of 4-6:6-8:3-10 ampholytes was used, while 3-10 ampholytes were used for the separation of cytoplasmic proteins. Focussing was performed using 20 mM NaOH and 10 mM H_3PO_4 as electrolytes, at 500 V for 10 minutes and at 750 V for either 2.0 h (membrane samples) or 1.0 h (cytoplasmic samples). In all cases, samples were focussed from the basic to the acidic end of the gels.

After NE-IEF, tube gels were equilibrated for 5.0 minutes in SDS-PAGE sample buffer (where indicated, 10.0 % β-mercaptoethanol was replaced with 5.0 mM DTT) and overlaid onto 12.5 % polyacrylamide gels of 1.0 mm thickness. SDS-PAGE was carried

out as described above (Section B.10.2) using gels of 12.5 % acrylamide for membrane samples and 15 % acrylamide for cytoplasmic samples.

B.10.4. Transfer of Proteins onto Membranes and Immunoblotting

This was performed according to a protocol supplied by Dr. Leonard Craig (R.G.W. Anderson Laboratory). Proteins were electrophoretically transferred to PVDF membranes immediately after SDS-PAGE, using a Biorad mini-transblot apparatus (Towbin et al., 1979). Prior to transfer, both membranes and gels were soaked in transfer buffer (21 mM tris, 192 mM glycine, pH 8.3) for 5.0 min. Transfer was for 2 h at 50 V and 4°C. Membranes were blocked by an overnight incubation at 4°C in 20 mM tris-HCl (pH 7.6) containing 137 mM NaCl (TBS), with 5.0% Carnation skim milk powder and 0.50 % tween-20. Reactions with primary antibodies were typically carried out at room temperature for 60 min at 2000-fold dilutions of antibodies in TBS containing 1.0% Carnation skim milk powder and 0.20% tween-20. Membranes were washed several times with TBS containing 0.20% skim milk powder and 0.20% tween-20. Blots were incubated for 60 min at room temperature with secondary antibodies (conjugated to horseradish peroxidase) in TBS containing 1.0% skim milk powder and 0.20% tween-20. Secondary antibodies were horseradish peroxidase conjugated to anti-mouse IgG (16, 000-fold dilution, for monoclonal primary antibodies) and horseradish peroxidase conjugated to anti-rabbit IgG (20,000-fold dilution, for rabbit polyclonal antibodies). After washing (as above) antibody binding was detected by chemiluminescence using the ECL method (Amersham).

B.10.5. Visualization of Proteins in Gels

Immediately after SDS-PAGE, polyacrylamide gels were stained by soaking for at least 1.0 h at room temperature in 0.050 % Coomassie Brilliant Blue R-250 in H_2O:isopropanol:acetic acid (65:25:10). Excess stain was removed with 10 % acetic acid (overnight at room temperature).

To visualize proteins labeled with tritium, gels were processed for fluorography by incubation for 15 min in 4 × their volume of fluorography reagent. Otherwise, fluorography was performed according to Bonner and Laskey (1974) with equivalent results. Briefly, stained gels were soaked twice for 15 min each in 20 × their volume of DMSO and incubated for 90 min in 4 × their volume in a solution of PPO (22.2 % in DMSO). PPO was precipitated in the gel by soaking for 30 min in an excess of H_2O. Fluorographed gels were dried at 80°C for 30 min and exposed to x-ray film at -80°C.

B.10.6. Measurement of Radioactivity in Labeled Proteins in Polyacrylamide Gels

Radioactively labeled bands located by exposure of fluorographed gels to x-ray film were excised from the dried gel and rehydrated by soaking in 500 µl of H_2O at 50°C for 30 min. Solvable gel and tissue solubilizer (500 µl) was added and samples were incubated at 50°C for 3.0 h. Atomlight scintillant (10.0 ml) was then added and radioactivity was determined by scintillation counting as described in Section B.4.3.

C. RESULTS AND DISCUSSION

C.1. Characterization of Oleate Uptake

C.1.1. Effect of Differentiation from Preadipocytes to Adipocytes

During the differentiation of 3T3-L1 preadipocytes to adipocytes, a variety of genes encoding proteins involved in LCFA metabolism and triglyceride synthesis become induced (Table 3). Among these are the genes encoding long chain ACS (Amri et al, 1994; Coleman et al., 1978) and ALBP (Bernlohr et al., 1984; Phillips et al., 1986; Spiegelman et al., 1983), both of which have been proposed to be involved in LCFA uptake (Noy and Zakim, 1993; Peeters and Veerkamp, 1989; Peeters, et al., 1989; Luxon and Weisiger, 1993; Stewart, 1991; Vork et al., 1991, 1993). The time-dependent changes in the specific activity of ACS and the level of ALBP during differentiation of 3T3-L1 preadipocytes to adipocytes are shown in figures 7 and 8, respectively.

In figure 7, the specific activities of ACS in cellular homogenates were measured using [9,10-^{3}H]oleate as substrate. Day 0 refers to the day in which the cells reached confluence and stimulation was initiated (as described in Section B 3.3). The rate of oleate activation to oleoyl-CoA began to increase at day 2 and continued to increase up to day 6, at which point it was 34-fold that of confluent, undifferentiated cells (day 0), in agreement with results reported by Coleman et al. (1978) for the specific activity of palmitate activation. The rate of oleate conversion to oleoyl-CoA by homogenates from

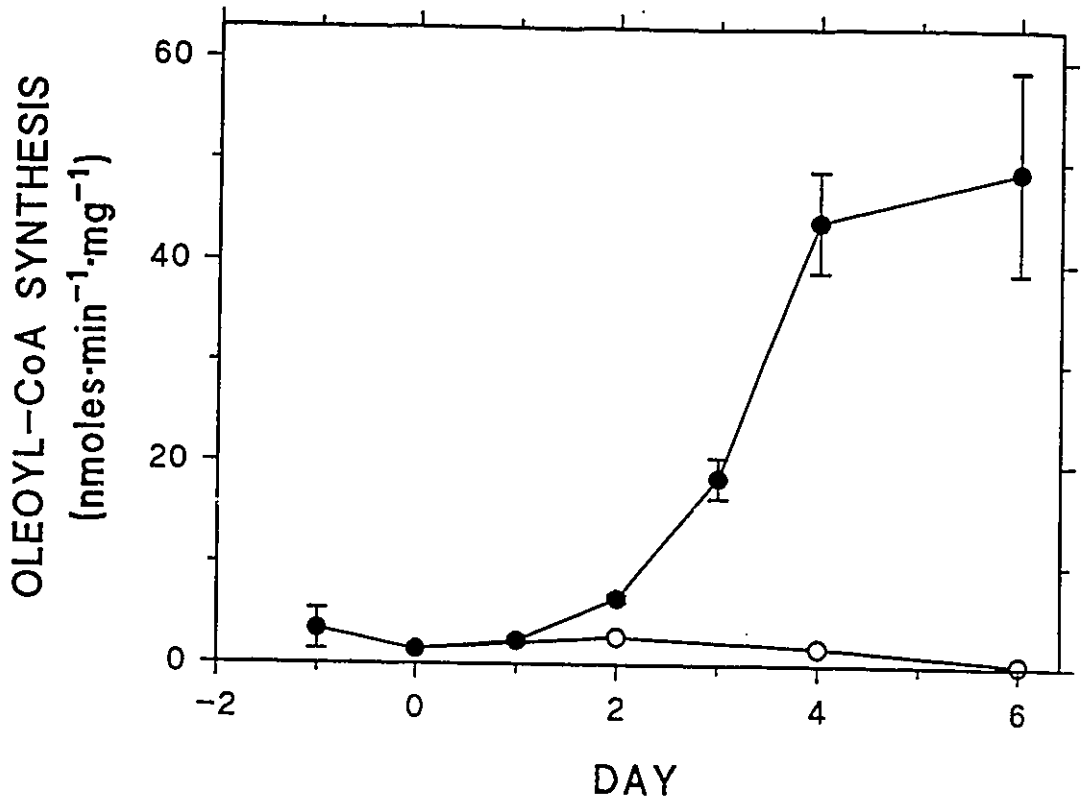

Figure 7. **Induction of long chain ACS activity upon differentiation of 3T3-L1 preadipocytes to adipocytes.** 3T3-L1 cells were either stimulated to differentiate (●) or maintained beyond confluence in an undifferentiated state (○) as described in Section B.3.3. On various days (day 0 denotes the day on which differentiation was initiated) cells were harvested and homogenized. Long chain ACS activities in homogenates were assayed as described in Section B.7.1, as the conversion of [9,10-^{3}H]oleate to [9,10-^{3}H]oleoyl-CoA. The results were normalized for total protein, and are expressed as the average rate of duplicate assays. Error bars indicate the variation.

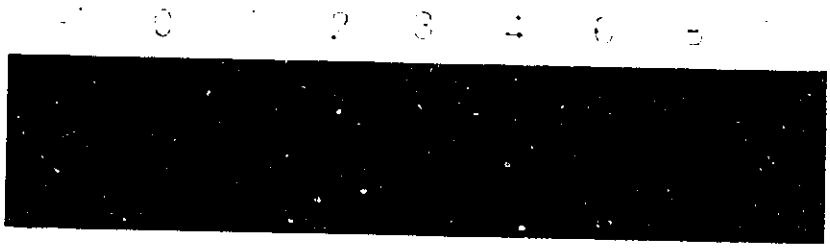

Figure 8. **Induction of ALBP upon differentiation of 3T3-L1 preadipocytes to adipocytes.** 3T3-L1 cells were stimulated to differentiate as described in Section B.3.3. Proteins from cells at various stages of differentiation were analysed by SDS-PAGE and transferred onto PVDF membranes. These were probed with an affinity-purified rabbit primary antibody specific for murine ALBP and horseradish peroxidase conjugated to a donkey, anti-rabbit secondary antibody. Antibody binding was detected by chemiluminescence using the ECL kit (Amersham). The numbers at the top of the panel indicate the stage of differentiation in days. Day -1 indicates preadipocytes, while day 0 denotes the day on which differentiation was initiated.

cells maintained beyond confluence in medium containing 9.0 % cat serum, which does not support differentiation (Kuri-Harcuch and Green, 1978), did not increase.

The levels of ALBP in homogenates from cells at various stages of differentiation were measured by Western analysis using an affinity purified anti-murine ALBP antibody (figure 8). No immunoreactive ALBP was observed prior to day 3 of differentiation (even in overexposures; data not shown). Immunoreactive ALBP increased substantially from day 3 to day 10. This was in agreement with increases observed at the mRNA level (Amri et al., 1995).

It has been reported that upon differentiation, 3T3-L1 cells utilize LCFAs in the culture medium at increased levels (Green and Kehinde, 1975). To investigate whether this was accompanied by increased LCFA uptake, and if so, whether the time dependence of increased uptake upon differentiation matched that observed for the induction of ACS and ALBP, cellular uptake of [9,10-^{3}H]oleate by 3T3-L1 preadipocytes and adipocytes was measured by a filtration assay using conditions described by Abumrad et al. (1981) and Stremmel and Berk (1986). Time courses of oleate uptake by preconfluent 3T3-L1 preadipocytes and differentiated 3T3-L1 adipocytes were linear for up to two minutes (figure 9). The rate of uptake by 3T3-L1 adipocytes was 50-fold higher than that by preadipocytes when normalized for cell number (14 nmoles/min/10^{6} adipocyte cells compared with 0.28 nmoles/min/10^{6} undifferentiated cells).

The differentiation of 3T3-L1 preadipocytes to adipocytes was accompanied by an increase in the cellular protein content (figure 10a), as reported by others (Student et al.,

1980). Oleate uptake, measured at various stages of differentiation was therefore expressed in figure 10b as the specific activity, normalized to the level of cellular protein. Uptake rates began to increase 2 days after cells were stimulated to differentiate, but remained relatively constant for those cells maintained in an undifferentiated state in the presence of cat serum (figure 10b). The rates of oleate uptake by differentiating cells continued to increase until day 5, at which time, stimulated cells showed an 8.5-fold higher activity than confluent, undifferentiated cells (5.3 compared with 0.62 nmoles/min/mg of cellular protein). After this point, uptake rates began to drop. This may have been due to increasing instability of the cells during the filter assay, since they accumulate more lipid and have higher levels of basal lipolysis with continued differentiation (Kawamura et al., 1981). Continued lipolysis has been shown to result in cell instability, probably due to the accumulation of fatty acids (Strålfors, 1990). This decrease in uptake activity was not studied further.

The induction of oleate uptake, ACS activity, and ALBP, therefore followed similar time courses (compare figures 7, 8 and 10b). This is consistent with, but does not show, the involvement of ACS and ALBP in LCFA uptake. It does indicate, however, that 3T3-L1 cells should represent a convenient model system in which to study the cellular components involved in the uptake process.

C.1.2. Effect of Uncomplexed LCFA Concentration on Uptake

The first step in the LCFA uptake process is the interaction of LCFAs with the cell surface. Non-esterified LCFAs circulate in the plasma of mammals complexed to

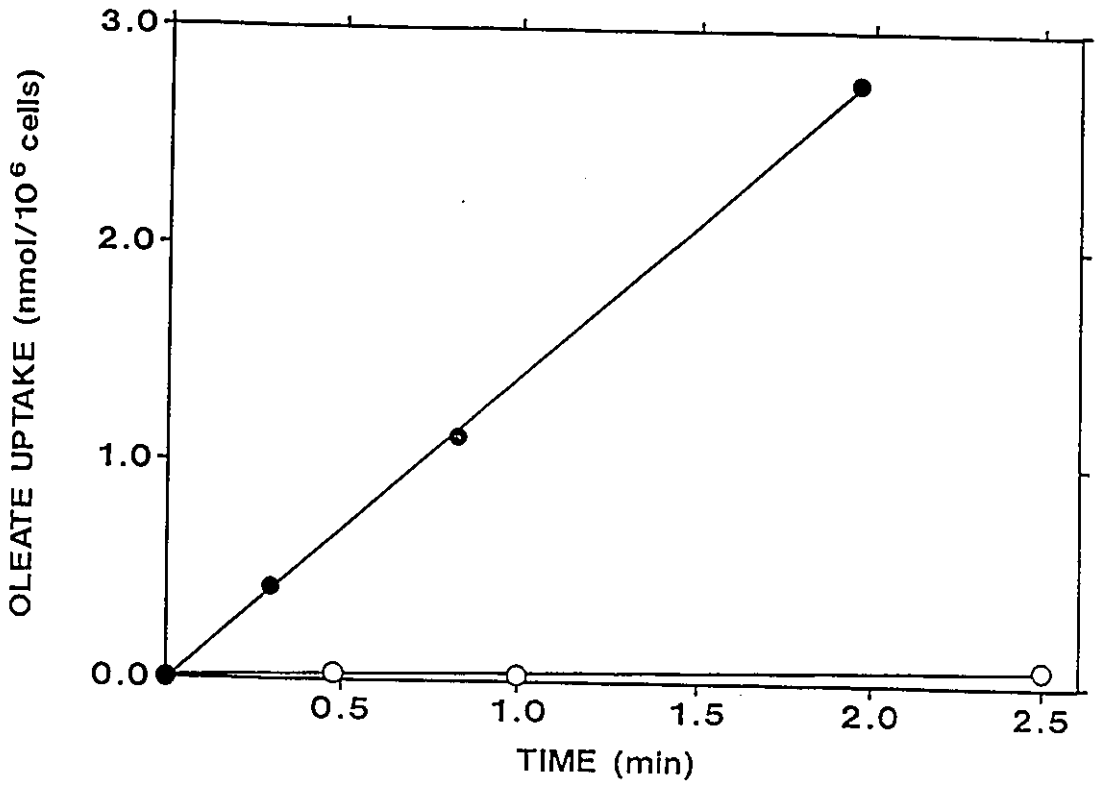

Figure 9. **Time-course of oleate uptake by 3T3-L1 adipocytes and preadipocytes.** 3T3-L1 adipocytes (●) were harvested 6 days after stimulation to differentiate, while preadipocytes (○) were harvested one day prior to confluence. A suspension of 5.0 x 10^5 cells/ml in PBS were incubated with a 1:1 molar ratio of [9,10-^{3}H]oleate:BSA (0.173 mM) at 37°C, aliquots were filtered at various times and the amount of radioactivity retained by the figures was determined as described in Section B.4.3.

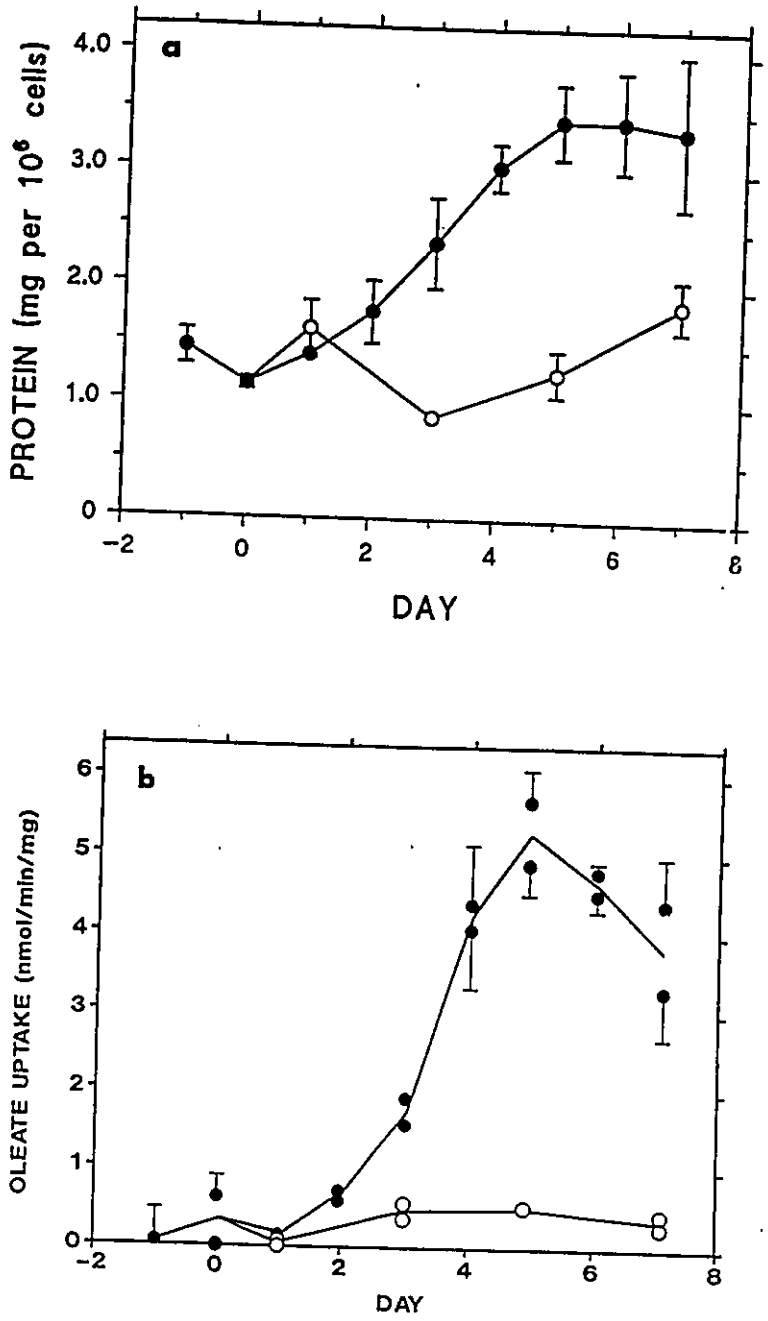

Figure 10. **Changes in cellular protein and [9,10-^{3}H]oleate uptake upon differentiation of 3T3-L1 preadipocytes to adipocytes.** 3T3-L1 cells were either stimulated to differentiate (●) or maintained beyond confluence in an undifferentiated state (○) as described in Section B.3.3. On various days (day 0 denotes the day on which differentiation was initiated) duplicate plates were harvested. **a.** Cellular protein and **b.** [9,10-^{3}H]oleate uptake rates (normalized for cellular protein) were measured as described in Sections B.7.8 and B.4.3, respectively. The results are expressed as the average rate of duplicate assays from each plate. Error bars indicate the variation between data points.

SA. The involvement of SA in LCFA uptake has generally been assumed to be in the solubilization of LCFA in the aqueous environment to provide a pool of bound LCFA to replenish uncomplexed LCFA that has been depleted by cellular uptake (Abumrad et al., 1981; Sorrentino and Berk, 1993; Sorrentino et al., 1989; Stremmel and Berk, 1986; Wolkoff, 1987). In this view, it is assumed that there is no direct interaction between the cells and LCFA:SA complexes which is relevant for LCFA uptake. Accordingly, uptake rates have routinely been plotted versus the concentration of uncomplexed oleate in equilibrium with oleate complexed to BSA (Abumrad et al., 1981; Schwieterman et al., 1988; Stremmel and Theilmann, 1986). The equilibrium binding of [9,10-^{3}H]oleate to BSA, as measured by the heptane partitioning method of Goodman (1958) as described by Spector et al. (1969, 1971), is shown in figure 11a. This was used as a standard curve to determine the concentration of uncomplexed [9,10-^{3}H]oleate in equilibrium with BSA at various [9,10-^{3}H]oleate:BSA ratios.

The rates of [9,10-^{3}H]oleate uptake were plotted versus the corresponding concentration of uncomplexed [9,10-^{3}H]oleate (figure 11b). Oleate uptake exhibited both saturable and non-saturable components. The latter (k of 1.57 nmoles/min/mg/μM, see equation 3, Section B.4.3) appears to be a general phenomenon, and has been thought to represent passive diffusion of LCFAs across the plasma membrane (Abumrad et al., 1981; Schwieterman et al., 1988; Sorrentino et al., 1988; Zhou et al., 1992). Because of its linear nature, it becomes a significant portion of total uptake only at high concentrations

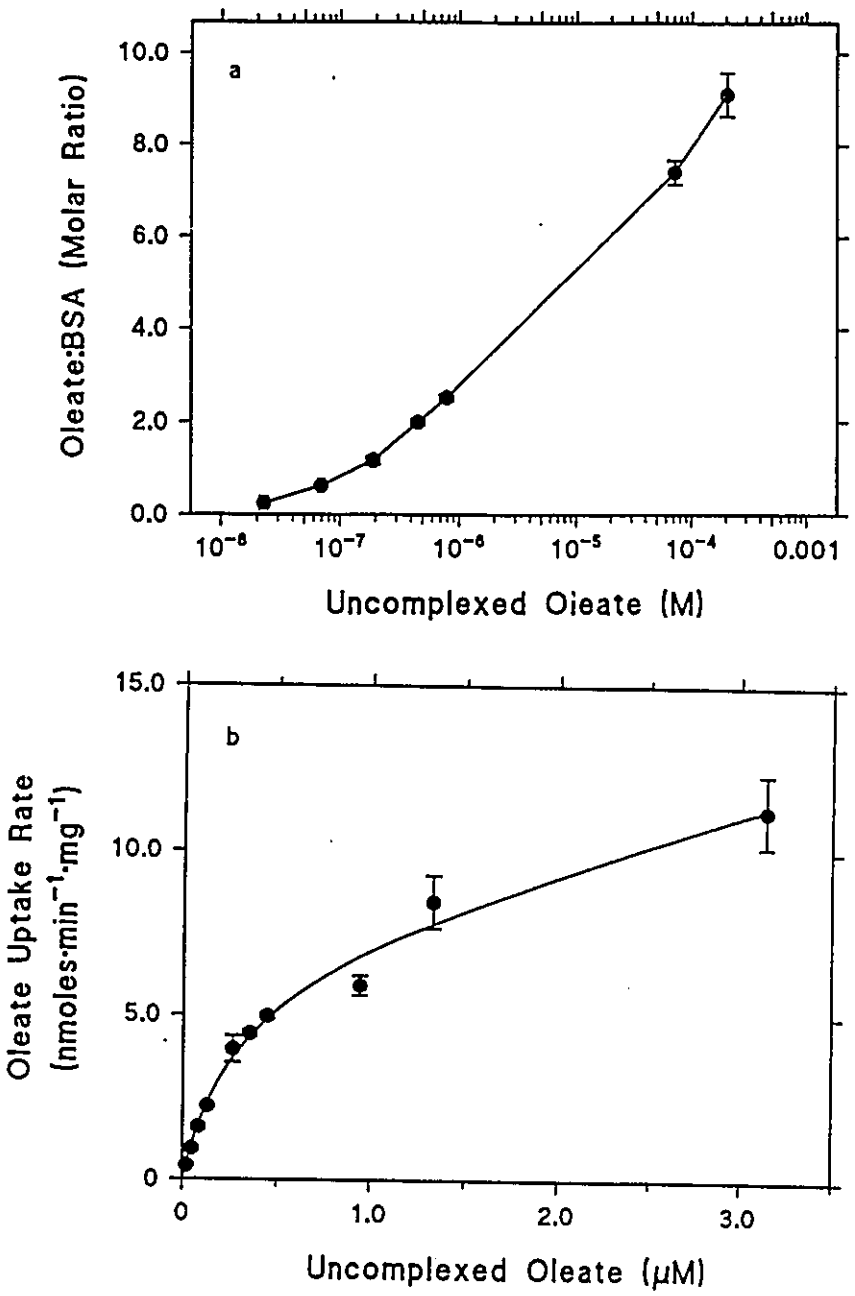

Figure 11. **[9,10-^{3}H]Oleate binding to BSA and uptake by 3T3-L1 adipocytes as a function of uncomplexed oleate concentration.** **a.** [9,10-^{3}H]Oleate binding to 0.50 mM BSA at 37°C was measured by the heptane partitioning method as described in Section B.4.2. Results are expressed as the average (two determinations) molar ratio of [9,10-^{3}H]oleate bound to BSA versus the concentration of uncomplexed [9,10-^{3}H]oleate. Error bars indicate the variation between datapoints. **b.** 3T3-L1 adipocytes were incubated at 37°C for 20 sec with increasing ratios of [9,10-^{3}H]oleate:BSA at a constant concentration of BSA of 173 μM, and oleate uptake was measured as described in Section B.4.3. Uptake rates (normalized to cellular protein) were plotted versus the concentration of uncomplexed oleate determined from the binding curve in **a.** The data represent the average ± S.E.M. of three determinations and were fit by equation (3).

Table 4. **Parameters for LCFA uptake in different cells.**

Cell Type	Ligand	$K_{0.5}$ (nM)	V_{max}
3T3-L1 Adipocyte	Oleate	301[a]	7.0 nmol/min/mg (16.1 nmol/min/10^6 cells)
		54[b]	6.6 nmol/min/mg
Rat Adipocyte	Oleate	300[c]	49.4 nmol/min/10^6cells
		60[d]	1.0 nmol/min/10 µl cells
	Stearate	160[d]	1.5 nmol/min/10 µl cells
	Palmitate	200[d]	2.5 nmol/min/10 µl cells
	Laurate	1500[d]	0.6 nmol/min/10 µl cells
Rat Hepatocyte	Oleate	83[e]	3.94 nmol/min/10^6cells
Rat Cardiomyocyte	Oleate	78[f]	1.9 nmol/min/10^6cells
		186[g]	9.5 nmol/min/10^6cells
X. laevis oocytes	Oleate	193[h]	110 pmol/h/oocyte

a. Present work, figure 5b.
b. Zhou et al., 1992.
c. Schweiterman et al., 1988.
d. Abumrad et al., 1984.
e. Stremmel et al., 1986.
f. Stremmel, 1988.
g. Sorrentino et al., 1988.
h. Zhou et al., 1994.

of uncomplexed LCFA, which are not physiologically relevant (Abumrad et al., 1981; Schwieterman et al., 1988; Sorrentino et al., 1988; Zhou et al., 1992).

From the parameters determined for oleate uptake from figure 11b, it is clear that 3T3-L1 adipocytes take up oleate with a high affinity ($K_{0.5}$ of 301 nM) and a high capacity (V_{max} of 7.0 nmoles/min/mg cellular protein). These parameters fall within the range of parameters measured for LCFA uptake by a variety of cells in different laboratories (Table 4). A substantial degree of variation can be observed, however, among analogous cell types. In part, this may be due to the assay conditions used; for instance, both $K_{0.5}$ and V_{max} for uncomplexed LCFA are dependent on the BSA concentration (Sorrentino et al., 1989; see next section).

C.1.3. Effect of SA on LCFA Uptake.

Under normal physiological conditions as well as conditions employed for most cellular LCFA uptake assays, the concentration of BSA, and therefore of LCFA-BSA complexes, greatly exceeds the concentration of uncomplexed LCFA (Spector, 1975; Spector et al., 1969). Furthermore, BSA has been shown to bind to the surface of a variety of cells (Dziarski, 1994; Horie et al., 1988; Popov et al., 1992; Reed and Burrington, 1989; Schnitzer et al., 1988; Torres et al., 1992b). This suggested that the concentration of LCFA complexed to SA at the cell surface might be significant. To test whether cells might utilize this rather than uncomplexed LCFA in the bulk medium, the effects of BSA on [9,10-^{3}H]oleate uptake by 3T3-L1 adipocytes were studied. In figure 12, the data from figure 11b were plotted as the rate of uptake versus the molar ratio of

oleate:BSA. Oleate uptake was linearly proportional to the ratio of oleate:BSA present. Furthermore, when the concentration of BSA was increased from 173 to 500 μM, the slope of the curve increased (from 2.75 to 8.29 nmoles/min/mg) indicating that BSA had a stimulatory effect on oleate uptake for each ratio of oleate:BSA, and therefore for each concentration of uncomplexed oleate tested. This effect was saturable with the concentration of BSA (figure 13). Values for $K_{0.5}$ and V_{max} of 379 μM BSA and 6.21 nmoles/min/mg of cellular protein, respectively were obtained when oleate uptake was measured at a constant ratio of oleate:BSA of 0.5:1 (figure 13a). When oleate uptake was measured at a ratio of oleate:BSA of 9:1 (figure 13b), $K_{0.5}$ and V_{max} values were 290 μM BSA and 278 μmoles/min/mg of cell protein, respectively. Results similar to those of figure 13a have been observed by others with rat hepatocytes, adipocytes and myocytes (Sorrentino and Berk, 1993; Sorrentino et al., 1988, 1989; Weisiger et al., 1981).

Berk and co-workers have proposed that this was the result of dissociation-limited uptake of LCFAs (described in Section A.5.3; Sorrentino and Berk, 1993; Sorrentino et al., 1989). However, the dissociation of LCFAs from SA has been reported to occur on the order of seconds or faster (Daniels et al., 1985). The data of figure 13b suggest that the saturability versus the BSA concentration was not the result of dissociation-limited uptake. Under the conditions of figure 13b (oleate:BSA of 9:1), the concentration of uncomplexed oleate was high (188 μM) and the rate of dissociation from BSA was fast (as oleate was loosely bound to BSA). Therefore, uncomplexed oleate was not likely to be depleted by uptake at any concentration of BSA. This suggests that the saturable

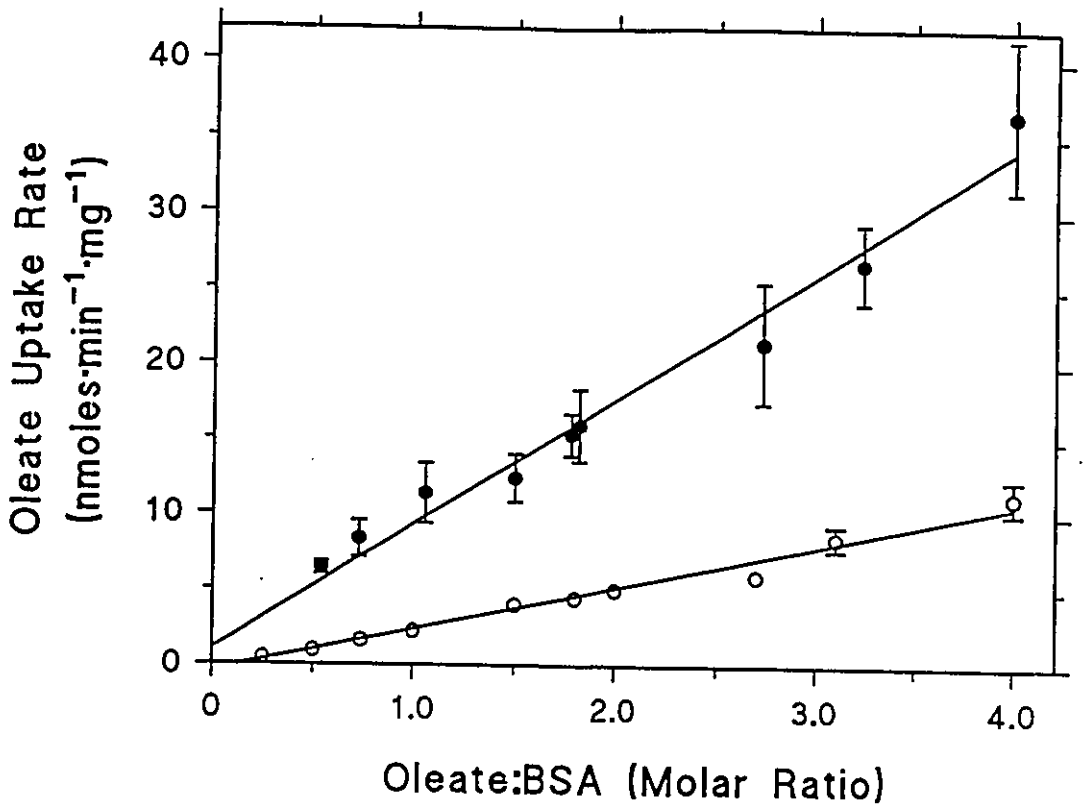

Figure 12. **Effect of BSA on the rate of [9,10-^{3}H]oleate uptake by 3T3-L1 adipocytes at increasing ratios of oleate:BSA.** [9,10-^{3}H]Oleate uptake by 3T3-L1 adipocytes was measured at increasing ratios of [9,10-^{3}H]oleate:BSA at fixed concentrations of BSA of 173 μM (○) and 500 μM (●) as described in Section B.4.3. Uptake rates were normalized for cellular protein. The data represent the average ± S.E.M. of three determinations.

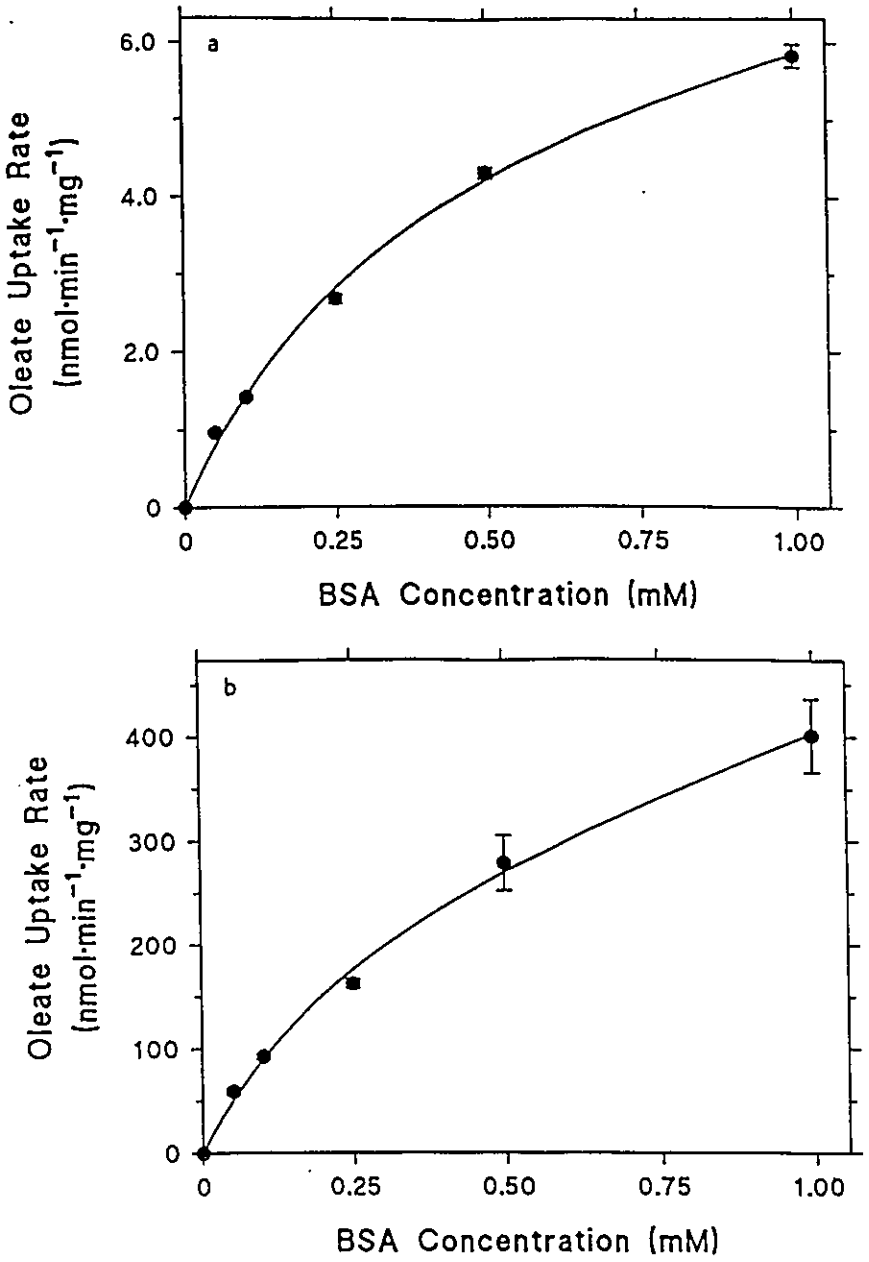

Figure 13. **The saturation of [9,10-^{3}H]oleate uptake by 3T3-L1 adipocytes with increasing concentrations of BSA.** The rates of [9,10-^{3}H]oleate uptake over 1.0 min time courses were determined as described in Section B.4.3. The concentrations of both BSA and oleate were varied so that the oleate:BSA ratio remained constant at **a.** 0.5:1 or **b.** 9:1, resulting in a constant concentration of uncomplexed oleate of 47 nM or 188 μM, respectively. The results are expressed as the average rates of oleate uptake ± S.E.M. of three determinations and are normalized for cellular protein content.

effect of BSA observed at lower oleate:BSA ratios might also not be the result of dissociation-limited uptake.

Further support for this is shown in figures 14 and 15. It was reasoned that if oleate uptake was limited by the dissociation of oleate from BSA at low BSA concentrations, then the rate of oleate uptake by 3T3-L1 adipocytes should have decreased as oleate became depleted by uptake and the limiting rate of dissociation from BSA became important. To vary the level of depletion of oleate, uptake was measured at increasing cell concentrations (figure 14). Oleate uptake was measured at a low BSA concentration (46.5 μM) in the range predicted to result in a limiting rate of dissociation of oleate from BSA (from figure 13). As the cell concentration was increased, the amount of oleate taken up approached and surpassed the amount of uncomplexed oleate initially present (figure 14, arrow). Furthermore, if the dissociation of oleate from BSA was rate-limiting, the time course of oleate uptake at low BSA concentrations should have appeared biphasic due to the increasing depletion of oleate with time, while the time course of oleate uptake at high BSA concentrations should have been linear. From figure 15, however, the time courses of oleate uptake by 3T3-L1 adipocytes were linear at both low and high BSA concentrations (50 μM and 500 μM BSA, at a constant oleate:BSA ratio of 2.0:1) even though the level of oleate uptake surpassed the calculated amount of oleate initially available as uncomplexed oleate (0.45 μM at the ratio of oleate:BSA used).

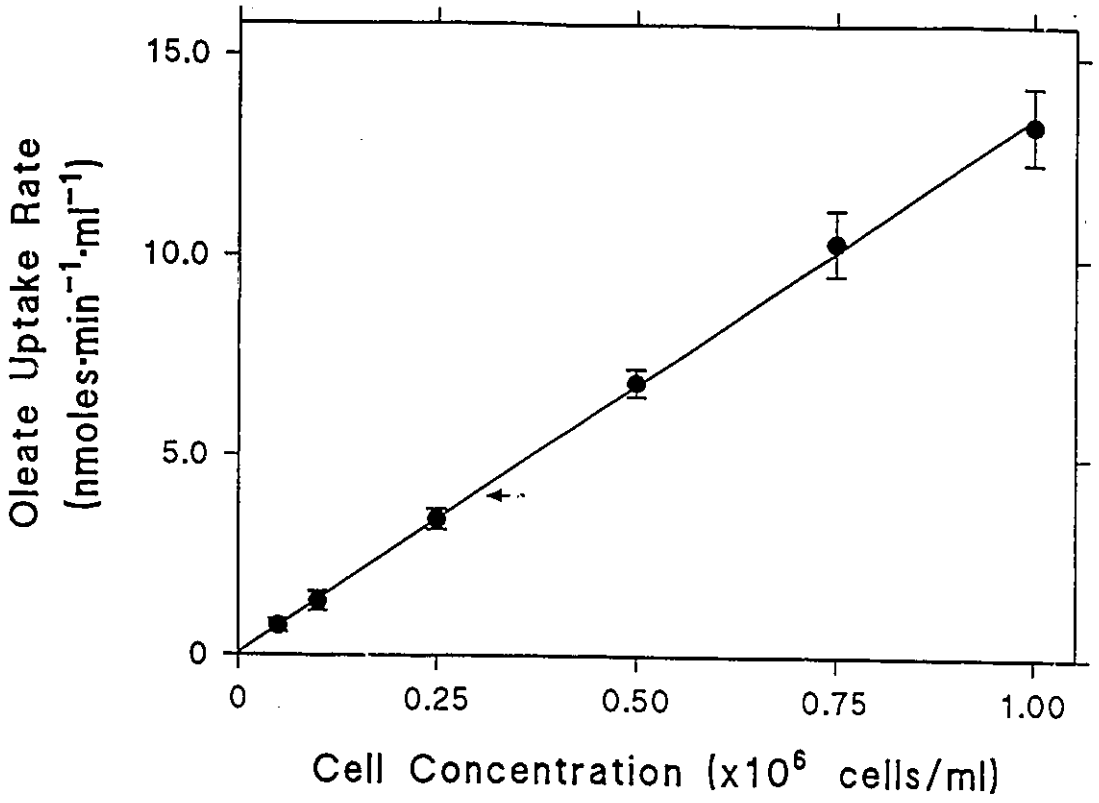

Figure 14. **Rate of [9,10-^{3}H]oleate uptake by 3T3-L1 adipocytes as a function of the cell concentration.** The rates of [9,10-^{3}H]oleate uptake were measured as a function of the concentration of 3T3-L1 adipocytes at a ratio of oleate:BSA of 4:1 in the presence of 46.5 μM BSA as described in the Experimental section. Results are expressed as the average rate of oleate uptake ± S.E.M. of three determinations. 10^6 cells contained 2.35 mg of protein. The arrow represents the point at which the amount of oleate taken up after 1.0 min was equivalent to the total amount of uncomplexed oleate initially present (4.0 μM).

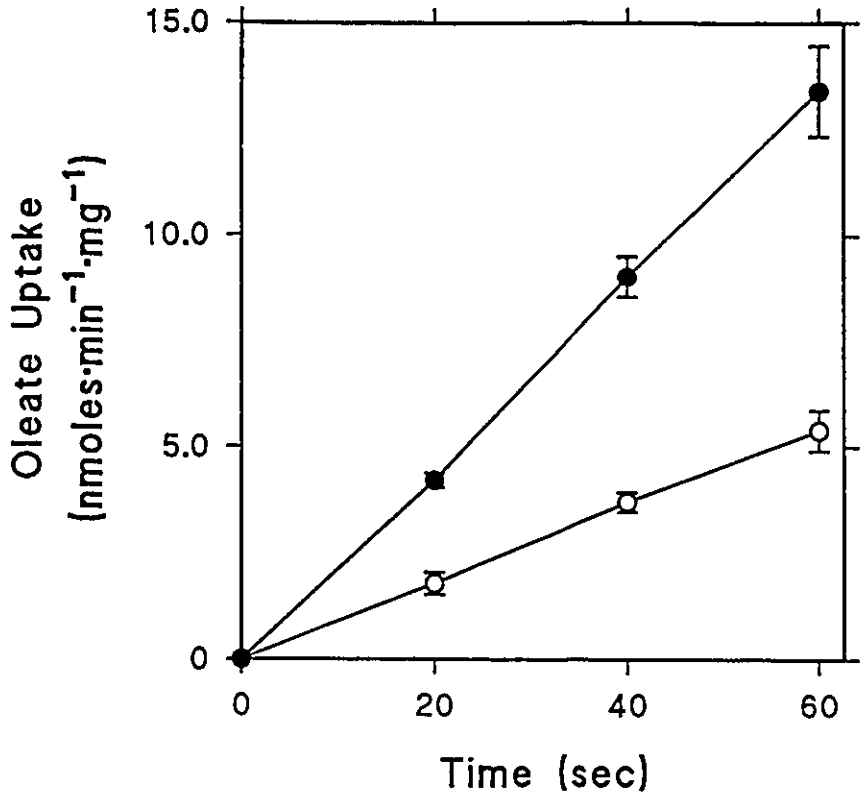

Figure 15. **Time courses of oleate uptake at different concentrations of BSA.** [9,10-^{3}H]Oleate uptake was measured as described in Section B.4.3. in the presence of either 50 (○) or 500 (●) μM BSA at an oleate:BSA ratio of 2:1, which results in an initial concentration of uncomplexed oleate of 450 nM. Results are expressed as the amount of oleate taken up per mg of cellular protein versus the time, in sec, of incubation with oleate:BSA and are the means ± S.E.M. of three determinations.

C.1.4. BSA Binding to the Cell Surface

These results demonstrate that the saturable effect of BSA was not due to dissociation-limited uptake, but rather to the concentration of oleate-BSA complexes. To test whether the stimulatory effect of BSA on oleate uptake may be due to a direct interaction between BSA and the cell surface, the cellular binding of BSA labeled with a photoreactive LCFA, 11-DAP-[11-^{3}H]undecanoate was studied (figure 16; the binding to and photoaffinity labeling of BSA by the photoreactive LCFA will be discussed in Section C.2). The data were modeled by equation 3 given in section B.4.3, as described in section B.9. Binding involved a saturable interaction with a K_d of 66.7 μM BSA and an apparent V_{max} of 0.675 nmoles bound per mg cellular protein. There was also a clearly non-saturable component to the binding (k of 2.1 nmoles/mg/μM, see Section B.9). This indicated the existence of a variety of binding sites for BSA on the cell surface which may be involved in BSA binding during uptake.

C.1.5. Implications for the Mechanism of LCFA Uptake.

Together, these results indicated that 3T3-L1 adipocytes could directly utilize BSA-complexed LCFAs as substrates for uptake and that this involved an interaction between BSA and the cell surface. Such an interaction might affect LCFA uptake in a number of ways (figure 17). For instance the cell surface might stimulate the dissociation of bound LCFA from BSA (figure 17, panel 1; Burczynski and Cai, 1994; Burczynski et al., 1993; Reed and Burrington, 1989; Weisiger, 1993). It has also been proposed that such an interaction might allow for a direct transfer of bound LCFA from BSA to the

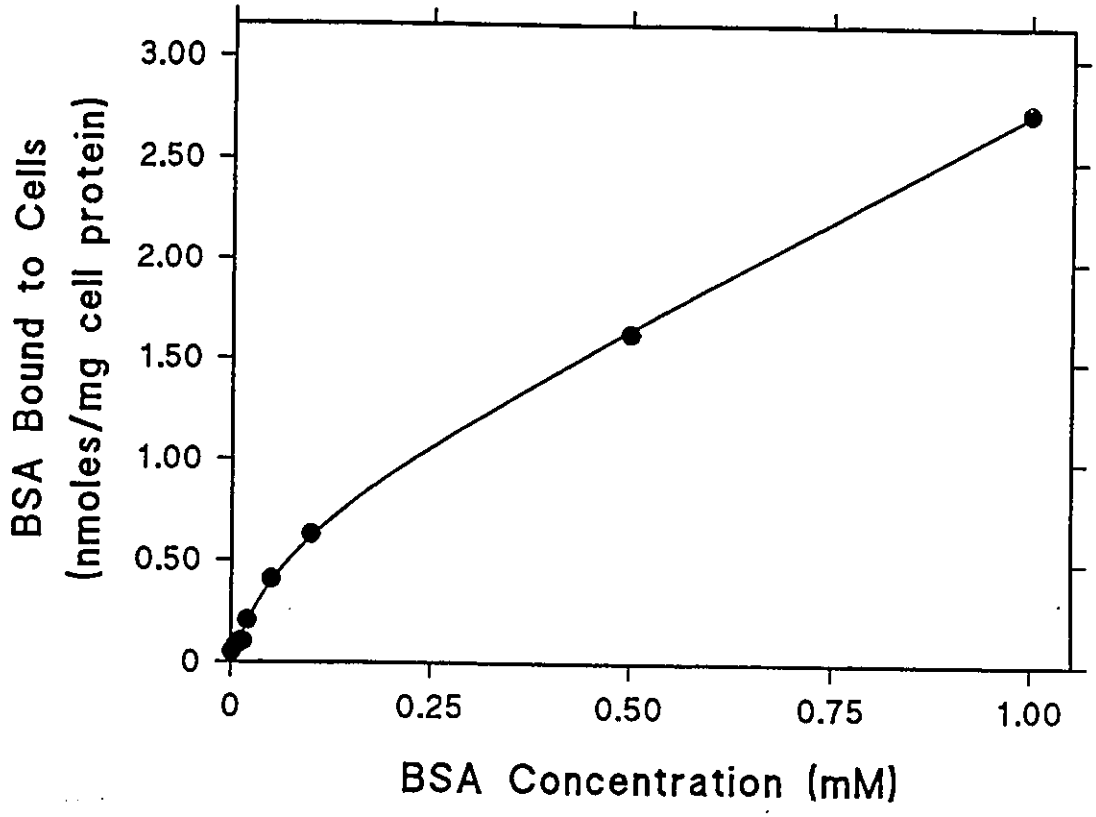

Figure 16. **The binding of 11-DAP-[11-^{3}H]undecanoate-labeled BSA by 3T3-L1 adipocytes.** The binding of BSA labeled with 11-DAP-[11-^{3}H]undecanoate to 3T3-L1 adipocytes was determined as described in Section B.9. Typical results are shown and are expressed as the amount of labeled BSA bound to cells versus the BSA concentration. The data were fit by equation (3).

lipid bilayer (figure 17, panel 2; Horie et al., 1988). Another alternative is that this might represent the targeting of LCFA-SA complexes to specific regions of the plasma membrane designated for transport (figure 17, panel 3). The possibility that caveolae (plasmalemmal vesicles) in the plasma membrane might represent such regions will be discussed in Section C.3.8.

The nature of the interaction of BSA with the cell surface is not clear. SA binding to cell surfaces is selective; while it binds to mammalian endothelial, heart, liver and lymphoblastoid cells, it does not bind to mammalian red blood cells, chicken cells or frog cells (Dziarski, 1994; Horie et al., 1988; Popov et al., 1992; Reed and Burrington, 1989; Schnitzer et al., 1988; Torres et al., 1992b). SA also binds nonspecifically to a variety of surfaces, including glass, various polymers and air-water interfaces (Weisiger, 1993). In contrast, BSA binds saturably to hepatocytes, cardiomyocytes and microvascular endothelium with somewhat lower K_d values (0.366, 1.1, and 15.5 μM, respectively) than that measured for 3T3-L1 adipocytes (figure 10; Popov et al., 1992; Reed and Burrington, 1989; Schnitzer et al., 1988).

Several putative BSA receptors have recently been identified (Ghinea et al., 1989, Schnitzer, 1992; Torres et al., 1992b). Two of these, of molecular weights 18 and 30 kDa, have been shown to be specific for chemically modified BSA (Schnitzer et al., 1992) and therefore appear to be scavenger receptors. A 60 kDa plasma membrane protein called albondin is specific for native albumin (Schnitzer et al., 1994). It is unclear whether these proteins are involved in LCFA uptake. As mentioned in section A.6.1.2,

CD36/FAT, a membrane protein which is known to be involved in LCFA uptake in adipocytes (Abumrad et al., 1993), has been shown to bind a variety of proteins, including chemically modified BSA (Acton et al., 1994), suggesting the possibility that it could be involved in binding LCFA-SA complexes.

Regardless of the exact nature of the interaction between the cell surface and LCFA-SA complexes, the results presented in this section indicate that such an interaction is directly involved in LCFA uptake. This does not appear to be restricted to SA; similar interactions with the cell surface have been shown to be involved in the uptake by T-lymphocytes of LCFA bound to α-fetoprotein (Torres et al., 1992a; Uriel et al., 1994). SA and α-fetoprotein belong to a multigene family which includes afamin and vitamin D-binding protein (Lichenstein et al., 1994). Cell binding of α-fetoprotein is thought to be mediated by the 18 and 30 kDa scavenger receptors mentioned above. The wide variety of ligands carried by these proteins (amino acids, bile acids, bilirubin, prostaglandins, steroids, and vitamin D; Lichenstein et al., 1994) suggests that this may be of general importance for the uptake of compounds circulating as complexes with carrier proteins (Torres et al., 1992a; Uriel et al., 1994).

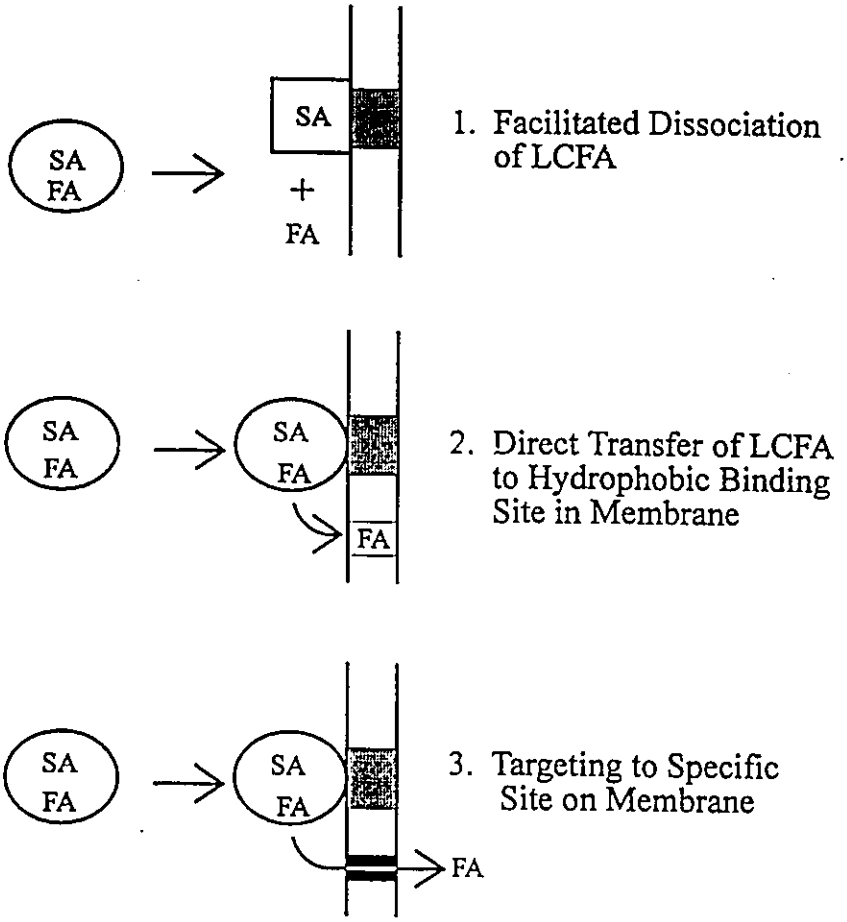

Figure 17. **Models by which SA-membrane interaction might affect LCFA uptake.** An interaction between SA and the plasma membrane of mammalian cells has been proposed to result in **1.** the facilitated dissociation of LCFAs from SA, resulting from a conformational change in SA upon membrane binding (Horie et al., 1988; Reed and Burrington, 1989) or **2.** the direct transfer of LCFAs from binding sites on SA to hydrophobic binding sites in the membrane (Horie et al., 1988); these might be proteins acting as LCFA receptors or the hydrophobic portion of the bilayer itself (represented by open box in the bilayer in **2**). **3.** An interaction between SA and the plasma membrane might also be involved in targeting LCFA-SA complexes to specific regions of the plasma membrane designated for LCFA uptake (represented by the black box in **3**). The interactions between the plasma membrane and SA (represented by the stippled box in the membrane in each of the three panels) might be mediated by putative protein receptors for SA or by lipids in the membrane. These three proposed models are not mutually exclusive.

C.2. Identification of Cellular FABPs Using a Photoreactive LCFA

C.2.1. Characteristics of 11-DAP-[11-^{3}H]undecanoate

To identify cellular LCFA binding proteins which may be involved in the uptake process, an approach based on photoaffinity labeling was used. This approach has proven to be useful for the identification of a number of receptors for a variety of ligands (Bayley, 1983; Brunner, 1993; Nielsen, 1988). Successful photoreactive probes for the identification of LCFA binding proteins should be chemically similar to LCFAs, so that they will bind specifically to LCFA binding sites on proteins, providing specificity to the labeling reaction (Bayley, 1983; Brunner, 1993). Furthermore, upon photolysis, the photoaffinity reagent should give rise to a highly reactive species which can react with C–C and C–H bonds, as they will be the prevalent groups in a hydrophobic environment, such as a LCFA binding pocket (Bayley, 1983; Brunner, 1993). The photoreactive LCFA 11-DAP-[11-^{3}H]undecanoate (compound 7 in figure 6) has these characteristics. The diazirine is stable in the dark but upon photolysis at 360 nm, it rearranges to form a carbene with the loss of N_2 (figure 18a). This species is sufficiently reactive to undergo insertion across C–H bonds as well as addition to C–C double bonds (figure 18b; Bayley, 1983; Brunner, 1993), enabling the facile labeling of hydrophobic LCFA-binding pockets. 11-DAP-[11-^{3}H]undecanoate has also been shown to mimic natural LCFAs by a variety of biochemical criteria. These include its ability to act as a substrate for LCFA uptake by

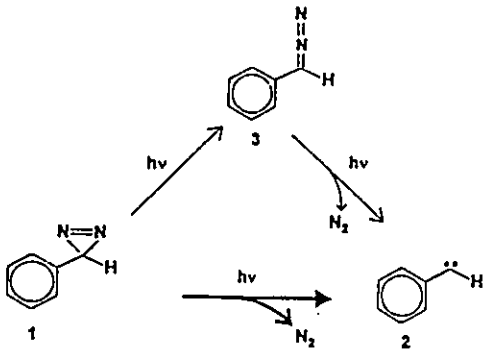

a. Photolysis of phenyldiazirine

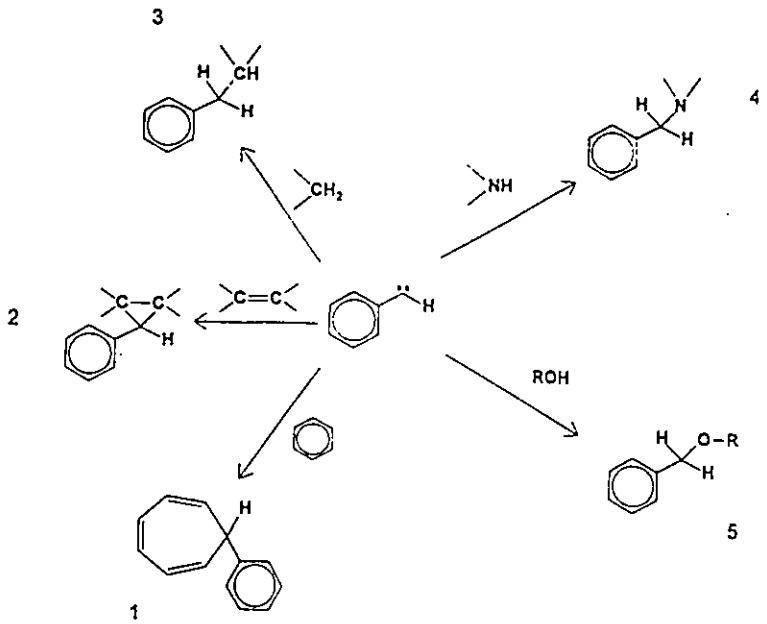

b. Reactions of carbenes

Figure 18. **Photolysis of phenyldiazirine and reactions of carbenes.** (adapted from Bayley, 1983, and Brunner, 1993) **a.** The conversion of phenyldiazirine (1) to a carbene (2) upon photolysis is shown (bold arrow with closed arrowhead) along with the conversion to the linear diazo-isomer (3) upon incomplete photolysis. This can be converted to a carbene upon further photolysis. **b.** Reactions of the carbene include addition to phenyl rings (1) and C=C bonds (2), addition across C–H bonds (3), N–H bonds (4) and O–H bonds (5).

E. coli (Mangroo and Gerber, 1992), acyl-CoA synthesis by rat liver microsomes (Leblanc and Gerber, 1984), and acylation of membrane proteins and phospholipid synthesis in L-cells (Capone et al., 1983; Leblanc et al., 1982). All of these processes are mediated by enzymes specific for LCFAs, indicating that the photoreactive reagent binds to LCFA binding sites.

These findings suggested that the cellular uptake of 11-DAP-[11-^{3}H]undecanoate should resemble that of other LCFAs. To test this, its uptake by 3T3-L1 adipocytes was measured using the filtration assay employed to study [9,10-^{3}H]oleate uptake in the previous section (B.1). The time courses of 11-DAP-[11-^{3}H]undecanoate uptake by both 3T3-L1 preadipocytes and adipocytes were linear for at least 1.0 min (figure 19). The rate of uptake by adipocytes (normalized to cellular protein) was approximately 7-fold higher than that by preadipocytes (1.95 compared with 0.264 nmoles/min/mg of cellular protein, respectively). This level of induction was comparable to that for oleate uptake observed in figure 10b, and reported by others (Zhou et al., 1992).

To enable the affinity of uptake for the uncomplexed photoreactive fatty acid to be measured, the concentrations of uncomplexed 11-DAP-[11-^{3}H]undecanoate in equilibrium with that bound to BSA were determined by the equilibrium phase partitioning method, as done for oleate (figure 11a). The relationship between the molar ratio of 11-DAP-[11-^{3}H]undecanoate to BSA and the concentration of uncomplexed 11-DAP-[11-^{3}H]undecanoate is shown in figure 20a. This was used to determine the concentrations of uncomplexed photoreactive LCFA in equilibrium with 11-DAP-[11-

^{3}H]undecanoate complexed to BSA in the uptake assay. Rates of 11-DAP-[11-^{3}H]undecanoate uptake, measured at various concentrations of uncomplexed photoreactive LCFA in the presence of BSA, were plotted versus the concentration of uncomplexed LCFA in figure 20b. Uptake was clearly saturable, exhibiting a high affinity ($K_{0.5}$ was 255 nM; figure 20b). The V_{max} determined from figure 20b (13.3 nmol/min/mg of cellular protein) was higher than that (7.0 nmoles/min/mg of cellular protein) determined for oleate uptake in figure 11b. This may reflect the different BSA concentrations used in the two experiments (see Section C.1.2.2 and figures 12 and 13). Therefore, the cellular uptake of 11-DAP-[11-^{3}H]undecanoate by 3T3-L1 adipocytes resembles that of other LCFAs, suggesting that the photoreactive probe is recognized as a LCFA by the cellular machinery responsible for LCFA uptake. This ability to mimic LCFAs in enzymatic reactions, binding to BSA, and cellular uptake indicate that the photoreactive probe should prove to be a suitable reagent for the identification of cellular LCFA binding proteins involved in the uptake process.

C.2.2. Photolysis Conditions

BSA was used as a probe to monitor photolysis conditions using 11-DAP-[11-^{3}H]undecanoate (figure 21a and b). BSA, incubated with the photoreactive LCFA for 60 min (at 37°C), was photolyzed for various times using a beam filtered through two Corning 7-51 filters (figure 21a) or through 0.020 % potassium hydrogen phthalate in a quartz cell of 5.0 cm pathlength (figure 21b). The Corning 7-51 filters transmitted light as a relatively narrow band centered at 360 nm, which corresponded to the absorbance

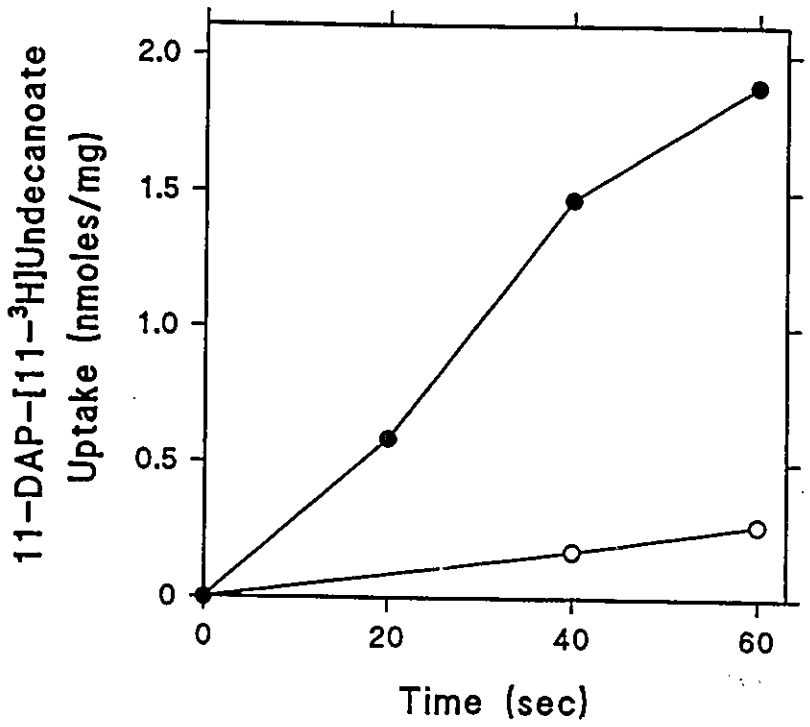

Figure 19. **Uptake of 11-DAP-[11-^{3}H]undecanoate by 3T3-L1 adipocytes and preadipocytes.** 3T3-L1 adipocytes (●) were harvested 6 days after stimulation to differentiate, while preadipocytes (○) were harvested one day prior to confluence. Cells, suspended in 0.50 ml of PBS at approximately 0.80 mg of cellular protein/ml were incubated at 37°C with a 1:1 molar ratio of 11-DAP-[11-^{3}H]undecanoate:BSA (each at 100 μM). 0.20 ml aliquots were removed at various times and filtered and the amount of radioactivity retained by the filters was determined as described in Section B.4.3. Typical results are shown as the rate of luptake (normalized for cellular protein) versus time.

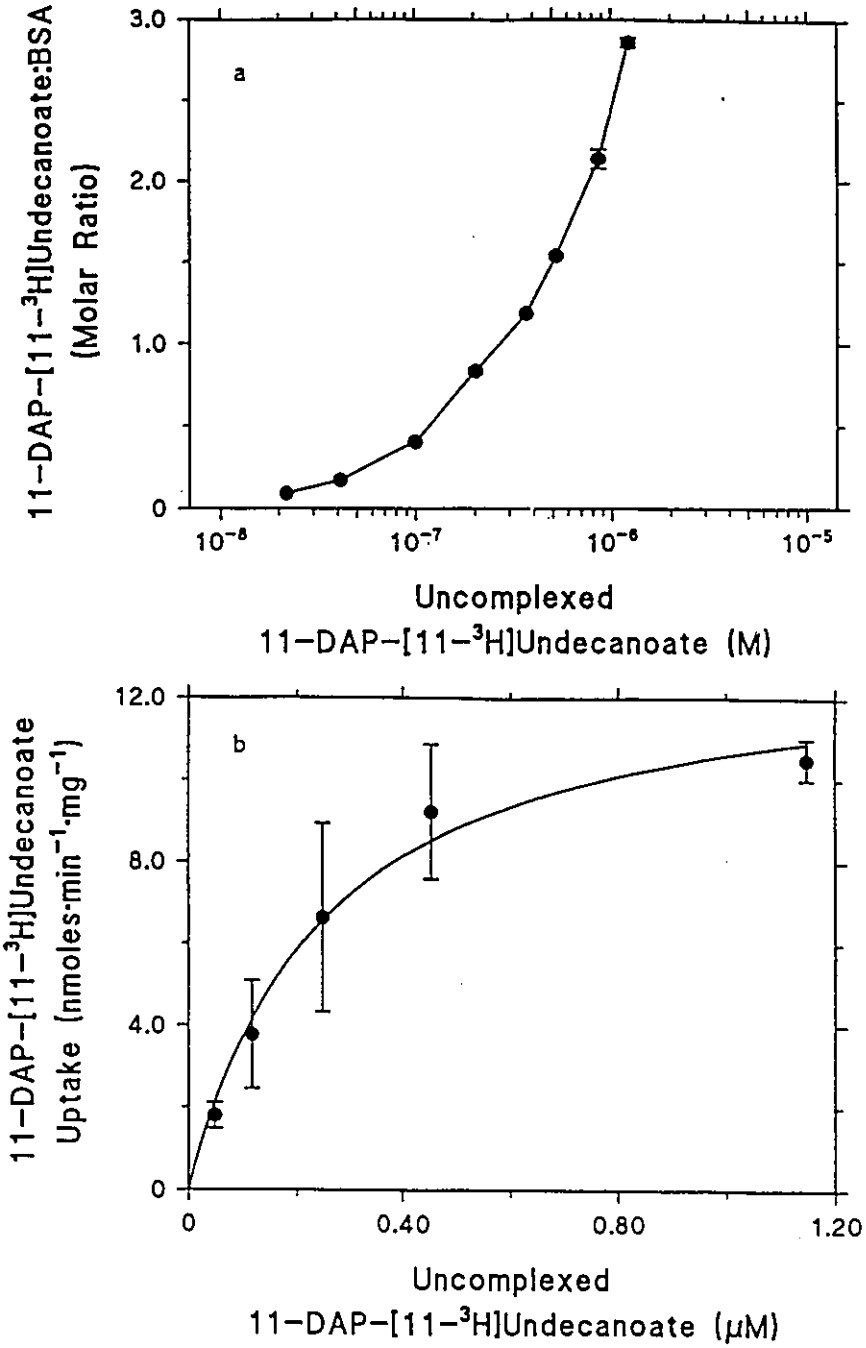

Figure 20. **11-DAP-[11-^{3}H]undecanoate binding to BSA and uptake by 3T3-L1 adipocytes as a function of uncomplexed 11-DAP-[11-^{3}H]undecanoate concentration.** **a.** 11-DAP-[11-^{3}H]undecanoate binding to 0.050 mM BSA at 37°C was measured by the heptane partitioning method as described in Section B.4.2. Results are expressed as the average (± S.E.M. of two determinations) molar ratio of 11-DAP-[11-^{3}H]undecanoate bound to BSA versus the concentration of uncomplexed 11-DAP-[11-^{3}H]undecanoate. **b.** 3T3-L1 adipocytes were incubated at 37°C for 20 sec with increasing ratios of 11-DAP-[11-^{3}H]undecanoate:BSA at a constant concentration of BSA of 0.50 mM, and 11-DAP-[11-^{3}H]undecanoate uptake was measured as described in Section B.4.3. Uptake rates (normalized for cellular protein) were plotted versus the concentration of uncomplexed 11-DAP-[11-^{3}H]undecanoate determined from the binding curve in **a**. The data represent the average ± S.E.M. of three determinations and were fit by equation (3).

maximum of the phenyldiazirine (Leblanc, 1991). Potassium hydrogen phthalate absorbed light below 300 nm (not shown), thereby transmitting light at which the phenyldiazirine absorbs. With either filter, the incorporation of the photoreactive probe into BSA was maximal by the earliest time-point (2.0 sec) and was stable for up to 30 sec. Furthermore, no significant photolytic degradation of the 66 kDa, BSA band could be observed (a slight time-dependent increase in the minor bands migrating below the 66 kDa band was observed when 0.020 % potassium hydrogen phthalate was used as a filter, however these bands were only observed because the film was purposefully overexposed to allow comparison with panels c and d; see below).

Upon incomplete photolysis, phenyldiazirines can rearrange to form linear diazo-isomers (figure 18a; Bayley, 1983; Brunner, 1993). Further photolysis at 360 nm leads to the generation of carbenes relatively slowly (Bayley, 1983). In fact, linear diazo-compounds are sufficiently stable for use as reagents for the non-photolytic, chemical modification of proteins (Bayley, 1983). This reaction can be distinguished from the desired photolytic reaction as it occurs in the dark. Therefore, the generation of the linear diazo-isomer can potentially complicate the interpretation of results from the labeling experiment since it is not reactive toward C–C or C–H bonds and therefore could dissociate from the hydrophobic, LCFA-binding pocket and react with functional groups at other sites on the protein or on other proteins in a complex biological sample.

To control for the generation of the linear diazo-isomer, the photoreactive LCFA was photolyzed (from 2.0 to 30 sec) using either Corning 7-51 filters (figure 21c) or 0.020

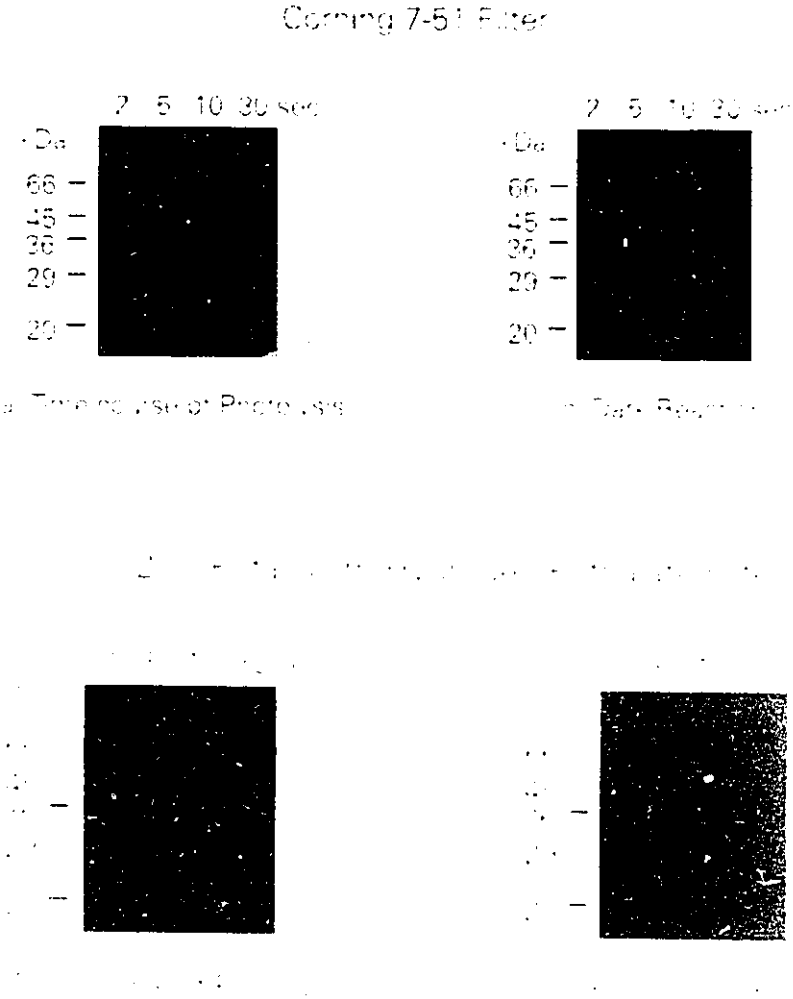

Figure 21. **Timecourse of photolysis of 11-DAP-[11-^{3}H]undecanoate.** A mixture of 11-DAP-[11-^{3}H]undecanoate and BSA (10μM each in PBS) was incubated at 37°C for 60 min in the dark. 50 μl aliquots of this (**a** and **b**) or 11 μM 11-DAP-[11-^{3}H]undecanoate in the absence of BSA (**c** and **d**) were photolyzed for the times indicated above each lane by exposure to light from a 1000W Xe-Hg lamp, filtered through two Corning 7-51 filters (**a** and **c**) or through a 0.020 % solution of potassium hydrogen phthalate in a 5.0 cm quartz cell (**b** and **d**). 11-DAP-[11-^{3}H]undecanoate photolyzed in the absence of BSA (**c** and **d**) was then mixed with BSA (1:1 molar ratio) to a final concentration of 10 μM and allowed to react for 5.0 hrs at 37°C, in the dark. Samples (0.66 μg of BSA) were analyzed by SDS-PAGE on 10 % acrylamide gels, which were subjected to fluorography. Numbers to the left indicate molecular masses of protein standards: BSA (66 kDa), chicken egg albumin (45 kDa), glyceraldehyde 3-phosphate dehydrogenase (36 kDa), carbonic anhydrase (29 kDa) and trypsin inhibitor (20 kDa).

% potassium hydrogen phthalate as a filter (figure 21d) as described above, and then incubated with BSA for 5.0 hours at 37°C in the dark. In both cases, no incorporation of the probe into BSA was observed, indicating that the rearrangement of the phenyldiazirine to the linear diazo-isomer was not significant under the photolysis conditions used.

C.2.3. Induction of Cellular FABPs During Differentiation of 3T3-L1 Preadipocytes to Adipocytes.

To identify FABPs induced upon the differentiation of 3T3-L1 preadipocytes to adipocytes, cells at various stages of differentiation were incubated at 37°C for 30 sec with 11-DAP-[11-^{3}H]undecanoate in the presence of BSA (figure 22). Protein bands of approximately 66, 40, 34 and 13 kDa were labeled upon photolysis of the subconfluent preadipocytes (P), cells maintained beyond confluence in an undifferentiated state by incubation in medium containing cat serum (U) and differentiated adipocytes (D). In addition to these, a major band of 15 kDa was labeled in differentiated adipocytes, but not in preconfluent preadipocytes, nor in confluent, undifferentiated cells. Furthermore, the 34 and 13 kDa bands were labeled more intensely in the differentiated cells than in preadipocytes.

To investigate the subcellular locations of the labeled bands, 3T3-L1 adipocytes labeled with the photoreactive LCFA were separated into various subcellular fractions by the method of Cushman and Wardzala (1980) as modified by Lange and Brandt (1990). Table 5 gives data from a typical fractionation for the recoveries and specific activities

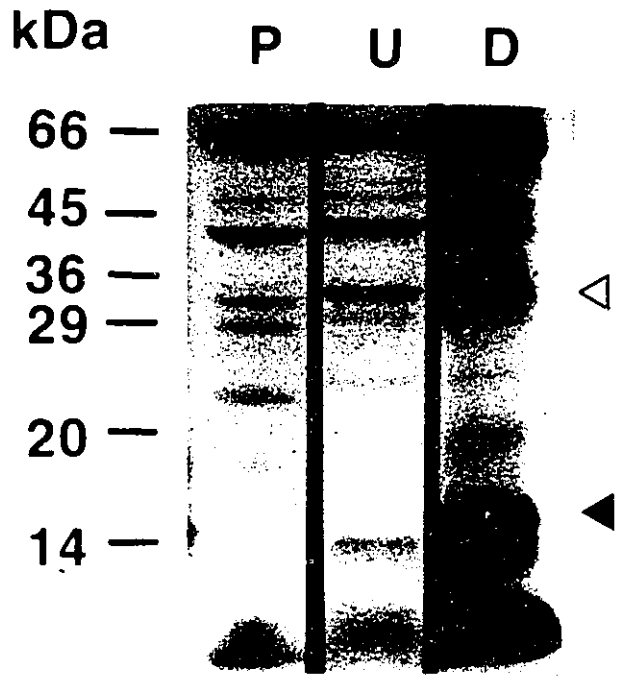

Figure 22. **Photoaffinity labeling with 11-DAP-[11-^{3}H]undecanoate of cellular proteins in intact 3T3-L1 cells.** 3T3-L1 preadipocytes harvested one day prior to confluence (P), or after maintenance in an undifferentiated state beyond confluence in 9.0 % cat serum (U), or differentiated 3T3-L1 adipocytes (D; harvested on the seventh day of differentiation) were incubated for 30 sec at 37°C with a mixture of 11-DAP-[11-^{3}H]undecanoate and BSA (1:1 molar ratio at 50 μM in PBS), prior to photolysis for 30 sec as described in the legend to figure 21, using two Corning 7-51 filters. Photolyzed cells were washed with 1.0 % BSA in PBS and analyzed by SDS-PAGE on 15 % acrylamide gels as described in Section B.10.2. 25 μg of cellular protein were applied to each lane. Numbers on the left of the panel indicate the positions of the protein standards as indicated in the legend to figure 21, including α-lactalbumin (14 kDa). Arrows indicate the bands of interest.

of 5'-nucleotidase, NADH dehydrogenase and cytochrome C oxidase, enzymatic markers for the plasma membrane, ER and mitochondria, respectively (Appelmans et al., 1955; Record et al., 1992; Touster et al., 1970). As expected, the plasma membrane fraction contained the highest specific activity of 5'-nucleotidase. It did, however appear to be contaminated by ER based on an increase in the specific activity of NADH-dehydrogenase, relative to that in the total homogenate. An alternate explanation, however, is suggested by the recent discovery of plasma membrane-localized NADH-ferricyanide reductase activities in a variety of cells (Howland et al., 1984; Mershel et al., 1984; Villalba et al., 1993). Furthermore, the patterns of proteins labeled by the photoreactive LCFA in each fraction differed substantially (figure 16), suggesting that cross-contamination was not significant.

Figure 23 shows the pattern of labeled proteins after SDS-PAGE analysis of various subcellular fractions prepared from 3T3-L1 adipocytes which had been subjected to photolysis after incubation at 37°C for 10 sec with 10 μM 11-DAP-[11-^{3}H]undecanoate; equal amounts of protein from each fraction were analyzed. Labeled proteins of approximately 66, 40, 34, 15 and 13 kDa were observed in the whole cell fraction (lane T). Of these, the labeled bands of low molecular weight (15 and 13 kDa) were soluble (lane S), suggesting that they were cytoplasmic. The 40 and 34 kDa bands appeared to be mitochondrial (compare lanes T and M). A number of other labeled bands were observed in plasma membranes (lane PM), but none of these appeared in the pattern from whole cells (lane T). A greater abundance of mitochondrial relative to plasma

membrane protein (approximately 10-fold) accounted for the observation of mitochondrial but not plasma membrane bands in the whole cell pattern. Therefore, while the labeling of intact adipocytes with a high concentration of photoreactive LCFA (10 μM is well above the $K_{0.5}$ observed for uptake from figure 20b) allowed the identification of intracellular FABPs, high affinity plasma membrane proteins were not easily recognized in the whole cell pattern. For this reason, isolated plasma membranes were labeled with the photoreactive probe to allow the identification of plasma membrane-bound LCFA binding proteins (Section B.3).

Table 5. **Activities of marker enzymes in various fractions of subcellular fractionation.** Percent yields were calculated relative to the level of activity in the homogenate. Specific activities were normalized for the protein content. The 5'-nucleotidase activity is expressed as the amount (in nmoles) of inorganic phosphate produced per min, while NADH dehydrogenase and cytochrome C-oxidase activities are expressed as the change in absorbance at either 410 or 550 nm, wavelength, respectively, per min.

	5'-Nucleotidase		NADH Dehydrogenase		Cytochrome-C Oxidase	
Fraction	% Yield	Specific Activity $\frac{\text{nmol } P_i}{\text{min}\bullet\text{mg}}$	% Yield	Specific Activity $\frac{\Delta A_{410}}{\text{min}\bullet\text{mg}}$	% Yield	Specific Activity $\frac{\Delta A_{550}}{\text{min}\bullet\text{mg}}$
Homogenate	100	5.02	100	1.89	100	1.71
Plasma Membrane	20.1	46.7	3.0	3.75	0.39	0.42
Microsomes	31.6	13.4	35.6	5.17	0.0	0.0
Mitochondria	40.3	8.26	40.7	3.07	89.0	13.4

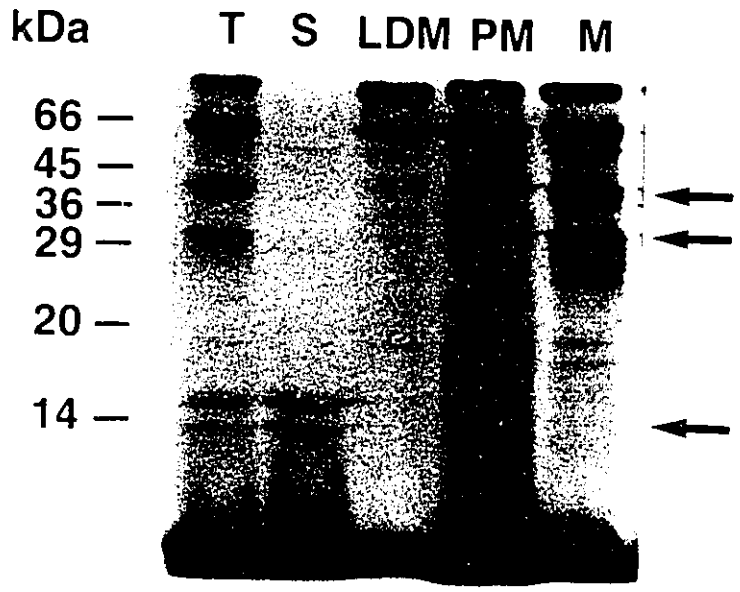

Figure 23. **Subcellular fractionation of differentiated cells prelabeled with 11-DAP-[11-^{3}H]undecanoate.** Differentiated cells (harvested on day 4 of differentiation), were incubated for 10 sec. at 37°C with 10 μM 11-DAP-[11-^{3}H]undecanoate in the absence of BSA. After photolysis as described in the legend to figure 22, an equal amount of unlabeled cells was added and the sample was pelleted at 450×*g* for 10 min. Subcellular fractions were isolated as described in Section B.6.4. Ten micrograms of protein from total homogenate (T), soluble (S), low density microsomal (LDM), plasma membrane (PM), and mitochondrial (M) fractions were solubilized and analyzed by SDS-PAGE on a 12.5% polyacrylamide gel, as described in Section B.10.2. The positions of protein standards are indicated as in figures 21 and 22. Arrows indicate the locations of bands of interest.

C.3. Photoaffinity Labeling of Plasma Membrane FABPs

C.3.1. Identification of Plasma Membrane FABPs

The primary site of interaction of LCFAs with cells may be in the plasma membrane via putative LCFA receptors. This is important not only for the cellular uptake of LCFAs but also for their involvement in a variety of crucial signaling cascades. LCFAs have been shown to regulate a diversity of cellular processes. These include gene expression and differentiation in adipocytes and preadipocytes, respectively (Amri et al., 1991a and b, 1994; Distel et al., 1992; Grimaldi et al., 1992; Safonova et al., 1994), platelet activating factor-induced platelet activation (Siafaka-Kapadai and Hanahan, 1993), insulin release by pancreatic β-cells (Opara et al., 1994; Warnotte et al., 1994) and the translocation of GluT4 to the plasma membrane in adipocytes (Hardy et al., 1991). LCFAs have also been shown to directly regulate the activities of a number of ion channels (Ordway et. al., 1989, 1991).

Despite the importance of the plasma membrane as the primary site of interaction of LCFAs with cells, very little is known about the details of this interaction. To identify high affinity, plasma membrane receptors for LCFAs, plasma membranes, purified from 3T3-L1 cells, were photolyzed after a 60 min incubation with 11-DAP-[11-^{3}H]undecanoate at 37°C. BSA was included in the reaction (at a ratio of photoreactive fatty acid:BSA of 0.5:1) to provide a concentration of uncomplexed 11-DAP-[11-^{3}H]undecanoate of 115 nM

(from figure 13a) to allow the specific labeling of high affinity FABPs (figure 24a). Two intensely labeled bands of 66 and 22 kDa were observed in plasma membranes from both adipocytes and cells maintained beyond confluence in an undifferentiated state. The 66 kDa band was due to BSA carried over from the labeling reaction as it migrated in the same position as BSA labeled with the probe in the absence of membranes and it could be competed from membranes with unlabeled BSA (not shown).

Measurement of the amount of radioactivity incorporated into the labeled bands indicated that the 22 kDa band in adipocyte plasma membranes contained two-fold more label than that in plasma membranes from undifferentiated cells. A protein of this molecular weight was not visible by Coomassie blue staining (figure 24c), which indicated that it was not a major protein. The intense labeling by the photoreactive LCFA and the fact that it was the only plasma membrane protein labeled under these conditions suggested that its labeling was specific and due to a high affinity for the probe.

The involvement of a number of proteins in LCFA uptake has been implicated as described in Sections A.6.2-A.6.4 of the Introduction. These proteins include the 43 kDa $FABP_{PM}$, the 63 kDa FATP, and the 85 kDa CD36/FAT (Abumrad et al., 1984, 1993; Schaffer and Lodish, 1994; Stremmel and Theilman, 1986). All have been shown to become induced in the plasma membranes of 3T3-L1 cells upon differentiation to adipocytes (Abumrad et al., 1993; Schaffer and Lodish, 1994; Zhou et al., 1992). Their labeling by the photoreactive LCFA was therefore expected based on the proposal that each functioned as a putative LCFA transporter (Abumrad et al., 1984, 1993; Potter and

Berk, 1993; Schaffer and Lodish, 1994). As seen in figure 24a, however, none of these proteins were labeled by the photoreactive LCFA under the conditions employed. This suggested that these proteins might have low affinities for the photoreactive LCFA.

To test this, plasma membranes were photolyzed after incubation with 10 μM 11-DAP-[11-^{3}H]undecanoate in the absence of BSA, to allow for the labeling of proteins with lower affinities for LCFAs (figure 24b). In addition to the intensely labeled band at 22 kDa, bands of apparent molecular weights of 67, 50, 36 and 29 kDa were labeled. Of these, only the 36 and 67 kDa bands were specific to plasma membranes from 3T3-L1 adipocytes (figure 24b). The apparent molecular weight and induced labeling of the 67 kDa band in 3T3-L1 adipocyte plasma membranes suggested that it may be related to the 63 kDa FATP (Schaffer and Lodish, 1994). Confirmation of this, however, must await the immunological characterization of the photoreactive LCFA-labeled protein with antibodies raised against the FATP (Schaffer and Lodish, 1994).

Proteins of 85 and 43 kDa were not labeled in plasma membranes from 3T3-L1 adipocytes when labeling was done with the high concentration of photoreactive LCFA (figure 24b). This suggested that neither CD36/FAT nor $FABP_{PM}$ in plasma membranes from 3T3-L1 adipocytes bound LCFAs. The reported binding of LCFAs by the liver $FABP_{PM}$ (Berk et al., 1990; Stremmel et al., 1985a) was based on the binding of radioactive LCFAs by plasma membranes isolated from liver as well as by the purified $FABP_{PM}$, in solution (Stremmel et al., 1985a). Clearly, the binding of LCFAs by plasma membranes cannot be taken as a measure of the specific binding by an individual protein.

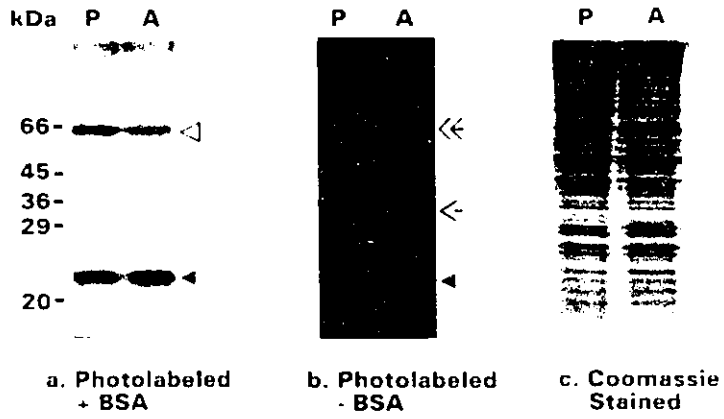

Figure 24. **Labeling of FABPs in plasma membranes from 3T3-L1 preadipocytes and adipocytes.** Plasma membranes (0.25 mg/ml in PBS) isolated from 3T3-L1 preadipocytes (**P**; maintained after confluence in an undifferentiated state) and adipocytes (**A**) were photolyzed, as described in the legend to figure 21 using two Corning 7-51 filters, after a 15 min incubation at 37°C with either **a.** 25 μM 11-DAP-[11-^{3}H]undecanoate in the presence of 50 μM BSA or **b.** 10 μM 11-DAP-[11-^{3}H]undecanoate in the absence of added BSA. Membranes labeled in the presence of BSA were washed at room temperature with 1.0% BSA in PBS, and then PBS alone. Those labeled in the absence of BSA were washed in PBS. 25 μg were analyzed by SDS-PAGE on a 12.5 % acrylamide gel which was stained with Coomassie blue (**c**) and then fluorographed (**a** and **b**). Numbers on the left indicate the molecular weights (in kDa) of protein standards as described in the legend to figure 21. Arrows indicate the bands of interest as follows: Open triangle, BSA carried over from the labeling reaction; closed triangle, 22 kDa protein; double arrowhead, 67 kDa protein; single arrowhead, 36 kDa protein.

In fact, others, being unable to repeat the results obtained by Stremmel and co-workers, have concluded that the binding of LCFAs to liver plasma membranes reflected mainly partitioning into the lipid phase (Cooper et al., 1989). The binding of radioactive-LCFA by purified $FABP_{PM}$ was measured by co-chromatography (Stremmel et al., 1985a). Very large amounts of the purified protein (0.30 mg) were required to detect LCFA binding (Stremmel et al., 1985a), suggesting that the level of binding may have been low.

Therefore, the results of figure 24 indicate that 3T3-L1 adipocyte plasma membranes contain a unique, apparently high affinity FABP of 22 kDa and two apparently low affinity FABPs which become induced upon differentiation. Based on similarities in apparent molecular weights, one of the low affinity proteins might be related to the recently described FATP; the identities of the unique, 22 kDa, high affinity FABP and the induced, 36 kDa low affinity FABP, however, remain unknown.

C.3.2. Localization of the 22 kDa Plasma Membrane FABP

The differentiation of 3T3-L1 preadipocytes to adipocytes is accompanied by increases in the number of caveolae on their cell surfaces (Fan et al., 1983). Caveolae are flask shaped pits in the plasma membrane which have been implicated in a variety of processes including the transport of and signalling by a variety of ligands (Anderson, 1993a and b; Anderson et al., 1992; Lisanti et al., 1994a). Procedures for the isolation of caveolae from different cell types have recently been developed (Chang et al., 1994; Lisanti et al., 1994b; Sargiacomo et al., 1993). Upon characterization, these preparations

have been found to contain a variety of proteins involved in signalling (Chang et al., 1994; Lisanti et al., 1994b).

To determine the plasma membrane localization of the 22 kDa protein labeled by the photoreactive LCFA, caveolae were isolated from plasma membranes of 3T3-L1 adipocytes. The fraction representing caveolae was identified by SDS-PAGE followed by immunoblotting with an anti-caveolin monoclonal antibody (mAb 2234; figure 25a). Caveolin is a 22 kDa resident protein of caveolae expressed in a variety of cells including 3T3-L1 adipocytes (Chang et al., 1994; Lisanti et al, 1994b; Rothberg et al., 1992; Scherer et al., 1994).

The fractions were also labeled with the photoreactive LCFA and equal amounts of protein from each fraction were analyzed by SDS-PAGE. The pattern of proteins labeled in the presence of BSA under conditions designed to allow for the specific labeling of high affinity FABPs (as in figure 24a) is shown in figure 25b. Proteins were also stained with Coomassie blue (figure 25c). As shown in figure 25b, the 22 kDa band labeled under specific conditions was found exclusively in caveolae.

The similarity in molecular weights between the 22 kDa, 11-DAP-[11-^{3}H]undecanoate-labeled protein and caveolin (figures 25a and b) suggested that they may be related. To test this, plasma membranes, labeled with the photoreactive LCFA, were solubilized and the extracts were subjected to immunoprecipitation with the anti-caveolin mAb, 2234 (figure 26). The labeled 22 kDa protein was immunoprecipitated by mAb 2234 but not by an irrelevant antibody, indicating that it was indeed murine caveolin.

Recently, this protein has been shown to become induced upon the differentiation of 3T3-L1 cells to adipocytes (Scherer et al., 1994). Induction of caveolin during differentiation is shown in figure 27 by Western analysis using a polyclonal antibody raised against a peptide corresponding to the C-terminal 13 amino acids predicted from the cDNA sequence of human caveolin. This antiserum detected two forms of caveolin (see the following Section). The level of induction was much higher than the two-fold increase in the labeling of the protein observed in figure 24 (a and b). The reasons for this discrepancy are unclear. It might relate to the use of plasma membranes isolated from cells maintained beyond confluence in 9.0 % cat serum as the undifferentiated control. This was done to increase the yield of plasma membranes, however it appears from figure 27 that caveolin begins to become induced at confluence (day 0), prior to the addition of hormones to stimulate differentiation. Alternatively, it might suggest that the binding of LCFAs by caveolin is differentially regulated in preadipocytes and adipocytes. These possibilities, however were not investigated further.

C.3.4. Different Forms of Caveolin.

Both canine and murine (3T3-L1 cell) caveolin have been reported to consist of two forms differing in molecular weight, as observed in figure 27 (Dupree et al., 1993; Kurzchalia et al., 1992; Scherer et al., 1994). To investigate whether both forms of murine caveolin interacted with the photoreactive LCFA, labeled 3T3-L1 adipocyte plasma membranes were analyzed by 2D-PAGE followed by either fluorography (figure 28a) or immunoblotting with caveolin specific antibodies (figure 28c and d). The photoaffinity

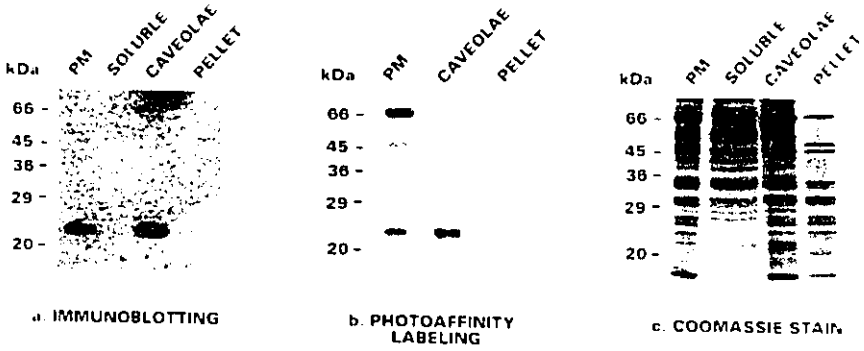

Figure 25. **Localization of the photoaffinity labeled, 22 kDa plasma membrane protein in caveolae.** Caveolae were isolated from 3T3-L1 adipocyte plasma membranes as described in Section B.6.5. Plasma membranes (**PM**), caveolae and the gradient pellet (**PELLET**) were labeled with 25 μM 11-DAP-[11-^{3}H]undecanoate in the presence of 50 μM BSA as described in the legend to figure 24. Triton X-100 solubilized plasma membrane proteins (**SOLUBLE**) were not labeled due to the presence of interfering detergent. Equal amounts (10 μg) of plasma membranes (**PM**), triton X-100 soluble (**SOLUBLE**), caveolae and the gradient pellet (**PELLET**) fractions were **a.** analyzed by SDS-PAGE and transferred to immobilon-P membranes and probed with a caveolin specific monoclonal antibody. Otherwise, 10μg of photoaffinity-labeled plasma membrane (**PM**), caveolae and gradient pellet (**PELLET**) fractions were analyzed by SDS-PAGE and either **b.** treated for fluorography and exposed to X-ray film or **c.** stained with Coomassie blue.

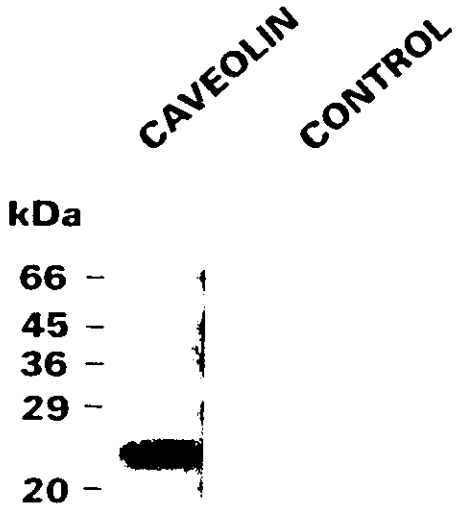

Figure 26. **Immunoprecipitation of the 22 kDa, adipocyte plasma membrane FABP with a monoclonal anti-caveolin antibody.** 3T3-L1 adipocyte plasma membranes labeled with 10 μM 11-DAP[11-^{3}H]undecanoate were solubilized, precleared by reaction with mouse IgG and then allowed to react with either monoclonal anti-caveolin antibody 2234 (**CAVEOLIN**) or an irrelevant antibody (non-immune rabbit serum, **CONTROL**) at 4.0°C overnight as described in Section B.10.1. Immunocomplexes were precipitated by reaction with protein A-sepharose beads. Immunoprecipitated proteins were solubilized by boiling for 1.5 min in 0.125 M Tris-HCl pH 6.8, containing 10 % SDS, 100 mM DTT, 12 % glycerol and 0.0070% bromophenol blue and analyzed by SDS-PAGE as described in the legend to figure 24. Numbers on the left indicate the positions of protein standards as described in the legend to figure 21.

Figure 27. **Induction of caveolin upon differentiation of 3T3-L1 preadipocytes to adipocytes.** 3T3-L1 cells were stimulated to differentiate as described in Section B.3.3. Proteins from cells at various stages of differentiation were analysed by SDS-PAGE and transferred onto PVDF membranes. These were probed with a polyclonal rabbit-primary antibody, specific for a peptide corresponding to the C-terminal 13 amino acids predicted from the cDNA sequence of human caveolin, and horseradish peroxidase conjugated to a donkey, anti-rabbit secondary antibody. Antibody binding was detected by chemiluminescence using the ECL kit (Amersham). The numbers at the top of the panel indicate the stage of differentiation in days. Day -1 indicates preadipocytes, while day 0 denotes the day on which differentiation was initiated.

labeled 22 kDa band was resolved into at least two spots of approximate pI's of 5.6 and 5.5 as determined by the measurement of the pH of an NE-IEF gel (first dimension) run in parallel (not shown). The two spots also differed in apparent molecular weight, the more acidic spot having a slightly lower apparent molecular weight (figure 28a).

Caveolin has been reported to be reversibly palmitoylated (R.G.W. Anderson, personal communication). 9-DAP-[9-^{3}H]nonanoate, a related photoreactive LCFA, could act as a substrate for the reversible acylation of membrane proteins (Capone et al., 1983). To determine whether 11-DAP-[11-^{3}H]undecanoate incorporation into the 22 kDa proteins resulted from acylation, its incorporation in the absence of photolysis was determined (figure 28b). Neither of the spots observed in figure 28a were labeled in the absence of photolysis. Therefore, the incorporation of the probe was the result of photolysis and not an enzymatic event such as acylation.

Both of the photoaffinity labeled spots were detected by immunoblotting with the polyclonal antiserum specific for the C-terminus of caveolin (figure 28c). However, only the more basic spot reacted with an antiserum specific for a peptide corresponding to amino acids 19-30 of the N-terminus of human caveolin (figure 28d). The mAb used in figures 25 and 26 gave a pattern identical to that obtained with the N-terminus specific antiserum (not shown). The nature of this difference in molecular weights and pI's is unknown (Dupree et al., 1993; Kurzchalia et al., 1992).

Dupree et al. (1993) have also found that an antibody generated against a peptide corresponding to amino acids 1-20, derived from the cDNA sequence of canine caveolin

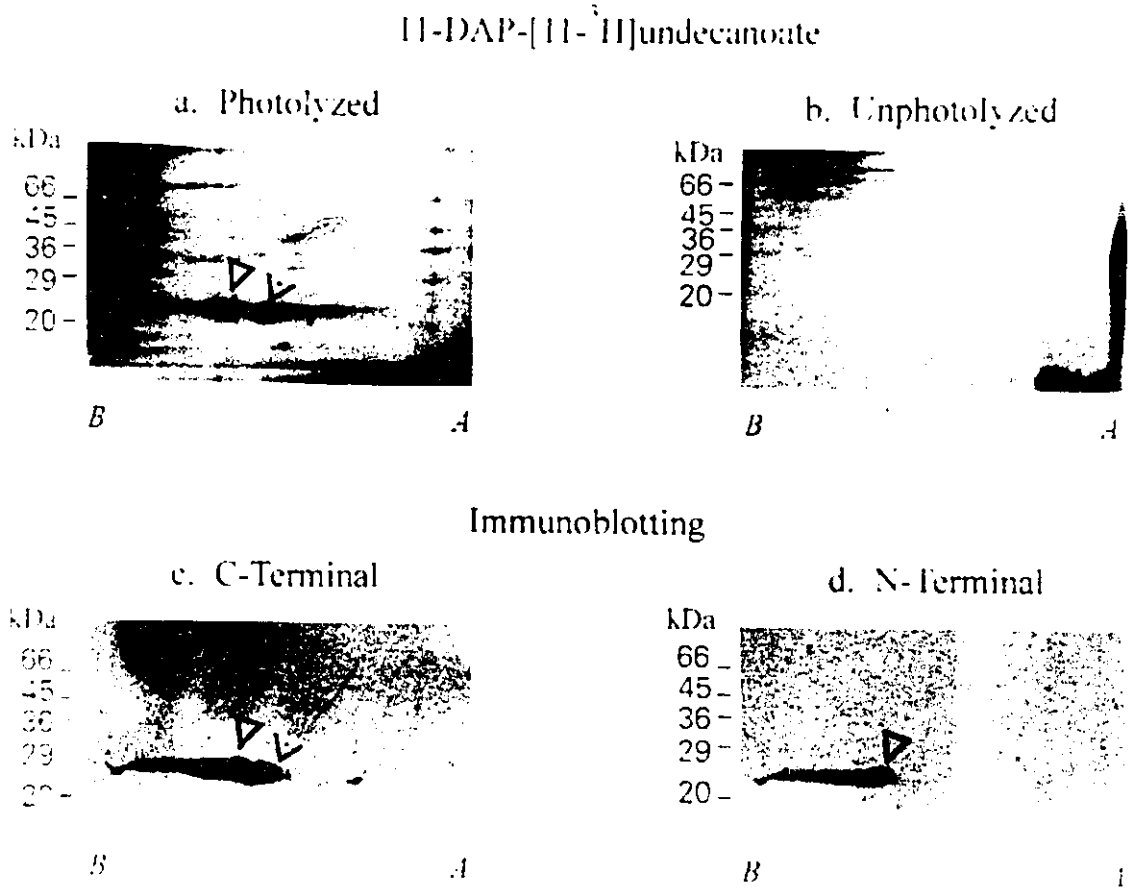

Figure 28. **2D-PAGE analysis of caveolin.** Plasma membranes isolated from 3T3-L1 adipocytes were incubated with 10 μM 11-DAP[11-^{3}H]undecanoate and were either photolyzed as described in the legend to figure 24 (**a.**, **c.** and **d.**) or kept protected from light without photolysis (**b.**). Samples (37.3 μg of protein) were subjected to NE-IEF for 2.0 hrs followed by SDS-PAGE as described in Section B.10.3. Gels were either subjected to fluorography to allow the visualization of radioactively labeled proteins (**a.** and **b.**), or were subjected to electrophoretic transfer to PVDF membranes followed by Western analysis as described in Sections B.10.5 and B.10.4, respectively. Blots were probed with the rabbit-primary antibodies of the following specificities: **c.** Specific for the C-terminal 13 amino acids and **d.** specific for amino acids 19-30 in the N-terminus, predicted from the cDNA sequence of human caveolin. In all panels, *B* and *A* indicate the basic and acidic ends of the gels, while numbers on the left of each panel indicate the positions of protein standards as in the legend to figure 21. The open triangle indicates the position of the higher molecular weight, more basic spot, whereas the arrowhead indicates the position of the lower molecular weight, more acidic spot.

recognized the high but not the low molecular weight form of caveolin. The results of figure 28 (c and d) and those of Dupree et al. (1993) suggest that the lower molecular weight, more acidic form of caveolin might entirely or partially lack the amino acid sequences to which the N-terminal antibodies were raised. This could be due to proteolytic processing of the protein (although caveolin does not have an N-terminal, membrane targeting sequence; Dupree et al., 1993), differential processing of the primary transcript (two transcripts corresponding to human caveolin have been detected; Glenney, 1992) or alternative translation initiation sites. To date, however, neither the cause, nor the functional significance of these different forms of caveolin are known.

The higher molecular weight more basic spot extended as a streak towards the more basic end of the gel when detected with the anti-caveolin antisera (figure 28c and d). This is consistent with reports that caveolin exists in multiple phosphorylation states (Glenney, 1989; Sargiacomo et al., 1994; Scherer et al., 1994; Tang et al., 1994). Similar streaking, however was not observed for 11-DAP-[11^{3}H]undecanoate-labeled caveolin (figure 28a) suggesting that not all forms bind LCFAs. The recent molecular cloning of murine caveolin and the identification of consensus phosphorylation sites within the derived protein sequence (Sargiacomo et al., 1994; Tang et al., 1994) should enable the effects of phosphorylation on LCFA binding to be investigated *in vitro*. Phosphorylation of caveolin might represent a means of regulation of LCFA binding in an analogous way to that described for ALBP (Section A.7.2; Buelt et al., 1991, 1992; Hresko et al., 1990).

C.3.5. Affinity of Caveolin for the Photoreactive LCFA

Recently, methodology has been described allowing the analysis of specific LCFA binding to high affinity, membrane-bound FABPs in the presence of high capacity non-specific binding of LCFAs by membrane bilayers and the surfaces of reaction vessels (Mangroo, 1992; Mangroo and Gerber, 1992). The ability of a large number of low affinity fatty acid binding sites on membranes and on the walls of reaction vessels to bind LCFAs has long been recognized (Vork et al., 1990; Weisiger, 1993). This results in the depletion of LCFAs at submicromolar concentrations, presenting a problem for the measurement of affinities of low abundance, high affinity FABPs.

One strategy to overcome this is to provide the photoreactive LCFA as a BSA-complex, as in figures 24a and 25b (Mangroo, 1992; Mangroo and Gerber, 1992). In the presence of BSA, a low concentration of uncomplexed LCFA is in equilibrium with a large pool of BSA-complexed LCFA; this effectively maintains a constant concentration of uncomplexed LCFA (Spector, 1975; Spector et al., 1969, 1971; Weisiger et al., 1981). Furthermore, the concentration of uncomplexed LCFA is dependent on the LCFA:BSA ratio (figure 20a) and is constant over a range of BSA concentrations (Weisiger, 1981).

As shown in figure 29, the level of incorporation of the photoreactive probe into caveolin was constant when the concentration of BSA was increased from 10 to 400 μM at a constant ratio of 11-DAP-[11-^{3}H]undecanoate:BSA of 1.0 and a concentration of uncomplexed 11-DAP-[11-^{3}H]undecanoate of 200 nM (as determined from figure 20a). This indicated that the labeling of caveolin was dependent on the concentration of

uncomplexed photoreactive LCFA, and that photoreactive LCFA was not depleted by plasma membranes. This satisfied the conditions required for utilizing BSA to control the concentration of uncomplexed 11-DAP-[11-^{3}H]undecanoate.

The affinities of the high molecular weight, basic and low molecular weight, acidic forms of caveolin for the photoreactive LCFA were determined by photolabeling 3T3-L1 adipocyte plasma membranes in the presence of 50 μM BSA. Labeling was done at different concentrations of uncomplexed 11-DAP-[11-^{3}H]undecanoate by varying the photoreactive LCFA:BSA ratio. The concentration of uncomplexed 11-DAP-[11-^{3}H]undecanoate at each ratio was determined from figure 20a. Labeled proteins were separated by 2D-PAGE as in figure 28. The amounts of 11-DAP-[11-^{3}H]undecanoate incorporated into the high molecular weight, basic spot and the low molecular weight, acid spot (figure 30a and b, respectively) was quantified after their excision from the gel and the elution of the radioactivity as described Section B.11.5.

Upon photolysis, the incorporation of the label into both forms of caveolin was saturable with respect to the concentration of uncomplexed 11-DAP-[11-^{3}H]undecanoate (figure 30). The high molecular weight, basic and low molecular weight, acidic spots displayed similar, high affinities for the photoreactive LCFA (K_d values were 0.373 and 0.388 μM, respectively). The levels of maximal binding were 13.5 and 11.0 pmoles/mg of plasma membrane protein, respectively. Thus, the difference in their N-termini did not affect labeling by the photoreactive LCFA, suggesting that the LCFA binding site is not localized to this region of the protein.

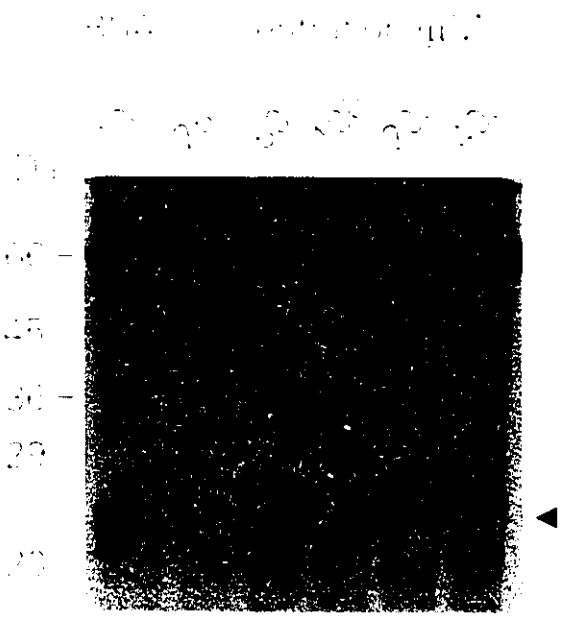

Figure 29. **Effect of BSA concentration on the labeling of caveolin at a constant ratio of 11-DAP[11-^{3}H]undecanoate:BSA.** Plasma membranes from 3T3-L1 adipocytes were photo-labeled (as described in the legend to figure 24) after incubation with varying concentrations of BSA (indicated at the top of each lane) in the presence of 11-DAP[11-^{3}H]undecanoate at a constant molar ratio of photoreactive LCFA:BSA of 1.0. Labeled membranes were washed and analyzed by SDS-PAGE as described in the legend to figure 24, except that the gel was allowed to continue to run after the dye front had run off the gel (until a prestained molecular weight marker of 18 kDa reached the bottom of the gel). Numbers on the left indicate the molecular weights of protein standards as described in the legend to figure 21. The arrow indicates the position of the 22 kDa, caveolin doublet.

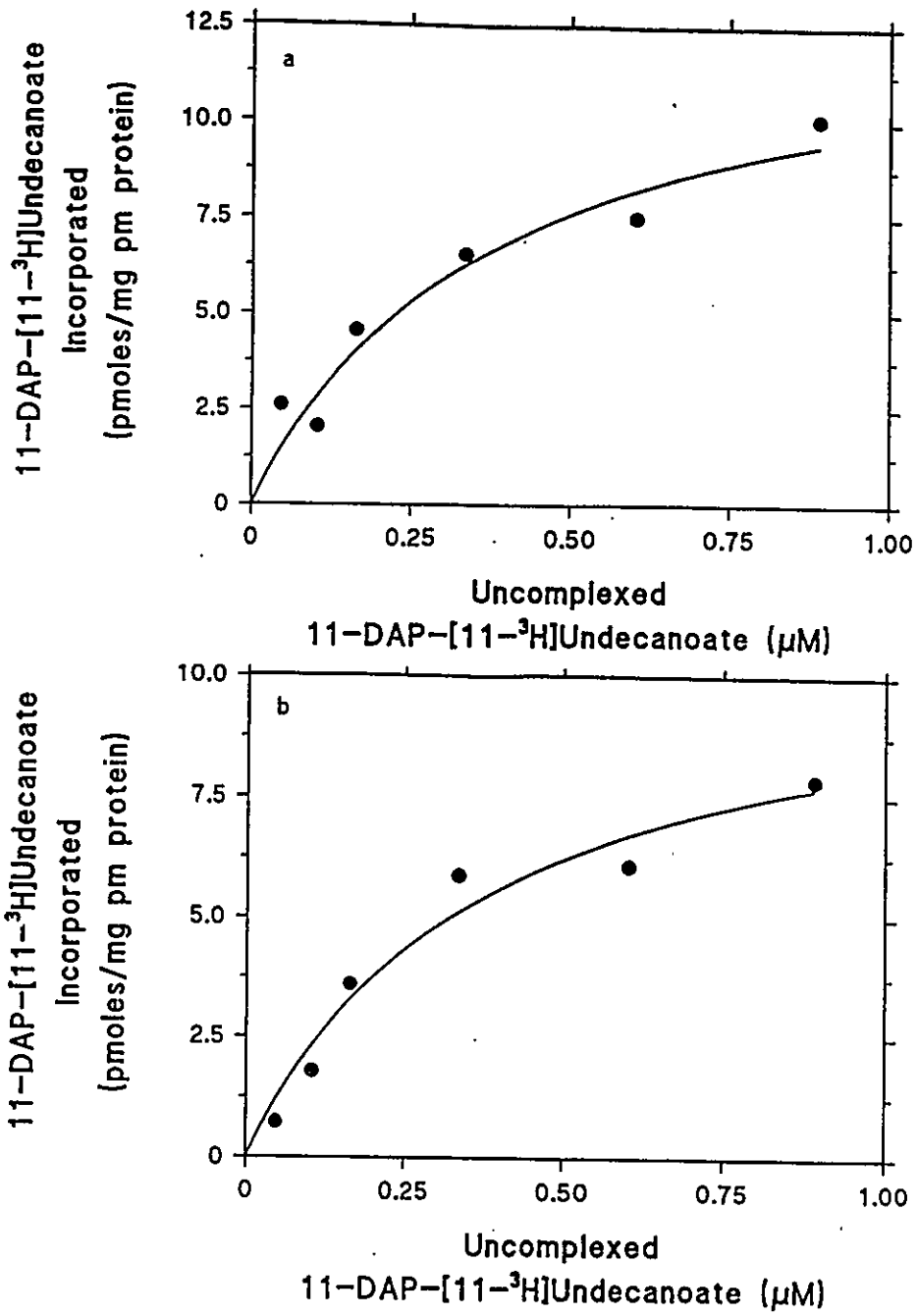

Figure 30. **Affinity of caveolin for 11-DAP-[11-^{3}H]undecanoate measured by photoaffinity labeling.** Plasma membranes isolated from 3T3-L1 adipocytes were labeled with varying concentrations of 11-DAP-[11-^{3}H]undecanoate in the presence of 50 μM BSA as described in the legend to figure 24. Labeled membranes were washed and subjected to 2D-PAGE as described in Section B.10.3. The incorporation of the radioactive label into **a.** the higher molecular weight, more basic and **b.** the lower molecular weight, more acidic spots corresponding to caveolin were quantified after excision of the spots from the dried gels as described in Section B.10.6. Each data point, presented as the number of pmoles of probe incorporated into caveolin per 10 μg of membrane protein represents the combined results of four determinations. The concentration of uncomplexed 11-DAP-[11-^{3}H]undecanoate were determined from the results of the analysis of 11-DAP-[11-^{3}H]undecanoate binding to BSA (figure 20a).

C.3.6. Organization of Caveolin in the Membrane

Pertinent to the potential functions of caveolin as a LCFA receptor, involved in LCFA uptake and/or signalling (discussed in the following Sections), is its orientation in the membrane (figure 31). Based on sequence analysis, caveolin is predicted to be a type II transmembrane protein (orientation 1 in figure 31) with a cytoplasmically oriented amino terminus (amino acid residues 1-101), a single transmembrane domain (amino acids 102-134) and an extra-cytoplasmic C-terminal domain (amino acids 135-178; Tang et al., 1994). This orientation is supported by results demonstrating the biotinylation of caveolin with non-permeant biotinylation reagents (Sargiacomo et al., 1993). In contrast, immunofluorescence studies with antibodies specific for either the carboxyl- or amino-terminal regions of the protein are consistent with a cytoplasmic orientation of both regions, suggesting that the long putative membrane spanning region might form a hairpin in the membrane (figure 31, orientation 2; Dupree et al., 1993; Kurzchalia et al., 1992, 1994). It has also been reported that caveolin oligomerizes in the membrane (Kurzchalia et al., 1994). It has been suggested that the transmembrane domain might form an amphipathic helix which could be organized into a hydrophilic pore in such an oligomeric structure (Kurzchalia et al., 1994).

C.3.7. Implications for the Function of Caveolin

The precise function(s) of caveolin are currently unclear. It has been localized to caveolae in a variety of cells (Lisanti et al., 1994b; Rothberg et al., 1992), as well as to vesicles derived from the *trans*-Golgi network in Madin-Darby canine kidney cells

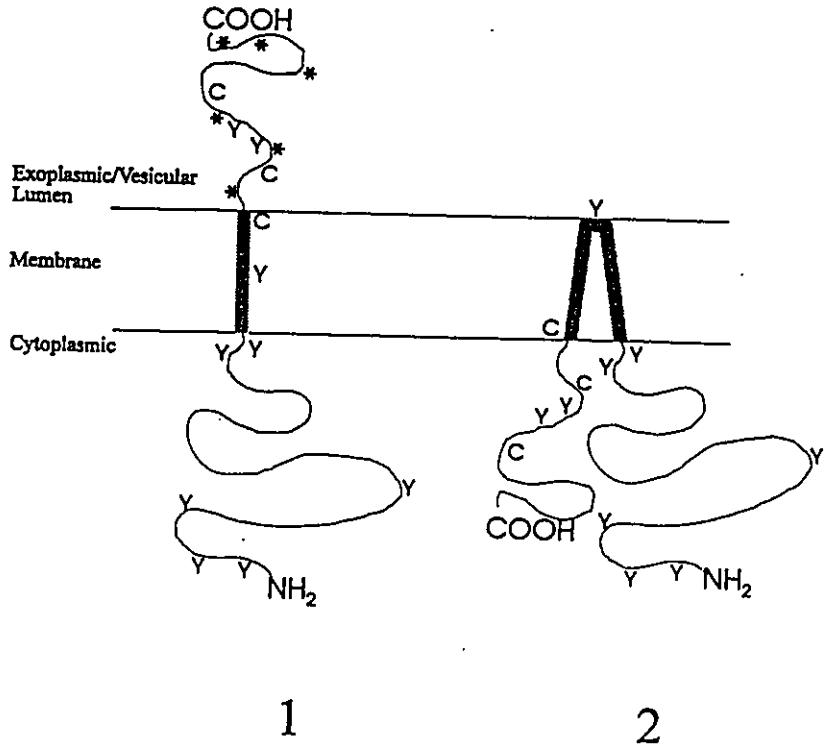

Figure 31. **Orientation of caveolin in the membrane.** Shown are two proposed models for the orientation of caveolin in the membrane. The first proposal, that caveolin spans the membrane, with its C-terminus oriented externally and N-terminus in the cytoplasm is based on evidence from surface biotinylation of cells using a non-permeant biotinylating reagent (Sargiacomo et al., 1993). The second model, that the membrane spanning domain of caveolin forms a hairpin such that both the C- and N-terminal domains are located in the cytoplasm, is based on studies with antibodies directed against the C- and N-termini, respectively (Dupree et al., 1993; Kurzchalia et al., 1992, 1994). The approximate locations of basic residues (Lys and Arg) in the C-terminal domain, which are succeptible to modification by the biotinylating reagent used by Sargiacomo et al. (1993) are indicated by asterisks. The approximate locations of Tyr (Y) and Cys (C) residues which are potential sites for phosphorylation and palmitoylation, respectively are also indicated.

(Kurzchalia et al., 1992; Glenney, 1992). These *trans*-Golgi-derived vesicles appear to share many characteristics with isolated caveolae, including high levels of cholesterol and glycosphingolipids and resistance to non-ionic detergents such as Triton X-100 (Kurzchalia et al., 1992; Lisanti et al., 1993, 1994b; Zurzolo et al., 1994). This has suggested that these might represent newly assembled caveolae on their way to the plasma membrane (Kurzchalia et al., 1992; Lisanti et al., 1993). Caveolin has been proposed to have a role in the targeting of these caveolae-like structures to the cell surface (Dupree et al., 1993; Kurzchalia et al., 1992, 1994; Lisanti et al., 1993; Zurzolo et al., 1994).

Caveolin has also recently been found in association with GluT4-containing intracellular vesicles in 3T3-L1 adipocytes (Scherer et al., 1994). GluT4 is recruited from this intracellular compartment to the plasma membrane in response to insulin stimulation (Cushman and Wardzala, 1980). It appears that GluT4 becomes localized to caveolae in the plasma membranes upon recruitment (Scherer et al., 1994). The presence of caveolin in GluT4-containing vesicles suggests that it may be involved in the targeting of these vesicles to caveolae in the plasma membrane (Scherer et al., 1994).

Alternatively, caveolin has been proposed to have a role in maintaining the structural integrity of caveolae at the cell surface (Rothberg et al., 1992). Caveolin is a component of the striated coat surrounding the cytoplasmic face of plasma membrane caveolae; treatment with cholesterol-binding drugs, such as filipin, resulted in the disassembly of caveolae and the disaggregation of the caveolin coat (Rothberg et al., 1992). Recent evidence, however, indicates that caveolin does not have a structural role;

treatment of cells with cholesterol oxidase results in the oxidation of cholesterol in caveolae which has no effect on their morphology or numbers, but results in the internalization of caveolin to a Golgi-derived location (Smart et al., 1994a). This has prompted speculation that caveolin might be involved in the shuttling of cholesterol between plasma membrane caveolae and the Golgi apparatus (Smart et al., 1994a).

Caveolin might serve as a LCFA receptor involved in LCFA uptake (discussed in the following section). Alternatively, the demonstration that LCFAs can stimulate the recruitment of GluT4 to the plasma membrane in rat adipocytes (Hardy et al., 1991), suggest that the LCFA binding activity of caveolin might be involved in mediating this effect. Caveolin associates in caveolae with a number of proteins involved in the transduction of signals. These include heterotrimeric G-proteins as well as the Src-related tyrosine kinase, c-Yes (Sargiacomo et al., 1993). Thus, caveolin might function as a LCFA receptor involved in mediating signalling cascades by LCFAs.

C.3.8. Involvement of Caveolae in LCFA Uptake

As suggested above, caveolin might be a LCFA receptor involved in LCFA uptake. Such a receptor could act in concert with putative SA receptors (discussed in Section C.1.5.) to sequester LCFAs in particular regions of the plasma membrane which may be designated for LCFA uptake. Certain lines of evidence suggest that these regions might be caveolae. First is the demonstration that caveolin, a resident protein of caveolae, is the only high affinity LCFA receptor in the plasma membrane (figure 24). Furthermore, the putative SA receptors described in Section C.1.5. (albondin,

glycoproteins 18 and 30, and CD36/FAT, which, itself, has been implicated in LCFA uptake) have all been localized to caveolae (Lisanti et al., 1994b; Schnitzer and Oh, 1994; Schnitzer et al., 1992, 1994). Finally, SA has been shown, by immuno-electron microscopy, to associate with caveolae (Schnitzer et al., 1988). Furthermore, SA remains associated after the isolation of caveolae (Lisanti et al., 1994b). It is surprising, therefore, that in the experiment of figure 25b, a band corresponding to labeled BSA was not present in the caveolae fraction. This could suggest either that labeled BSA did not become associated with caveolae or that unlabeled BSA displaced it more efficiently from caveolae than from plasma membranes. The availability of isolated caveolae should allow these alternatives to be investigated.

Caveolae have been proposed to be involved in the uptake of a variety of solutes through a process called potocytosis (figure 32; Anderson, 1993a; Anderson et al., 1992). In general, this involves the dynamic cycling of caveolae between open and closed states (Anderson, 1993a; Anderson et al., 1992; Parton et al., 1994; Smart et al., 1994b). When caveolae are open to the extracellular environment, solutes have access to the caveolar space and can bind to receptors located within caveolae (figure 32, step 1). Upon closing of the caveolae to the extracellular space, changes are believed to be elicited in some as yet unidentified parameters, resulting in the dissociation of the solute from its receptor and its subsequent uptake, driven by a large concentration gradient across the caveolar membrane (figure 32, step 2; Anderson 1993a; Anderson et al., 1992). The reopening of

the caveolae to the extracellular space (figure 32, step 3) completes the cycle (Anderson 1993a; Anderson et al., 1992).

According to this potocytotic model (figure 32), SA-LCFA complexes and uncomplexed LCFAs would bind to SA receptors and caveolin, respectively, in caveolae. Upon closing of the caveolar compartment, and dissociation of bound LCFAs, they would be taken up into the cytoplasm. The mechanism of transmembrane movement of LCFAs during uptake (black box in figure 32) will be addressed in Section C.6. The use of cell lines not expressing caveolin (such as FRT, a rat thyroid epithelial cell line; Sargiacomo et al., 1993) and reagents which affect caveolae functions should allow this model of LCFA uptake to be tested. Such reagents include filipin, which results in the disassembly of caveolae in a variety of cells (Rothberg et al., 1992; Schnitzer et al., 1994), cholesterol oxidase which stimulates the removal of caveolin from caveolae of human skin fibroblasts (Smart et al., 1994a), and protein kinase C activators which inhibit the closing off of caveolae in epithelial cells (Smart et al., 1994b).

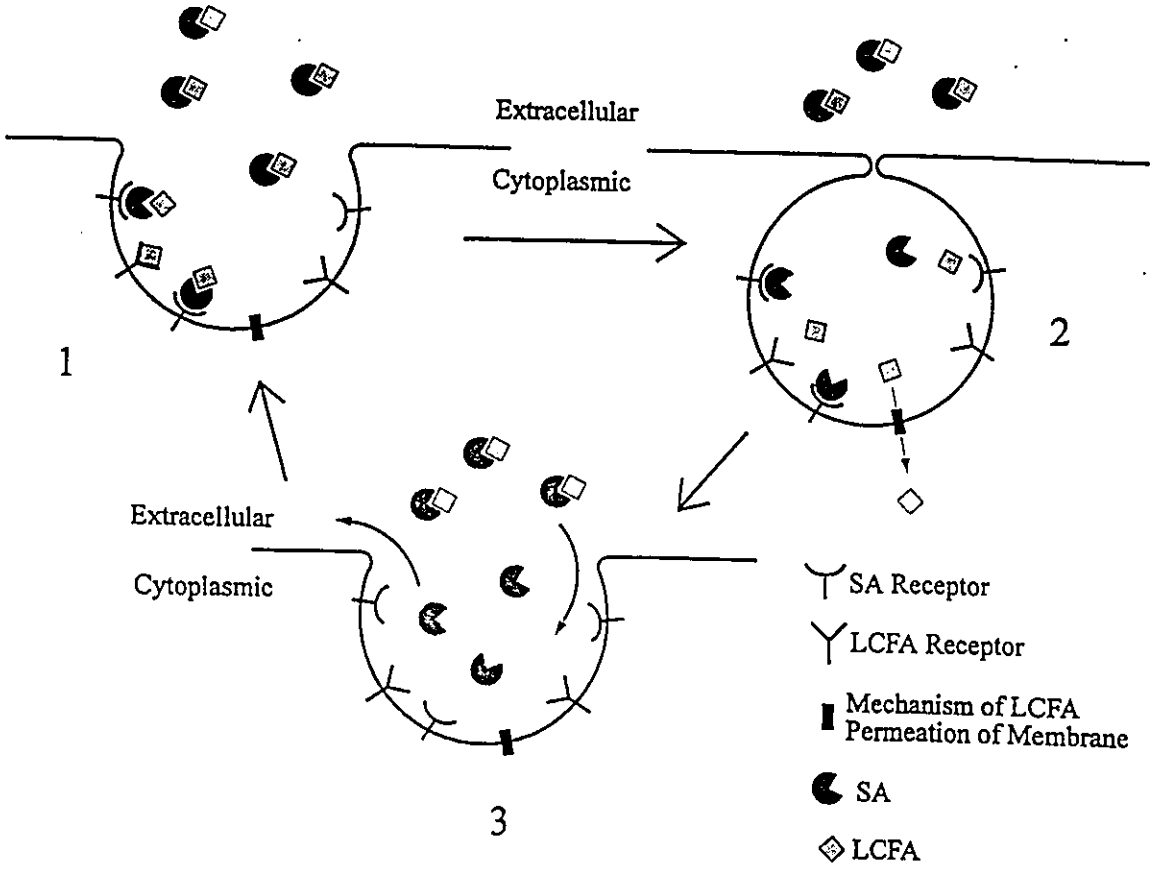

Figure 32. **Model for LCFA uptake mediated by potocytosis.** Caveolae are believed to be involved in the uptake of solutes by potocytosis (Anderson, 1993; Anderson et al., 1992). This process is shown schematically for the case of LCFA uptake. **1.** LCFA-SA complexes and uncomplexed LCFAs are believed to bind to their respective receptors when caveolae are open to the external medium. **2.** The caveolae then close off and LCFAs dissociate from their receptors and SA as a result of some putative change in an undefined parameter. The resulting high concentration of LCFA within the caveolar compartment then drives LCFA permeation across the membrane which occurs by an as yet undefined process (indicated by a black box in the figure). **3.** Caveolae re-open to begin the cycle again.

C.4. Labeling and Characterization of the ALBP

C.4.1. Identification of the 15 kDa FABP as ALBP

The labeling of a 15 kDa cytoplasmic protein in intact 3T3-L1 adipocytes with 11-DAP-[11^{3}H]undecanoate (figures 22 and 23) indicated that the photoreactive LCFA was internalized by these cells. The absence of labeling of the protein in undifferentiated cells (figure 22 lanes P and U) was most likely the result of the absence of the protein, since these cells internalized the photoreactive probe as shown by the labeling of mitochondrial proteins (compare figures 22 and 23).

To confirm the absence of the protein from undifferentiated cells, cytoplasm was isolated from differentiated and undifferentiated cells and labeled by photolysis after incubation with 10μM 11-DAP-[11-^{3}H]undecanoate (figure 33). A 66 kDa band was labeled in both cases. This was most likely due to BSA carried over from the growth medium. A 15 kDa protein was also labeled in cytoplasm from differentiated adipocytes but not in cytoplasm from undifferentiated cells (figure 33a). A protein of corresponding molecular weight was lightly stained by Coomassie blue in cytoplasm from differentiated cells but not in cytoplasm from undifferentiated cells (figure 33b), suggesting that it was induced upon differentiation.

Based on its specific labeling by the probe, molecular weight, cytoplasmic location and induction in adipocytes, the protein appeared to be a low molecular weight,

adipocyte-specific FABP, suggesting that it might be the ALBP. To confirm this, cytoplasm was prepared from 3T3-L1 adipocytes labeled with the photoreactive LCFA (as in the legend to figure 23) and was analyzed by 2D-PAGE followed by Western blotting using the affinity purified anti-ALBP antibody (figure 34a) or by fluorography to detect the incorporation of photoreactive probe (figure 34b). Western analysis revealed that the ALBP migrated as two spots of apparent molecular weight of 15 kDa but different pI values. This is consistent with the ALBP existing as phosphorylated and non-phosphorylated forms (Bernier et al., 1987; Hresko et al., 1990). The photoaffinity labeled 15 kDa protein migrated as a single spot coincident with the more basic of the two spots detected with the anti-ALBP antibody (compare panels a and b). The reason that only the more basic of the two spots detected by the antibody was labeled with the photoreactive LCFA is unclear, however it might relate to the reported inhibition of LCFA binding by phosphorylation of the protein (Buelt et al., 1992).

These results confirmed the identity of the 11-DAP-[11-^{3}H]undecanoate-labeled, 15 kDa cytoplasmic protein as the ALBP. Waggoner and Bernlohr (1990) have also demonstrated the photolabeling of the ALBP in intact 3T3-L1 adipocytes with a photoreactive lipid, 4-azido-N-hexadecylsalicylamide. This reagent, however lacked a carboxyl-group, which has been shown to be involved in the binding of LCFAs to the ALBP (Sacchettini and Gordon, 1993; Xu et al., 1993). Furthermore, it is not clear whether the labeling obtained was specific for the LCFA binding site of the protein. This is because the photoreactive group used was an aryl-azide. These compounds give rise

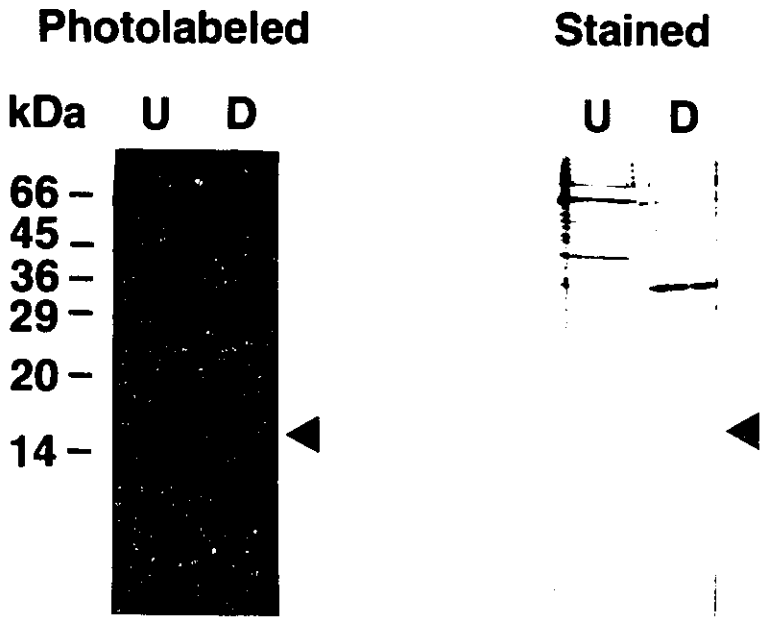

Figure 33. **Photoaffinity labeling of cytoplasmic proteins from 3T3-L1 adipocytes.** Delipidated cytoplasmic fractions were isolated as described Section B.6.2. from undifferentiated (**U**) or differentiated (**D**) cells and were incubated with 10 μM 11-DAP-[11-^{3}H]undecanoate for 10 min at 37°C in 10 mM sodium phosphate, pH 7.4. Photolysis was done as described in the legend to figure 24. Samples containing 5 μg of protein were analyzed by SDS-PAGE on a 15% polyacrylamide gel, which was stained with Coomassie blue (right panel) and subjected to fluorography (left panel). Numbers on the left indicate molecular masses of markers as in the legends to figures 21 and 22. The arrowheads indicate the positions of the bands of interest.

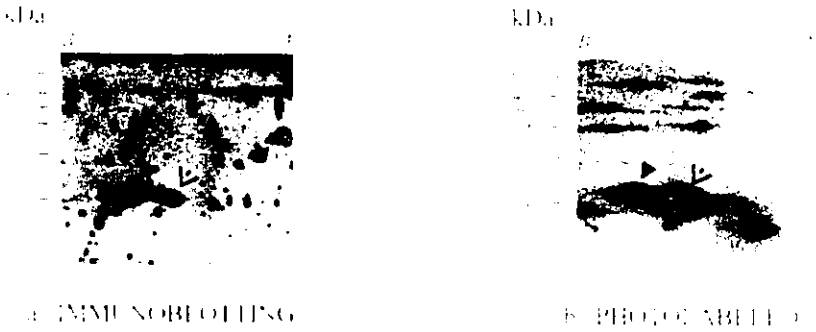

Figure 34. **2D-PAGE analysis of photoaffinity-labeled cytoplasmic proteins.** 3T3-L1 adipocytes were labeled with 11-DAP-[11-^{3}H]undecanoate and cytoplasm was prepared as described in the legend to figure 23. Labeled cytoplasm was subjected to 2D-PAGE as described in Section B.10.3. Gels were either **a.** transferred to PVDF membranes which were probed with an affinity purified antibody specific for murine ALBP (as described in the legend to figure 8 and Section B.10.4), or **b.** subjected to fluorography. Arrows indicate the spots of interest and numbers on the left of each panel indicate the molecular weights of protein standards as described in the legends to figures 21 and 22. *B* and *A* indicate the basic and acidic ends of the gel, respectively.

upon photolysis to aryl-nitrenes, which are considerably less reactive than carbenes (Bayley, 1983). In fact, because aryl-nitrenes rely on the presence of functional groups on the protein for reaction, aryl-azides have been considered unsuitable for the labeling of hydrophobic sites, such as LCFA binding sites (Bayley, 1983).

C.4.2. Affinity of ALBP for 11-DAP-[11-^{3}H]undecanoate

To investigate the affinity of the ALBP for the photoreactive LCFA, its labeling in the presence of BSA was studied. BSA was included in the labeling reaction to provide a submicromolar concentration of uncomplexed photoreactive LCFA which would not be depleted by nonspecific binding (as described in Section C.3.5). Appropriate conditions were determined by labeling 3T3-L1 adipocyte cytoplasm with 11-DAP-[11-^{3}H]undecanoate added as a 1:1 molar ratio with BSA (figure 35, lanes marked as A). The resulting concentration of uncomplexed 11-DAP-[11-^{3}H]undecanoate was 266 nM (from figure 20a). The level of labeling of the 15 kDa band in cytoplasm from differentiated cells was relatively constant when the concentration of BSA was varied from 5 to 25 μM. Cytoplasm isolated from cells maintained in an undifferentiated state after confluence was also labeled (figure 35, lanes marked with P) as a control for background. As another control, BSA was labeled in the absence of cytoplasmic proteins (lanes marked C). While protein bands in the vicinity of 15 kDa were not labeled by the photoreactive LCFA when BSA concentrations were low (5.0-10 μM) they did become labeled at higher concentrations of BSA. These labeled bands were most likely derived from BSA, since they appeared when BSA was labeled in the absence of cytoplasm. Based on these

results, 10 μM BSA was chosen as a convenient compromise between sufficient LCFA buffering and reduced background.

When labeling was done in the presence of 10 μM BSA, the incorporation of the photoreactive LCFA into ALBP (determined as described in Section B.10.6) was saturable with respect to the concentration of uncomplexed 11-DAP-[11-^{3}H]undecanoate (figure 36). Values for K_d and maximal binding were 0.91 μM and 111 pmoles/mg of cytoplasmic protein, respectively. Thus the affinity of the ALBP for 11-DAP-[11-^{3}H]undecanoate is in the same range of affinities for a variety of natural LCFAs and derivatives (Table 6; Buelt et al., 1992; Lalond et al., 1994b; Matarese and Bernlohr, 1988; Sha et al., 1993).

C.4.3. Interaction of ALBP with Natural LCFAs

To confirm that the photoreactive LCFA interacted with the ALBP at its LCFA binding site, cytoplasm prepared from adipocytes was labeled with 10 μM 11-DAP-[11-^{3}H]undecanoate in the presence of increasing concentrations of oleic and palmitic acids (figure 37). Labeling was carried out in the absence of BSA to avoid effects of the competitor LCFAs on the equilibrium concentration of uncomplexed photoreactive LCFA. The level of incorporation of the photoreactive LCFA into the ALBP upon photolysis was plotted versus the concentration of competitor LCFA (figure 37). Both oleate (figure 37a) and palmitate (figure 37b) resulted in apparently saturable decreases in the level of labeling of the ALBP. The concentrations at which inhibition was half of maximal (apparent K_d) were 2.97 and 3.52 μM for oleic and palmitic acids, respectively. These values are similar to K_d values determined for the binding of a variety of LCFAs to

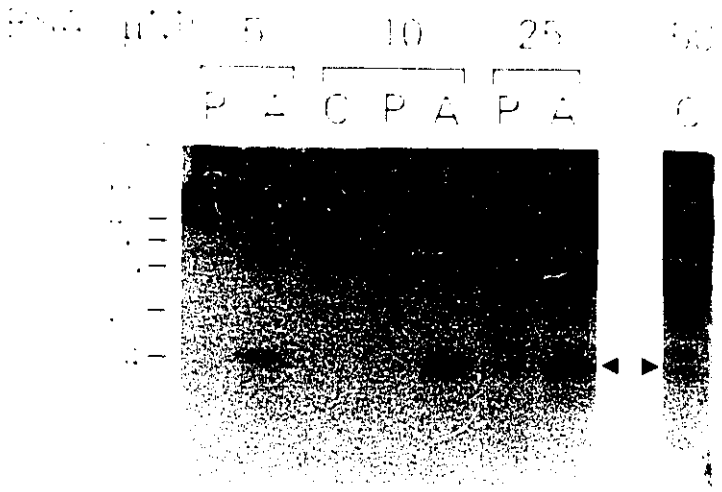

Figure 35. **Labeling of cytoplasm from 3T3-L1 adipocytes *in vitro* in the presence of increasing concentrations of BSA at a constant molar ratio of 11-DAP-[11-^{3}H]undecanoate:BSA.** Delipidated cytoplasm was isolated from 3T3-L1 adipocytes (A) or cells maintained beyond confluence in an undifferentiated state (P), as described in Section B.6.2. Samples (0.5 mg cytoplasmic protein/ml in 10 mM sodium phosphate, pH 7.4) were incubated for 10 min at 37°C with either 5, 10 or 25 μM BSA in the presence of an equivalent concentration of 11-DAP-[11-^{3}H]undecanoate. Samples lacking cytoplasmic protein (C) but containing either 10 or 50 μM BSA were also included. Photolysis was as described in the legend to figure 22. Labeled samples (equivalent to 6.25 μg of cytoplasmic protein) were analysed by SDS-PAGE as described in Section B.10.2, on 15 % acrylamide gels which were processed for fluorography. Numbers on the left indicate molecular masses of markers as in the legends to figures 21 and 22. The arrowheads indicate the positions of the bands of interest.

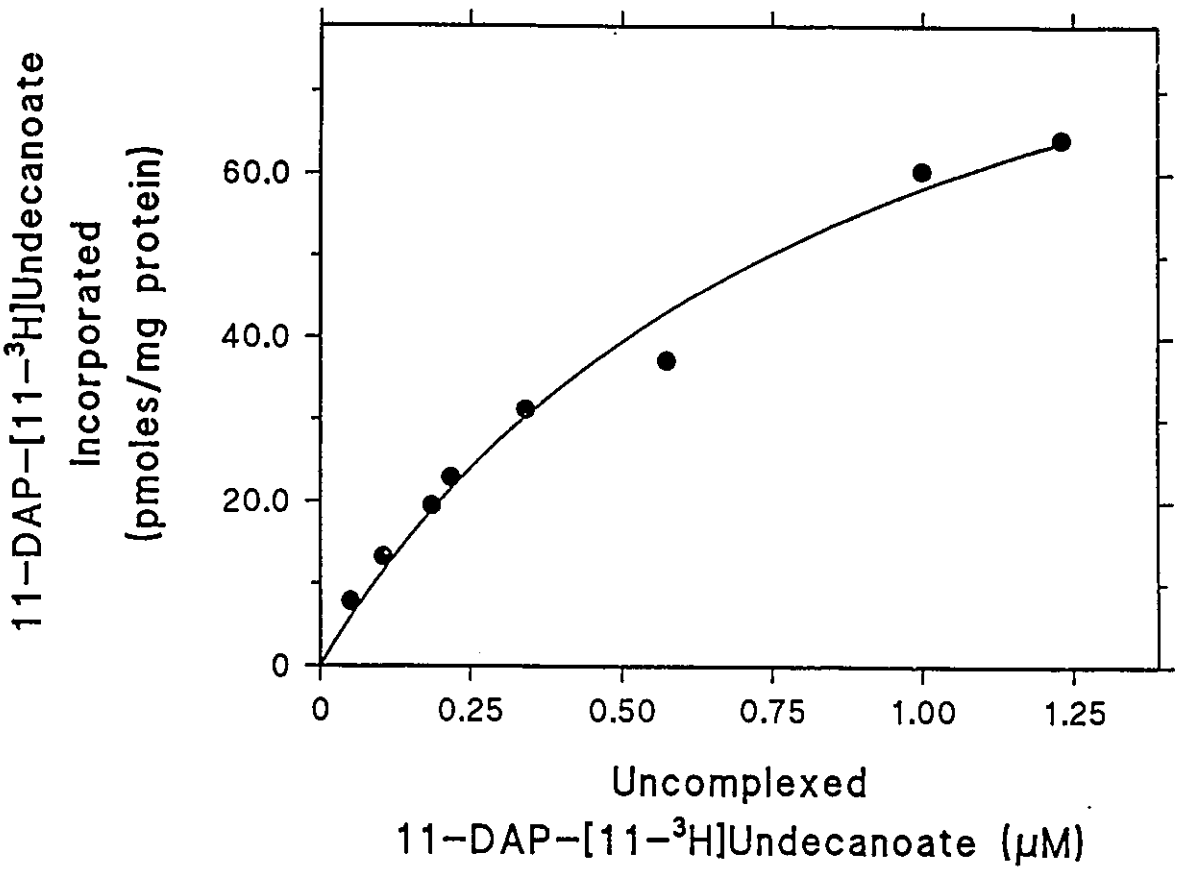

Figure 36. **Affinity of ALBP for 11-DAP-[11-^{3}H]undecanoate as measured by photoaffinity labeling.** Delipidated cytoplasm, isolated from 3T3-L1 adipocytes, was labeled with varying concentrations of 11-DAP-[11-^{3}H]undecanoate in the presence of 10 μM BSA and subjected to SDS-PAGE as described in the legend to figure 33. The incorporation of the radioactive label into the band corresponding to ALBP was quantified after excision from the dried gel as described in Section B.10.6. The concentrations of uncomplexed 11-DAP-[11-^{3}H]undecanoate were determined from the results of the analysis of 11-DAP-[11-^{3}H]undecanoate binding to BSA (figure 20a).

purified ALBP using a variety of techniques, including standard radiochemical methods, fluorescence assays with fluorescent LCFA analogues, and titration calorimetry (Table 6; Buelt et al., 1992; Matarese and Bernlohr, 1988; Lalond et al., 1994b; Sha et al., 1993). This both confirms that the photoreactive LCFA interacts with the ALBP at its LCFA binding site and demonstrates the usefulness of this technique for the measurement of the binding of natural LCFAs to cytoplasmic FABPs in complex mixtures, such as crude cytoplasmic fractions. It has the advantage over standard radiochemical methods of overcoming problems associated with the separation of bound from unbound forms of the FABP for detection (Glatz and Veerkamp, 1983; Vork et al., 1990). Furthermore, it has the advantage over all other methods currently in use by allowing the measurement of specific binding of LCFAs by relatively low levels of cytoplasmic FABPs in crude mixtures, avoiding the requirement for large amounts of purified proteins.

While the majority of binding constants reported for the ALBP (Table 6) and other cytoplasmic FABPs are in the low micromolar range, Richieri et al. (1994) have recently reported binding constants 1-2 orders of magnitude lower. The reasons for this discrepancy are unknown, although they might be related to the fact that Richieri et al. measured LCFA binding indirectly. They indirectly measured the concentration of uncomplexed LCFA in equilibrium with bound LCFA, with the use of the intestinal-FABP derivatized with a fluorescent group that was sensitive to LCFA binding (called acrylodated-intestinal FABP, or ADIFAB; Richieri et al, 1992); this was then used as an indirect measure of the level of LCFA binding to a second FABP present in large

amounts (Richieri et al., 1994). In contrast, all other techniques monitor the amount of bound LCFA either directly or by monitoring the change in some property of the protein upon LCFA binding (Buelt et al., 1992; Matarese and Bernlohr, 1988; Lalond et al., 1994b; Sha et al., 1993). The use of the photoreactive LCFA also has the advantage of allowing the direct measurement of the interaction of LCFAs with FABPs.

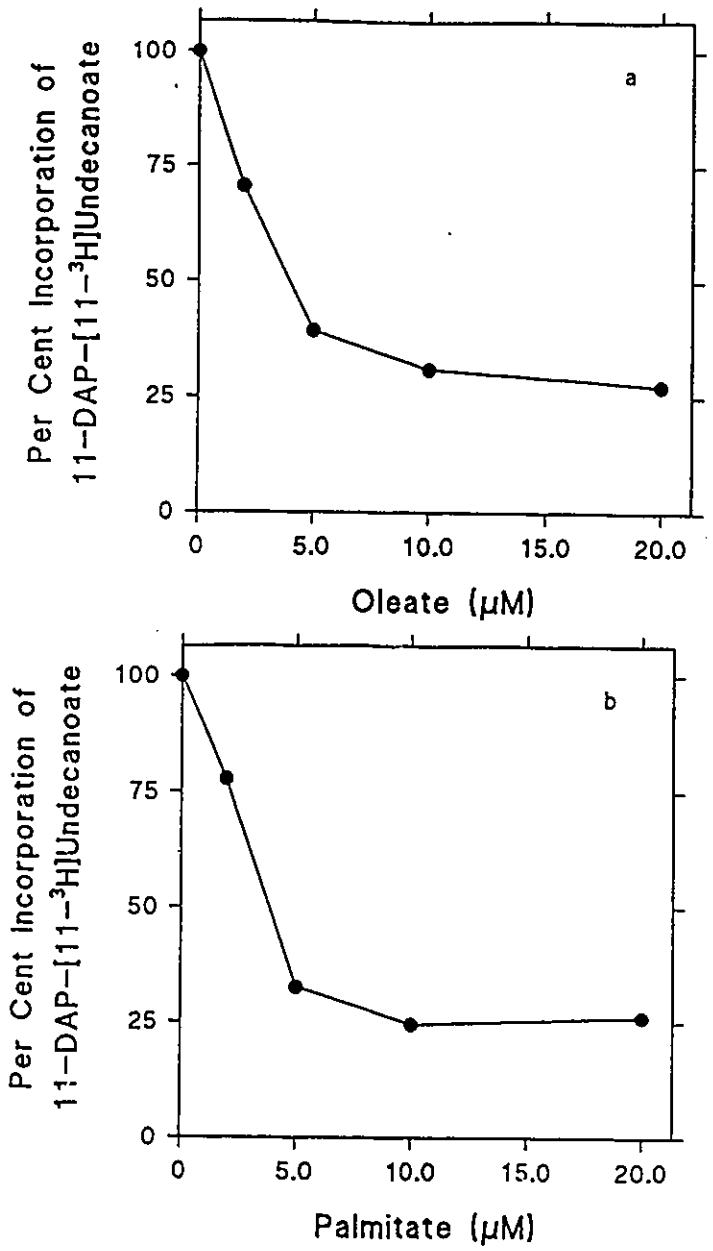

Figure 37. **Oleate and palmitate compete out the photoaffinity labeling of ALBP by 11-DAP-[11-^{3}H]undecanoate.** Delipidated cytoplasm, isolated from 3T3-L1 adipocytes, was incubated at 37°C for 10 min at a protein concentration of 0.50 mg/ml in 10 mM sodium phosphate, pH 7.4, with 10 μM 11-DAP-[11-^{3}H]undecanoate in the presence of increasing concentrations of **a.** oleate or **b.** palmitate, each added as ethanolic stocks. The final concentration of ethanol was 1.0 % and did not, itself, affect the level of incorporation of the photoreactive LCFA into ALBP upon photolysis. Samples were photolyzed as described in the legend to figure 22. After photolysis, samples were subjected to SDS-PAGE on 15 % acrylamide gels, followed by fluorography. The incorporation of 11-DAP-[11-^{3}H]undecanoate into ALBP was determined as described in Section B.10.6.

Table 6. **Dissociation constants for the binding of various LCFAs and derivatives to the murine 3T3-L1 ALBP.**

Ligand	K_d (μM)
Palmitate	3.5±2.2[a] 0.077[b]
α-Iodopalmitate	4.20±0.71[c]
Oleate	2.97±0.94[d] 3.0[e] 2.4±1.0[f] 0.056±0.009[b]
Retinoate	50[e]
Arachidonate	4.4±1.1[f] 0.139±0.013[b]
12-Anthroyloxy-oleate	1.0[g] 2.0±0.4[h] 2.3±0.1[i]
cis-Parinarate	1.7±0.2[h] 0.5±0.1[i]
11-DAP-[11-^{3}H]-undecanoate	0.91±0.17[j]

a. Competition with 11-DAP-[11-^{3}H]undecanoate. This work, figure 37b.
b. Use of ADIFAB as probe for concentration of uncomplexed fatty acid (Richieri et al., 1994)
c. As a.; figure 50 a.
d. As a.; figure 37 a.
e. Liposome method of delivery of fatty acid (Matarese and Bernlohr, 1988).
f. Titration calorimetry (Lalond et al., 1994b).
g. Fluorescence based assay (Buelt et al., 1992).
h. Fluorescence based assay. Used recombinant ALBP (Sha et al., 1993).
i. As h., but with ALBP-GST fusion protein.
j. Photoaffinity labeling. This work, figure 36.
a., c., d., j. Done with crude 3T3-L1 adipocyte cytoplasmic fraction.
b., e.-i. Used purified proteins.

C.5. Involvement of ALBP in LCFA Trafficking *In Vivo*

C.5.1. The Photoaffinity Labeling of ALBP in Intact Cells is Dynamic

As mentioned previously, photoaffinity labeling is well suited for the analysis of the time-dependent interaction of the probe with cellular proteins. This is due the fact that photoaffinity reagents are inert until exposed to a brief flash of intense light, allowing the labeling reaction to be initiated at timed intervals (Bayley, 1983). Because photolysis results in the covalent attachment of the radioactive probe to binding proteins, the interaction of the probe with individual proteins can be followed. Therefore, the spatial and temporal distribution of the probe can be determined in intact cells.

The finding that the ALBP was labeled when intact 3T3-L1 adipocytes were photolyzed in the presence of the photoreactive LCFA suggested that it could be used to monitor the internalization of the photoreactive probe and its trafficking to intracellular sites of utilization in intact cells. Therefore, the effect of the time of incubation (at 37°C) of intact 3T3-L1 adipocytes with 11-DAP-[11-^{3}H]undecanoate on the labeling of ALBP was investigated (figure 38). The labeling of ALBP (arrow) increased with incubation time up to 20 sec, after which it began to decrease until it was virtually zero by 100 sec. The level of labeling of the mitochondrial 34 kDa protein, however, continued to increase over the entire time course. This provides direct evidence that newly internalized LCFAs interact with the cytoplasmic ALBP in a dynamic way. It indicates that *in vitro*, LCFAs,

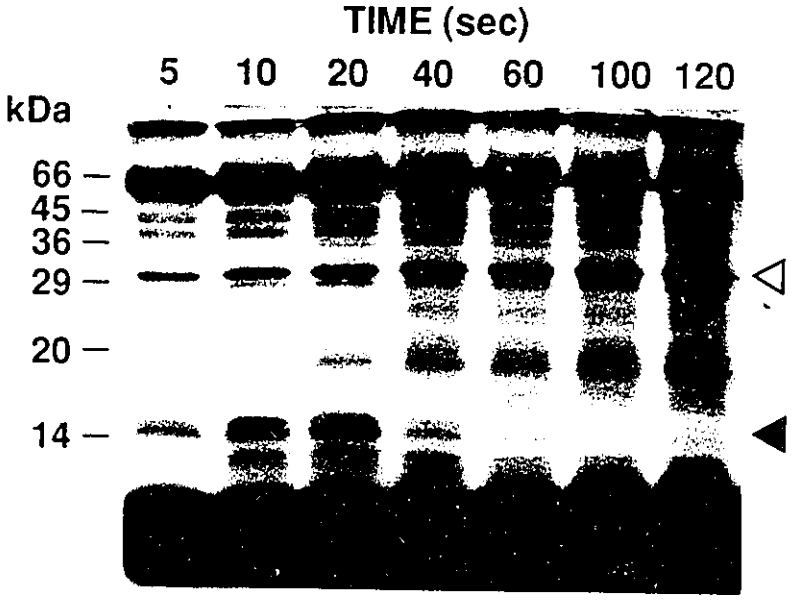

Figure 38. **Time dependance of labeling of intracellular FABPs in intact 3T3-L1 adipocytes with 11-DAP-[11-^{3}H]undecanoate.** Cells were incubated for various times (indicated at the top of each lane) at 37°C with 200 μM 11-DAP-[11-^{3}H]undecanoate in the presence of 50 μM BSA at 8.0 mg cell protein/ml in PBS. They were then photolyzed by a 2.0 sec exposure to light from a 1000 W Xe-Hg lamp, filtered by passage through 0.020 % potassium hydrogen phthalate as described in the legend to figure 21. An equal amount of each sample (25 μg cellular protein) was analyzed by SDS-PAGE on a 15 % acrylamide gel which was subjected to fluorography (as described in Sections B.10.2 and B.10.5, respectively). Arrowheads on the right indicate the positions of the mitochondrial fatty acid binding protein (open arrowhead) and the cytoplasmic ALBP (solid arrowhead). Numbers on the left indicate molecular weights in kDa of protein standards as described in the legend to figures 21 and 22.

upon entering the cytoplasm first bind to the ALBP and are then transferred to other intracellular sites. This is consistent with a role for the ALBP in intracellular LCFA trafficking.

C.5.2. Effect of DIDS Treatment of Cells on the Internalization of LCFAs

To determine whether the labeling of the ALBP in intact cells responded to the inhibition of the internalization of the probe, cells were treated with DIDS, a known inhibitor of LCFA uptake in rat adipocytes (Abumrad et al., 1984; Harmon et al., 1991). Because it is highly charged, it does not permeate the plasma membrane of cells; therefore, it is presumed to act at the plasma membrane to inhibit early events in LCFA uptake, such as the delivery of LCFAs to the membrane by SA, or the permeation of LCFAs across the membrane (Abumrad et al., 1984). Consistent with this, DIDS has been found to covalently modify an 85 kDa rat adipocyte plasma membrane protein recently identified as CD36/FAT (Abumrad et al., 1984, 1993; Harmon et al., 1991). The effect of DIDS on oleate uptake in 3T3-L1 adipocytes is shown in figure 39. As reported for rat adipocytes, a 45 min pre-incubation of 3T3-L1 adipocytes with DIDS at 37°C resulted in the inhibition of oleate uptake. Furthermore, this inhibition was irreversible since it was not affected by washing the cells after treatment with DIDS. This is consistent with the covalent modification of one or more proteins by DIDS, as reported for rat adipocytes.

The effect of DIDS pretreatment on the photoaffinity labeling of the ALBP in intact cells with the photoreactive LCFA is shown in figure 40. The pretreatment of cells

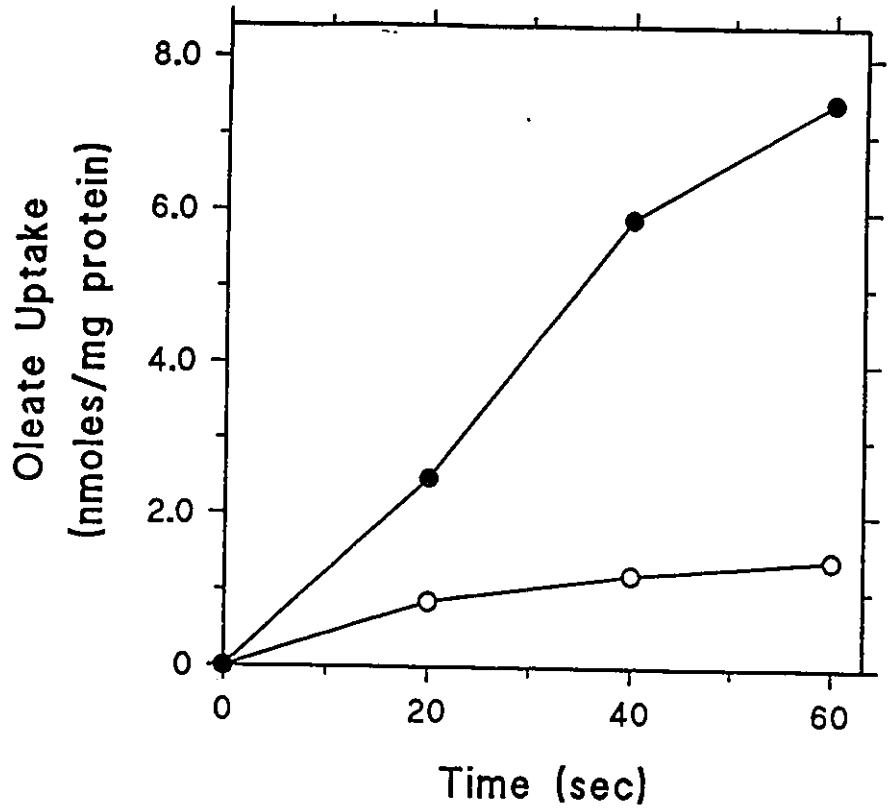

Figure 39. **Effect of pretreatment of 3T3-L1 adipocytes with DIDS on [9,10-^{3}H]oleate uptake.** 3T3-L1 adipocytes, harvested as described in Section B.3.4, were treated with 1.0 mM DIDS (O) at 1.0 mg of cellular protein/ml in PBS, at 37°C for 45 min, in the dark. DIDS was added from a 100-fold stock in DMSO, such that the concentration of DMSO was 1.0 %. DMSO was also included in the absence of DIDS as a control (●). After treatment, cells were pelleted for 10 min at 450×*g*, at 4.0°C, and then resuspended gently to 1.0 mg/ml in PBS and the uptake of [9,10-^{3}H]oleate was measured as described in Section B.4.3. Results represent typical time courses of uptake.

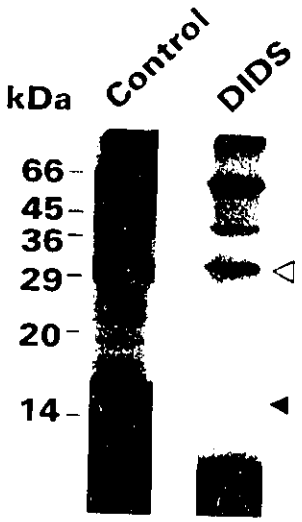

Figure 40. **Effect of the pretreatment with DIDS on the labeling of intracellular FABPs in intact 3T3-L1 adipocytes.** Cells were treated at 4.0 mg cell protein/ml in PBS for 60 min at 37°C with either 1.0% DMSO (lane marked **Control**) or 1.0 mM DIDS (lane marked **DIDS**), as described in the legend to figure 40. They were then incubated for 15 sec at 37°C with 100 μM 11-DAP-[11-^{3}H]undecanoate in the presence of 50 μM BSA and photolabeled as described in the legend to figure 39. Cellular protein (25 μg) was analyzed by SDS-PAGE on a 15% acrylamide gel which was subjected to fluorography as described in Sections B.10.2 and B.10.5, respectively. Arrowheads on the right indicate the positions of the mitochondria, 34 kDa protein (open arrowhead) and the cytoplasmic ALBP (solid arrowhead). Numbers on the left indicate molecular weights (in kDa) of protein standards as indicated in the legends to figures 21 and 22.

with 1.0 mM DIDS for 45 min. resulted in almost complete inhibition of the labeling of the ALBP in cells irradiated after a 15 sec incubation, at 37°C, with 200 μM 11-DAP-[11-^{3}H]undecanoate in the presence of 100 μM BSA. Similarly, the labeling of the 34 and 40 kDa proteins (which fractionated with the mitochondria, see figure 23) was also reduced in DIDS-treated relative to control cells (figure 40). The fact that labeling of these proteins was still observed, however, suggests that DIDS did not fully inhibit the internalization of the photoreactive probe. This is consistent with the observation that DIDS did not completely inhibit oleate uptake in either 3T3-L1 or rat adipocytes (figure 39; Abumrad et al., 1984). These results confirm the proposal that DIDS inhibits LCFA uptake by affecting one or more early steps in process (see p. 167). They also demonstrate that the labeling of the ALBP by the photoreactive LCFA in intact cells reflects the cytoplasmic concentration of the probe. Furthermore, they confirm that the photolabeling of ALBP in intact cells can be used to monitor the internalization of the probe by the cells, as an alternative to standard assays for LCFA uptake which measure the total accumulation of tracer LCFA.

C.5.3. Effect of α-Iodopalmitate on the Internalization of LCFAs

α-Halo-fatty acids are also known to inhibit LCFA uptake in both rat hepatocytes (Mahadevan and Sauer, 1971) and adipocytes (Abumrad et al., 1984). α-Iodopalmitate treatment of 3T3-L1 adipocytes resulted in the inhibition of [9,10-^{3}H]oleate uptake (figure 41) and the incorporation of radioactivity into cellular lipids, including acyl-CoA, polar lipids and triglycerides (figure 42a-c, respectively).

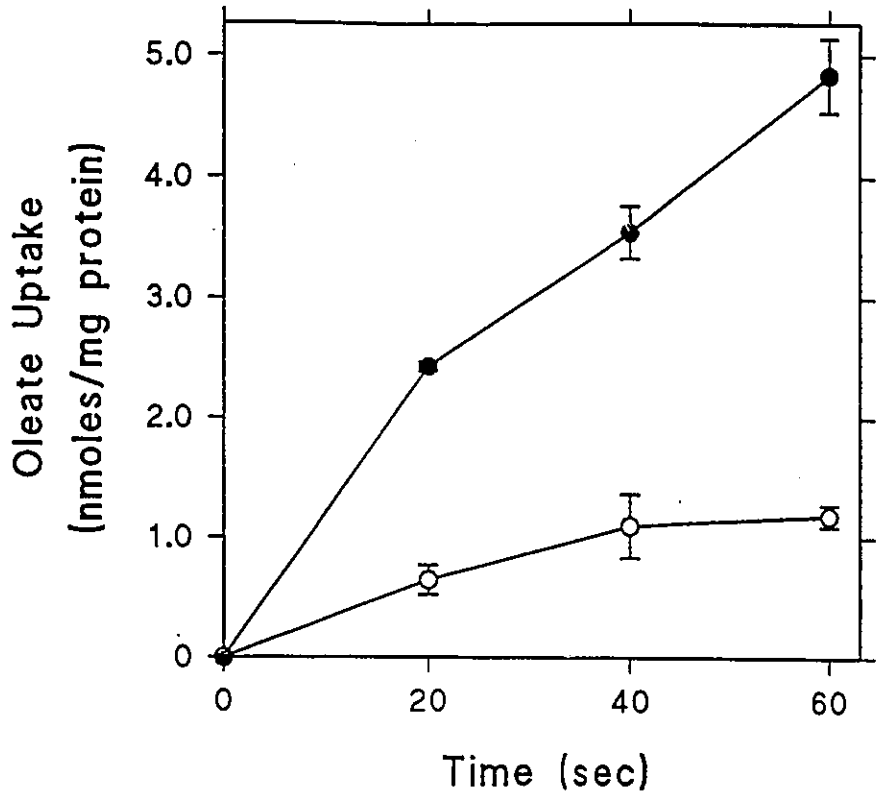

Figure 41. **Inhibition of [9,10-^{3}H]oleate uptake by α-iodopalmitate treatment of 3T3-L1 adipocytes.** Cells (1.0 mg cellular protein/ml) were treated with 50 μM α-iodopalmitate (○) in PBS, pH 7.5 for 15 min at 37°C with shaking. Control cells (●) were treated in parallel in the absence of α-iodopalmitate. Both treated and control cells were pelleted at 450×*g* for 10 min, at 4.0°C and resuspended to 1.0 mg of cellular protein/ml in PBS. [9,10-^{3}H]oleate uptake was measured as described in Section B.4.3. Results represent the means ± S.E.M. of three determinations.

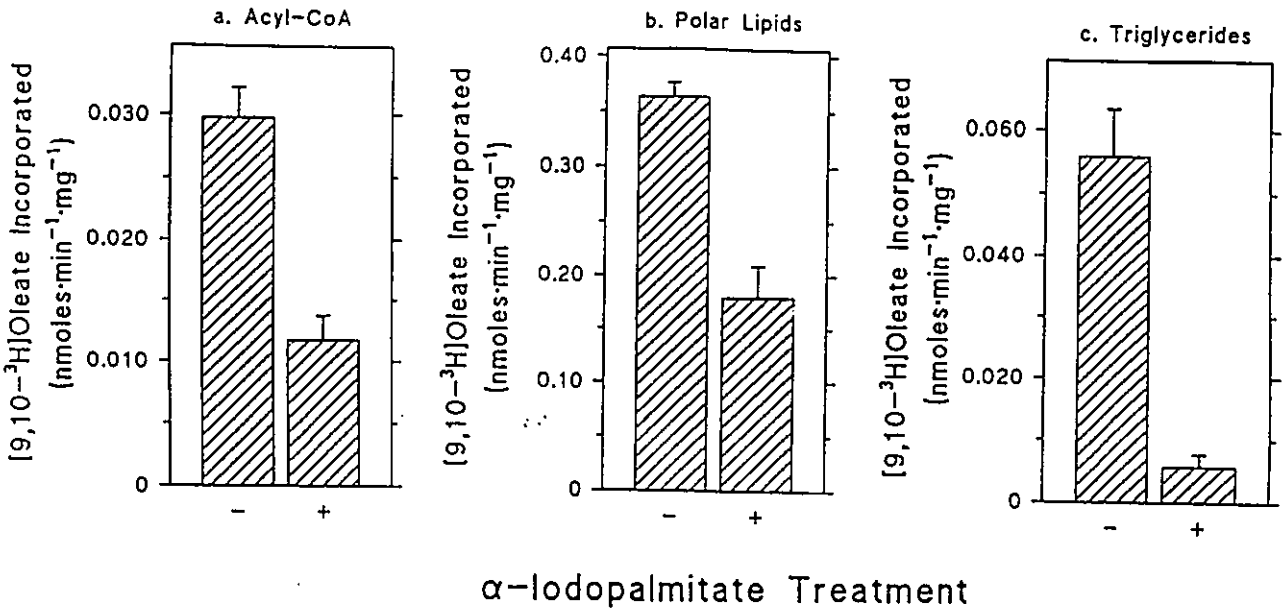

Figure 42. **Effect of α-iodopalmitate treatment of 3T3-L1 adipocytes on the incorporation of [9,10-^{3}H]oleate into cellular lipids.** 3T3-L1 adipocytes in 3.5 cm diameter cell culture dishes were treated with α-iodopalmitate as described in the legend to figure 41. Control cells treated in parallel in the absence of α-iodopalmitate were also included. Immediately after treatment, cells were incubated with 2.0 ml of PBS containing 0.20 mM [9,10-^{3}H]oleate and 0.10 mM BSA at 37°C. The incorporation of radioactivity into cellular lipids (**a.** acyl-CoA, **b.** polar lipids and **c.** triglycerides) was determined as described in Section B.4.4. Results are expressed as the average ± S.E.M. of three determinations of the rate of incorporation normalized to the level of cellular protein.

While it has been assumed that α-halo-fatty acids inhibit the movement of LCFAs across the plasma membrane (Abumrad et al., 1984; Mahadevan and Sauer, 1971) this is not known with certainty. This is due to their hydrophobic nature, which suggests that α-halo-fatty acids could cross membranes by passive diffusion (as discussed in Section A.6.2 of the Introduction). Therefore, their site of action may be intracellular rather than at the cell membrane. Thus, it is not clear whether the inhibition of LCFA uptake by α-halo-fatty acids reflects effects on the movement of LCFAs across the plasma membrane or on intracellular events (as outlined in Section A.4 of the Introduction).

The photoaffinity labeling of the ALBP in intact cells was used to resolve this issue. Because the ALBP appears to be an intermediate in the trafficking of newly internalized LCFAs (figure 38), its labeling by the photoreactive probe should respond differently to the inhibition of early events in LCFA uptake (such as their delivery to and movement across the plasma membrane) and late events (such as their trafficking or conversion to LCFA-CoA). 3T3-L1 adipocytes were, therefore, treated either without ('control' cells) or with α-iodopalmitate and then labeled with the photoreactive LCFA in the presence of BSA (figure 43). As expected from figure 38, the time-dependent labeling of the ALBP in control cells (Panel a, arrow) was dynamic, initially increasing up to a maximum level at 45 sec, and then dropping to virtually zero by 120 sec. In cells treated with α-iodopalmitate (Panel b), the ALBP was labeled to a much higher level than in control cells, at the earliest time-point (5.0 sec); furthermore, its labeling was constant up

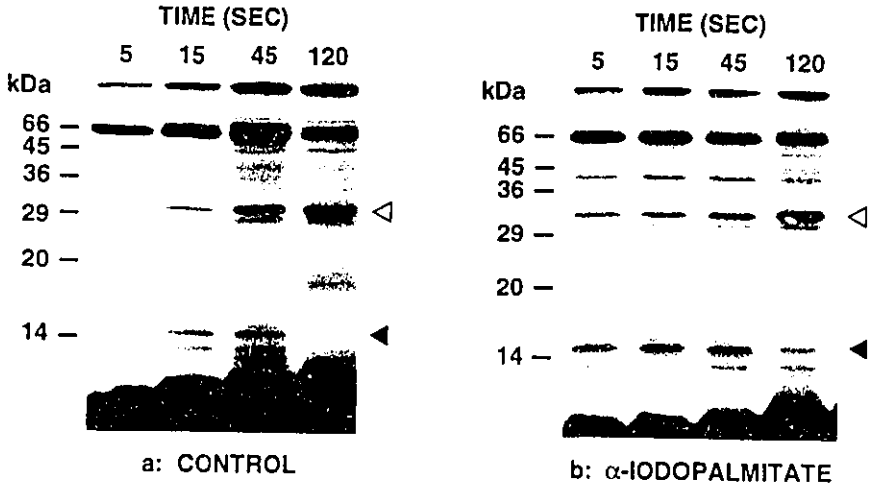

Figure 43. **The effect of pretreatment of 3T3-L1 adipocytes with α-iodopalmitate on the time dependant photoaffinity labeling of cellular FABPs in intact cells.** 3T3-L1 adipocytes were treated in the absence (**a.**) or the presence (**b.**) of α-iodopalmitate as described in the legend to figure 41. Cells were then incubated for various times (indicated above each lane) with 11-DAP-[11-^{3}H]undecanoate and subjected to photolysis as described in the legend to figure 39. Labeled cells were washed and analyzed by SDS-PAGE as described in the legend to figure 39 and Section B.10.2. Gels were treated for fluorography as described in Section B.10.5. The 15 kDa band corresponding to the ALBP is indicated with the solid arrowhead; the mitochondrial, 34 kDa band is indicated with the open arrowhead. Numbers on the left of each panel indicate the positions of protein standards of the indicated molecular weights, as described in the legends to figures 21 and 22.

to 45 sec, and the decline in the level of labeling occurring at 120 sec was not as pronounced as for control cells.

The finding that the pretreatment of 3T3-L1 adipocytes with α-iodopalmitate (figure 43, panel b) did not reduce the level of photoaffinity-labeling of the ALBP indicated that the transbilayer movement of the photoreactive LCFA was not inhibited by α-iodopalmitate. Instead, the earlier and more prolonged labeling of the ALBP in α-iodopalmitate-treated cells (figure 43, Panel b) is consistent with the inhibition of one or more late events in LCFA uptake. These might include the delivery or utilization of the photoreactive LCFA (figure 44). The further investigation of the nature of this step will be presented in Section C.7.

C.5.4. Implications

Together, these results demonstrate that the labeling of the ALBP in intact 3T3-L1 adipocytes with the photoreactive LCFA is dynamic (figures 38 and 44a), consistent with an involvement of the protein in the delivery of newly internalized LCFAs to sites of utilization within the cell. Furthermore, its labeling in intact cells is sensitive to decreases in the cytoplasmic concentration of the photoreactive LCFA, resulting from the inhibition of one or more early steps in LCFA uptake (figures 40 and 44), as well as to the accumulation of the probe in the cytoplasm, resulting from the inhibition of one or more late steps in LCFA uptake (figures 43 and 44).

The use of this photolytic assay for LCFA uptake has allowed a long standing issue to be resolved; this is the step at which α-halo-fatty acids act to inhibit LCFA

uptake. It was shown (figure 43) that the transbilayer movement of LCFAs was unaffected by treatment of cells with α-iodopalmitate, contrary to what had been assumed from earlier studies with α-bromopalmitate (Abumrad et al., 1984; Mahadevan and Sauer, 1971). Instead, α-iodopalmitate appeared to inhibit one or more late steps in LCFA uptake. Thus, this photolytic assay used in conjunction with inhibitors has, for the first time, allowed the uptake process to be differentiated into early and late steps *in vivo* (figure 44). This has not been possible with conventional methods which measure the intracellular accumulation of radioactively labeled, natural LCFAs or fluorescent LCFA analogues (Abumrad et al., 1981; Luxon and Weisiger, 1993; Storch et al., 1991; Stremmel and Berk, 1986).

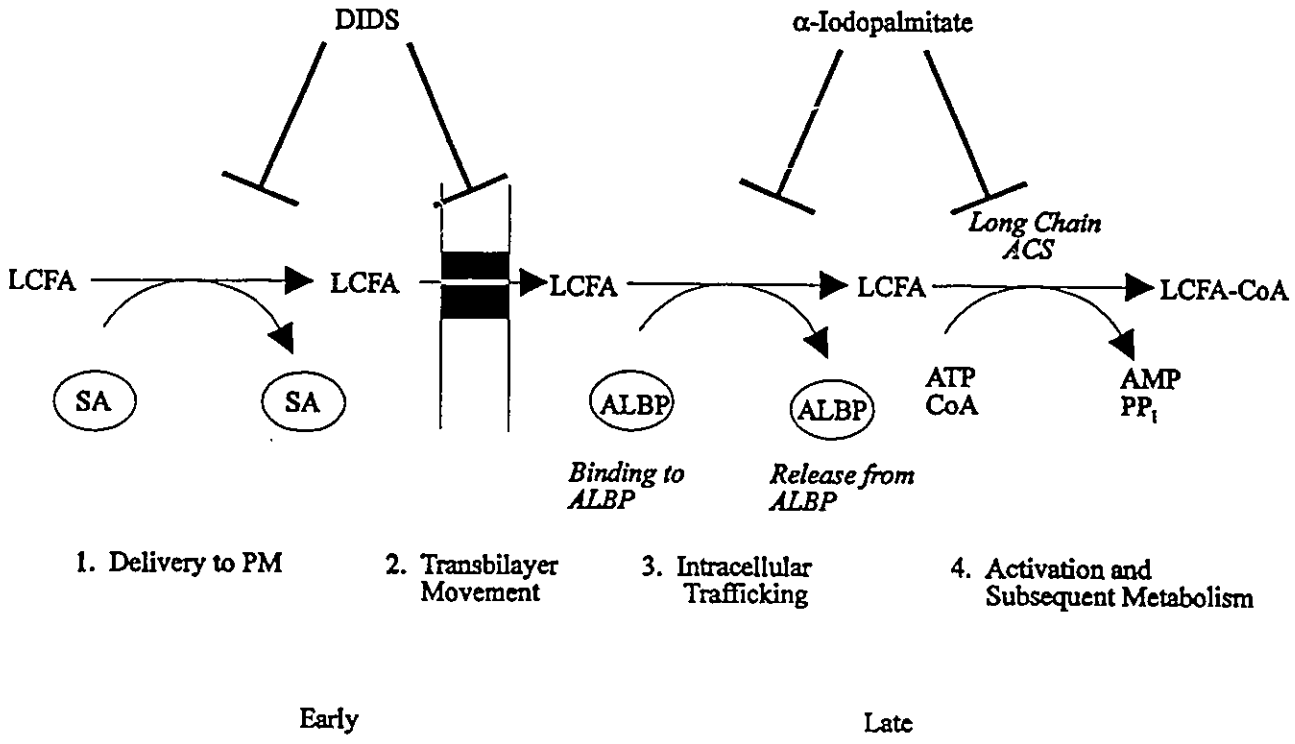

Figure 44. **Steps involved in LCFA uptake and sites of action of DIDS and α-iodopalmitate.** The steps involved in LCFA uptake in 3T3-L1 adipocytes are shown schematically (numbered 1-4). They are roughly divided into early steps, including LCFA delivery to and movement across the plasma membrane (PM), and late steps including the dissociation of LCFA from ALBP and LCFA activation to LCFA-CoA and subsequent metabolism. The respective steps which appear to be inhibited by DIDS and α-iodopalmitate are indicated.

C.6. Mechanism of LCFA Permeation of the Plasma Membrane: Effect of Intracellular pH on LCFA Uptake

As discussed in Section A.6.5, the lipophilic nature of protonated LCFAs has led many to propose that they move across plasma membranes of cells by the partitioning into and non-specific diffusion across the lipid bilayer (Hamilton et al., 1994; Kamp and Hamilton, 1992, 1993; Noy and Zakim, 1993; Noy et al., 1986). The permeation of LCFAs across model membranes is fast (Doody et al., 1980; Kamp and Hamilton, 1992, 1993; Noy and Zakim, 1993). Furthermore, at very high concentrations, LCFAs have been shown to enter cells by this mechanism (Hamilton et al., 1994).

As demonstrated in figures 11b and 20b, and discussed in Section C.1.2, LCFA uptake by mammalian cells involve both saturable and non-saturable processes, with respect to the concentration of uncomplexed LCFA (Abumrad et al., 1981; Schwieterman et al., 1988; Sorrentino et al., 1988; Zhou et al., 1992). The non-saturable process, manifested by a linear increase in the uptake rate versus the concentration of uncomplexed LCFA, is generally believed to represent the passive diffusion of protonated LCFAs across the plasma membrane (Abumrad et al., 1981; Schwieterman et al., 1988; Sorrentino et al., 1988; Zhou et al., 1992). Under normal physiological conditions, the concentration of uncomplexed LCFA in equilibrium with SA is in the nanomolar range. However, the contribution of the linear increase in the uptake rate is significant only at very high

(micromolar) concentrations of uncomplexed LCFA, and therefore is thought to be physiologically irrelevant. As a result of these considerations, the high concentrations of uncomplexed LCFA (35 μM) employed by Hamilton et al. (1994) in their demonstration that LCFAs enter cells by passive diffusion brings the physiological relevance of this result into question.

Uptake at lower, more physiologically relevant concentrations of uncomplexed LCFAs is saturable, as demonstrated in figures 11b and 20b (Abumrad et al., 1981; Schwieterman et al., 1988; Sorrentino et al., 1988; Zhou et al., 1992). It has been presumed that this represents protein mediated permeation of LCFAs across the plasma membrane (Abumrad et al., 1981; Schwieterman et al., 1988; Sorrentino et al., 1988; Zhou et al., 1992). Others, however, have argued that it could represent protein-mediated events within the cell, such as binding or metabolism of LCFAs (Noy and Zakim, 1993; Noy et al., 1986). In their view, the permeation of low concentrations of LCFA across the plasma membrane should occur by the same mechanism as that of high concentrations, namely by the passive permeation of the protonated species.

To resolve this issue, the effects of the intracellular pH on LCFA uptake in 3T3-L1 adipocytes was studied. In membrane vesicles composed of artificial lipid bilayers, LCFA has been shown to distribute between the two leaflets in response to changes in the pH gradient across the bilayer; due to the permeability of the lipid bilayer to the protonated but not the ionized LCFA (Hope and Cullis, 1987). If the movement of LCFAs across the plasma membrane of mammalian cells was the result of passive

diffusion of the protonated species, and not of protein mediated transport, then it also should respond to changes in the pH gradient across the plasma membrane in a manner consistent with that demonstrated in model membrane systems. Therefore, the effect of a decrease in the internal pH on LCFA uptake in 3T3-L1 adipocytes was studied.

C.6.1. Reduction of pH_c in 3T3-L1 Adipocytes

The pH_C of 3T3-L1 adipocytes was reduced by the NH_4Cl prepulsing technique (Frelin et al., 1988; Moolenaar et al., 1983, 1984). This is shown diagrammatically in figure 45a. It involved the loading of the cells with NH_4^+ by incubating them with 45 mM NH_4Cl (figure 45a, step 1), which results in an initial increase in the cytoplasmic pH due to the protonation of NH_3 in the cytoplasm to give NH_4^+, followed by a gradual recovery brought about by the action of the cellular homeostatic mechanisms. This is followed by the replacement of the medium containing NH_4Cl with one lacking it, leading to the efflux of NH_3 from the cell, resulting in a rapid drop in the cytoplasmic pH due to the dissociation of NH_4^+, and a gradual recovery due to the cellular homeostatic mechanisms (figure 45a, step 2). During this experiment, the pH_C was monitored with the fluorescent indicator, BCECF. Prior to prepulsing, the pH_C was 7.3 (figure 45b). After prepulsing, the cytoplasm rapidly became acidified to a pH of 6.7. The pH_C recovered by 10 min reaching a level of almost 7.6, overshooting the normal resting value of 7.3. The external pH was maintained at 7.4 throughout the experiment.

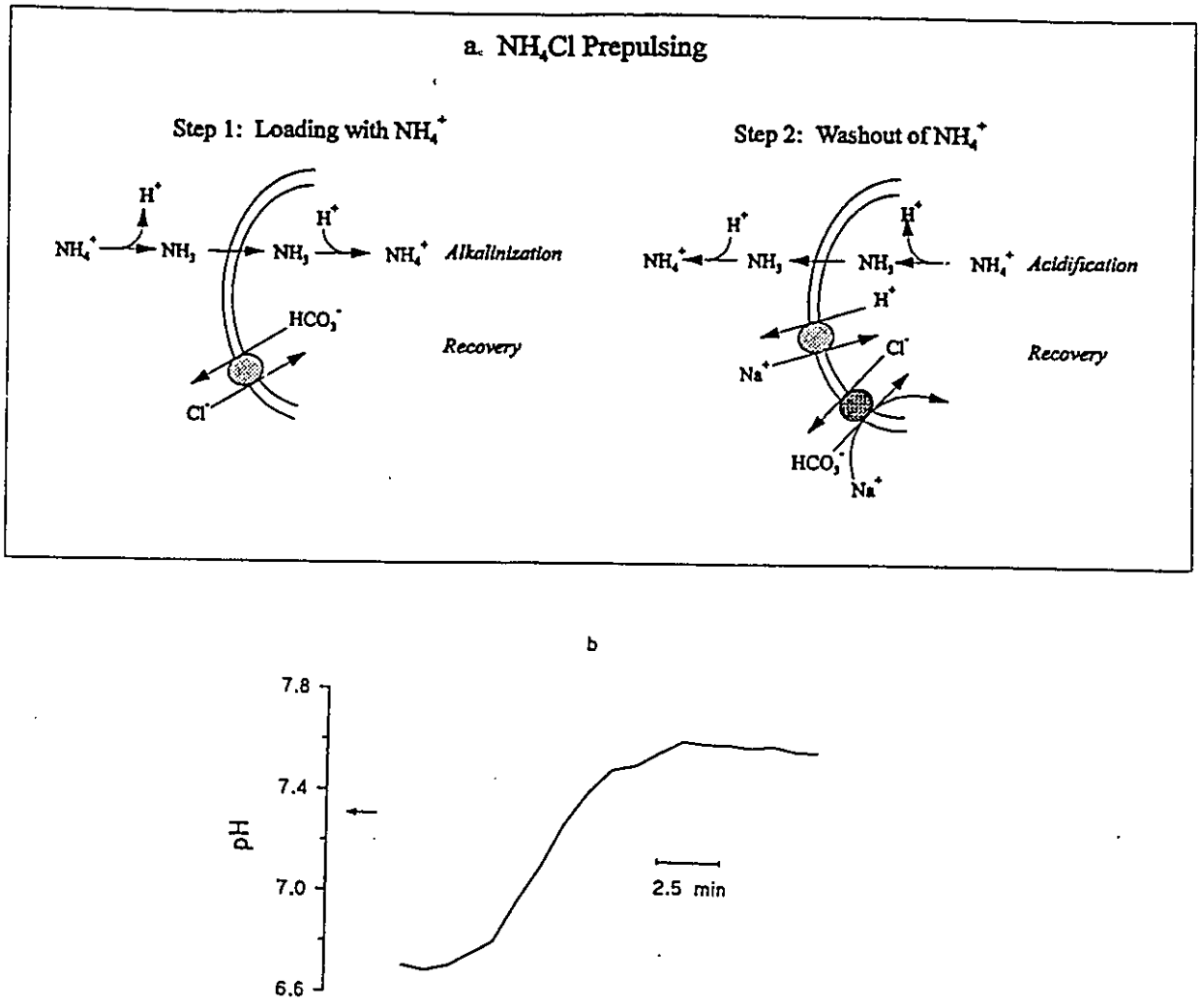

Figure 45. **NH_4Cl prepulsing and effect on intracellular pH in 3T3-L1 adipocytes.** **a.** Illustration of the NH_4Cl prepulsing technique (adapted from Frelin et al., 1988). In the first step (left), cells are incubated in medium containing NH_4Cl. While NH_4^+ is non-permeant, NH_3 readily crosses the plasma membrane and becomes protonated within the cytoplasm. This results in a very rapid increase in the cytoplasmic pH. The cellular homeostatic machinery, in this case represented by the Na^+-independent Cl^-/HCO_3^- exchanger, restors the pH_C to normal levels during a slower recovery phase. In the second step (right), cells are removed from the NH_4Cl. This causes the efflux of NH_3 from the cell, and therefore the dissociation of NH_4^+ within the cytoplasm. This results in a rapid acidification of the cytoplasm. Again, the cellular homeostatic machinery, in this case represented by a Na^+/H^+ exchanger and a Na^+-dependant Cl^-/HCO_3^- exchanger, restore pH_C to normal levels during a slower recovery phase. **b.** The effect of NH_4Cl prepulsing on the pH_C in in 3T3-L1 adipocytes was monitored using the fluorescent, pH_C indicator, BCECF, as described in Section B.5.2. The pH_C prior to prepulsing was 7.3 (indicated by the arrow). The acidification of the cytoplasm and the recovery of pH_C after removal of NH_4Cl (step 2 in **a**) are shown. The external pH was maintained at 7.4 throughout the experiment. The timescale is indicated by the horizontal bar.

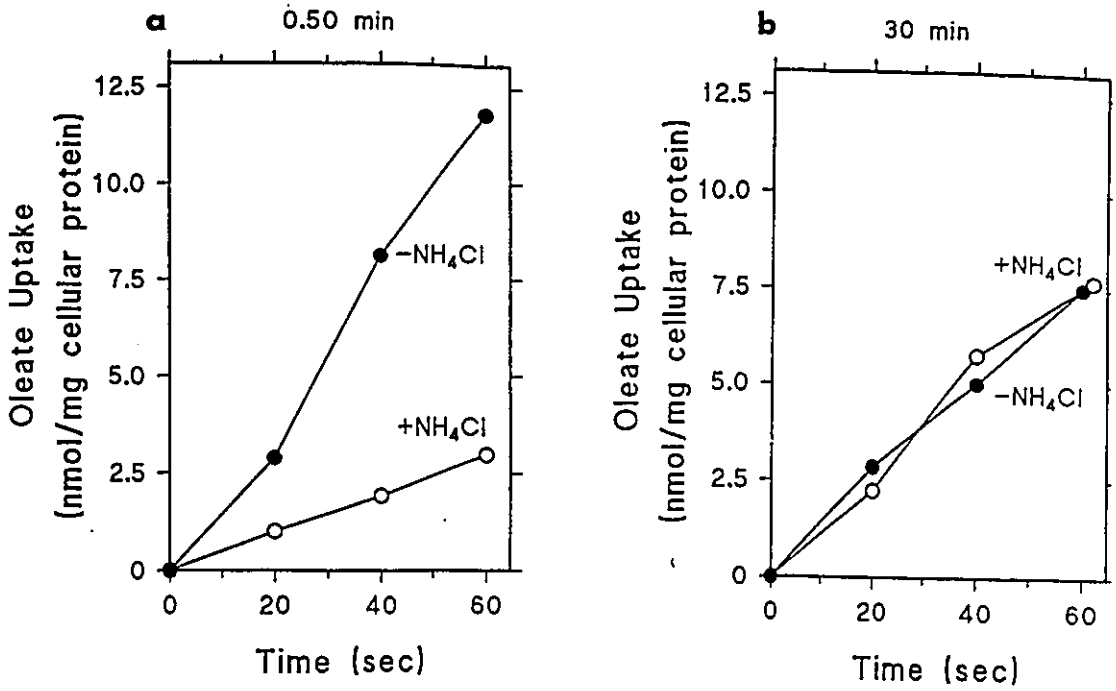

Figure 46. **The effect of NH_4Cl prepulsing on [9,10-^{3}H] oleate uptake in 3T3-L1 adipocytes.** A suspension of 3T3-L1 adipocytes was incubated with (+) or without (-) NH_4Cl as described Section B.5.1. The cells were pelleted, resuspended in PBS containing 10 mM glucose and incubated for either **a.** 0.50 or **b.** 30 min at 37°C prior to the measurement of [9,10-^{3}H]oleate uptake as described in Section B.4.3. Typical results obtained are presented as the amount of oleate taken up, normalized for cellular protein content.

C.6.2. Effect of pH_c on Oleate Uptake by 3T3-L1 Adipocytes

The rapid acidification of the cytoplasm upon prepulsing with NH_4Cl (figure 45b) was accompanied by a 70 % reduction in the rate of oleate uptake (figure 46a), while the recovery of pH_c to more alkaline levels was accompanied by the recovery of normal levels of [9,10-^{3}H]oleate uptake (figure 46b). In that experiment, oleate uptake was measured under physiologically relevant conditions; in particular, the concentration of uncomplexed [9,10-^{3}H]oleate in equilibrium with BSA was 47 nM. This was consistent with oleate uptake involving the passive permeation of the protonated species across the plasma membrane; however, the effects of the reduction of the intracellular pH on other steps in the uptake process may have also affected the level of uptake and therefore were investigated.

C.6.3. Effect of pH on LCFA Binding to ALBP and Activation by Long Chain ACS

Filtration assays measure the net accumulation of radioactively labeled LCFAs within cells; therefore, results may reflect both the permeation of the radioactive LCFA across the plasma membrane as well as intracellular events such as binding to cytoplasmic FABPs, such as ALBP, and conversion to LCFA-CoA by long chain ACS. The effect of the pH on the *in vitro* photoaffinity labeling of ALBP in cytoplasm isolated from 3T3-L1 adipocytes is shown in figure 47. The level of 11-DAP-[11-^{3}H]undecanoate incorporated into ALBP upon photolysis was relatively constant when pH was varied from 5.5-7.5. This agrees with studies on the binding of oleic acid to the rat liver-FABP,

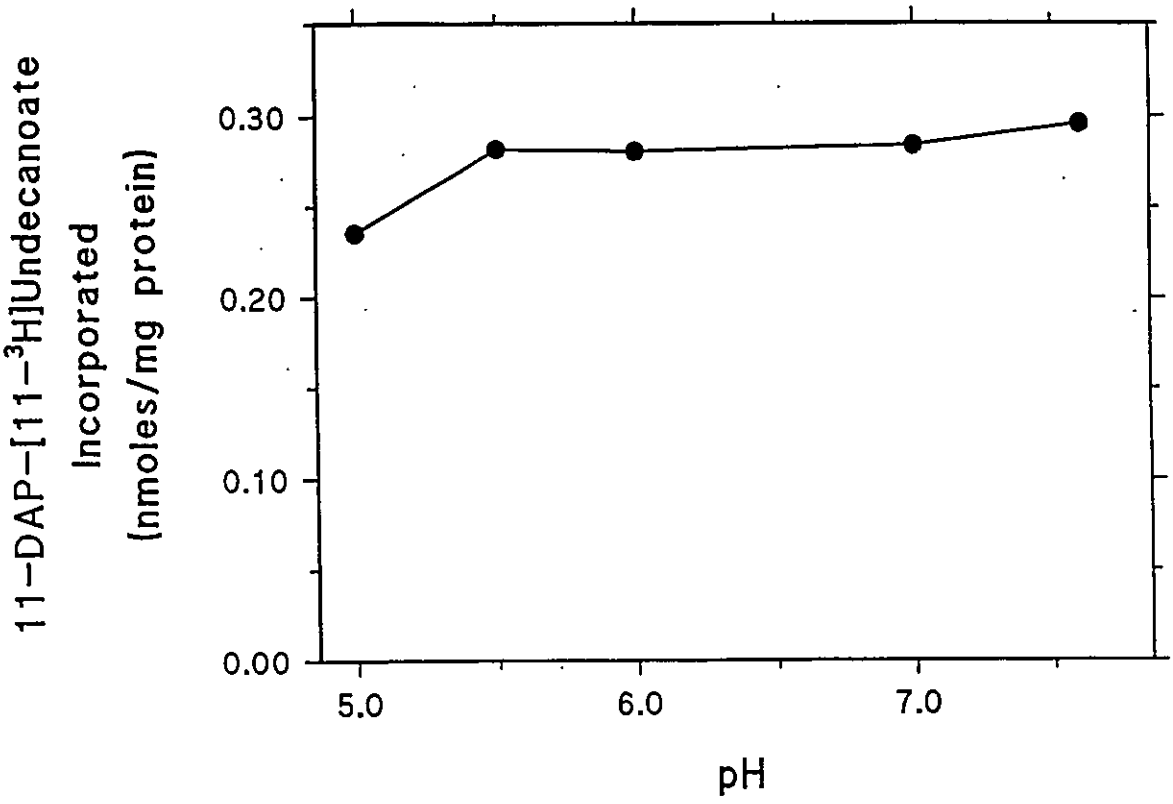

Figure 47. **Effect of pH on the *in vitro* photoaffinity labeling of ALBP with 11-DAP-[11-^{3}H]undecanoate.** Delipidated cytoplasm, isolated from 3T3-L1 adipocytes, was photolyzed as described in the legend to figure 22 after incubation at 0.50 mg of cytoplasmic protein/ml with 10 μM 11-DAP-[11-^{3}H]undecanoate in 10 mM sodium phosphate, at the indicated pH values. The level of incorporation of the photoreactive fatty acid into the ALBP as a function of pH. The level of incorporation of the probe into ALBP upon photolysis was determined as described in the legend to figure 37.

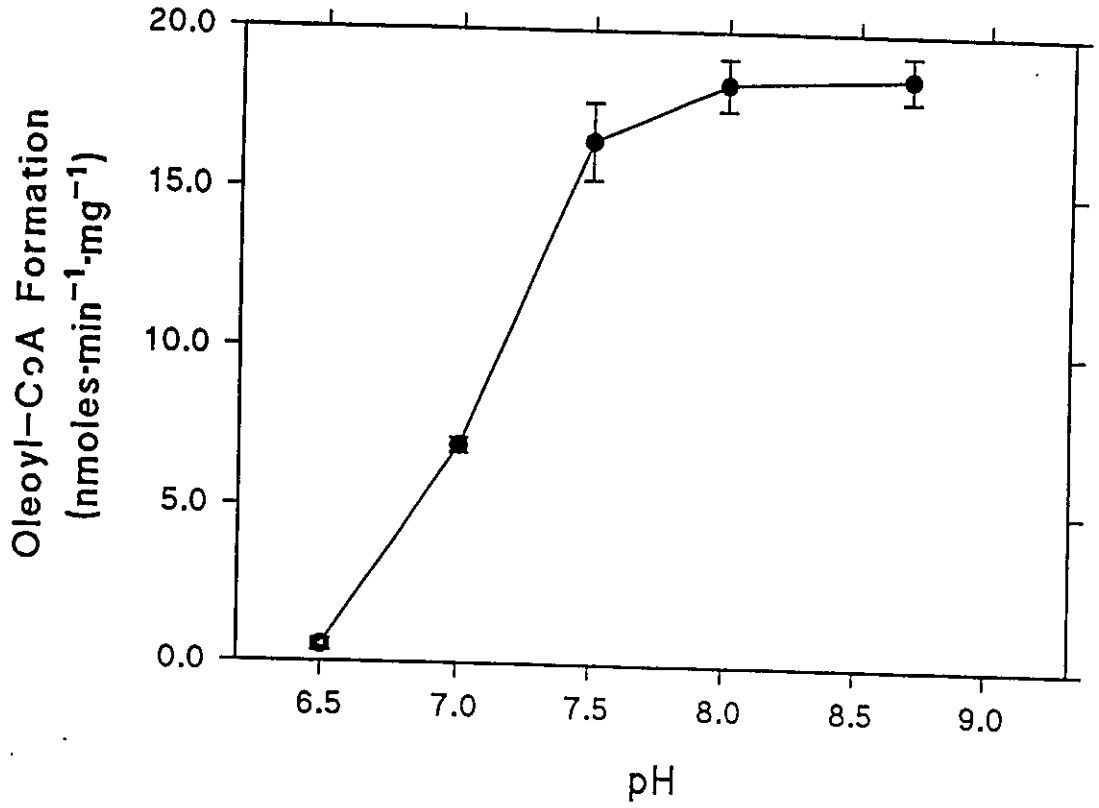

Figure 48. **Effect of pH on the activity of long chain ACS in cell homogenates:** ACS activities in homogenates of 3T3-L1 adipocytes were measured at various pH's as described in Section B.7.1. Results are presented as the rate of formation of [9,10-^{3}H]oleoyl-CoA from [9,10-^{3}H]oleate and are normalized for protein content. Results are the means ± S.E.M. of three determinations.

which found little effect of pH on the level of binding from pH 6.4 to 8.5 (Cistola et al., 1988b).

The effect of pH on the activity of long chain ACS in homogenates from 3T3-L1 adipocytes was measured using [9,10-^{3}H]oleate as the substrate (figure 48). ACS activities were maximal above pH 7.5, but dropped off rapidly as the pH was decreased. The activity of ACS was virtually zero at pH 6.5. Therefore, the reduction of pH_c from 7.3 to 6.7 during the prepulsing procedure could have resulted in a substantial decrease in the activity of long chain ACS, and therefore in activation of oleate for further metabolism. As mentioned previously, this is believed to be the rate limiting step in LCFA uptake in *E. coli* (Mangroo, 1992; Mangroo and Gerber, 1993) and has been proposed to represent an important step in LCFA uptake in mammalian cells (Noy and Zakim, 1993). Its involvement in LCFA uptake in 3T3-L1 adipocytes will be investigated in Section C.7. This suggests the possibility that the decrease in oleate uptake accompanying the drop in pH_c upon prepulsing with NH_4Cl (figure 46) may have resulted from a decrease in the activity of long chain ACS.

C.6.4. Effect of Intracellular pH on the Labeling of ALBP with the Photoreactive LCFA in Intact 3T3-L1 Adipocytes.

As demonstrated in Section C.5 (figures 40 and 43), the labeling of ALBP by 11-DAP-[11-^{3}H]undecanoate in intact cells was sensitive to the cytoplasmic concentration of the photoreactive LCFA, and could be used to differentiate between effects on early or late events in LCFA uptake. The insensitivity of the *in vitro* labeling of ALBP by the

photoreactive LCFA to changes in pH from 5.5 to 7.5 indicated that the binding of LCFAs by the protein should not be affected by the reduction in the pH_c to 6.7 arising from the prepulsing procedure (figure 45b). Therefore, any change in the labeling of ALBP in intact cells, accompanying prepulsing should be a reflection of the affects of the intracellular pH on the permeation of the photoreactive LCFA across the plasma membrane.

A solution of 75 μM 11-DAP-[11-^{3}H]undecanoate and 50 μM BSA in PBS was added to 3T3-L1 adipocyte monolayers immediately after they were prepulsed in the absence or presence of NH_4Cl (figure 49, lanes marked 0.50 min). Upon photolysis, after a 5.0 sec incubation with the probe at 37°C, the level of labeling of the ALBP (arrow), and other intracellular proteins, was reduced in cells prepulsed with NH_4Cl relative to those prepulsed in the absence of NH_4Cl (figure 49, lanes marked 0.5 min). NH_4Cl itself had no effect on the *in vitro* labeling of the ALBP by 11-DAP-[11-^{3}H]undecanoate (not shown). When monolayers were labeled 30 min after prepulsing, normal levels of labeling of ALBP and other intracellular proteins were observed (figure 49, lanes marked 30 min). This indicated that the permeation of the photoreactive LCFA across the plasma membrane was reduced 30 sec after prepulsing, when the pH_c was reduced, but was restored to normal levels by 30 min after prepulsing, when the pH_c had recovered.

C.6.5. Implications for the Mechanism of LCFA Movement across the Plasma Membrane

At the concentration of uncomplexed probe used in the experiment of figure 49 (470 nM at a molar ratio of probe:BSA of 1.5, as determined in figure 20a) the major

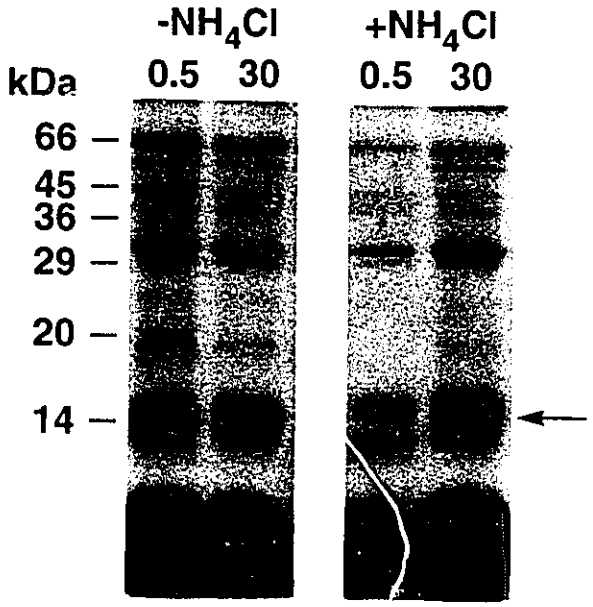

Figure 49. **The effect of decreased pH_c, by NH_4Cl prepulsing, on the photoaffinity labeling of intracellular proteins in intact 3T3-L1 adipocytes with 11-DAP-[11-^{3}H]undecanoate.** Monolayers of 3T3-L1 adipocytes on tissue culture dishes (1.5 cm diameter) were carried through prepulsing in the presence (right-hand panel) or absence (left-hand panel) of NH_4Cl as described in Section B.5.1. After removal of the NH_4Cl or control solution, monolayers were allowed to recover in PBS containing 10 mM glucose for either 0.50 or 30 min (indicated at the top of each lane) prior to incubation with 75 μM 11-DAP-[11-^{3}H]undecanoate in the presence of 50 μM BSA for 5 sec and photolysis as described in the legend to figure 39. Labeled proteins were analyzed by SDS-PAGE followed by fluorography as described in Sections B.10.2 and B.10.5, respectively. Numbers on the left indicate the migration of marker proteins of the specified molecular weights as described in the legends to figures 21 and 22. The arrow indicates the band of interest.

contribution to uptake was by the saturable process (figure 20b). This indicated that the physiologically relevant, saturable phase of LCFA uptake observed in figure 20b, involved the permeation of the protonated LCFA across the plasma membrane, presumably by means of diffusion through the lipid bilayer. Alternatively, LCFAs may traverse the plasma membrane by means of a fatty anion-proton cotransporter, which appears unnecessary in view of the lipophilic nature of protonated LCFAs and the evidence that LCFA permeation of model membranes is fast as discussed in Section A.6.2 (Doody etal., 1980; Kamp and Hamilton, 1992, 1993; Noy and Zakim, 1993).

These results can be explained by changes in the ΔpH affecting either the net flux or the equilibrium distribution of LCFAs across the plasma membrane. In the first case the net flux of LCFAs across the plasma membrane may be determined by the balance between those moving from the outer to the inner leaflet and those moving in the opposite direction. Acidification of the inside would lead to a shift in this equilibrium favouring movement to the outer leaflet. Alternatively, if LCFA uptake was driven by the intracellular trapping of LCFAs by binding or metabolism, this would be sensitive to the concentration of LCFA on the inner leaflet of the membrane, which is determined by the distribution of LCFAs across the bilayer in response to the ΔpH.

The decrease in pH_c by 0.6 units as a result of prepulsing (figure 45b) corresponded to an increase in the ΔpH from 0.1 to 0.7 (inside acidic). This is expected to result in a change in the ratio of LCFAs partitioned into the inner versus the outer leaflet of the plasma membrane from 0.8 to 0.2. Thus, the LCFA concentration in the

inner leaflet of the plasma membrane should have been reduced by 75 %, leading to the prediction of a 75 % decrease in LCFA uptake. This agrees well with the 70% reduction in uptake observed upon reduction of the intracellular pH (figure 46).

Evidence does, however, indicate that LCFA uptake by a variety of mammalian cells involves one or more plasma membrane proteins as already discussed in Sections A.6 and C.3. The results presented in Section C.3 suggested that caveolin is a LCFA receptor which might be involved in targeting LCFAs to caveolae, or in responding to LCFAs as signalling molecules. The specific functions of other plasma membrane proteins implicated in LCFA uptake are unclear. While the results presented above indicate that LCFA movement across the plasma membrane is not mediated by a transport protein, it remains possible that these proteins are involved in an uptake step other than LCFA movement across the plasma membrane. One such step is the interaction of SA with the cell surface (See Sections C.1.4 and C.1.5 and discussion in Section C.3.9). Alternatively, one or more of these proteins might be involved in the regulation of LCFA uptake (Abumrad et al., 1993). The finding that LCFA permeation across the plasma membrane is affected by the intracellular pH suggests the possibility that uptake of LCFAs could potentially be regulated by the modulation of the ΔpH across the membrane.

C.7. Inhibition of LCFA Uptake by α-Iodopalmitate: Role of ACS in Long Chain Fatty Acid Uptake.

α-Halo-fatty acids such as α-bromo- or α-iodopalmitate are known inhibitors of LCFA uptake (Abumrad et al., 1984; Mahadevan and Sauer, 1971). As observed in Section C.5.3, the pretreatment of 3T3-L1 adipocytes for 15 min with 50 μM α-iodopalmitate resulted in a substantial decrease in the level of [9,10-^{3}H]oleate uptake (figure 41) and incorporation into cellular lipids (figure 42), and this was due to the inhibition of one or more late steps in the uptake process, such as LCFA delivery or activation to LCFA-CoA (figures 43 and 44).

C.7.1. Effect of α-Iodopalmitate on LCFA Binding to ALBP.

To determine the effect of α-iodopalmitate on LCFA delivery by ALBP, cytoplasm isolated from 3T3-L1 adipocytes was labeled *in vitro* with the photoreactive LCFA in the presence of α-iodopalmitate (figure 50). α-Iodopalmitate resulted in a decrease in the incorporation of 11-DAP-[11-^{3}H]undecanoate into ALBP in a concentration-dependent manner (figure 50a). This inhibition of photoaffinity labeling was saturable, as was observed with oleate and palmitate (figure 37). It exhibited an apparent K_d for α-iodopalmitate of 4.2 μM (figure 50a and Table 6), which was slightly higher than those values determined for oleate and palmitate (figure 37 and Table 6), indicating a lower affinity for α-iodopalmitate.

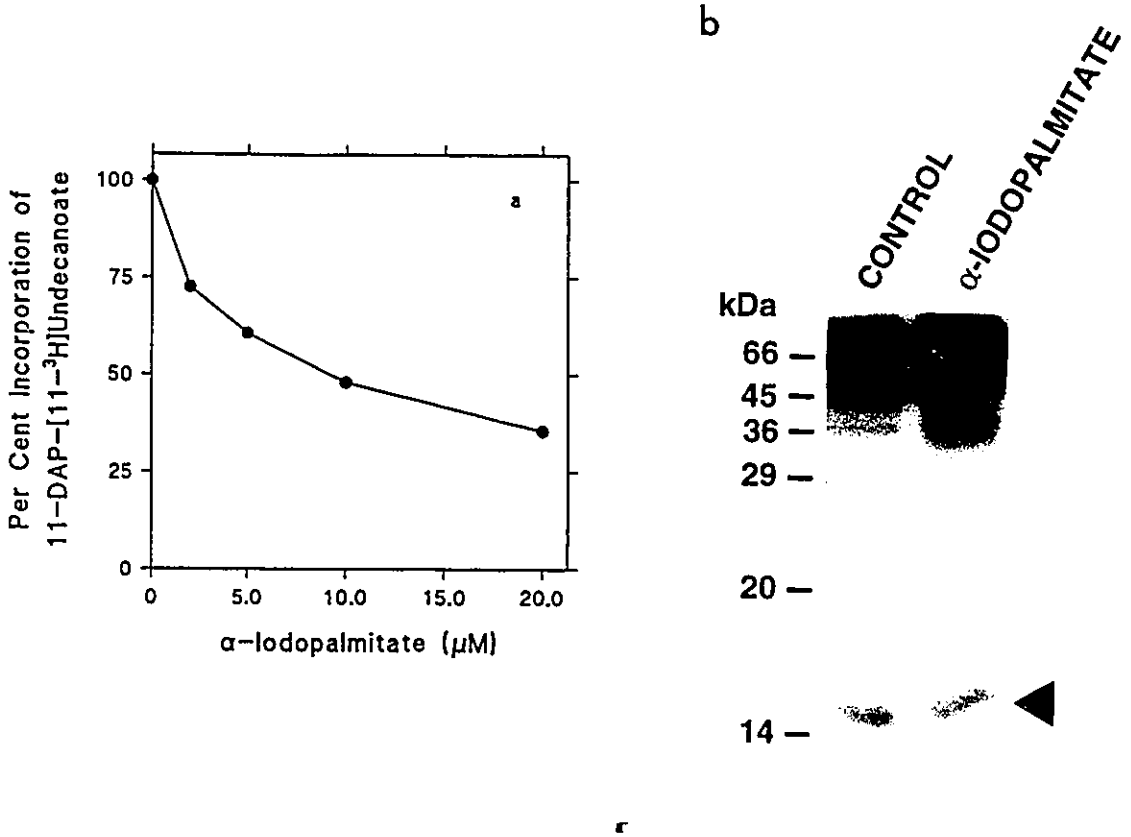

Figure 50. **Inhibition of 11-DAP-[11-^{3}H]undecanoate-labeling of ALBP *in vitro* by α-iodopalmitate. a.** The effect of α-iodopalmitate on the incorporation of 11-DAP-[11-^{3}H]undecanoate into ALBP *in vitro* was determined as described in the legend to figure 38. **b.** Cytoplasm (1.0 ml of 1.0 mg protein/ml in 50 mM sodium phosphate, pH 7.4) was treated for 15 min at 37°C either with or without 50 μM α-iodopalmitate (as indicated above each lane) and then passed through 1.0 ml of packed lipidex 1000 at 37°C. Delipidated samples were incubated with 10 μM 11-DAP-[11-^{3}H]undecanoate at 0.50 mg protein/ml at 37°C for 15 min. in the dark. Samples were photolyzed as described in the legend to figure 22 and were analyzed by SDS-PAGE, followed by fluorography as described in Sections B.10.2 and b.10.5, respectively. The 15 kDa band corresponding to ALBP is indicated by the solid arrowhead.

Lipidex 1000 treatment at 37°C is known to remove LCFAs from their binding sites on FABPs (Glatz and Veerkamp, 1983; Vork et al., 1990). When cytoplasm treated with α-iodopalmitate, and then delipidated with lipidex 1000 at 37°C, was photolyzed with 11-DAP-[11-^{3}H]undecanoate, normal labeling of the ALBP was observed (figure 50b), indicating that the inhibition of LCFA binding by α-iodopalmitate was reversible. This is important since α-halo-long chain fatty acids have been shown to irreversibly inhibit a variety of enzymes by the covalent modification of essential residues (Coleman et al., 1992). Thus, α-iodopalmitate inhibited the binding of LCFAs to ALBP in a reversible manner. This, together with the finding that ALBP was labeled *in vivo* in 3T3-L1 adipocytes pretreated with α-iodopalmitate (figure 43), indicated that LCFA trafficking (i.e. LCFA binding and release by ALBP) was not inhibited by α-iodopalmitate. In fact, the *in vitro* binding of α-iodopalmitate by ALBP (figure 50a) suggested that ALBP may have bound α-iodopalmitate *in vivo*, while the reversible nature of the binding (figure 50b) and the demonstration that ALBP was involved in LCFA delivery *in vivo* strongly suggested that α-iodopalmitate bound to ALBP *in vivo* was delivered to intracellular sites by the protein. Thus, it appeared that α-iodopalmitate inhibited a step in LCFA uptake after the delivery of LCFAs.

C.7.2. Effect of α-Iodopalmitate on Long Chain ACS.

α-Bromopalmitate is known to inhibit a number of membrane associated enzymes involved in fatty acid metabolism and triglyceride synthesis. These include rat liver mitochondrial ACS and mono- and diacylglycerol acyltransferases (Mahadevan and Sauer,

1971; Coleman et al., 1992). To determine the effect of α-iodopalmitate on long chain ACS in 3T3-L1 adipocytes, total membranes were prepared, treated with 50 μM α-iodopalmitate for 15 min at 37°C, and assayed for [9,10-^{3}H]oleoyl-CoA synthesis either directly or after washing in the presence of 100 μM BSA (figure 51). α-Iodopalmitate treatment of total membranes resulted in the inhibition of long chain ACS; this was not affected by washing the membranes with BSA after treatment, indicating that it was irreversible. This suggested a mechanism by which α-iodopalmitate inhibited LCFA uptake; namely, through the inhibition of cellular long chain ACS.

To investigate the effects of pretreatment of 3T3-L1 adipocytes with α-iodopalmitate on the levels of cellular long chain ACS, the activities of long chain ACS were determined in subcellular fractions, prepared by centrifugation of cell homogenates on gradients of 0-42 % sucrose. Figure 52 shows the results of a typical gradient. ER, mitochondria and peroxisomes, the three mammalian organelles which have been found to contain long chain ACS (Suzuki et al., 1990) were recovered in a single membrane band (designated the "organellar band") at approximately 33 % sucrose, as assessed by following the activities of glucose-6-phosphatase, cytochrome C-oxidase and catalase, enzymatic markers for these organelles.

The fat cake, which floated to the top of the gradient, was also recovered (fraction designated "lipid droplet" in figure 52). This has been shown to consist of the cytoplasmic triglyceride droplets together with the membranes that enclose them (Egan et al., 1992; Greenberg et al., 1991). This fraction was devoid of enzymatic activities

associated with the ER, mitochondria and peroxisomes (figure 52), indicating that it was not contaminated by these organelles.

Intact 3T3-L1 adipocytes, treated either with or without 50 μM α-iodopalmitate for 15 min at 37°C in PBS, were homogenized and fractionated as described above. The total homogenates, cytoplasmic (recovered from fractions 1 and 2 of the gradient; figure 52), lipid droplet and organellar fractions were assayed for long chain ACS activity using [9,10-^{3}H]oleate as substrate (figure 53). A slight but reproducible decrease in the level of ACS activity was observed in total homogenates from α-iodopalmitate-treated cells relative to control cells. α-Iodopalmitate treatment of intact cells appeared to have no effect on long chain ACS in the organellar fraction, since no difference in the activity of [9,10-^{3}H]oleate conversion to [9,10-^{3}H]oleoyl-CoA was observed. This was surprising in light of the sensitivity of long chain ACS in total 3T3-L1 adipocyte membranes to α-iodopalmitate *in vitro* (figure 51).

Treatment of cells with α-iodopalmitate did, however, have an effect on the level of long chain ACS activity associated with the lipid droplet fraction. The activity of [9,10-^{3}H]oleoyl-CoA synthesis in the lipid droplet fraction prepared from cells treated with α-iodopalmitate was only 34 % of that in the lipid droplet fraction prepared from control cells. The level of the reduction in the lipid droplet-associated long chain ACS activity was similar to the level of inhibition of oleate uptake and incorporation into cellular lipids by α-iodopalmitate observed in figures 41 and 42.

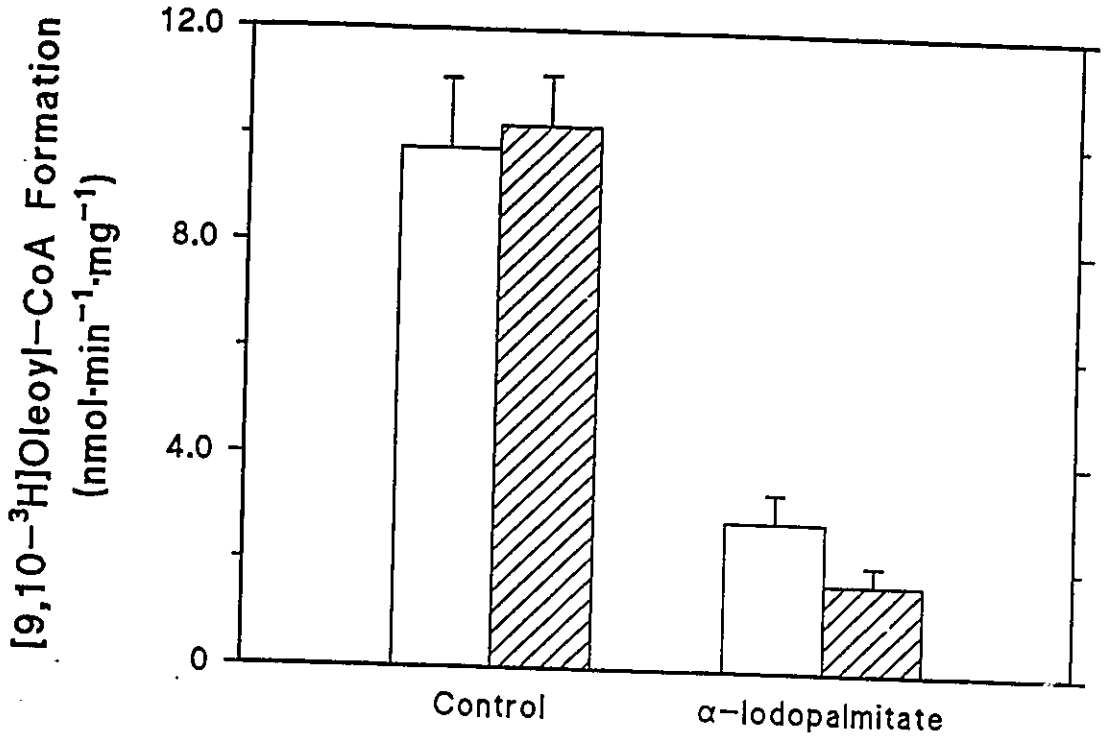

Figure 51. **Inhibition of ACS upon treatment of total membranes with α-iodopalmitate *in vitro*.** Total membranes, isolated from 3T3-L1 adipocytes as described in Section B.6.1, were incubated at 25 mg membrane protein/ml for 15 min at 4.0°C in 0.35 M tris-HCl, pH 7.4 containing 8.0 mM $MgCl_2$ and 5.0 mM β-mercaptoethanol. They were then treated at 1.25 mg membrane protein/ml in 0.35 M tris-HCl, pH 7.4 containing 8.0 mM $MgCl_2$ and 5.0 mM β-mercaptoethanol either with or without 50 μM α-iodopalmitate for 10 min at 37°C. The conversion of [9,10-^{3}H]oleate to [9,10-^{3}H]oleoyl-CoA was assayed either directly (open bars) or after washing with 0.10 mM BSA (hatched bars). Assays were carried out at 0.0125 mg membrane protein/ml as described in Section B.7.1. Results are the mean ± S.E.M. of three determinations.

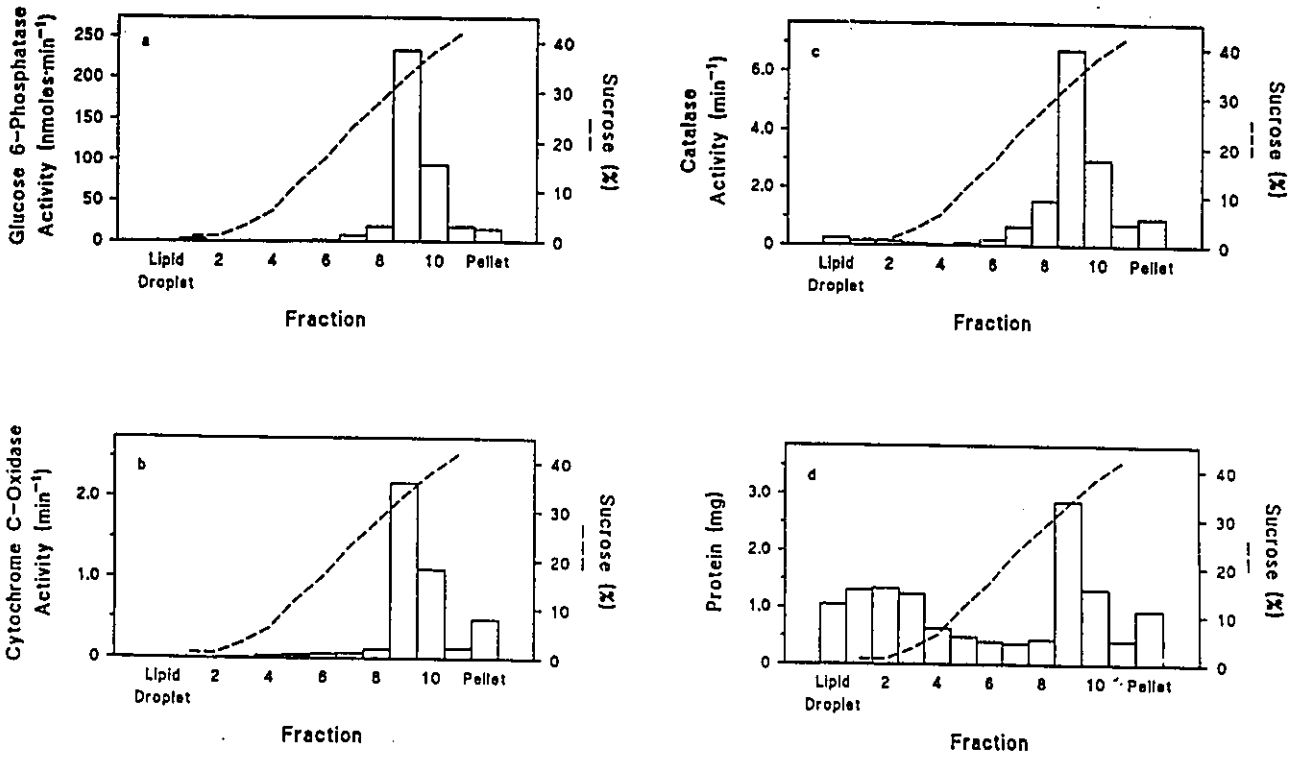

Figure 52. **Separation of lipid droplets from other organelles by sucrose density gradient centrifugation.** Homogenates of 3T3-L1 adipocytes (1.5 ml), prepared as described in Section B.6.3, were layered onto discontinuous sucrose gradients and were centrifuged as described in Section B.6.3. The gradients were fractionated as described in Section B.6.3, and each fraction was assayed for the following (vertical axes on left): **a.** glucose 6-phosphatase (expressed as the nmoles of inorganic phosphate produced per min), **b.** cytochrome C-oxidase (expressed as the decrease in absorbence at 550 nm, wavelength per min), **c.** catalase (expressed as the decrease in absorbence at 240 nm, wavelength per min) and **d.** protein content expressed as mg of protein), as described in Section B.7. The sucrose concentration in each fraction (vertical axis on right of each panel) was determined from the refractive index and is expressed as the percent sucrose (*w/v*).

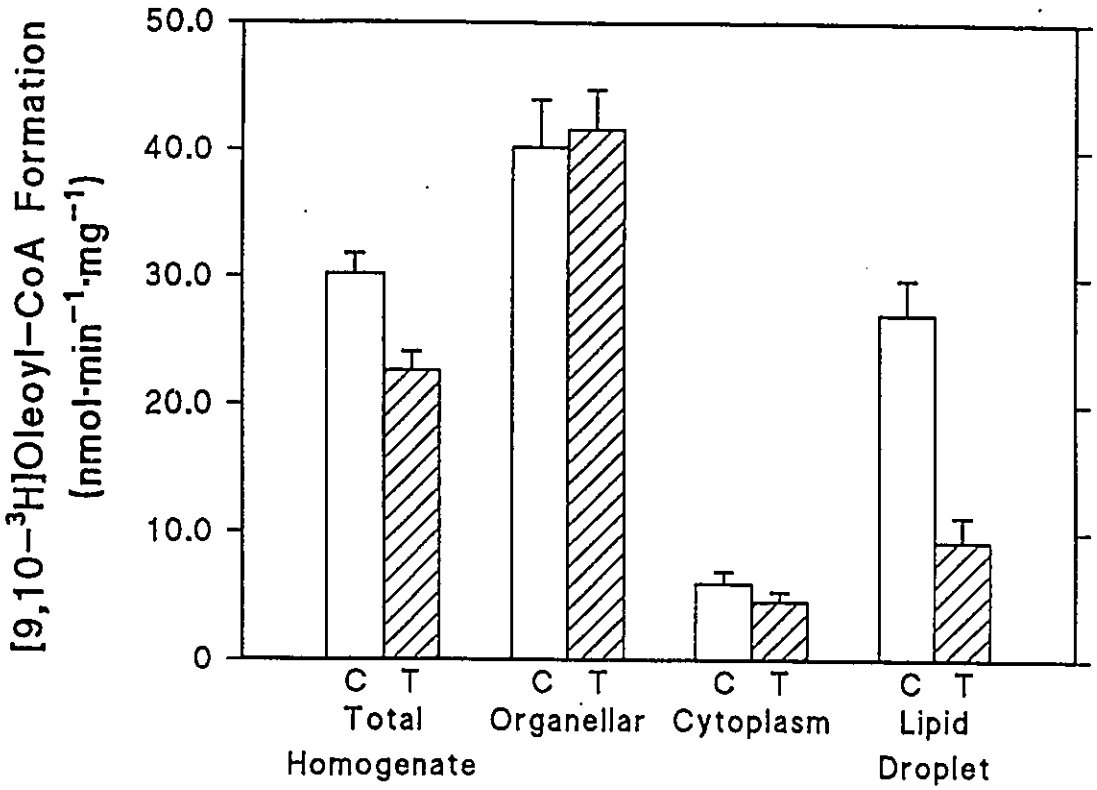

Figure 53. **Effect of treatment of intact 3T3-L1 adipocytes with α-iodopalmitate on cellular long chain ACS activities.** 3T3-L1 adipocyte monolayers were treated with α-iodopalmitate as described in the legend to figure 43 (hatched bars). Control cells were carried through the treatment in the absence of α-iodopalmitate (open bars). Cells were then homogenized and fractionated as described in the legend to figure 53 and Section B.6.3. Long chain ACS activities were determined as described in Section B.7.1. The following fractions were assayed: total homogenate, organellar fraction (the membrane band containing the bulk of the enzymatic marker activities which migrated to approximately 30 % sucrose, as indicated in figure 53), cytoplasm (fractions 1 and 2 in figure 53) and the lipid droplet. The activities of long chain ACS were normalized to the amount of protein and are presented as the average ± S.E.M. of three determinations.

The presence of long chain ACS in lipid droplets of adipocytes had not previously been described; however, it was expected based on the function of the lipid droplet as the site of triglyceride storage (Egan et al., 1992; Greenberg et al., 1991). The specific activity of [9,10-^{3}H]oleoyl-CoA synthesis in the lipid droplet fraction of control cells was similar to that of total homogenates. This may have been due to the contamination of the lipid droplet fraction with cytoplasm (figure 52d), resulting in an underestimate of the specific activity due to an overestimate of the amount of protein associated with the lipid droplet.

The reduction of the level of lipid droplet-associated long chain ACS activity in cells treated with α-iodopalmitate was most likely due to the irreversible inhibition of the enzyme associated with the lipid droplet rather than a redistribution of the enzyme to a different fraction. This is based on the following lines of evidence: Firstly, no significant increase in the enzymatic activity in the other fractions was observed. This includes the cytoplasmic fraction; in fact, the specific activity of long chain ACS in the cytoplasm was much lower than that in the total homogenate, suggesting that it may have been due to contamination from other fractions. Secondly, although FadD, the long chain ACS from *E. coli*, redistributes between cytoplasmic and membrane associated fractions (Mangroo and Gerber, 1993), and a number of distinct long chain ACSs (Faa1p-3p) from the yeast *S. cerevisiae* appear to be soluble (Knoll et al., 1994), mammalian long chain ACS appears to be an integral membrane protein (Hesler et al., 1990; Suzuki et al., 1990). Therefore, the results shown in figure 53 suggest that long chain ACS in the lipid droplet

of 3T3-L1 adipocytes was selectively inhibited by α-iodopalmitate treatment of intact cells.

C.7.3. Implications for the Role of Long Chain ACS in LCFA Uptake

The finding that treatment of 3T3-L1 adipocytes with α-iodopalmitate resulted in the inhibition of the lipid droplet-associated long chain ACS activity (figure 53) and, concomitantly of cellular LCFA uptake (figure 41) and incoproration into cellular lipids (figure 42) but not permeation of LCFAs across the plasma membrane (figure 43), suggested that α-halo-LCFAs exert their effects on LCFA uptake through the inhibition of LCFA activation rather than LCFA movement across the plasma membrane.

Therefore, in mammalian cells, as in *E. coli*, long chain ACS appears to play an important role in LCFA uptake. Further support for this includes the finding that cell lines exhibiting decreased arachidonyl-CoA synthetase activity could be obtained by tritium suicide selection for decreased arachidonate uptake (Laposata, 1990; Neufeld et al., 1984). Similarly, Schaffer and Lodish (1994) have reported that the forced expression of long chain ACS conferred increased LCFA uptake to cells normally expressing only low levels of the enzyme. These results, together with the demonstration that the inhibition of long chain ACS resulted in decreased LCFA uptake (figures 41 and 53) support the argument of Noy and Zakim (1993) that LCFA uptake in mammalian cells is driven by the conversion of LCFAs to LCFA-CoA by cellular ACS.

C.7.4. Implications for Functions of Cytoplasmic FABPs

The selective inhibition of the lipid droplet-associated long chain ACS activity upon treatment of intact cells with α-iodopalmitate, together with the sensitivity of long chain ACS in the organellar fraction to α-iodopalmitate *in vitro* but not *in vivo* suggests that in intact cells, α-iodopalmitate was targeted specifically to the lipid droplet. This is the first demonstration of such an exclusive intracellular targeting of LCFAs to a subcellular location in mammalian cells. As demonstrated in figure 38, the time dependence of labeling of ALBP in intact 3T3-L1 adipocytes by the photoreactive LCFA indicates an involvement for the protein in the intracellular delivery of newly internalized LCFAs to sites of utilization. As discussed above (Section C.7.1.) ALBP binds α-iodopalmitate with an affinity slightly lower than for natural LCFAs (figure 50a and Table 6). This strongly suggested that it was involved in the targeting of α-iodopalmitate to the lipid droplet in 3T3-L1 adipocytes.

A role for the ALBP in the targeted delivery of newly internalized LCFAs to the lipid droplets of adipocytes does not require the ALBP to increase the rate of diffusion of LCFAs through the cytoplasm or to drive LCFA uptake. Therefore, it amounts to a shift in the emphasis of the role of the ALBP in LCFA delivery from increasing the rate of delivery to providing a means for the delivery to a specific intracellular site, namely the lipid droplet, where triglycerides are stored.

C.7.5. Mechanisms of LCFA Targeting to the Lipid Droplet.

The mechanism by which the ALBP might accomplish this targeting of LCFAs to the lipid droplet is unclear. LCFA transfer from ALBP to artificial membranes involves a direct interaction between ALBP and the membrane and is affected by the membrane lipid composition (Wootan and Storch, 1994; Wootan et al., 1993). *In vivo*, it is possible that ALBP interacts with the lipid portion of the fat droplet membrane. While the binding of ALBP to membranes has not been investigated, at least one member of the cytoplasmic FABP family (the ileal lipid binding protein) has been shown to associate with membranes (Kramer et al., 1993).

It is possible that specific interaction with the lipid droplet membrane might be accomplished by receptors for the ALBP in that membrane. While the lipid droplet membrane is originally derived from the ER, its protein composition changes during the maturation of the lipid droplet (Greenberg et al., 1991; Hare et al., 1994). A 62 kDa protein, called perilipin, has recently been identified as a specific component of the surface of the lipid droplet in adipocytes (Greenberg et al. 1991). It exhibits a high degree of sequence similarity over a stretch of 105 amino acids with the adipose differentiation-related protein (ADRP), a 425 amino acid protein localized to the cytoplasmic side of the plasma membrane (Greenberg et al., 1993; Jiang and Serrero, 1992). It has been proposed that perilipin and ADRP, via their homologous region may act as receptors on the lipid droplet and the plasma membrane, respectively, for a soluble factor involved in lipid metabolism, which shuttles between the two compartments

(Greenberg et al., 1993). The ALBP appears to be such a factor, although it has not been determined whether it interacts with either of these proteins.

Alternatively, as discussed in Section A.7.2., it has been proposed that phosphorylation of ALBP at Tyr-19, which becomes exposed upon LCFA binding, locks the LCFA in a bound state, while hydrolysis of the phosphate allows LCFA release from the binding site (Buelt et al, 1992; Hresko et al., 1990). This potential requirement of phosphotyrosine hydrolysis for the release of bound LCFA suggests that the targeted delivery of LCFAs might be accomplished by the subcellular distribution of one or more specific protein tyrosine phosphatases. Liao et al. (1991) have identified a novel, membrane bound, phospho-ALBP phosphatase in 3T3-L1 adipocytes; however, its subcellular location is not known. As yet, no lipid droplet-associated protein tyrosine phosphatase activity has been described.

C.7.6. Implications for Triglyceride Synthesis

The finding that LCFAs are delivered exclusively to the lipid droplet in 3T3-L1 adipocytes, and the discovery of a lipid droplet associated long chain ACS activity also have implications for triglyceride synthesis in adipocytes. All of the enzymatic activities involved in the synthesis of triglycerides from glycerol 6-phosphate and LCFAs have been detected on the ER (Hare et al., 1994; Moller et al., 1981; Suzuki et al., 1990) and triglyceride synthesis has been shown to occur there (Greenberg et al., 1991; Hare et al., 1994). However, none of these enzymatic activities had been reported to be associated with the lipid droplet. Despite this, triglycerides are constantly hydrolysed and re-acylated

in mature lipid droplets (Edens et al., 1990), suggesting that triglyceride synthesis also occurs at the lipid droplet itself. The finding of a long chain ACS activity associated with the lipid droplet of 3T3-L1 adipocytes (figure 53) is consistent with this. Recent evidence has suggested that at some point during their *de novo* formation at and separation from the ER, triglyceride droplets acquire a membrane which is derived from the ER membrane (Greenberg et al., 1991; Hare et al., 1994). It is therefore possible that the lipid droplet associated ACS activity was acquired along with the ER membrane. Similarly, other enzymes involved in triglyceride synthesis, in particular acyl-CoA:diacylglycerol acyl transferase, might also be associated with the lipid droplet membrane, allowing LCFA activation and triglyceride synthesis to occur there.

C.8. Model for LCFA uptake in Mammalian cells

A model for LCFA uptake in 3T3-L1 adipocytes, based on the results presented in sections C.1 through C.7, is shown in figure 54. As indicated in Section A.4, LCFA uptake in mammalian cells involves a number of steps. These include the delivery of LCFAs to the cell surface by SA (Step 1a), which may interact with cellular receptors to facilitate the transfer of bound LCFA to the cell, possibly to caveolin, a high affinity LCFA receptor in caveolae on the cell surface (Step 1b). LCFAs appear to traverse the plasma membrane by passive diffusion (Step 2), and are delivered by the ALBP exclusively to the lipid droplet (Step 3), where activation to LCFA-CoA (Step 4) and incorporation into triglycerides are thought to occur.

This model is by no means complete, as indicated by the question marks in figure 54. Firstly, the nature of the interaction of SA with the membrane (indicated by the stippled box in figure 17) has yet to be resolved, although accumulating evidence suggests that it may be mediated by one or more cell surface proteins, such as albondin (Schnitzer et al., 1994), the scavenger receptors gp18 and gp30 (Schnitzer et al., 1992) and possibly CD36/FAT, an unrelated scavenger receptor (Acton et al., 1994).

Furthermore, the mechanism by which this association of SA and the cell membrane facilitates LCFA uptake is also unclear (figure 17). It has been proposed that it may 1) lead to facilitated dissociation of LCFA from SA, increasing the uncomplexed

LCFA concentration in the vicinity of the plasma membrane (Reed and Burrington, 1989); or 2) allow a direct transfer of bound LCFA from SA to hydrophobic binding sites (either LCFA receptors or the lipid bilayer itself) on the plasma membrane. Alternatively, it may allow for the targeting of LCFA-SA complexes to regions of the plasma membrane designated for LCFA uptake. Evidence is beginning to accumulate which suggests that caveolae might be such regions. This includes the identification of caveolin, a resident protein of caveolae, as a unique high affinity LCFA receptor (Section C.3) as well as the localization within caveolae of albondin and gp's 18 and 30, receptors for native and chemically modified SA, respectively, and CD36/FAT, a receptor for modified SA which has been implicated in LCFA uptake in adipocytes (Lisanti et al., 1994b; Rothberg et al., 1992; Schnitzer and Oh, 1994; Schnitzer et al., 1992,1994).

The cell surface proteins, CD36/FAT, FATP and $FABP_{PM}$, are known to be involved in LCFA uptake (Abumrad et al., 1984; Schaffer and Lodish, 1994; Stremmel and Theilmann, 1986). The nature of their involvement, however remains unclear. Results presented in Section C.6 as well as by others (Hamilton et al., 1994) clearly indicate that LCFA movement across the plasma membrane (Step 2 of figure 54) occurs by passive diffusion of the protonated LCFA, indicating that the above proteins do not act as LCFA transporters. It remains possible, however that they may participate in one or more other steps in LCFA uptake. As mentioned above, CD36/FAT is a scavenger receptor which binds chemically modified SA (Acton et al., 1994) suggesting that it might mediate the interaction of LCFA-SA complexes with the plasma membrane. Otherwise,

it is possible that these proteins might be involved in the regulation of LCFA uptake.

The mechanism by which LCFAs are targeted by the ALBP to the lipid droplet is also unknown. As discussed in Section C.7.5, targeting could involve an interaction between the ALBP and the lipid droplet surface, mediated either by the lipid composition of the membrane (Wootan and Storch, 1994; Wootan et al., 1993) or by receptor proteins (Greenberg et al., 1993). Alternatively, it may be regulated by the phosphorylation state of the ALBP (Hresko et al., 1990).

Finally, the nature of the lipid droplet-associated long chain ACS activity is unknown. Its relationship with long chain ACS located in other organelles would be of particular interest. As discussed previously (Section A.8.2), evidence suggests that mammalian cells contain a single long chain ACS which is distributed among the ER, mitochondria and peroxisomes (Suzuki et al., 1990). This is in contrast to *S. cerevisiae*, which contains at least five separate long chain ACSs (Johnson et al., 1994b).

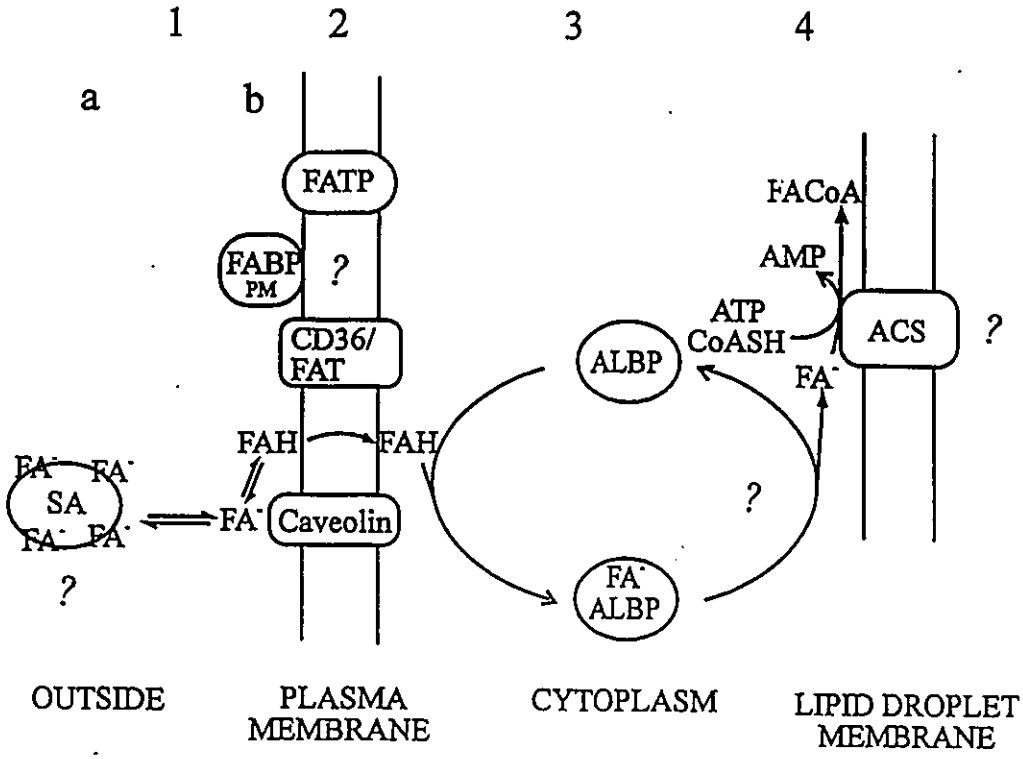

Figure 54. **Model of LCFA uptake in 3T3-L1 adipocytes.** LCFA uptake in 3T3-L1 adipocytes involves a number of distinct steps. In step 1, LCFAs are delivered to the cell surface by SA (**a**) where they interact with LCFA receptors, such as caveolin (**b**). The localization of caveolin as well as putative SA receptors within caveolae suggests that these may be the sites of LCFA uptake. LCFAs partition into the lipid bilayer and become protonated (FAH) crossing the bilayer by passive diffusion (step 2). They are targeted to specific organelles, such as the lipid droplet of 3T3-L1 adipocytes by cytoplasmic FABPs such as the ALBP (step 3). There, they are converted to LCFA-CoA by long chain ACS (step 4), preventing their efflux and activating them for further metabolism. Question marks indicate aspects of the model which are currently unclear. These include the nature of the interaction of SA with the cell membrane and the mechanism by which it affects LCFA uptake. Furthermore, while the plasma membrane proteins, CD36/FAT, $FABP_{PM}$ and FATP have been shown to be involved in LCFA uptake, the nature of their roles is currently unclear; they may be involved in the regulation of the process. The mechanism of targeting of LCFAs to the lipid droplet by ALBP is also unclear, but may be related to the lipid composition of the lipid droplet membrane or to the phosphorylation state of the protein. Finally, the nature of the lipid droplet associated ACS activity is not clear. The presence of these or related proteins in a variety of cells which exhibit high levels of LCFA uptake suggests the generality of this model.

C.9. Future Directions

C.9.1. Generality of Model for LCFA Uptake: Studies in Other Cell Types

While the working model for LCFA uptake presented above (figure 54) has been derived from studies on 3T3-L1 adipocytes, evidence suggests that it may be applicable to other mammalian cell types exhibiting high levels of LCFA uptake and metabolism. For example, SA binds to the surfaces of (Popov et al., 1992; Reed and Burrington, 1989; Torres et al., 1992b) and exerts stimulatory effects on LCFA uptake by cardiomyocytes, hepatocytes and T-lymphocytes (Sorrentino et al., 1989; Uriel et al., 1994). Furthermore, caveolin, CD36/FAT, $FATP_{PM}$ and FATP are expressed in a variety of these cells including adipocytes and cardiomyocytes (Abumrad et al., 1993; Glenney, 1992; Potter et al., 1987; Schaffer and Lodish, 1994; Scherer et al., 1994). As mentioned in Section A.7.1, a variety of cells express cytoplasmic FABPs. The heart-FABP and mP2 share a high degree of sequence identity with ALBP (Veerkamp et al., 1991). The mechanism of transfer of LCFAs from the heart-FABP to model membranes is similar to that mediated by the ALBP (Kim and Storch, 1992b). The heart-FABP has also been shown to be phosphorylated on Tyr-19, suggesting that LCFA binding might be regulated by phosphorylation in an analogous manner to that found for ALBP (Nielsen and Spener, 1993). The proposal that membrane interaction and reversible phosphorylation might be

involved in LCFA targeting by the ALBP suggests that the heart-FABP might mediate similar targeting events.

The photoaffinity labeling methodologies, developed for the study of LCFA uptake in 3T3-L1 adipocytes, can be applied to other cell types to test the generality of the model for LCFA uptake presented in the preceding section (figure 54). This will include the identification of membrane associated and soluble FABPs, the characterization of their binding to LCFAs, and the study of their time-dependent labeling in intact cells as a measure of the trafficking of newly internalized LCFAs.

As indicated above, cardiomyocytes represent an attractive cell type with which to pursue such studies. The reasons for this include their reliance on LCFAs as their major energy source, their expression of a number of proteins whose involvement in LCFA uptake has been implicated in 3T3-L1 adipocytes (as mentioned above), and their sensitivity to high levels of LCFAs (Liedtke et al., 1988), which suggests that a mechanism by which LCFAs are targeted directly to sites of metabolism might be beneficial by minimizing the non-specific diffusion of LCFAs throughout the cytoplasm.

Yeasts also represent a potentially useful system in which to carry out such studies. Although many types of yeast, including *S. cerevisiae*, can utilize LCFAs as their sole carbon and energy sources (Johnson et al., 1994b), very little is known about the mechanisms of LCFA uptake in these cells (Johnson et al., 1994b; Kohlwein and Paltauf, 1983). *S. cerevisiae* is very amenable to genetic manipulation, allowing the generation

of null mutants and complementation analyses. Such studies should allow the roles of proteins identified by photoaffinity labeling to be assigned *in vivo*.

C.9.2. Characterization of LCFA Binding Site of Caveolin

The saturable labeling by the photoreactive LCFA, of both the high molecular weight, basic and low molecular weight, acidic forms of caveolin (figure 30) indicated that each form contained a high affinity LCFA binding site. The characterization of the amino acid residues in the vicinity of these binding sites can be accomplished through a combination of photoaffinity labeling with the radioactive probe and protein chemistry, involving the fragmentation of the protein, analysis of peptides and protein sequencing.

The availability of the cDNA clones for caveolin from a variety of species (Glenney, 1992; Kurzchalia et al., 1992; Tang et al., 1994) should facilitate the analysis of the LCFA binding site. This can be accomplished by expressing and labeling different regions of the protein to identify the location of the LCFA binding site, and measuring the effects on photoaffinity labeling of random and specific mutations introduced into the primary sequence of the protein.

C.9.3. Characterization of Effect of Phosphorylation on LCFA Binding by Caveolin

The result of figure 28, that both forms of caveolin migrate on 2D-PAGE with multiple pI values, is consistent with the reported phosphorylation of caveolin (Glenney, 1989; Sargiacomo et al., 1994; Scherer et al., 1994). However, only the most acidic spot of the two molecular weight forms of caveolin are labeled with the photoreactive LCFA, suggesting the possibility that phosphorylation might affect LCFA binding. The effects

of phosphorylation or dephosphorylation of caveolin *in vitro* on labeling with the photoreactive LCFA will determine whether LCFA binding is regulated by phosphorylation of the protein. Furthermore, several putative phosphorylation sites have been identified in the primary sequence of caveolin (Sargiacomo et al., 1994; Tang et al., 1994). The affects of mutations introduced at these sites on LCFA binding can also be studied, to gain insight into the mechanism of this potential regulation of LCFA binding.

C.9.4. Characterization of Involvement of Caveolin in LCFA Uptake

Caveolin was identified as the only high affinity LCFA binding protein present in 3T3-L1 adipocyte plasma membranes (figure 24a), suggesting that it may be involved in LCFA uptake or signalling. The availability of cDNA clones for caveolin from various sources (as mentioned above) should enable this to be tested. This could be accomplished by the expression recombinant genes encoding caveolin or antisense RNA corresponding to caveolin in cells either not expressing or expressing caveolin, respectively. Therefore, the ability of caveolin expression to confer increased LCFA uptake or signalling, or the ability of the reduction of caveolin expression to reduce LCFA uptake or signalling could be determined.

C.9.5. Identification of SA Receptor in Adipocytes

The involvement of known SA receptors in LCFA uptake in 3T3-L1 adipocytes can be tested through the use of antibodies for those proteins a) to determine whether they are expressed by these cells and if so, b) to inhibit SA binding to the cell surface and c) to determine whether a concomitant inhibition of LCFA uptake is observed.

Alternatively, the identification of novel SA receptors can be accomplished through the use of a variety of techniques, including ligand blotting with labeled SA and studies with chemical crosslinking agents to chemically fix SA to its putative receptor(s).

C.9.6. Mechanism of ALBP Mediated Targeting of LCFAs to the Lipid Droplet

The development of an *in vitro* assay for LCFA targeting by the ALBP, consisting of membranes from different organelles should enable targeting to be easily manipulated experimentally. The potential involvement of receptors for the ALBP on the lipid droplet membrane can be tested by the analysis of ALBP binding to that membrane as well as through the use of ligand blotting and/or crosslinking techniques, as discussed in section C.9.5. The involvement of phosphorylation in the targeting can be studied in the *in vitro* system through the use of phosphorylated or unphosphorylated ALBP, as well as through the search for lipid droplet associated protein tyrosine phosphatases with specificity for phospho-ALBP.

C.9.7. Characterization of Lipid Droplet Associated ACS

The data of figure 53 has been the first description of a lipid droplet-associated long chain ACS activity in adipocytes. The relationship between this enzyme and that in mitochondria, ER and peroxisomes of mammalian cells can be investigated through enzymatic as well as immunological analysis, the latter with antibodies specific to the mitochondrial, ER and peroxisomal enzyme. Furthermore, if found to be different, the enzyme can be isolated from lipid droplets, used to generate antibodies, and the isolation of its cDNA by molecular cloning can be undertaken.

C.9.8. Identification and Characterization of LCFA Binding Sites on Proteins

Recent evidence implicates the involvement of LCFAs in the regulation of a variety of cellular processes. For example, it has been proposed that they may be ligands for proteins of the PPAR family, regulating their activities as transcription factors (Amri et al., 1995; Chawla and Lazar, 1994; Chawla et al, 1994; Tontonoz et al. 1994a and b). Sequence comparison has indicated that Tsp, a periplasmic protease expressed in *E. coli* and recently implicated in LCFA uptake in that organism (Azizan and Black, 1994), shares homology with members of the mammalian cytoplasmic FABP family (Silber et al., 1992). A portion (residues 263-393) of the *N*-methyl-D-aspartate receptor, a ligand gated ion channel whose activity has been found to be modulated by LCFAs, also shares significant sequence similarity with a variety of cytoplasmic FABPs (Petrou et al., 1993). As yet, however, LCFA binding to these proteins has not been demonstrated. The use of the methodologies described in Sections C.3.5 and C.4 for the identification and analysis of LCFA binding to membrane bound as well as soluble FABPs, should allow the proposed binding of LCFAs to these and other proteins of interest to be tested.

REFERENCES

Abe, T., Fujino, T., Fukuyama, R., Minoshima, S., Shimizu, N., Toh, H., Suzuki, H., and Yamamoto, T. (1992) Human long-chain acyl-CoA synthetase: Structure and chromosomal location. *J. Biochem.* **111**, 123-128.

Abumrad, N.A., Perkins, R.C., Park, J.H. and Park, C.R. (1981) Mechanism of long-chain fatty acid permeation in isolated adipocyte. *J. Biol. Chem.* **256**, 9183-9191.

Abumrad, N.A., Park, J.H., and Park, C.R. (1984) Permeation of long-chain fatty acid into adipocytes. Kinetics, specificity, and evidence for involvement of a membrane protein. *J. Biol. Chem.* **259**, 8945-8953.

Abumrad, N.A., Forest, C., Regen, D.M., Barnella, U.S. and Melki, S.A. (1991) Metabolism of oleic acid in differentiating BFC-1 preadipoose cells *Am. J. Physiol.* **261**, E76-E86.

Abumrad, N.A., El-Maghrabi, M.R., Amri, E.-Z., Lopez, E. and Grimaldi, P.A. (1993) Cloning of a rat adipocyte membrane protein implicated in binding or transport of long-chain fatty acids that is induced during preadipocyte differentiation. Homology with CD36. *J. Biol. Chem.* **268**, 17665-17668.

Acton, S.L., Scherer, P.E., Lodish, H.F., and Krieger, M. (1994) Expression cloning of SR-BI, a CD36-related class B scavenger receptor. *J.Biol. Chem.* **269**, 21003-21009.

Ames, B.N. (1966) Assay for inorganic phosphate, total phosphate and phosphatases. *Methods Enzymol.* **8**, 115-118.

Ames, G.F.-L. and Nikaido, K. (1976) Two-dimensional gel electrophoresis of membrane proteins. *Biochemistry* **15**, 616-623.

Amri, E.-Z., Bertrand, B., Ailhaud, G. and Grimaldi, P. (1991a) Regulation of adipose cell differentiation. I. Fatty acids are inducers of the aP2 gene expression. *J. Lipid Res.* **32**, 1449-1456.

Amri, E.-Z., Ailhaud, G. and Grimaldi, P. (1991b) Regulation of adipose cell differentiation. II. Kinetics of induction of the aP2 gene by fatty acids and modulation by dexamethasone. *J. Lipid Res.* **32**, 1457-1463.

Amri, E.-Z., Ailhaud, G. and Grimaldi, P.-A. (1994) Fatty acids as signal transducing molecules: Involvement in the differentiation of preadipose to adipose cells. *J. Lipid Res.* **35**, 930-937.

Amri, E.-Z., Bonino, F., Ailhaud, G., Abumrad, N.A., and Grimaldi, P.A. (1995) Cloning of a protein that mediates transcriptional effects of fatty acids in preadipocytes. Homology to peroxisome proliferator-activated receptors. *J. Biol. Chem.* **270**, 2367-2371.

Andersen, O.S. (1989) Kinetics of ion movement mediated by carriers and channels. *Methods Enzymol.* **171**, 62-112.

Anderson, R.G.W. (1993a) Potocytosis of small molecules and ions by caveolae. *Trends Cell Biol.* **3**, 69-72.

Anderson, R.G.W. (1993b) Caveolae: Where incoming and outgoing messages meet. *Proc. Natl. Acad. Sci. USA*. **90**, 10909-10913.

Anderson, R.G.W., Kamen, B.A., Rothberg, K. and Lacey, S.W. (1992) Potocytosis: Sequestration and transport of small molecules by caveolae. *Science* **255**, 410-411

Appelmans, F., Wattiaux, R. and de Duve, C. (1955) Tissue fractionation studies. 5. The association of acid phosphatase with a special class of cytoplasmic granules in rat liver. *Biochem. J.* **59**, 438-445.

Azizan, A. and Black, P.N. (1994) Use of transposon Tn*phoA* to identify genes for cell envelope proteins of *Escherichia coli* required for long-chain fatty acid transport: The periplasmic protein Tsp potentiates long-chain fatty acid transport. *J. Bacteriol.* **176**, 6653-6662.

Baldini, G., Hohl, T., Lin, H.Y., and Lodish, H.F. (1992) Cloning of a Rab3 isotype predominantly expressed in adipocytes. *Proc. Natl. Acad. Sci. USA*. **89**,5049-5052.

Bar-Tana, J., Rose, G., and Shapiro, B. (1971) The purification and properties of microsomal palmitoyl-coenzyme A synthetase. *Biochem. J.* **122**, 353-362.

Bass, N.M. (1993) Cellular binding proteins for fatty acids and retinoids: Similar or specialized functions? *Mol. Cell. Biochem.* **123**, 191-202.

Bayley, H.C. (1983) *Photogenerated reagents in biochemistry and molecular biology* (Work, T.S. and Burdon, R.H., eds) Elsevier, New York.

Beavo, J.A., Rogers, N.L., Crofford, O.B., Hardman, J.G., Sutherland, E.W., and Newman, E.V. (1970) Effects of xanthine derivatives on lipolysis and on adenosine 3',5'-monophosphate phosphodiesterase activity. *Mol. Pharm.* **6**, 597-603.

Becker, M.M., Kalinna, B.H., Waine, G.J., and McManus, D.P. (1994) Gene cloning, overproduction and purification of a functionally active cytoplasmic fatty acid-binding protein (Sj-FABP$_c$) from the human blood fluke *Schistosoma japonicum*. *Gene* **148**, 321-325.

Beers, R.F., Jr. and Sizer, I.W. (1952) A spectrophotometric method for measuring the breakdown of hydrogen peroxide by catalase. *J. Biol. Chem.* **195**, 133-140.

Bell, G.L., Burant, C.F., Takeda, J., and Gould, G.W. (1993) Structure and function of mammalian facilitative sugar transporters. *J. Biol. Chem.* **268**, 19161-19164.

Bennett, E., Stenvers, K.L., Lund, P.K., abnd Popko, B. (1994) Cloning and characterization of a cDNA encoding a novel fatty acid binding protein from rat brain. *J. Neurochem.* **63**, 1616-1624.

Benning, M.M., Smith, A.F., Wells, M.A., and Holden, H.M. (1992) Crystallization, structure determination and least-squares refinement to 1.75 Å resolution of the fatty-acid-binding protein isolated from *Manduca sexta* L. *J. Mol. Biol.* **228**, 208-219.

Berk, P.D., Wada, H., Horio, Y., Potter, B.J., Sorrentino, D., Zhou, S.-L., Isola, L.M., Stump, D., Kiang, C.-L. and Thung, S. (1990) Plasma membrane fatty acid-binding protein and mitochondrial glutamic-oxaloacetic transaminase of rat liver are related. *Proc. Natl. Acad. Sci. USA.* **87**, 3484-3488.

Bernier, M., Laird, D.M. and Lane, M.D. (1987) Insulin-activated tyrosine phosphorylation of a 15-kilodalton protein in intact 3T3-L1 adipocytes. *Proc. Natl. Acad. Sci. USA.* **84**, 1844-1848.

Bernlohr, D.A., Angus, C.W., Lane, M.D., Bolanowski, M.A. and Kelley, T.J., Jr. (1984) Expression of specific mRNAs during adipose differentiation: Identification of an mRNA encoding a homologue of myelin P2 protein. *Proc. Natl. Acad. Sci. USA.* **81**, 5468-5472.

Birkenmeier, E.H., Gwynn, B., Howard, S., Jerry, J., Gordon, J.I., Landschulz, W.H., and McKnight, S.L. (1989) Tissue-specific expression, developmental regulation, and genetic mapping of the gene encoding CCAAT/enhancer binding protein. *Genes & Dev.* **3**, 1146-1156.

Black, P.N. and DiRusso, C.C. (1994) Molecular and biochemical analysis of fatty acid transport, metabolism and gene regulation in *Escherichia coli*. *Biochim. Biophys. Acta* **1210**, 123-145.

Black, P.N., Said, B., Ghosn, C.R., Beach, J.V., and Nunn, W.D. (1987) Purification and characterization of an outer membrane-bound protein involved in long-chain fatty acid transport in *Escherichia coli*. *J. Biol. Chem.* **262**, 1412-1419.

Black, P.N., DiRusso, C.C., Metzger, A.K., and Heimert, T.L. (1992) Cloning, sequencing and expression of the *fadD* gene of *Escherichia coli* encoding acyl coenzyme A synthetase. *J. Biol. Chem.* **267**, 25513-25520.

Bligh, E.G. and Dyer, W.J. (1959) A rapid method of total lipid extraction and purification. *Can. J. Biochem. Physiol.* **31**, 911-917.

Bonner, W.M. and Laskey, R.A. (1974) Quantitative film detection of ^{3}H and ^{14}C in polyacrylamide gels by fluorography. *Eur. J. Biochem.* **46**, 83-88.

Brecher, P., Saouaf, R., Sugarman, J.M., Eisenberg, D., and LaRosa, K. (1984) Fatty acid transfer between multilamellar liposomes and fatty acid-binding proteins. *J. Biol. Chem.* **259**, 13395-13401.

Brown, M.S. and Goldstein, J.L. (1983) Lipoprotein metabolism in the macrophage: Implications for cholesterol deposition in atherosclerosis. *Annual Review Biochem.* **52**, 223-261.

Brunner, J. (1993) New photolabeling and crosslinking methods. *Annual Review Biochem.* **62**, 483-514.

Buelt, M.K., Shekels, L.L., Jarvis, B.W., and Bernlohr, D.A. (1991) *In vitro* phosphorylation of the adipocyte lipid-binding protein (p15) by the insulin receptor. Effects of fatty acid on receptor kinase and substrate phosphorylation. *J. Biol. Chem.* **266**, 12266-12271.

Buelt, M.K., Xu, Z., Banaszak, L.J. and Bernlohr, D.A. (1992) Structural and functional characterization of the phosphorylated adipocyte lipid-binding protein (pp15). *Biochemistry* **31**, 3493-3499.

Bull, H.A., Brickell, P.M., and Dowd, P.M. (1994) *src*-related protein tyrosine kinases are physically associated with the surface antigen CD36 in human dermal microvascular endothelial cells. *FEBS Lett.* **351**, 41-44.

Burczynski, F.J. and Cai, Z.-S. (1994) Palmitate uptake by hepatocyte suspensions: Effect of albumin. *Am. J. Physiol.* **267**, G371-G379.

Burczynski, F.J., Cai, Z.-S, Moran, J.B. and. Forker, E.L. (1989) Palmitate uptake by cultured hepatocytes: Albumin binding and stagnant layer phenomena. *Am. J. Physiol.* **257**, G584-G593.

Burczynski, F.J., Moran, J.B. and Cai, Z.-S. (1993) Uptake of organic anions by hepatocyte monolayers: Codiffusion versus facilitated dissociation. *Can. J. Physiol. Pharmacol.* **71**, 863-867.

Campbell, F.M., Gordon, M.J., and Dutta-Roy, A.K. (1994) Plasma membrane fatty acid-binding protein ($FABP_{pm}$) of the sheep placenta. *Biochim. Biophys. Acta* **1214**, 187-192.

Canfield, W.K. and Arion, W.J. (1988) The glucose-6-phosphatase system in rat hepatic microsomes displays hyperbolic kinetics at physiological glucose 6-phosphate concentrations. *J. Biol. Chem.* **263**, 7458-7460.

Capone, J., Leblanc, P., Gerber, G.E., and Ghosh, H.P. (1983) Localization of membrane proteins by the use of a photoreactive fatty acid incorporated *in vivo* into vesicular somatitis virus. *J. Biol. Chem.* **258**, 1395-1398.

Chanarin, I., Patel, A., Slavin, G., Wills, E.J., Andrews, T.M., and Stewart, G. (1975) Neutral-lipid storage disease: A new disorder of lipid metabolism. *British Med. J.* **1**, 553-555.

Chang, W.-J., Ying, Y., Rothberg, K.G., Hooper, N.M., Turner, A.J., Gambiel, H.A., DeGunzburg, J., Mumby, S.M., Gilman, A.G. and Anderson, R.G.W. (1994) Purification and characterization of smooth muscle cell caveolae. *J. Cell Biol.* **126**, 127-138.

Chawla, A. and Lazar, M.A. (1994) Peroxisome proliferator and retinoid signalling pathways co-regulate preadipocyte phenotype and survival. *Proc. Natl. Acad. Sci. USA* **91**, 1786-1790.

Chawla, A., Schwarz, E.J., Dimaculangan, D.D., and Lazar, M.A. (1994) Peroxisome proliferator-activated receptor (PPAR) γ: Adipose-predominant expression and induction early in adipocyte differentiation. *Endocrinology* **135**, 798-800.

Cistola, D.P., Hamilton, J.A., Jackson, D., and Small, D.M. (1988a) Ionization and phase behaviour of fatty acids in water: Application of the Gibbs phase rule. *Biochemistry* **27**, 1881-1888.

Cistola, D.P., Walsh, M.T., Corey, R.P., Hamilton, J.A. and Brecher, P. (1988b) Interactions of oleic acid with liver fatty acid binding protein: A carbon-13 NMR study. *Biochemistry*. **27**, 711-717.

Clark, S. (1992) Protein isoprenylation and methylation at carboxyl-terminal cysteine residues. *Annual Review Biochem.* **61**, 355-386.

Coleman, R.A., Reed, B.C., Mackall, J.C., Student, A.K., Lane, M.D., and Bell, R.M. (1978) Selective changes in microsomal enzymes of triacylglycerol, phosphatidylcholine, and phosphatidylethanolamine biosynthesis during differentiation of 3T3-L1 preadipocytes. *J. Biol. Chem.* **253**, 7256-7261.

Coleman, R.A., Rao, P., Fogelsong, R.J., and Bardes, E.S-G. (1992) 2-Bromopalmitoyl-CoA and 2-bromopalmitate: Promiscuous inhibitors of membrane-bound enzymes. *Biochim. Biophys. Acta* **1125**, 203-209.

Cooper, R., Noy, N., and Zakim, D. (1989) Mechanism for binding of fatty acids to hepatocyte plasma membranes. *J. Lipid Res.* **30**, 1719-1726.

Cornelius, P., MacDougald, O.A., and Lane, M.D. (1994) Regulation of adipocyte development. *Annual Review Nutr.* **14**, 99-129.

Cowan, S.W., Newcomer, M.E., and Jones, T.A. (1993) Crystallographic studies on a family of cellular lipophilic transport proteins. Refinement of P2 myelin protein and the structure determination and refinement of cellular retinol-binding protein in complex with all-*trans*-retinol. *J. Mol. Biol.* **230**, 1225-1246.

Cushman, S.W. and Wardzala, L.J. (1980) Potential mechanism of insulin action on glucose transport in the isolated rat adipose cell. Apparent translocation of intracellular transport systems to the plasma membrane. *J. Biol. Chem.* **255**, 4758-4762.

Daniels, C., Noy, N. and Zakim, D. (1985) Rates of hydration of fatty acids bound to unilamellar vesicles of phosphatidylcholine or to albumin. *Biochemistry* **24**, 3286-3292.

DeGrella, R.F., and Light, R.J. (1980) Uptake and metabolism of fatty acids by dispersed adult rat heart myocytes. II. Inhibition by albumin and fatty acid homologues, and the effect of temperature and metabolic reagents. *J. Biol. Chem.* **255**, 9739-9745.

De Jong, J.W. and Hülsmann, W.C. (1970) A comparative study of palmitoyl-CoA synthetase activity in rat liver, heart and gut mitochondrial and microsomal preparations. *Biochim. Biophys. Acta* **197**, 127-135.

Diede, H.E., Rodilla-Sala, E., Gunawan, J., Manns, M., and Stremmel, W. (1992) Identification and characterization of a monoclonal antibody to the membrane fatty acid binding protein. *Biochim. Biophys. Acta* **1125**, 13-20.

Distel, R.J., Robinson, G.S. and Spiegelman, B.M. (1992) Fatty acid regulation of gene expression. Transcriptional and post-transcriptional mechanisms. *J. Biol. Chem.* **267**, 5937-5941.

Doglio, A., Dani, C., Fredrikson, G., Grimaldi,P., and Ailhaud, G. (1987) Acute regulation of insulin-like growth factor-I gene expression by growth hormone during adipose cell differentiation. *EMBO J.* **6**, 4011-4016.

Doglio, A., Dani, C., Grimaldi,P., and Ailhaud, G. (1986) Growth hormone regulation of the expression of differentiation-dependant genes in preadipocyte Ob1771 cells. *Biochem. J.* **238**, 123-129.

Doody, M.C., Pownall, H.J., Kao, Y.J., and Smith, L.C. (1980) Mechanism and kinetics of transfer of a fluorescent fatty acid between single-walled phosphatidylcholine vesicles. *Biochemistry* **19**, 108-116.

Dupree, P., Parton, R.G., Raposo, G., Kurzchalia, T.V., and Simons, K. (1993) Caveolae and sorting in the *trans*-Golgi network of epithelial cells. *EMBO J.* **12**, 1597-1605.

Dziarski, R. (1994) Cell-bound albumin is the 70-kDa peptidoglycan-, lipopolysaccharide-, and lipoteichoic acid-binding protein on lymphocytes and macrophages. *J. Biol. Chem.* **269**, 20431-20436.

Edens, N.K., Leibel, R.L., and Hirsch, J. (1990) Mechanism of free fatty acid re-esterifecation in human adipocytes in vitro. *J. Lipid Res.* **31**, 1423-1431.

Egan, J.J., Greenberg, A.S., Chang, M.-K., Wek, S.A., Moos, M.C., Jr. and Londos, C. (1992) Mechanism of hormone-stimulated lipolysis in adipocytes: Translocation of hormone-sensitive lipase to the lipid storage droplet. *Proc. Natl. Acad. Sci. USA* **89**, 8537-8541.

Einerhand, A.W.C., Kos, W.T., Distel, B., and Tabak, H.F. (1993) Characterization of a transcriptional control element involved in proliferation of peroxisomes in yeast in response to oleate. *Eur. J. Biochem.* **214**, 323-331.

Endemann, G., Stanton, L.W., Madden, K.S., Bryant, C.M., White, R.T., and Protter, A.A. (1993) CD36 is a receptor for oxidized low density lipoprotein. *J. Biol. Chem.* **268**, 11811-11816.

Enerbäck, S., Ohlsson, B.G., Samuelsson, L., and Bjursell, G. (1992) Characterization of the human lipoprotein lipase (LPL) promoter: Evidence of two *cis*-regulatory regions, LP-α and LP-β, of importance for the differentiation-linked induction of the LPL gene during adipogenesis. *Mol. Cell. Biol.* **12**, 4622-4633.

Fan, J.Y., Carpentier, J.-L., van Obberghen, E., Grunfeld, D., Gorden, P., and Orci, L. (1983) Morphological changes of the 3T3-L1 fibroblast plasma membrane upon differentiation to the adipocyte form. *J. Cell Sci.* **61**, 219-230.

Ferguson, M.A.J. and Williams, A.F. (1988) Cell-Surface anchoring of proteins via glycosyl-phosphatidylinositol structures. *AnnualReview Biochem.* **57**, 285-230.

Fève, B., Emorine, L.J., Lasnier, F., Blin, N., Baude, B., Nahamias, C., Strosberg, D., and Piarault, J. (1991) Atypical β-adrenergic receptor in 3T3-F442A adipocytes. Pharmacological and molecular relationship woth the human β_3-adrenergic receptor. *J. Biol. Chem.* **266**, 20329-20336.

Flier, J.S. (1995) The adipocyte: Storage depot or node on the energy information superhighway. *Cell* **80**, 15-18.

Frelin, C., Vigne, P., Ladoux, A., and Lazdunski, M. (1988) The regulation of the intracellular pH in cells from vertebrates. *Eur. J. Biochem.* **174**, 3-14.

Freytag, S.O. and Geddes, T.J. (1992) Reciprocal regulation of adipogenesis by Myc and C/EBPα. *Science.* **256**, 379-382.

Fujino, T. and Yamamoto, T. (1992) Cloning and functional expression of a novel long-chain acyl-CoA synthetase expressed in brain. *J. Biochem.* **111**, 197-203.

Gao, G. and Serrero, G. (1990) Phospholipase A_2 is a differentiation-dependent enzymatic activity activity for adipogenic cell line and adipocyte precursors in primary culture. *J. Bi Chem.* **265**,2431-2434.

Gaskins, H.R., Kim, J.-W., Wright, J.T., Rund, L.A., and Hausman, G.J. (1990) Regulation of insulin-like growth factor-I ribonucleic acid expression, polypeptide secretion, and binding protein activity by growth hormone in porcine preadipocyte cultures. *Endocrinology* **126**, 622-630.

Ghinea, N., Eskenasy, M., Simionescu, M. and Simionescu, N. (1989) Endothelial a'bumin binding proteins are membrane-associated components exposed on the cell surface. *J. Biol. Chem.* **264**, 4755-4758.

Gibbons, G.F. (1990) Assembly and secretion of hepatic very-low-density lipoprotein. *Biochem. J.* **268**, 1-13.

Glatz, J.F.C. and Veerkamp, J.H. (1983) A radiochemical procedure for the assay of fatty acid binding by proteins. *Anal. Biochem.* **132**, 89-95.

Glenney, J.R., Jr. (1989) Tyrosine phosphorylation of a 22-kDa protein is correlated with transformation by Rous sarcoma virus. *J. Biol. Chem.* **264**, 20163-20166.

Glenney, J.R., Jr. (1992) The sequence of human caveolin reveals identity with VIP21, a component of transport vesicles. *FEBS Lett.* **314**, 45-48.

Goodman, D.S. (1958) The distribution of fatty acids between *n*-heptane and aqueous phosphate buffer. *J. Am. Chem. Soc.* **80**, 3887-3892.

Green, H. and Kehinde, O. (1975) An established preadipose cell line and its differentiation in culture II. Factors affecting the adipose conversion. *Cell* **5**, 19-27.

Greenberg, A.S., Egan, J.J., Wek, S.A., Garty, N.B., Blanchette-Mackie, E.J. and Londos, C. (1991) Perilipin, a major hormonally regulated adipocyte-specific phosphoprotein associated with the periphery of lipid storage droplets. *J. Biol. Chem.* **266**, 11341-11346.

Greenberg, A.S., Egan, J.J., Wek, S.A., Moos, M.C.Jr., Londos, C., and Kimmel, A.R. (1993) Isolation of cDNAs for perilipins A and B: Sequence and expression of lipid droplet-associated proteins of adipocytes. *Proc. Natl. Acad. Sci. USA*. **90**, 12035-12039.

Greenwalt, D.E., Lipsky, R.H., Ockenhouse C.F., Ikeda, H., Tandon, N.N., and Jamiesson, G.A. (1992) Membrane glycoprotein CD36: A review of its roles in adherence, signal transduction, and transfusion medicine. *Blood* **80**, 1105-1115.

Grimaldi, P.A., Knobel, S.M., Whitsell, R.R. and Abumrad, N.A. (1992) Induction of aP2 gene expression by nonmetabolized long-chain fatty acids. *Proc. Natl. Acad. Sci. USA*. **89**, 10930-10934.

Groot, P.H.E., Scholte, H.R., and Hülsmann, W.C. (1976) Fatty acid activation: Specificity, localization, and function. *Adv. Lipid Res.* **14**,75-126.

Guest, S.J., Hadcock, J.R., Watkins, D.C., and Malbon, C.C. (1990) β_1- and β_2-adrenergic receptor expression in differentiating 3T3-L1 cells. Independant regulation at the level of mRNA. *J. Biol. Chem.* **265**, 5370-5375.

Hall, M. and Saggerson, E.D. (1985) Reversible inactivation of long-chain fatty acyl-CoA synthetase in rat adipocytes. *Biochem. J.* **226**, 275-282.

Hamilton, J.A. and Cistola, D.P. (1986) Transfer of oleic acid between albumin and phospholipid vesicles. *Proc. Natl. Acad. Sci. USA*. **83**:82-86.

Hamilton, J.A., Civelek, V.N., Kamp, F., Tornheim, K. and Corkey, B.E. (1994) Changes in internal pH caused by movement of fatty acids into and out of clonal pancreatic β-cells (HIT). *J. Biol. Chem.* **269**, 20852-20856.

Hancock, R.E.W. (1991) Bacterial outer membranes: Evolving concepts. Specific structures provide gram-negative bacteria with several unique advantages. *ASM News* **57**, 175-182.

Hansen, H.O., Andreasen, P.H., Mandrup, S., Kristiansen, K., and Knudsen, J. (1991) Induction of acyl-CoA-binding protein and its mRNA in 3T3-L1 cells by insulin during preadipocyte-to-adipocyte differentiation. *Biochem. J.* **277**, 341-344.

Hardy, R.W., Ladenson, J.H., Henriksen, E.J., Holloszy, J.O. and McDonald, J.M. (1991) Palmitate stimulates glucose transport in rat adipocytes by a mechanism involving translocation of the insulin sensitive glucose transporter (GluT4). *Biochem. Biophys. Res. Commun.* **177**, 343-349.

Hare, J.F., Taylor, K., and Holocher, A. (1994) Energy-dependent protein-triacylglycerol interaction in a cell-free system from 3T3-L1 adipocytes. *J. Biol. Chem.* **269**, 771-776.

Harmon, C.M., Luce, P., Beth, A.H. and Abumrad, N.A. (1991) Labeling of adipocyte membranes by sulfo-*N*-succinimidyl derivatives of long-chain fatty acids: Inhibition of fatty acid transport. *J. Membrane Biol.* **121**, 261-268.

Harmon, C.M. and Abumrad, N.A. (1993) Binding of sulfosuccinimidyl fatty acids to adipocyte membrane proteins: Isolation and amino-terminal sequence of an 88-kD protein implicated in transport of long-chain fatty acids. *J. Membrane Biol.* **133**, 43-49.

Hesler, C.B., Olymbios, C., Haldar, D. (1990) Transverse-plane topography of long-chain acyl-CoA synthetase in the mitochondrial outer membrane. *J. Biol. Chem.* **265**, 6600-6605.

Hope, M.J. and Cullis, P.R. (1987) Lipid asymmetry induced by transmembrane pH gradients in large unilamellar vesicles. *J. Biol. Chem.* **262**, 4360-4366.

Horie, T., Mizuma, T., Kasai, S. and Awazu, S. (1988) Conformational change in plasma albumin due to interaction with isolated rat hepatocyte. *Am. J. Physiol.* **254**, G465-G470.

Houslay, M.D. and Stanley, K.K. (1982) *Dynamics of Biological Membranes. Influence on Synthesis, Structure and Function.* John Wiley and Sons Ltd. Chichester, UK. pp23, 43-47.

Howland, J.L., Osrin, D., Donatelli, M., and Theofrastous, J.P. (1984) Inhibition of erythrocyte plasma membrane NADH dehydrogenase by nucleotides and uncouplers. *Biochim. Biophys. Acta.* **778**, 400-404.

Hresko, R.C., Hoffman, R.D., Flores-Riveros, J.R. and Lane, M.D. (1990) Insulin receptor tyrosine kinase-catalyzed phosphorylation of 422(aP2) protein. Substrate activation by long-chain fatty acid. *J. Biol. Chem.* **265**, 21075-21085.

Huang, M.-M., Bolen, J.B., Barnwell, J.W. Shattil, S.J., and Brugge, J.S. (1991) Membrane glycoprotein IV (CD36) is physically associated with the Tyn, Lyn, and Yes protein-tyrosine kinases in human platelets. *Proc. Natl. Acad. Sci. USA*. **88**, 7844-7848.

Jamdar, S.C. and Fallon, H.J. (1973) Glycerolipid biosynthesis in rat adipose tissue. I. Properties and distribution of glycerophosphate acyltransferase and effect of divalent cations on neutral lipid formation. *J. Lipid. Res.* **14**, 509-516.

Jencks, W.P. (1989) Utilization of binding energy and coupling rules for active transport and other coupled vectorial processes. *Methods Enzymol.* **171**, 145-164.

Jiang, H.-P. and Serrero, G. (1992) Isolation and characterization of a full-length cDNA coding for an adipose differentiation-related protein. *Proc. Natl. Acad.Sci. USA*. **89**, 7856-7860.

Johnson, D.R., Bhatnagar, R.S., Knoll, L.J., and Gordon, J.I. (1994a) Genetic and biochemical studies of protein N-myristoylation. *Annual Review Biochem.* **63**, 869-914.

Johnson, D.R., Knoll, L.J., Levin, D.E., and Gordon, J.I. (1994b) *Saccharomyces cerevisiae* contains four fatty acid activation (FAA) genes: An assessment of their role in regulating protein N-myristoylation and cellular lipid metabolism. *J. Cell Biol.* **127**, 751-762.

Jones, T.A., Bergfors, T., Sedzik, J., and Unge, T. (1988) The three-dimensional structure of P2 myelin protein. *EMBO J.* 7, 1597-1604.

Kaestner, K.H., Christy, R.J., McLenithan, J.C., Braiterman, L.T., Cornelius, P., Pekala, P.H., and Lane, M.D. (1989) Sequence, tissue distribution, and differential expression of mRNA for a putative insulin-responsive glucose transporter in mouse 3T3-L1 adipocytes. *Proc. Natl. Acad. Sci. USA*. **86**, 3150-3154.

Kaikaus, R.M., Bass, N.M. and Ockner, R.K. (1990) Functions of fatty acid binding proteins. *Experientia* **46**, 617-630.

Kameda, K. and Nunn, W.D. (1981) Purification and characterization of acyl coenzyme A synthetase from *Escherichia coli*. *J. Biol. Chem.* **256**, 5702-5707.

Kamp, F. and Hamilton, J.A. (1992) pH gradients across phospholipid membranes caused by fast flip-flop of un-ionized fatty acids. *Proc. Natl. Acad. Sci., USA* **89**, 11367-11370.

Kamp, F. and Hamilton, J.A. (1993) Movement of fatty acids, fatty acid analogues, and bile acids across phospholipid bilayers. *Biochemistry* **32**, 11074-11086.

Kates, M. (1986) Techniques of Lipidology. Isolation, Analysis and Identification of Lipids , 2nd ed. *Laboratory Techniques in Biochemistry and Molecular Biology* **3** (pt. 2) Burdon, R.H. and van Knippenberg, P.H., editors) Elsevier, Amsterdam. pp. 238-327.

Kawamura, M., Jensen, D., Wancewicz, E., Joy, L., Khoo, J. and Steinberg, D. (1981) Hormone-sensitive lipase in differentiated 3T3-L1 cells and its activation by cyclic AMP-dependant protein kinase. *Proc. Natl. Acad. Sci. USA* **78**, 732-736.

Kim, H.-K., and Storch, J. (1992a) Free fatty acid transfer from rat liver fatty acid-binding protein to phospholipid vesicles. Effect of ligand and solution properties. *J. Biol. Chem.* **267**, 77-82.

Kim, H.-K., and Storch, J. (1992b) Mechanism of free fatty acid transfer from rat heart fatty acid-binding protein to phospholipid membranes: Evidence for a collisional process. *J. Biol. Chem.* **267**, 20051-20056.

Knoll, L.J. and Gordon, J.I. (1993) Use of *Escherichia coli* strains containing *fad* mutations plus a triple plasmid expression system to study the import of myristate, its activation by *Saccharomyces cerevieiae* acyl-CoA synthetase, and its utilizatiuon by *S. cerevisiae* myristoyl-CoA:protein *N*-myristoyltransferase. *J. Biol. Chem.* **268**, 4281-4290.

Knoll, L.J., Johnson, D.R., and Gordon, J.I. (1994) Biochemical studies of three *Saccharomyces cerevisiae* acyl-CoA synthetases, Faa1p, Faa2p, and Faa3p. *J. Biol. Chem.* **269**, 16348-16346.

Kohlwein, S.D. and Paltauf, F. (1983) Uptake of fatty acids by the yeasts, *Saccharomyces uvarum* and *Saccharomycopsis lipolytica*. *Biochim. Biophys. Acta* **792**, 310-317.

Kramer, W., Girbig, F., Gutjahr, U., Kowalewski, S., Jouvenal, K., Müller, G., Tripier, D., and Wess, G. (1993) Intestinal bile acid absorption. Na^+-dependant bile acid transport activity in rabbit small intestine correlates with the coexpression of an integral 93-kDa and a peripheral 14-kDa bile acid-binding membrane protein along the duodenum-ileum axis. *J. Biol. Chem.* **268**, 18035-18046.

Kumar G.B. and Black, P.N. (1991) Linker mutagenesis of a bacterial fatty acid transport protein. Identification of domains with functional importance. *J. Biol. Chem.* **266**, 1348-1353.

Kumar G.B. and Black, P.N. (1993) Bacterial long-chain fatty acid transport. Identification of amino acid residues within the outer membrane protein FadL required for activity. *J. Biol. Chem.* **268**, 15469-15476.

Kuri-Harcuch, W. and Green, H. (1978) Adipose conversion of 3T3 cells depends on a serum factor. *Proc. Natl. Acad. Sci. USA* **75**, 6107-6109.

Kurtz, A., Zimmer, A., Schnütgen, Brüning, G., Spener, F., and Müller, T. (1994) The expression pattern of a novel gene encoding brain-fatty acid binding protein correlates with neuronal and glial cell development. *Development* **120**, 2637-2649.

Kurzchalia, T.V., Dupree, P., Parton, R.G., Kellner, R., Virta, H., Lehnert, M., and Simons, K. (1992) VIP21, a 21-kD membrane protein is an integral component of *trans*-Golgi-network-derived transport vesicles. *J. Cell Biol.* **118**, 1003-1014.

Kurzchalia, T.V., Dupree, P., and Monier, S. (1994) VIP21-caveolin, a protein of the *trans*-Golgi network and caveolae. *FEBS Lett.* **346**, 88-91.

Laemmli, U.K. (1970) Cleavage of structural proteins during the assembly of the head of bacteriophage T4. *Nature* **227**, 680-685.

Lalonde, J.M., Bernlohr, D.A. and Banaszak, L.J. (1994a) X-ray crystallographic structures of adipocyte lipid-binding protein complexed with palmitate and hexadecanesulfonic acid. Properties of cavity binding sites. *Biochemistry* **33**, 4885-4895.

Lalonde, J.M., Levenson, M.A., Roe, J.J., Bernlohr, D.A., and Banaszak, L.J. (1994b) Adipocyte lipid-binding protein complexed with arachidonic acid. Titration calorimetry and X-ray crystallographic studies. *J. Biol. Chem.* **269**,25339-25347.

Lange, K. and Brandt, U. (1990) Insulin-responsive glucose transporters are concentrated in a cell surface-derived membrane fraction of 3T3-L1 adipocytes. *FEBS Lett.* **261**, 459-463.

Laposata, M. (1990) Solubilization of arachidonate-CoA ligase from cell membranes, chromatographic separation from non-specific long-chain fatty acid CoA ligase, and isolation of mutant cell line defective in arachidonate-CoA ligase. *Methods Enzymol.* **187**, 237-242.

Lazo, O., Contreras, M., Hashmi, M., Stanley, W., Irazu, C., and Singh, I. (1988) Peroxisomal lignoceryl-CoA ligase deficiency in childhood adrenoleukodistrophy and adrenomyeloneuropathy. *Proc. Natl. Acad. Sci. USA* **85**, 7647-7651.

Lazo, O., Contreras, M., and Singh, I. (1990) Topographical localization of peroxisomal acyl-CoA ligases: Differential localization of palmitoyl-CoA and lignoceryl-CoA ligases. *Biochemistry* **29**, 3981-3986.

Leblanc, P. (1991) *Radioactive photoreactive fatty acid analogues: Synthesis, biological utilization and tools for the study of fatty acid transport.* Ph.D. Thesis, McMaster University, Canada.

Leblanc, P., and Gerber, G.E. (1984) Biosynthetic utilization of photoreactive fatty acids by rat liver microsomes. *Can. J. Biochem. Cell Biol.* **62**, 375-378.

Leblanc, P., Capone, J. and Gerber, G.E. (1982) Synthesis and biosynthetic utilization of radioactive photoreactive fatty acids. *J. Biol. Chem.* **257**, 14586-14589.

Li, W.-X., Howard, R.J., and Leung, L.L.K. (1993) Identification of SVTCG in thrombospondin as the conformation-dependant, high affinity binding site for its receptor, CD36. *J. Biol. Chem.* **268**, 16179-16184.

Liao, K., Hoffman, R.D., and Lane, M.D. (1991) Phosphotyrosyl turnover in insulin signalling. Characterization of two membrane-bound pp15 protein tyrosine phosphatases from 3T3-L1 adipocytes. *J. Biol. Chem.* **266**, 6544-6553.

Lichenstein, H.S., Lyons, D.E., Wurfel, M.M., Johnson, D.A., McGinley, M.D., Leidli, J.C., Trollinger, D.B., Mayer, J.P., Wright, S.D., and Zukowski, M.M. (1994) Afamin is a new member of the albumin, α-fetoprotein, and vitamin D-binding protein gene family. *J.Biol.Chem.* **269**:18149-18154.

Liedtke, A.J., DeMaison L., Eggleston, A.M., Cohen, L.M., and Nellis, S.H. (1988) Changes in substrate metabolism and effects of excess fatty acids in reperfused myocardium. *Circulation Res.* **62**, 535-542.

Lin, F.-T. and Lane, M.D. (1994) CCAAT/enhancer binding protein α is sufficient to initiate the 3T3-L1 adipocyte differentiation program. *Proc. Natl. Acad. Sci. USA*. **91**, 8757-8761.

Lisanti, M.P., Tang, Z.-L. and Sargiacomo, M. (1993) Caveolin forms a hetero-oligomeric protein complex that interacts with an apical GPI-linked protein: Implications for the biogenesis of caveolae. *J. Cell Biol.* **123**, 595-604.

Lisanti, M.P., Scherer, P.E., Tang, Z.-L., and Sargiacomo, M. (1994a) Caveolae, caveolin and caveolin-rich membrane domains: A signalling hypothesis. *Trends Cell Biol.* **4**, 231-235.

Lisanti, M.P., Scherer, P.E., Vidugiriene, J., Tang, Z.-L., Hermanowski-Vosatka, A., Tu, Y.-H., Cook, R.F. and Sargiacomo, M. (1994b) Characterization of caveolin-rich membrane domains isolated from an endothelial-rich source: Implications for human disease. *J. Cell Biol.* **126**, 111-126.

Lowry, O., Rosenbrough, N., Farr, A. and Randall, R. (1951) Protein measurement with the Folin phenol reagent. *J. Biol. Chem.* **193**, 265-275.

Luxon, B.A. and Weisiger, R.A. (1993) Sex differences in intracellular fatty acid transport: Role of cytoplasmic binding proteins. *Am. J. Physiol.* **265**, G831-G841.

Maatman, R.G.H.J., Degano, M., van Moerkerk, H.T.B., van Marrewijk, W.J.A., van der Horst, D.J., Sacchettini, J.C., and Veerkamp, J.H. (1994) Primary structure and binding characteristics of locust and human muscle fatty acid-binding proteins. *Eur. J. Biochem.* **221**, 801-810.

Mahadevan, S. and Sauer, F. (1971) Effect of α-bromo-palmitate on the oxidation of palmitic acid by rat liver cells. *J. Biol. Chem.* **246**, 5862-5867.

Mahadevan, S. and Sauer, F. (1974) Effect of trypsin, phospholipases, and membrane-impermeable reagents on the uptake of palmitic acid by isolated rat liver cells. *Arch. Biochem. Biophys.* **164**, 185-193.

Mangroo, D. (1992) *Fatty Acid Uptake in* Escherichia coli*: Development of a Photoaffinity Labeling Approach for Identifying Proteins Involved in the Transmembrane*

Movement of Long Chain Fatty Acids. Ph.D. Thesis, McMaster University, Hamilton, Canada.

Mangroo, D., and Gerber, G.E. (1992) Photoaffinity labeling of fatty acid-binding proteins involved in long chain fatty acid transport in *Escherichia coli. J. Biol. Chem.* **267**, 17095-17101.

Mangroo, D., and Gerber, G.E. (1993) Fatty acid uptake in *Escherichia coli*: Regulation by recruitment of fatty acyl-CoA synthetase to the plasma membrane. *Biochem. Cell Biol.* **71**, 51-56.

Maniscalco, W.M., Stremmel, W., and Heeney-Campbell, M. (1990) Uptake of palmitic acid by rabbit alveolar type II cells. *Am. J. Physiol.* **259**, L206-L212.

Matarese, V. and Bernlohr, D.A. (1988) Purification of murine adipocyte lipid-binding protein. Characterization as a fatty acid- and retinoic acid-binding protein. *J. Biol. Chem.* **263**, 14544-14551.

Mersel, M., Malviya, A.N., Hindelang, C., and Mandel, P. (1984) Plasma membrane isolated from astrocytes in primary cultures. Its acceptor oxidoreductase properties. *Biochim. Biophys. Acta.* **778**, 144-154.

Minor, L.K., Rothblat, G.H., and Glick, J.M. (1989) Triglyceride and cholesteryl ester hydrolysis in a cell culture model of smooth muscle foam cells. *J. Lipid Res.* **30**, 189-197.

Mishina, M., Kamiryo, T., Tashiro, S.-I., Hagihara, T., Tanakas, A., Fukui, S., Osumi, M., and Numa, S. (1978a) Subcellular localization of two long-chain acyl-coenzyme-A synthetases in *Candida lipolytica. Eur. J. Biochem.* **89**, 321-328.

Mishina, M., Kamiryo, T., Tashiro, and Numa, S. (1978b) Separation and characterization of two long-chain acyl-CoA synthetases from *Candida lipolytica. Eur. J. Biochem.* **82**, 347-354.

Moller, F., Wong, K.H., and Green, P. (1981) Control of fat cell phosphatidate phosphohydrolase by lipolytic agents. *Can. J. Biochem.* **59**, 9-15.

Moolenaar, W.H., Tsien, R.Y., van der Saag, P.T. and de Laat, S.W. (1983) Na^+/H^+ exchange and cytoplasmic *p*H in the action of growth factors in human fibroblasts. *Nature* **304**, 645-648.

Moolenaar, W.H., Tertoolen, L.G.J., and de Laat, S.W. (1984) The regulation of cytoplasmic pH in human fibroblasts. *J. Biol. Chem.* **259**, 7563-7569.

Moustaid, N. and Sul, H.S. (1991) Regulation of expression of the fatty acid synthase gene in 3T3-L1 cells by differentiation and triiodothyronine. *J. Biol. Chem.* **266**, 18550-18554.

Neufeld, E.J., Bross, T.E., Majerus, P.W. (1984) A mutant $HSDM_1C_1$ fibrosarcoma line selected for defective eicosanoid precursor uptake lacks arachidonate-specific acyl-CoA synthetase. *J. Biol.Chem.* **259**:1986-1992.

Nielsen, P.E. (ed.) (1989) *Photochemical Probes in Biochemistry* Kulwer Academic Publishers. Dordrecht, The Netherlands.

Nielsen, S.U. and Spener, F. (1993) Fatty acid-binding protein from rat heart is phosphorylated on Tyr^{19} in response to insulin stimulation. *J. Lipid Res.* **34**, 1355-1366.

Nikaido, H. (1976) Outer membrane of *Salmonella typhimurium*. Transmembrane diffusion of some hydrophobic substances. *Biochim. Biophys. Acta* **433**, 118-132.

Nikaido, H. (1994) Porins and specific diffusion channels in bacterial outer membranes. *J. Biol. Chem.* **269**, 3905-3908.

Nikaido, H. and Vaara, M. (1985) Molecular basis of bacterial outer membrane permeability. *Microbiol. Rev.* **49**, 1-32.

Noy, N. and Zakim, D. (1993) Physical chemical basis for the uptake of organic compounds by cells. in *Hepatic Transport and Bile Secretion: Physiology and Pathophysiology* (N. Tavolini and P.D. Berk, eds) Raven Press Ltd., New York p. 313-335.

Noy, N., Donnelley, T.M., and Zakim, D. (1986) Physical-chemical model for the entry of water-insoluble compounds into cells. Studies of fatty acid uptake by the liver. *Biochemistry* **25**, 2013-2021.

Nunn, W.D., Simons, R.W., Egan, P.A., and Maloy, S.R. (1979) Kinetics of the utilization of medium and long chain fatty acids by a mutant of *Escherichia coli* defective in the *fadL* gene. *J. Biol. Chem.* **254**, 9130-9134.

Opara, E.C., Garfinkle, M., Hubbard, V.S. Burch, W.M. and Akwari, O.E. (1994) Effect of fatty acids on insulin release: Role of chain length and degree of unsaturation. *Am. J. Physiol.* **266**, E635-E639.

Ordway, R.W., Walsh, J.V., Jr. and Singer, J.J. (1989) Arachidonic acid and other fatty acids directly activate potassium channels in smooth muscle cells. *Science* **244**,1176-1179.

Ordway, R.W., Singer, J.J. and Walsh, J.V., Jr (1991) Direct regulation of ion channels by fatty acids. *Trends Neurosci.* **14**, 96-100.

Pande, S.V. and Mead, J.F. (1968) Long chain fatty acid activation in subcellular preparations from rat liver. *J. Biol. Chem.* **243**, 352-361.

Parsons, P. and Scribner, D. (1988) Purified microsomal long chain fatty acyl CoA ligase: A novel mechanism. *FASEB J.* **2**, A1544 (Meeting abstract).

Parton, R.G., Joggerst, B., and Simons, K. (1994) Regulated internalization of caveolae. *J. Cell Biol.* **127**, 1199-1215.

Peeters, R.A. and Veerkamp, J.H. (1989) Does fatty acid-binding protein play a role in fatty acid transport? *Mol. Cell. Biochem.* **88**, 45-49.

Peeters, R.A., Veerkamp, J.H. and Demel, R.A. (1989) Are fatty acid-binding proteins involved in fatty acid transfer? *Biochim. Biophys. Acta* **1002**, 8-13.

Peterson, J., Bihan, B.E., Bengtsson-Olivecrona, G., Deckelbaum, R.J., Carpentier, Y.A., and Olivecrona, T. (1990) Fatty acid control of lipoprotein lipase: A link between energy metabolism and lipid transport. *Proc. Natl. Acad. Sci. USA.* **87**, 909-913.

Petrou, S., Ordway, R.W., Singer, J.J. and Walsh, J.V., Jr. (1993) A putative fatty acid-binding domain of the NMDA receptor. *Trends Biochem. Sci.* **18**, 41-42.

Phillips, M., Djian, P. and Green, H. (1986) The nucleotide sequence of three genes participating in the adipose differentiation of 3T3 cells. *J. Biol. Chem.* **261**, 10821-10827.

Popov, D., Hasu, M., Ghinea, N., Simionescu, N. and Simionescu, M. (1992) Cardiomyocytes express albumin binding proteins *J. Mol. Cell. Cardiol.* **24**, 989-1002.

Potter, B.J. and Berk, P.D. (1993) Liver plasma membrane fatty acid binding protein. in *Hepatic Transport and Bile Secretion: Physiology and Pathophysiology* (N. Tavolini and P.D. Berk, eds) Raven Press Ltd., New York p. 253-267.

Potter, B.J., Stump, D., Schweiterman, W., Sorrentino, D., Jacobs, L.N. Kiang, C.-L., Rand, J.H. and Berk, P.D. (1987) Isolation and partial characterization of plasma

membrane fatty acid binding proteins from myocardium and adipose tissue and their relationship to analogous proteins in liver and gut. *Biochem. Biophys. Res. Comm.* **148**, 1370-1376.

Raderath, K. (1970) An evaluation of film detection methods for weak β-emitters, particularly tritium. *Anal. Biochem.* **34**, 188-205.

Record, M., Bes, J.-C., Chap, H. and Douste-Blazy, L. (1982) Isolation and characterization of plasma membranes from Krebs II ascite cells using percoll gradient. *Biochim. Biophys. Acta* **688**, 57-65.

Reed, B.C. and Lane, M.D. (1980) Insulin receptor synthesis and turnover in differentiating 3T3-L1 adipocytes. *Proc. Natl.. Acad. Sci. USA* 77, 285-289.

Reed, R.G. and Burrington, C.M. (1989) The albumin receptor effect may be due to a surface-induced confomational change in albumin. *J. Biol. Chem.* **264**, 9867-9872.

Resh, M.D. (1994) Myristylation and palmitylation of Src family members: The fats of the matter. *Cell* **76**, 411-413.

Rice, K.M., Leinhard, G.E., and Garner, C.W. (1992) Regulation of the expression of pp160, a putative insulin receptor signal protein, by insulin, dexamethasone, and 1-methyl-3-isobutylxanthine in 3T3-L1 adipocytes. *J. Biol. Chem.* **267**, 10163-10167.

Richieri, G.V., Ogata, R.T., and Kleinfeld, A.M. (1992) A fluorescently labeled intestinal fatty acid binding protein. Interactions with fatty acids and its use in monitoring free fatty acids. *J. Biol. Chem.* **267**, 23495-23501.

Richieri, G.V., Ogata, R.T., and Kleinfeld, A.M. (1994) Equilibrium constants for the binding of fatty acids with fatty acid-binding proteins from adipocyte, intestine, heart, and liver measured with the fluorescent probe ADIFAB. *J. Biol. Chem.* **269**, 23918-23930.

Ringold, G.M., Chapman, A.B., and Knight, D.M. (1986) Glucocorticoid control of developmentally regulated adipose genes. *J. Steroid Biochem.* **24**, 69-75.

Rothberg, K.G., Heuser, J.E., Donzell, W.C., Ying, Y.-S., Glenney, J.R., and Anderson, R.G.W. (1992) Caveolin, a protein component of caveolae membrane coats. *Cell* **68**, 673-682.

Rotin, D., Wan, P., Grinstein, S. and Tannock, I. (1987) Requirement of the Na^+/H^+ exchanger tor tumor growth. *Cancer Res.* **47**, 1497-1504.

Rubin, C.S., Hirsch, A., Fung, C., and Rosen, O.M. (1978) Development of hormone receptors and hormonal responsiveness *in vitro*. *J. Biol. Chem.* **253**, 7570-7578.

Russo, J.J., Manuli, M.A., Ismail-Beigi, F., Sweander, K.J., and Edelman, I.S. (1990) Na^+-K^+-ATPase in adipocyte differentiation in culture. *Am. J. Physiol.* **259**, C968-C977.

Sacchettini, J.C., and Gordon, J.I. (1993) Rat intestinal fatty acid binding protein. A model system for analyzing the forces that can bind fatty acids to proteins. *J. Biol. Chem.* **268**, 18399-18402.

Sacchettini, J.C., Gordon, J.I., and Banaszak, L.J. (1988) The structure of crystalline *Escherichia coli*-derived rat intestinal fatty acid-binding protein at 2.5-Å resolution. *J. Biol. Chem.* **263**, 5815-5819.

Sacchettini, J.C., Gordon, J.I., and Banaszak, L.J. (1989a) Crystal structure of rat intestinal fatty-acid-binding protein. Refinement and analysis of the *Escherichia coli*-derived protein with bound palmitate. *J. Mol. Biol.* **208**, 327-339.

Sacchettini, J.C., Scapin, G., Gopaul, D., and Gordon, J.I. (1989b) Refinement of the structure of *Escherichia coli*-derived rat intestinal fatty acid-binding protein with bound oleate to 1.75-Å resolution. Correlation with the structures of the apoprotein and the protein with bound palmitate. *J. Biol. Chem.* **267**, 23534-23545.

Sachs, G. and Fleischer, S. (1989) Transport machinery: An overview. *Methods Enzymol.* **171**, 3-12.

Safonova, I., Reichert, U., Shroot, B., Ailhaud, G., and Grimaldi, P. (1994) Fatty acids and retinoids act synergistically on adipose cell differentiation. *Biochem. Biophys. Res. Commun.* **204**, 498-504.

Sargiacomo, Sudol, M., Tang, Z.-L., and Lisanti, M.P. (1993) Signal transducing molecules and glycosyl-phosphatidylinositol-linked proteins form a caveolin-rich insoluble complex in MDCK cells. *J. Cell Biol.* **122**, 789-807.

Sargiacomo, M., Scherer, P.E., Tang, Z.-L., Casanova, J.E., and Lisanti, M.P. (1994) *In vitro* phosphorylation of caveolin-rich membrane domains: Identification of an associated serine kinase activity as a casein kinase II-like enzyme. *Oncogene* 9, 2589-2595.

Scapin, G., Spandon, P., Pengo, P., Mammi, M., Zanotti, G., and Monaco, H.L. (1988) Chicken liver basic fatty acid-binding prpotein (pI=9.0). Purification, crystallization and preliminary X-ray data. *FEBS Lett.* **240**, 196-200.

Scapin, G., Spandon, P., Mammi, M., Zanotti, G., and Monaco, H.L. (1990) Crystal structure of chicken liver basic fatty acid-binding protein at 2.7 Å resolution. *Mol. Cell. Biochem.* **98**, 95-99.

Scapin, G., Gordon, J.I., and Sacchettini, J.C. (1992) Refinement of the structure of recombinant rat intestinal fatty acid-binding apoprotein at 1.2-Å resolution.. *J. Biol. Chem.* **267**, 4253-4269.

Schaffer, J.E. and Lodish, H.F. (1994) Expression cloning and characterization of a novel adipocyte long chain fatty acid transport protein. *Cell* **79**, 427-436.

Scherer, P.E., Lisanti, M.P., Baldini, G., Sargiacomo, M., Mastick, C.C., and Lodish, H.F. (1994) Induction of caveolin during adipogenesis and association of GLUT4 with caveolin-rich vesicles. *J. Cell Biol.* **127**,1233-1243.

Schnitzer, J.E. (1992) gp60 is an albumin-binding glycoprotein expressed by continuous endothelium involved in albumin transcytosis. *Am. J. Physiol.* **262**, H246-H254.

Schnitzer, J.E., and Oh, P. (1994) Albondin-mediated capillary permeability to albumin. Differential role of receptors in endothelial transcytosis and endocytosis of native and modified albumins. *J. Biol. Chem.* **269**, 6072-6082.

Schnitzer, J.E., Carley, W.W. and Palade, G.E. (1988) Specific albumin binding to microvascular endothelium in culture. *Am. J. Physiol.* **254**, H425-H437.

Schnitzer, J.E., Sung, A., Horvat, R. and Bravo, J. (1992) Preferential interaction of albumin-binding proteins, gp30 and gp18, with conformationally modified albumins. Presence in many cells and tissues with a possible role in catabolism. *J. Biol. Chem.* **267**, 24544-24553.

Schnitzer, J.E., Oh, P., Pinney, E. and Allard, J. (1994) Filipin-sensitive caveolae-mediated transport in endothelium: Reduced transcytosis, scavenger endocytosis, and capillary permeability of select macromolecules. *J. Cell Biol.* **127**, 1217-1232.

Schroeder, F., Jefferson, J.R., Powell, D., Incerpi, S., Woodford, J.K., Colles, S.M., Myers-Payne, S., Emge, T., Hubbell, T., Moncecchi, D., Prows, D.R., and Heyliger, C.E. (1993) Expression of rat L-FABP in mouse fibroblasts: Role in fat absorption. *Mol. Cell. Biochem.* **123**:73-83.

Schürer, N.Y., Stremmel, W., Grundmann, J.-U., Schliep, V., Kleinert, H., Bass, N.M., and Williams, M.L. (1994) Evidence for a novel keratinocyte fatty acid uptake mechanism with preference for linoleic acid: Comparison of oleic and linoleic acid

uptake by cultured human keratinocytes, fibroblasts and a human hepatoma cell line. *Biochim. Biophys. Acta* **1211**, 51-60.

Schwieterman, W., Sorrentino, D., Potter, B.J., Rand, J., Kiang, C.-L., Stump, D. and Berk, P.D. (1988) Uptake of oleate by isolated rat adipocytes is mediated by a plasma membrane fatty acid binding protein closely related in liver and gut. *Proc. Natl. Acad. Sci. USA*. **85**, 359-363.

Scow, R.O. and Blanchette-Mackie, E.J. (1992) Endothelium, the dynamic interface in cardiac lipid transport. *Mol. Cell. Biochem*. **116**, 181-191.

Semenkovich, C.F., Wims, M., Noe, L., Etienne, J., and Chan, L. (1989) Insulin regulation of lipoprotein lipase activity in 3T3-L1 adipocytes is mediated at posttranscriptional and posttranslational levels. *J. Biol. Chem*. **264**, 9030-9038.

Sha, R.S., Kane, C.D., Xu, Z., Banaszak, L.J. and Bernlohr, D.A. (1993) Modulation of ligand binding affinity of the adipocyte lipid-binding protein by selective mutation. Analysis *in vitro* and *in situ*. *J. Biol. Chem*. **268**:7885-7892.

Siafaka-Kapadai, A. and Hanahan, D. (1993) An endogenous inhibitor of PAF-induced platelet aggregation, isolated from rat liver, has been identified as free fatty acid. *Biochim. Biophys. Acta*. **1166**, 217-221.

Silber, K.R., Keiler, K.C., and Sauer, R.T. (1992) Tsp: A tail-specific protease that selectively degrades proteins with nonpolar C termini. *Proc. Natl. Acad. Sci. USA*. **89**, 295-299.

Smart, E.J., Ying, Y.-S., Conrad, P.A., and Anderson, R.G.W. (1994a) Caveolin moves from caveolae to the Golgi apparatus in response to cholesterol oxidation. *J. Cell Biol.* **127**, 1185-1197.

Smart, E.J., Foster, D.C., Ying, Y.-S., Kamen, B.A., and Anderson, R.G.W. (1994b) Protein kinase C activators inhibit receptor-mediated potocytosis by preventing internalization of caveolae. *J. Cell Biol.* **124**, 307-313.

Smith, P.J., Wise, L.S., Berkowitz, R., Wan, C., and Rubin, C. (1988) Insulin-like growth factor-I is an essential regulator of the differentiation of 3T3-L1 adipocytes. *J. Biol. Chem*. **263**, 9402-9408.

Smith, A.F., Tsuchida, K., Suzuki, T.C., and Wells, M.A. (1992) Isolation, characterization, and cDNA sequence of two fatty acid-binding proteins from the midgut of *Manduca sexta* larvae. *J. Biol. Chem*. **267**, 380-384.

Sorrentino, D. and Berk, P.D. (1993) Free fatty acids, albumin, and the sinusoidal plasma membrane: Concepts, trends and controversies. in *Hepatic Transport and Bile Secretion: Physiology and Pathophysiology* (N. Tavolini and P.D. Berk, eds) Raven Press Ltd., New York p. 197-210.

Sorrentino, D., Stump, D., Potter, B.J., Robinson, R.B., White, R., Kiang, C.-L. and Berk, P.D. (1988) Oleate uptake by cardiac myocytes is carrier mediated and involves a 40-kDa plasma membrane fatty acid binding protein similar to that in liver, adipose tissue, and gut. *J. Clin. Invest.* **82**, 928-935.

Sorrentino, D., Robinson, R.B., Kiang, C.-L. and Berk, P.D. (1989) At physiologic albumin/oleate concentrations oleate uptake by isolated hepatocytes, cardiac myocytes and adipocytes is a saturable function of the unbound oleate concentration. Uptake kinetics are consistent with the conventional theory. *J. Clin. Invest.* **84**, 1325-1333.

Spector, A.A. (1975) Fatty acid binding to plasma albumin. *J. Lipid Res.* **16**, 165-179.

Spector, A.A., John, K. and Fletcher, J.E. (1969) Binding of long chain fatty acids to bovine serum albumin. *J. Lipid Res.* **10**, 56-67.

Spector, A.A., Fletcher, J.E., and Ashbrook, J.D. (1971) Analysis of long-chain free fatty acid binding to bovine serum albumin by determination of stepwise equilibrium constants. *Biochemistry* **10**, 3229-3232.

Spiegelman, B.M. and Green, H. (1980) Control of specific protein biosynthesis during the adipose conversion of 3T3 cells. *J. Biol. Chem.* **255**, 8811-8818.

Spiegelman, B.M., Frank, M., and Green, H. (1983) Molecular cloning of mRNA from 3T3 adipocytes. Regulation of mRNA content for glycerophosphate dehydrogenase and other differentiation dependant proteins during adipocyte development. *J. Biol. Chem.* **258**, 10083-10089.

Stein, W.D. (1989) Kinetics of transport: Analyzing, testing, and characterizing models using kinetic approaches. *Methods Enzymol.* **171**, 23-62.

Stewart, J.M. (1991) Fatty acid-binding protein and facilitated diffusion of fatty acids. *Biochem. J.* **280**, 835-836.

Storch, J. (1993) Diversity of fatty acid-binding protein structure and function: Studies with fluorescent ligands. *Mol. Cell. Biochem.* **123**, 45-53.

Storch, J, and Bass, N.M. (1990) Transfer of fluorescent fatty acids from liver and heart fatty acid-binding proteins to model membranes. *J. Biol. Chem.* **265**, 7827-7831.

Storch, J, Lechene, C., and Kleinfeld, A.M. (1991) Direct determination of free fatty acid transport across the adipocyte plasma membrane using quantitative fluorescence microscopy. *J. Biol. Chem.* **266**, 13473-13476.

Strålfors, P. (1990) Autolysis of isolated adipocytes by endogenously produced fatty acids. *FEBS Lett.* **263**, 153-154.

Stremmel, W. (1988) Fatty acid uptake by isolated rat heart myocytes represents a carrier-mediated process. *J. Clin. Invest.* **81**, 844-852

Stremmel, W. and Berk, P.D. (1986) Hepatocellular influx of [^{14}C]oleate reflects membrane transport rather than intracellular metabolism or binding. *Proc. Natl. Acad. Sci., USA* **83**, 3086-3090.

Stremmel, W., and Theilmann, L. (1986) Selective inhibition of long-chain fatty acid uptake in short-term cultured rat hepatocytes by an antibody to the rat liver plasma membrane fatty acid-binding protein. *Biochim. Biophys. Acta* **877**, 191-197.

Stremmel, W., Lotz G., Strohmeyer, G. and Berk, P.D. (1985b) Identification, isolation, and partial characterization of a fatty acid binding protein from rat jejunal microvillus membranes. *J. Clin. Invest.* **75**, 1068-1076.

Stremmel, W., Strohmeyer, G., Borchard, F., Kochwa, S. and Berk, P. D. (1985a) Isolation and partial characterization of a fatty acid binding protein in rat liver plasma membranes. *Proc. Natl. Acad. Sci. USA* **82**, 4-8.

Stremmel, W., Strohmeyer, G. and Berk, P.D. (1986) Hepatocellular uptake of oleate is energy dependant, sodium linked and inhibited by an antibody to a hepatocyte plasma membrane fatty acid binding protein. *Proc. Natl. Acad. Sci. USA* **83**, 3584-3588.

Stryer, L. (1988) *Biochemistry*, 3rd Ed.,W.H. Freeman and Co., New York. pp.479, 548.

Student, A.K., Hsu, R.Y. and Lane, M.D. (1980) Induction of fatty acid synthetase synthesis in differentiating 3T3-L1 preadipocytes *J. Biol. Chem.* **255**, 4745-4750.

Stump, D.D., Zhou, S.-L., and Berk, P.D. (1993) Comparison of plasma membrane FABP and mitochondrial isoform of aspartate aminotransferase from rat liver. *Am. J. Physiol.* **265**, G894-G902.

Suzuki, H., Kawarabayasi, Y., Kondo, J., Abe, T., Nishikawa, K., Kimura, S., Hashimoto, T., ajd Yamamoto, T. (1990) Structure and regulation of rat long-chain acyl-CoA synthetase. *J. Biol. Chem.* **265**, 8681-8685.

Swick, A.G. and Lane, M.D. (1992) Identification of a transcriptional repressor down-regulated during preadipocyte differentiation.. *Proc. Natl. Acad. Sci. USA* **89**, 7895-7899.

Tang, Z.-L., Scherer, P.E., and Lisanti, M.P. (1994) The primary sequence of murine caveolin reveals a conserved consensus site for phosphorylation by protein kinase C. *Gene* **147**, 299-300.

Thomas, J.A., Buschbaum, R.N., Zimmiak, A., and Racker, E. (1979) Intracellular pH measurements in Erlich ascites tumor cells utilizing spectroscopic probes generated in situ. *Biochemistry* **18**, 2210-2218.

Tiara, M., Hockman, S.C., Calvo, J.C., Tiara, M., Belfrage, P., and Manganiello, V.C. (1993) Molecular cloning of the rat adipocyte hormone-sensitive cyclic GMP-inhibited cyclic nucleotide phosphodiesterase. *J. Biol. Chem.* **268**, 18573-18579.

Tontonoz, P., Kim, J.B., Graves, R.A., and Spiegelman, B.M. (1993) ADD1: A novel helix-loop-helix transcription factor associated with adipocyte determination and differentiation. *Mol. Cell. Biol.* **13**, 4753-4759.

Tontonoz, P., Hu, E., Graves, R.A., Budavari, A.I., and Spiegelman, B.M. (1994a) mPPARγ2: Tissue-specific regulator of an adipocyte enhancer. *Genes & Dev.* **8**, 1224-1234.

Tontonoz, P., Hu, E., and Spiegelman, B.M. (1994b) Stimulation of adipogenesis in fibroblasts by PPARγ2, a lipid-activated transcription factor. *Cell* **79**, 1147-1156.

Torres, J.-M., Anel, A. and Uriel, J. (1992a) Alpha-fetoprotein-mediated uptake of fatty acids by human T lymphocytes. *J. Cell. Physiol.* **150**, 456-462.

Torres, J.-M., Darracq, N. and Uriel, J. (1992b) Membrane proteins from lymphoblastoid cells showing cross-affinity for α-fetoprotein and albumin. Isolation and characterization. *Biochim. Biophys. Acta* **1159**, 60-66.

Touster, O., Aronson, N.N., Jr., Dulaney, J.T. and Hendrickson, H. (1970) Isolation of rat liver plasma membranes. Use of nucleotide pyrophosphatase and phosphodiesterase I as marker enzymes. *J. Cell Biol.* **47**, 604-618.

Towbin, H., Staehelin, T., and Gordon, J. (1979) Electrophoretic transfer of proteins from polyacrylamide gels to nitrocellulose sheets: Procedure and some applications. *Proc. Natl. Acad. Sci. USA*. **76**, 4350-4354.

Uriel, J., Torres, J.-M. and Anel, A. (1994) Carrier-protein-mediated enhancement of fatty-acid binding and internalization in human T-lymphocytes. *Biochim. Biophys. Acta* **1220**, 231-240.

van Adelsberg, J., Barasch, J., and Al-Awqati, Q. (1989) Measurement of pH of intracellular compartments in living cells by fluorescent dyes. *Methods Enzymol.* **172**, 85-95.

van Beilen, J.B., Eggink, G., Enequist, H., Bos, R., and Witholt, B. (1992) DNA sequence determination and functional characterization of the OCT-plasmid-encoded *alkJKL* genes of *Pseudomonas oleovorans*. *Mol. Microbiol.* **6**, 3121-3136.

Vasseur-Cognet, M. and Lane, M.D. (1993a) *Trans*-acting factors involved in adipogenic differentiation. *Curr. Opin. Gen. Dev.* **3**, 238-245.

Vasseur-Cognet, M. and Lane, M.D. (1993b) CCAAT/enhancer binding protein α (C/EBPα) undifferentiated protein: A developmentally regulated nuclear protein that binds to the C/EBPα gene promoter. *Proc. Natl. Acad. Sci. USA*. **90**, 7312-7316.

Veerkamp, J.H., Peeters, R.A., and Maatman, R.G.H.J. (1991) Structural and functional features of different types of cytoplasmic fatty acid-binding proteins. *Biochim. Biophys. Acta* **1081**, 1-24.

Veerkamp, J.H., van Kuppevelt, T.H.M.S.M., Maatman, R.G.H.J. and Prinsen, C.F.M. (1993) Structural and functional aspects of cytosolic fatty acid-binding proteins. *Prostaglandins, Leukotrienes and Essential Fatty Acids*. **49**, 887-906.

Villalba, J.M., Canalejo, A., Rodriguez-Aguilera, J.C., Buron, M.I., Moore, D.J., and Navas, P. (1993) NADH-ascorbate free radical and -ferricyanide reductase activities represent different levels of plasma membrane electron transport. *J. Bioenerget. Biomemb.* **25**, 411-417.

Vork, M.M., Glatz, J.F.C., Surtel, D.A.M., and van der Vusse, G.J. (1990) Assay of the binding of fatty acids by proteins: Evaluation of the lipidex 1000 procedure. *Mol. Cell. Biochem.* **98**, 111-117.

Vork, M.M., Glatz, J.F.C. and van der Vusse, G.J. (1991) Does fatty acid-binding protein facilitate the diffusion of oleic acid? *Biochem. J.* **280**, 835.

Vork, M.M., Glatz, J.F.C., and Van Der Vusse, G.J. (1993) On the mechanism of long chain fatty acid transport in cardiomyocytes as facilitated by cytoplasmic fatty acid-binding protein. *J. Theor. Biol.* **160**, 207-222.

Waggoner, D.W. and Bernlohr, D.A. (1990) *In situ* labeling of the adipocyte lipid binding protein with 3-[^{125}I]Iodo-4-azido-*N*-hexadecylsalicylamide. Evidence for a role of fatty acid binding proteins in lipid uptake. *J. Biol. Chem.* **265**, 11417-11420.

Warnotte, C., Gilon, P., Nenquin, M. and Henquin, J.-C. (1994) Mechanisms of the stimulation of insulin release by saturated fatty acids. A study of palmitate effects in mouse β-cells. *Diabetes*, **43**, 703-711.

Watkins, D.C., Northup, J.K., and Malbon, C.C. (1987) Regulation of G-proteins in differentiation. Altered ratio of α- to β-subunits in 3T3-L1 cells. *J.Biol.Chem.* **262**, 10651-10657.

Weisiger, R.A. (1993) The role of albumin binding in hepatic organic anion transport. in *Hepatic Transport and Bile Secretion: Physiology and Pathophysiology* (N. Tavolini and P.D. Berk, eds) Raven Press Ltd., New York p. 171-196.

Weisiger, R., Gollan, J. and Ockner, R. (1981) Receptor for albumin on the liver cell surface may mediate uptake of fatty acids and other albumin-bound substances. *Science* **211**, 1048-1051.

Weisiger, R.A., Pond, S.M., and Bass, L. (1989) Albumin enhances unidirectional fluxes of fatty acid across a lipid-water interface: Theory and experiments. *Am. J. Physiol.* **257**, G904-G916.

Winter, N.S., Bratt, J.M., and Banaszak, L.J. (1993) Crystal structures of holo and apo-cellular retinol-binding protein II. *J. Mol. Biol.* **230**, 1247-1259.

Wolkoff, A.W. (1987) The role of an albumin receptor in hepatic organic anion uptake: The controversy continues. *Hepatology* **7**, 777-779.

Wootan, M.G. and Storch, J. (1994) Regulation of fluorescent fatty acid transfer from adipocyte and heart fatty acid bindig proteins by acceptor membrane lipid composition and structure. *J. Biol. Chem.* **269**, 10517-10523.

Wootan, M.G., Bernlohr, D.A., and Storch, J. (1993) Mechanism of fluorescent fatty acid transfer from adipocyte fatty acid binding protein to membranes. *Biochemistry* **32**, 8622-8627.

Xu, Z., Bernlohr, D.A., and Banaszak, L.J. (1992) Crystal structure of recombinant murine adipocyte lipid-binding protein. *Biochemistry* **31**, 3484-3492.

Xu, Z., Bernlohr, D.A., and Banaszak, L.J. (1993) The adipocyte lipid-binding protein at 1.6-Å resolution. Crystal structures of the apoprotein and with bound saturated and unsaturated fatty acids. *J. Biol. Chem.* **268**, 7874-7884.

Yang, V.W., Christy, R.J., Cook, J.S., Kelley, T.J. and Lane, M.D. (1989) Mechanism of regulation of the 422(aP2) gene by cAMP during preadipocyte differentiation. *Proc. Natl. Acad. Sci. USA*. **89**, 3629-3633.

Yang, Y., Spitzer, E., Kenney, N., Zschiesche, W., Li, M., Kromminga, A., Müller, T., Spener, F., Lezius, A., Veerkamp, J.H., Smith, G.H., Salomon, D.S., and Grosse, R. (1994) Members of the fatty acid binding protein family are differentiation factors for the mammary gland. *J. Cell Biol.* **127**, 1097-1109.

Young, A.C.M., Scapin, G., Kromminga, A., Patel, S.B., Veerkamp, J.H., and Sacchettini, J.C. (1994) Structural studies on human muscle fatty acid binding protein at 1.4 Å resolution: Binding interactions with three C18 fatty acids. *Structure* **2**, 523-534.

Zanotti, G., Scapin, G., Spadon, P., Veerkamp, J.H., and Sacchettini, J.C. (1992) Three-dimensional structure of recombinant human muscle fatty acid-binding protein. *J. Biol. Chem.* **267**, 18541-18550.

Zezulak, K.M. and Green, H. (1986) The generation of insulin-like growth factor-1-sensitive cells by growth hormone action. *Science* **233**, 551-553.

Zhou, S.-L., Stump, D., Sorrentino, D., Potter, B.J. and Berk, P.D. (1992) Adipocyte differentiation of 3T3-L1 cells involves augmented expression of a 43-kDa plasma membrane fatty acid-binding protein. *J. Biol. Chem.* **267**, 14456-14461.

Zhou, S.-L., Stump, D., Isola, L. and Berk, P.D. (1994) Constitutive expression of a saturable transport system for non-esterified fatty acids in *Xenopus laevis* oocytes. *Biochem. J.* **297**, 315-319.

Zovich, D.C., Orologa, A., Okuno, M., kong, L.W.Y., Talmage, D.A., Piantedosi, R., Goodman, D.S., and Blaner, W.S. (1992) Differentiation-dependent expression of retinoid-binding protein in BFC-1β adipocytes. *J. Biol. Chem.* **267**, 13884-13889.

Zurzolo, C., van't Hof, W., van Meer, G., and Rodriguez-Boulan, E. (1994) VIP21/caveolin, glycosphingolipid clusters and the sorting of glycosylphosphatidylinositol-anchored proteins in epithelial cells. *EMBO J.* **13**, 42-53.